Linking sill morphology to emplacement mechanisms

by

Nick Schofield

A thesis submitted to
The University of Birmingham
For the degree of
DOCTOR OF PHILOSOPHY

Department of Earth Sciences
School of Geography, Earth
And environmental sciences
The University of
Birmingham
May 2009

Abstract

Mafic sill complexes are increasingly being shown to play a major role in the movement of magma around the upper crust in volcanic terranes and to have a role in mass extinction events in Earth history.

Most of the current models of sill emplacement assume that brittle fracture operates at all points of sill emplacement. Within this thesis, a series of observations are presented from sheet intrusions in South Africa, USA and the UK showing that in certain situations, dependent on host rock lithology, the propagation of magma through normal brittle fracture can cease. In this circumstance a prevalent fluid/fluid or fluid/ductile relationship between host rock and intruding magma is often developed. Once this occurs, the evolution of a given sheet intrusion becomes distinctly different from that produced by normal brittle fracture alone. The break down in brittle fracture often leads to the development of magma fingers, which accelerate ahead of the main sheet of magma. It is important to note that it is ultimately the host rock lithology and its coupled response to intrusion of magma that dictates the ongoing evolution of the morphology of sheet intrusions in high-level magmatic systems.

Words: 200

Acknowledgement

Undertaking this PhD has been an interesting journey, it has been one of the best experiences of my life, but it has equally been tinged with much sadness.

I've been very lucky throughout my PhD to have had five (having mysteriously gained another supervisor post-viva) excellent supervisors who have all contributed to this project in their own unique ways.

Particular thanks/apologies should go to Prof. Tim Reston who took over lead supervision after Ken's death. Although he has an unusual (possibly unhealthy) fascination with lithospheric stretching, he has equally been an invaluable source of advice and encouragement. A bottle of whisky is in order, however drink it properly Tim!

Prof. Donny Hutton provided many discussions on sill emplacement, life and experiences. The field season which I spent with Donny in South Africa has provided me many good memories.

Prof. Graham Westbrook provided critical discussions in general. He is also thanked for allowing me to take part in the HERMES TTR-16 cruise on the Norwegian Margin in June 2005.

Dr. Carl Stevenson (one of the members of the Northern Ireland structural mob) deserves a big mention. He has been a both a good friend and a colleague. We have had many discussions on igneous emplacement, mainly at the Pub. So cheers mate, I couldn't have done it without you. It should also be noted that the school of GEES decided post-viva that Dr. Stevenson was one of my supervisors! Talk about sitting on the fence!

Thanks should also go to Dr. Jonathan Turner, who gave many words of encouragement during the PhD. "Alright Jonathan……Three lobster thermidor's please"!

Prof. John Underhill (Kens former PhD supervisor) is thanked for encouragement, advice, discussions and post-doc references! In bad times it was nice to know that I had somebody looking out for me back in Edinburgh.

Dr Chris Cornelius of Cuadrilla Resources is thanked for his hospitality and introduction to the sills of the Raton Basin which cemented many of the ideas presented in the thesis. Dr Pete Turner of Cuadrilla Resources is thanked for help during the PhD and introducing me to Chris, as well as introducing me to plethora of 'interesting' individuals.

The late Dr Bill Owens is thanked for early advice on AMS in Skye and for accompanying me in the field along with Donny on my first trip to the Trotternish Peninsula. He is sadly missed.

John Smallwood of Hess is thanked for continued support and providing 3D seismic data sets.

Funding from NERC studentship (NER/S/A/2005/13237) is gratefully acknowledged.
AAPG Grants-In-Aid program is thanked for awarding the Horst & Jessie von Bandat Memorial Grant which enabled USA fieldwork to be undertaken.

I would like to thank my examiners Dr. Mike Curtis (BAS) and Dr. Andy Chambers (Birmingham), I thank them both for seeing through my abysmal English skills to provide an opportunity for an in-depth and stimulating discussion on the thesis. Mike is particularly thanked for making me realise the need for complete precision and conciseness, as well as getting me to take more care in reading conclusions of papers!

On more personal notes, several people deserve mentions;

Dr. Neil Davies, did his best and succeeded in making the first half of my PhD a bizarre experience. Luckily for UK citizens, he is now in Canada.

Fellow members of Rm 116 “The office of glory” a.k.a. “Subsurface office and Phil” deserve a mention. These include Craig “Magma” Magee, Ken “Keys” Mcdermot, Phil “Palynology” Jardine and Baba “Faults” Jibrin……..I’m sure you are all destined for great things, how about “The School of the Subsurface and Phil”?

Other mentions should go to people who have made my time at Birmingham very enjoyable. In no particular order, these include; Aruna Mistry, Ian Boomer, Paula Cole, Sarah King, Andy Rees, Richard Greswell, June Morris, Russel Exley, Simon Holford, Liam Herrigshaw, Andy Chambers, Kate Thatcher, Sam Spendlove, Ruth Hughes, Chloe Parker.

Other notable mentions should also include the VMSG crew, who I have shared many a pint with over the years and in some cases ‘romantic’ sunset cruises under the Golden Gate bridge. The usual suspects consist of Dr Davie Brown (Glasgow), Dr Simon Passey (Faroes), Simon “Hang about, when I’m cleaning windows, fingers” Drake (UCL/Birkbeck).

Finally I would particularly like to mention two people who have kept me on the right side of normality in recent years;

My housemate, Kate Faloon a.k.a Loser, has been a source of very un-witty banter and given much amusement (often at her own expense, red-light bulbs maybe?). She has plied me with wine, whisky and chocolate brownies when the stress kicked in. In addition she has done my washing up on one to many occasions (well actually on most occasions to be trueful). For all this I am extremely grateful to her, but ultimately Kate, just remember…….I’m right, you’re wrong, so…...?

The final thank mention goes to Holly who has been a source of great patience (generally). She has also kept a smile on my face in difficult times mainly due to her confusion with the general world around. So Holly in response to some of the questions you’ve raised or shown utter shock at in recent years (I know you don’t mind me saying these), the answers are as follows. 1) People do indeed eat monkeys 2) Clouds on the ground are generally referred to as fog and 3) The Bismarck did not take part in Falklands conflict and did not sink off the Falkland Islands. I hope this has cleared a few things up!

Dedication

This thesis is dedicated to the memory of Dr. Ken Thomson (1966 – 2007)

Ken unexpectedly passed away in April of 2007 while in the department. He was a brilliant supervisor, academic and polymath! Along with Donny he set an excellent PhD project which I've had the honour of getting my teeth into, for which I am extremely grateful.

So Ken, if your about somewhere in the ether, I hope your happy with the result. It would have been nice to have a pint with you afterwards.

"Sentries have come in from the hill, sir.... They report Zulus to the southeast. Four thousand of them" *from the film Zulu (1965)*

“Mk.1 Eyeballs” – British military term

Contents

List of Figures

Chapter 4: The geometry and flow directions of the Trotternish Sill Complex, Trotternish peninsula, Isle of Skye

Chapter 1
Introduction and models of sill emplacement

Constraining the geometry and architecture of sub-volcanic intrusions is fundamental to understanding the transport, delivery and storage of magma in the upper crust and its eventual eruption at the Earth's surface. The intrusive components of a volcanic system generally represent the volumetrically most significant part but are largely inaccessible unless exposed in eroded epicontinental terrains (e.g. Palisades Sill, Newark Basin, USA, Husch, 1990) or after rapid and dramatic uplift (e.g. Tuscan magmatic province, Italy, Rocchi et al., 2002).

In the shallow subsurface, magma transport is dominated by dykes (Callot et al., 2001) and sills (Cartwright and Hansen, 2006). Traditionally dykes have been assumed to play the largest role in feeding magma around high level magmatic systems (Pollard, 1987; Ernst et al., 2001; Gudmundsson, 2003). However an increasing amount of evidence suggests that in shallow level systems, mafic sill complexes can play a major role in transporting magma and feeding overlying eruptive complexes (Thomson and Hutton, 2004; Cartwright and Hansen, 2006; Thomson, 2007). Cartwright and Hansen (2006) gave convincing evidence for movement of magma not just vertically, but over 10's of km laterally through sills. Evidence for long distance (~ 4000km) lateral movement of magma in sills has been recently confirmed by the geochemical study of the Ferrar sills, Antarctica, by Leat (2008). The main implication of the work of Cartwright and Hansen (2006), Leat (2008) and others (Stevenson et al., 2008) is that eruptive centres and shallow level intrusive complexes may not necessarily overly the source region of magmatism in the lower crust.

1.1 Models of sill initiation and emplacement

Sills are traditionally defined as concordant sheet like igneous bodies with large length: thickness ratios (Corry, 1988; Liss, 2004). Many current models of sill emplacement have their roots in models developed up to 132 years ago. Some of the main models are outlined briefly in the following section.

1.1.1 Gilbert (1877)

Gilberts beautifully illustrated account of laccolithic intrusion probably gave the first detailed account of sill and laccolith intrusion. In field observations Gilbert realised that the vertical

inflation of laccolithic bodies in the Henry Mountains, Utah, USA, had led to doming of the overlying roof rock (Fig. 1.1a and Fig. 1.1b).

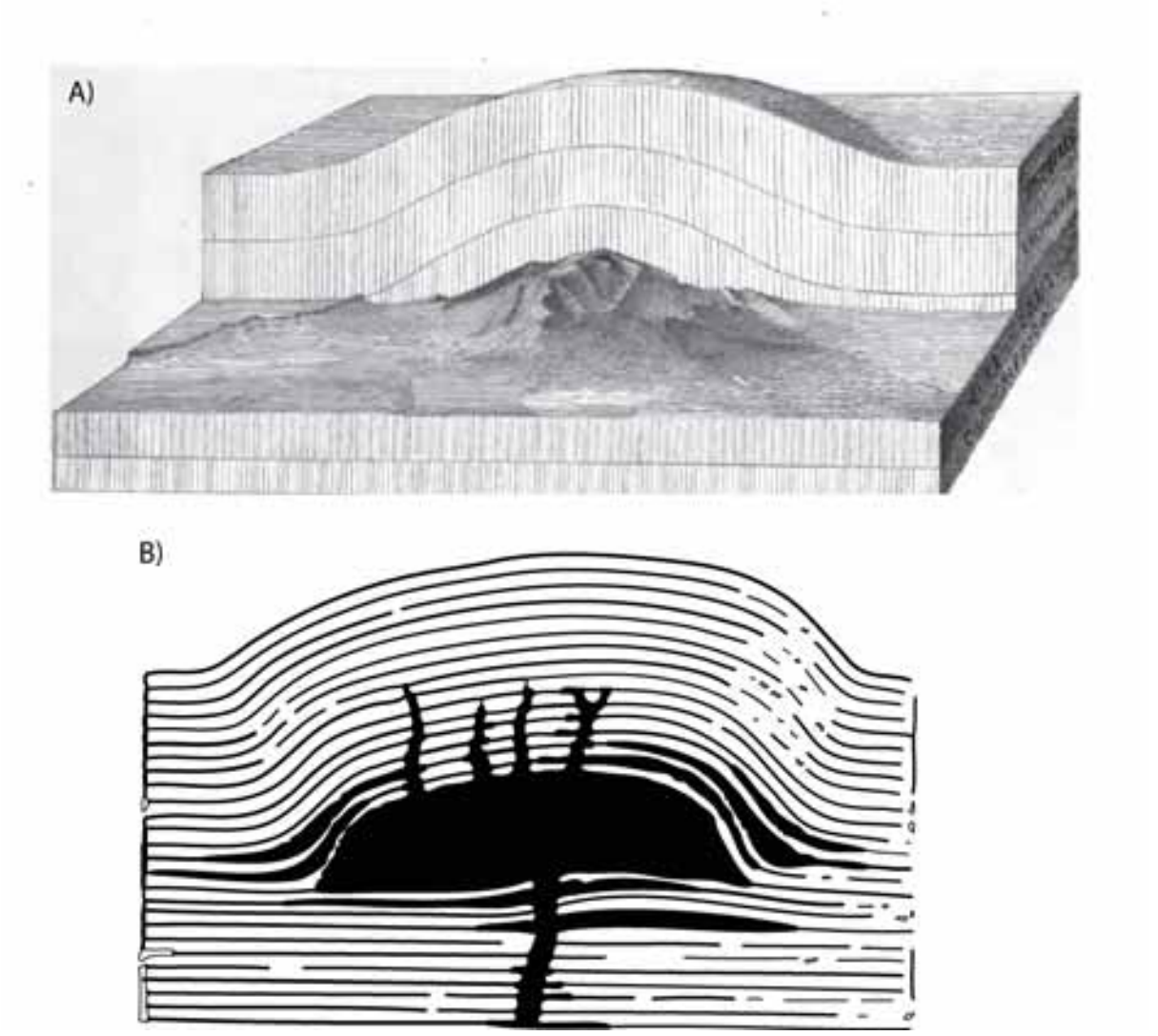

Fig. 1.1 – From Gilbert (1877), A) Shows the schematic sketch of the Mt. Elsworth laccolith, and Gilberts reconstruction of the doming which would have occurred over the body B) Re-drawn from Gilbert (1877), showing idealised schematic across a laccolith

Gilbert essentially proposed that laccolith emplacement could be viewed as a hydraulic piston, so that for laccoliths/sills to form the magmatic pressure must be higher then the lithostatic pressure, leading to the uplift of a central block bounded by a ring fault overlying the a central disc of inflating magma. On this basis, Gilbert proposed that sill and laccolith intrusion initiated at the point that magmatic pressure was sufficient to overcome the weight of the overburden.

For a model developed over 132 years ago, Gilbert's model was highly advanced for its time. In particular Gilbert (1877) noted that the highest strain within the domed overburden would be expected to develop at the periphery of the sill/laccolith. This has been subsequently shown to be the case (Johnson and Pollard, 1973; Goulty and Schofield, 2008).

1.1.2 Anderson (1951)

Anderson proposed that sill emplacement takes place perpendicular to the direction of least compressive stress as a result of magma taking the path of least resistance through the crust. To explain the transition from dyke to sill, Anderson (1951) invoked a mechanism of rotation of the stress field at a given point in the intrusion of the dyke to explain its rotation onto a horizontal plane. For stress rotation to occur Anderson (1951) proposed that repeated injection of dykes into the earth's crust could effectively change the orientation of the stress field. Anderson's (1951) premise has been shown to be possible, with various workers showing that rotation in the stress field can occur in various circumstances promoting the emplacement of sills (Parsons and Thompson, 1991; Parsons et al., 1992; Valentine and Krogh, 2006; Burchardt, 2008).

1.1.3 Mudge (1968)

Mudge (1968) collated data from 54 sill and laccolith intrusions. In this analysis Mudge discovered the paleo-depth of emplacement ranged from ~ 900m to 2300m in depth. He also noted that most bodies were overlain by impermeable mudstone-siltstone beds and that the intrusions themselves had appeared to have intruded well-defined bedding planes. In the model of emplacement, Mudge (1968) proposed that the overlying impermeable mudstone-siltstone beds had acted as fluid barriers to both magma and steam, retarding upward movement of magma and causing it to emplace laterally to form either a sill or laccolith.

Mudge (1968) proposed that sills and laccoliths were absent at depths above 900m as the shale was acting in a brittle manner, compared to below 900m depth were it was acting in a ductile fashion. He presumed that above 900m, the fracturing allowed the transit of magma more easily to the surface, thus inhibiting the formation of sill intrusions at shallow depths. To explain the lack of sill intrusions below 2300m Mudge hypothesised that at this level the magmatic overpressure was insufficient to lift the weight of overlying overburden, similar to the deduction of Gilbert (1877).

The identification by Mudge (1968) of the importance of impermeable barriers preventing the escape and dissipation of superheated water vapour within host rock is

significant, as impermeable barriers and overpressured horizons are now thought to play a large role in governing the emplacement of shallow level sheet intrusions (Whin Sill, Liss, 2004).

1.1.4 Gretener (1969)

Gretener (1969) disagreed with Mudge's (1968) hypothesis of sill intrusion triggered by impermeable shale/mudstone barriers preventing the upward flow of magma. Instead he proposed that the state of stress between stratigraphic units of varying elastic modulus and Poisson's ratio will be different, which may lead to them acting as effective stress barriers preventing upward movement of magma, causing the magma to intrude horizontally thus initiating sill emplacement.

1.1.5 Johnson and Pollard (1973)

Johnson and Pollard (1973) showed that when magma intruded onto a horizontal plane it could easily propagate through host rock by stress concentrations at the sill tip effectively splitting the rock apart. They also observed that the vertical inflation and doming of a sill body led to the opening of tensile fractures particularly at the periphery of sill/laccolith, where sub-vertical dykes could be seen to develop, sometimes flattening at higher levels forming a step-stair configuration to the edge of the sill/laccolith.

The importance of Johnson and Pollard's model is significant and it has continued to be applied in the context of laccolith emplacement (Roman-Berdiel et al., 1995; Kerr and Pollard, 1998) and models of saucer-shaped sill emplacement (see chapter 2).

1.1.6 Leamen (1975)

In Leamen's study of the sill intrusions of Hobart, Tasmania, he observed that the sills showed a stepped (saucer-shaped) morphology on all scales. Leamen (1975) noted that sills often intruded along Permian-aged calcareous rock, arguing that the exploitation by magma of these preferential horizons was due to a poorly developed pre-existing fracture network which did not allow easy intrusion of magma through host rock.

1.1.7 Kavanagh et al. (2008)

Kavanagh et al. (2008) extended the analogue modelling experiments of Pollard (1973) which found that sills tended to form from a dyke at planar discontinuities in the form of bedding planes, foliation and unconformities, whatever the orientation of least compressive stress.

Within the analogue experiments of Kavanagh et al. (2008) they found that dyke arrest occurred when a high rigidity ratio existed between two layers. Sill intrusion however only initiated when the interface between the two layers of different rigidities was weak, creating a suitable parting surface for the sills to intrude along. Menand (2008) argued that after the emplacement of a sill at a rigidity contrast *sensu* Kavanagh (2008), the rigidity contrast created by the sill itself created favourable rigidity anisotropy promoting the emplacement of successive sills and formation of a laccolith.

Evidence of dyke arrest in the field at rigidity contrasts has been reported by Gudmundsson (2005) who found evidence of dyke arrest at interfaces between layers possessing large rigidity contrasts e.g. tuff and lava (Fig 1.2).

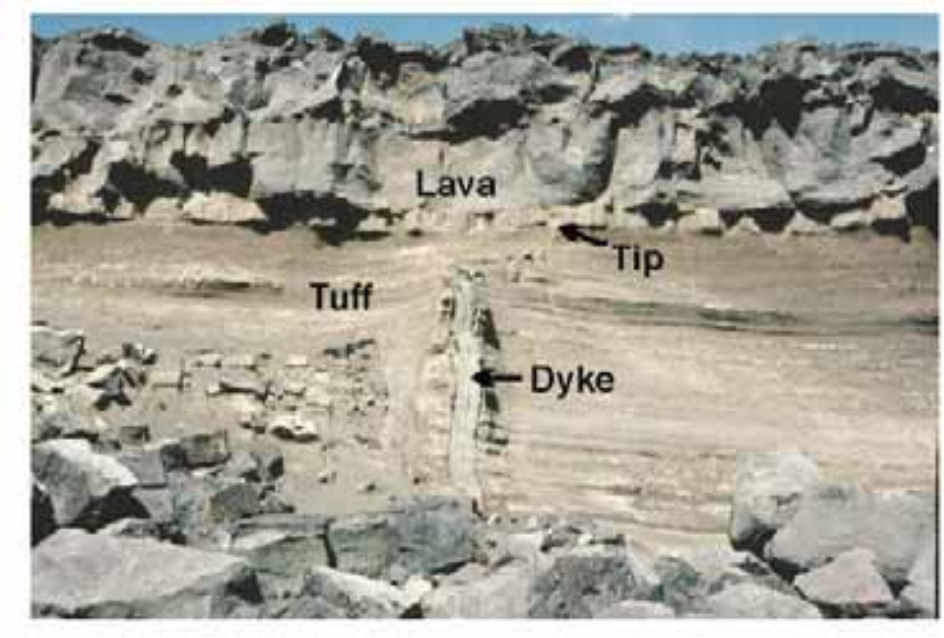

Fig. 1.2 – Photo taken from Gudmundson (2005) showing arrested dyke in tuff 5m beneath lava.

1.2 Models of saucer-shaped sill emplacement (Pre 3D seismic)

Although Leamen (1975) did notice the presence of stepped sills, it was Francis (1982) who first stated that sills in sedimentary basins tended to form a saucer-shaped morphology. This observation has subsequently been confirmed in recent years from sills imaged using 3D seismic data (Chapter 2). However it is important to outline the models of sill emplacement which are applicable to the formation of saucer-shaped sills and which have mainly been derived from field observations.

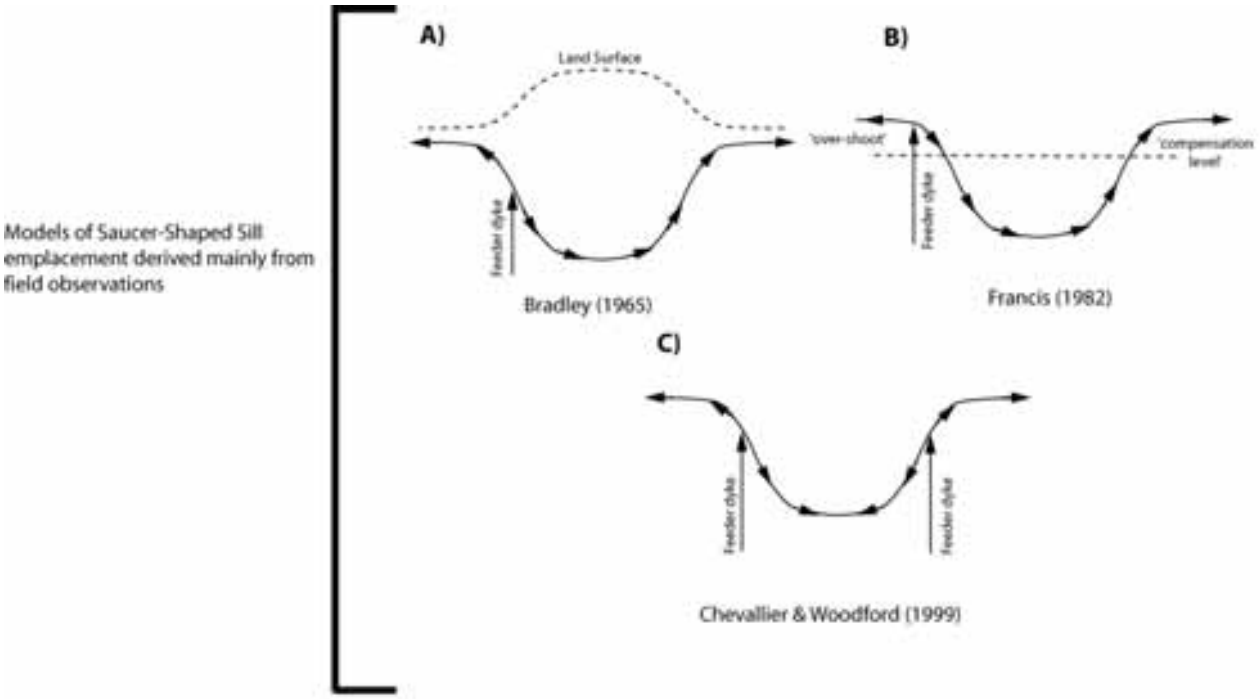

Fig. 1.3 – Saucer-shaped sill emplacement models mostly derived from field data (re-drawn and modified from Thomson and Hutton, 2004) (see text for details).

1.2.1 Bradley (1965)

Bradley (1965) (Fig. 1.3a) proposed that sills intrude along an isobaric surface, where magma pressure equals that of the lithostatic pressure. This resulted in the sill effectively following the overlying topography, with structurally high areas of the sill corresponding to topographic lows, and structurally low areas corresponding to topographic highs. The model has come under criticism by various workers for being essentially un-testable due to uncertainty in the form of the paleo-landsurface at time of intrusion (Francis, 1982; Liss, 2004; Thomson and Hutton, 2004). However by using flood basalt sequences as an approximate guide to the paleo-landsurface, Thomson and Hutton (2004) showed that underlying sills, which are temporally connected with the lavas, do not parallel overlying topography, questioning the validity of Bradley's (1965) model. Also within Bradley's (1965) model, a drop in magma pressure would lead to higher intrusions, which is counter-intuitive.

In addition, the model of Bradley (1965) has the feeder for the saucer located off-centre on the outer rim of the saucer, implying that magma flow must be directed downwards to the base of the sill. Both of these aspects are incompatible with seismic evidence, which

shows magma flow up and away from a centrally located feeder zone in the inner saucer (Thomson and Hutton, 2004; Hansen and Cartwright, 2004).

1.2.2 Francis (1982)

Based on work on the basic sills of the Midland Valley, Scotland, Francis (1982) proposed a model of saucer-shaped sill emplacement consisting of aspects of neutral buoyancy and gravitational flow (Fig.1.3b). The model consists of a feeder dyke intruded off axis from the basin centre which 'overshoots' the level of neutral buoyancy that exists at the point in which the density of magma equals the density of the surrounding country rock. At the point that the vertical stress (due to the overburden) becomes smaller then the horizontal stress, the dyke re-orientates onto the horizontal plane, instigating sill intrusion. However the density of the magma (now propagating horizontally) exceeds that of the surrounding rock. To return to equilibrium, Francis (1982) proposed that magma must flow down dip under gravity towards the centre of the basin, exploiting bedding planes and joint surfaces to accomplish this. Francis (1982) argues that for the magma to reach hydrostatic equilibrium it may then flow up the other side of the basin, thus forming a saucer-shaped sill.

Francis's model was widely accepted by the geological community for a number of years (Mcphie, 1993), and is still invoked in models of sill emplacement (Goulty, 2005). However several key observations have raised serious questions regarding the validity of the model in understanding sill emplacement into the upper crust (Trendall, 1994). Firstly, the presumption that sills occur at the point were vertical stress becomes smaller then horizontal stress is incorrect, as in such a circumstance sills would never be expected to occur in extensional terranes, which is widely known not to be the case (Bell and Butcher, 2002; Davies *et al.,* 2002; Thomson and Hutton, 2004). Secondly, as with the model of Bradley (1965), the model of Francis (1982) requires magma flow to be directed downwards to the base of the saucer, which together with the placement of the magma source off-centre away from the central sill axis, is in direct contradiction to the findings of Thomson and Hutton (2004) and Hansen and Cartwright (2006) (see chapter 2).

1.2.3 Chevalier and Woodford (1999)

Chevalier and Woodford (1999) developed a model of saucer-shaped sill emplacement based on work on saucer-shaped sills within the Karoo Basin, South Africa (Fig. 1.3c). In this model a ring dyke ascends vertically and at a given point the dyke re-orientates to form an inclined

sheet, inflating as it does so. This inflation causes the overburden of country rock to be lifted, allowing magma to flow downwards into the central section, forming the base of a saucer-shaped sill. Again this model of emplacement requires downwards flow of magma, in contradiction to the findings of Thomson and Hutton (2004). In addition studies of saucer-shaped sills within the Karoo have not led to any reporting of ring-dykes in association with saucer-shaped sills (Polteau et al*.,* 2008; this study).

1.3 Discussion

Various controlling factors for sill emplacement have been proposed covering variety of emplacement mechanisms. These include;

- Regional stress fields (Anderson, 1951).
- Impermeable barriers (Mudge, 1968).
- Stress barriers (Gretener, 1969).
- Splitting of host rock at magma tips (Pollard and Johnson, 1973).
- Discontinuities and rigidity contrasts (Pollard, 1973; Kavanagh et al., 2008).
- Zones of equipotential pressure (Gilbert, 1877, Bradley, 1965).
- Neutral buoyancy (Francis, 1982).

In the above models of sill emplacement, all models assume brittle fracture operating, aside from the model of Mudge (1968) who proposed that ductile deformation in shale/mudstone beds inhibited fracturing and steam escape, promoting sill intrusion rather then vertical dyke emplacement. Although the model of Mudge (1968) is flawed, his identification of the importance of the possible importance of host rock rheology on the emplacement of sills is an important observation and which will be argued to play a major role in the emplacement of sills later within this thesis.

1.4 Preface to remaining chapters

This thesis investigates the emplacement of sills within sedimentary basins, drawing on a variety of different lines of evidence from sheet intrusions in both field and seismic data before proposing a generalised model for their emplacement.

Chapter 2 - This chapter deals with observations and models of sill emplacement derived mainly from 3D seismic data, both through past work and new observations.

Chapter 3 - This chapter deals with common structural elements seen within sills in both seismic data and field data. It also proposes that such structures need to be classified genetically and not just purely on morphology.

Chapter 4 - This chapter deals with the emplacement and flow directions of the Trotternish/Little Minch Sill Complex, exposed within the Trotternish peninsula, Isle of Skye. The work shows the presence of convex-up finger structures within the sills which are related to flow and shows that the sills are made of multiple pulses of magma which have not been differentiated by previous petrological or geochemical studies of the sill complex.

Chapter 5 - This chapter deals with the morphology of field examples of saucer-shaped sills. Most work is concentrated on the Golden Valley Sill, South Africa which shows evidence of the same convex-up flow structures as seen in Skye. The morphology of these features indicates that they are similar to magma fingers as described by Pollard et al. (1975) caused by the creation of a fluid-fluid relationship between host rock and intruding magma.

Chapter 6 - This chapter reviews the mechanism of magma finger formation and explores how a prevailing fluid-fluid relationship can be created between intruding magma and host rock. Fluidization *sensu* Kokelaar (1982) is evaluated and the concept of fluidization is applied to the model of emplacement of the Golden Valley Sill, which is also presented within this chapter.

Chapter 7 - This chapter links the emplacement mechanisms of sills to their morphology by showing that the response of host rock rheology during intrusion of magma ultimately governs the final morphology of the sill produced.

Chapter 8 - This chapter gives concluding remarks and possible future work.

Chapter 2 – Contribution of 3D seismic data in the understanding of sill emplacement mechanisms

Within recent years arguably the largest breakthrough in the study of sub-volcanic sill complexes has come about as a result of exploitation of oil industry 3D seismic data in offshore basins containing intrusive sill complexes (*see* Thomson and Hutton, 2004). This has enabled detailed morphologies of sills and flow pathways of magma in the upper crust to be studied directly (Bell and Butcher, 2002; Smallwood and Maresh, 2002; Thomson and Hutton, 2004; Cartwright and Hansen, 2006; Thomson, 2007; Thomson and Schofield, 2008).

Although the use of 3D seismic data has yielded a great deal of information regarding the gross morphology of sills (Trude, 2006), their occurrence (Bell and Butcher, 2002; Smallwood and Maresh, 2002; Thomson and Hutton, 2004; Cartwright and Hansen, 2006; Rocchi et al., 2007; Thomson, 2007; Thomson and Schofield, 2008) and large-scale relationships with the magmatic system (Cartwright and Hansen, 2006), the main limitation of 3D seismic data is its inability to elucidate the underlying mechanisms of magma intrusion.

2.1 3D seismic investigation of sills

Before dealing with the emplacement models of sill emplacement derived either directly from 3D seismic data, or based on observations from it, it is important to review some of the key observations which have been made from seismic data with regard to sills and sill emplacement.

2.1.1 Sills in 3D seismic data – An introduction

Many major sedimentary basins worldwide contain a large volume of mafic intrusive volcanics, particularly those basins related to major rifting events. These include the Parana Basin (Brazil), Faroe-Shetland Basin (North West European Margin) and NE Rockall Trough (NW Atlantic). Past studies of sill complexes have mainly been restricted to field relationships and geochemical analysis on exposed sill complexes (Du Toit, 1920; Francis, 1982; Leamen, 1975; Pollard et al*.,* 1975; Walker, 1993; Gibson and Jones, 1991; Horsman et al*.,* 2005). The increased availability of 3D seismic data in offshore sedimentary basins, has enabled the study of un-eroded submerged sill complexes to take place which has led to major advances in recent years on how magma is emplaced, moved and accommodated in the upper

crust (Planke et al., 2005; Hansen and Cartwright, 2006; Davies et al., *2002;* Smallwood and Maresh, 2002; Thomson and Hutton, 2004; Thomson, 2007; Thomson and Schofield, 2008).

Investigations using 3D seismic data confirmed the observation of Francis (1982) that sills within sedimentary basins dominantly possess a saucer-shaped morphology at high-levels, consisting of a concordant inner sill, which at its edges rapidly steepens forming an arcuate inclined sheet, typically at an angle of 20 – 35° (Fig. 2.1) (Goulty and Schofield, 2008). Some sills display a roughly concordant outer rim, which sometimes shows a ragged appearance at its leading edge, and further transgressions of the sill can take place away from the outer rim, giving a step-stair appearance to some sills (Malthe-Sørenssen et al., 2004; Thomson and Hutton, 2004; Goulty and Schofield, 2008). However, flat outer rims are not always developed in all sills, with some only showing an arcuate transgressive rim that does not flatten (e.g. Solsikke Sill, Norwegian Margin, Hansen and Cartwright, 2006).

2.1.2 Imaging of sills on seismic data

On seismic data sills are typically characterised by very high amplitude reflections (Smallwood and Maresh, 2002; Thomson and Hutton, 2004), as sills have higher density and seismic velocities compared to surrounding sediments (Smallwood and Maresh, 2002), this leads to large acoustic impedance contrasts, resulting in strong reflection coefficient being developed at contacts between host rock and sill. The main implication of this, aside from producing bright reflectors, is that the transmitted seismic energy through the sills is somewhat reduced leading to poor imaging beneath the sills (Smallwood and Maresh, 2002).

Imaging of sills and the sub-volcanic system within seismic data can be further inhibited by overlying lava sequences. The problem of imaging beneath basalts is well known in both industry and academia (Silva and Corcoran, 2002; Roberts, 2005: Rohrman, 2007) and arises from the attenuation of the seismic signal through the basalt sequence caused by high impedance contrast and high frequency noise, caused by scattering of the seismic wave in the top few metres of a basalt sequence (Gallagher and Dromgoole, 2007). This coupled with poorly constrained velocities of basalt and sub-basalt sequences used in stacking and migration algorithms further compounds the sub-basalt imaging problem (Gallagher and Dromgoole, 2007). Despite this, the high acoustic impedance contrasts developed by sills within 3D seismic data may be exploited by employing processes such as opacity rendering (Thomson and Hutton, 2004; Thomson, 2004, Thomson, 2007; Thomson and Schofield, 2008).

2.1.3 Opacity rendering

In most seismic studies of sill complexes, investigations of 3D morphology of the sill complex have been conducted using traditional seismic picking techniques (Davies et al., 2002; Hansen et al., 2004; Hansen et al., 2006; Hansen and Cartwright, 2006). The main disadvantage of this technique holds is that the seismic data is treated in a passive sense, in so much that the 3D images produced e.g. time maps of sills, are a function of host user's interpretation.

As sills typically form the highest amplitude events in a given seismic volume, the display of the seismic volume can be manipulated to leave only the high amplitude events, making the generally lower amplitude sediments transparent (*see* Smallwood and Maresh, 2002; Thomson and Hutton, 2004; Thomson and Schofield, 2008). This is termed opacity rendering and has the advantage that a seismic volume can be examined without any prior need of interpretation of data, which is both quick and prevents interpretational bias by the user. In addition to this, as the 3D seismic cube viewed is a function of amplitude, relative lateral changes in thicknesses can be assessed across a sill (Fig. 2.2) (*see* Thomson, 2004).

Figure 2.2 from (Thomson, 2005) demonstrates how opacity rendering works. Figure 2.2a and Figure 2.2b show the seismic response for basalt of varying thickness and the seismic response of sediment with varying thickness. Figure 2.2c shows the amplitude/thickness plot based on Fig a) and Fig b). In both cases the peak amplitude in both the basalt and sediments corresponds to the seismic tuning thickness, i.e. that when the seismic response of the top and bottom contact of the sill constructively interfere to give a single high amplitude event. As seen in Fig. 2.2c the peak amplitude of sediment (0.15) equals that of 7m of basalt, so by removing amplitudes of 0.15 and below, the host rock will become transparent, but basalt with a thickness greater then 7m will remain (Thomson and Hutton, 2004). In addition thickness variation of between 7-20 m can be assessed, in this respect although an opacity rendered sill will not be representative of absolute thickness variations, it will still be representative of relative thickness variations, allowing potentially thicker and thinner areas of the sill to be identified.

The major pitfall of opacity rendering is that although it has the ability to display relative thickness changes in a sill, this is based on the assumption that amplitude is only controlled by the sill thickness. In reality however, other effects, such as roughness, porosity and alteration of host rock will effect the amplitude response from the sill/host rock contact.

Despite the pitfalls and the fact that opacity rendering does render the thinnest part of a sill transparent, e.g. at the sill tips, the overall access to large-scale geometry and relative

thickness changes make it a very powerful tool in the interpretation of volcanic sequences within seismic data (*see* Thomson, 2004; Thomson and Hutton, 2004; Thomson and Schofield, 2008).

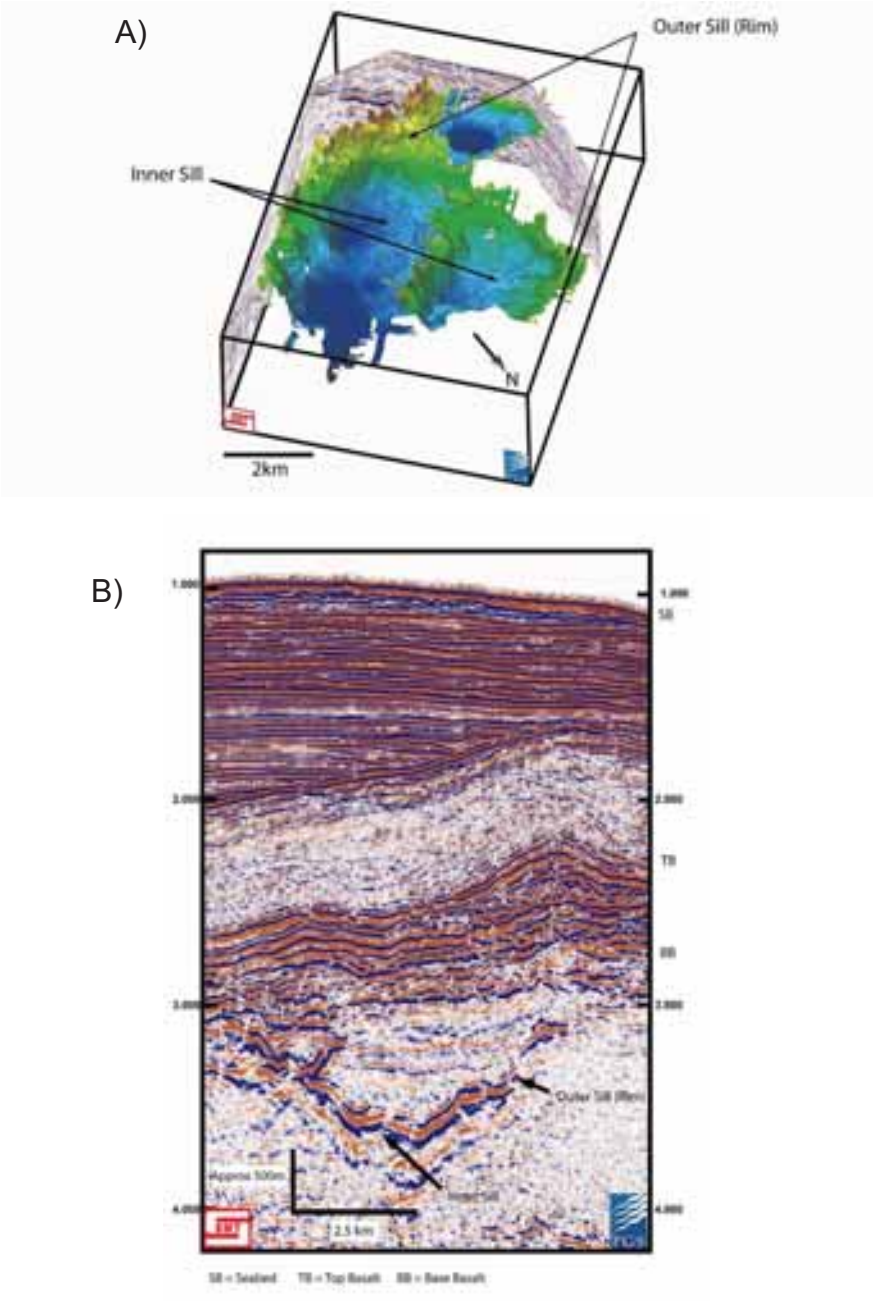

Fig. 2.1 – Typical form of sills as imaged within 3D seismic surveys (NE Rockall Trough). The sills are generally characterised by a saucer-shaped morphology, with approximately concordant inner sill, surrounded by a transgressive inclined sheet, which sometimes flattens to form a ragged outer rim (as seen in the top figure). A) Shows horizon pick of top sill reflector B) 2D seismic line showing cross-sectional view from a saucer-shaped sill. Note the high amplitude nature of the sill. SB = Sea Bed, TB = Top Basalt, BB = Base Basalt

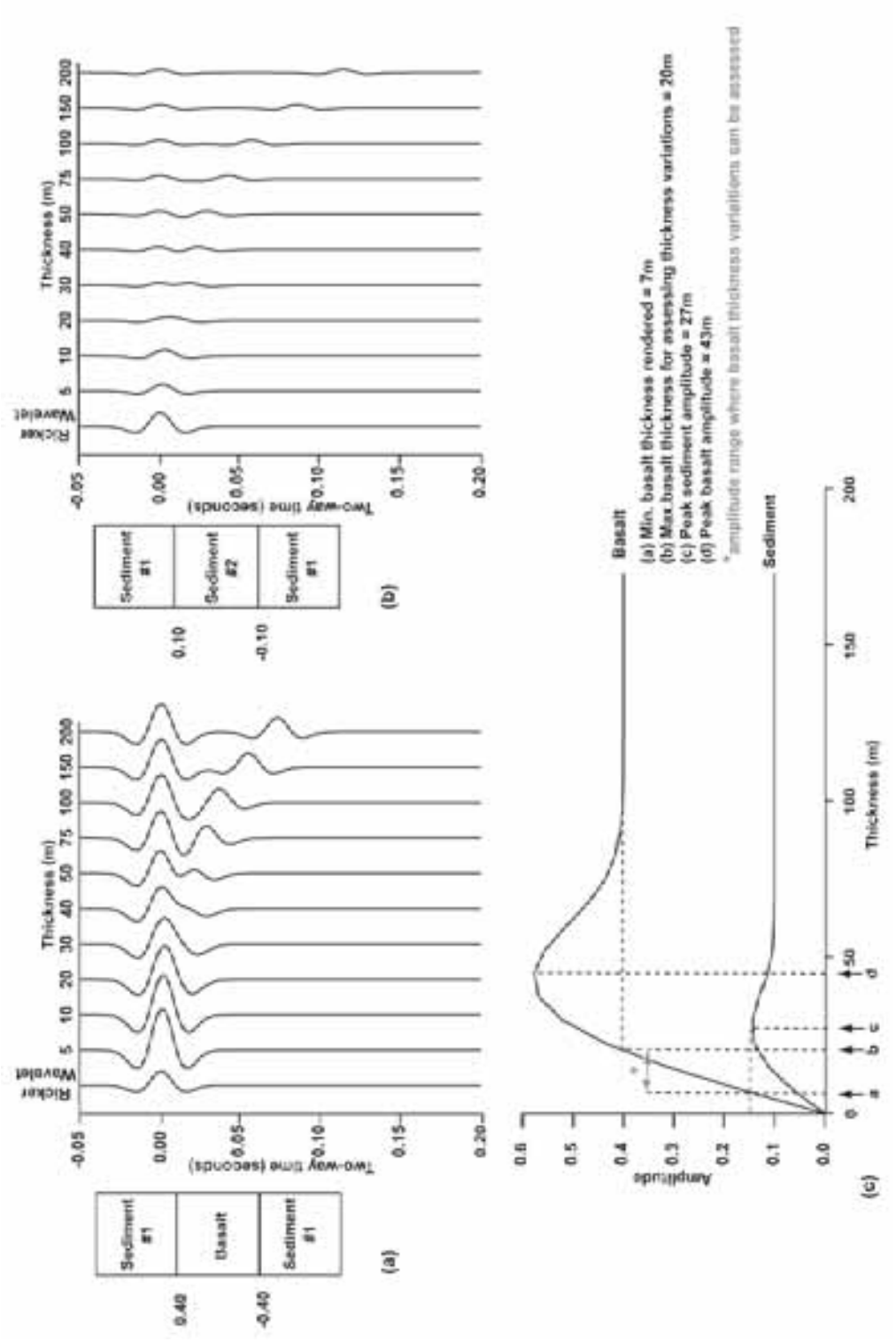

Fig. 2.2 – From Thomson (2005) showing seismic response for basalt and sediments (see text for details).

2.1.4 Sill feeding regimes

The movement of magma through the upper crust has long been an area of debate (Lister and Kerr, 1991; Rubin, 1995; Cartwright and Hansen, 2006). Much of the physical view of sub-volcanic systems has been determined by field studies (Du toit, 1920; Anderson, 1951) and geochemical analysis (Klausen and Larsen, 2002). From this, the movement of magma in the upper brittle crust has been thought to be mainly the result of vertical and horizontal movement of magma within dykes (j; Cartwright and Hansen, 2006). The main inference of these models is that eruptive centres, fed via dykes, overlie the source region of magma below. However this is not necessarily the case as laterally extensive sills are capable of feeding one another without the need for intervening dykes (Cartwright and Hansen, 2006)

Figure 2.3 (modified from Thomson and Schofield, 2008) shows opacity rendered sills from the NE Rockall trough , sill A, an elliptical saucer shaped sill 3 × 5 km in diameter, can be seen being fed from sill B, sitting stratigraphically below. Such a relationship is confirmed by the branching relationships of sill A, which branch away from the feeder extending upwards from sill B.

Figure 2.4 shows an opacity rendered sill from the Flett basin, illustrating the feeding of a sill at higher stratigraphic level by the sill below. Of note are the finger-like forms within the sill, which are representative of areas of the sill with relative changes in thickness.

The feeding of laterally continuous sills by other sills has major implications for the understanding of the sub-volcanic system. Firstly models suggesting that neutral buoyancy in the upper crust controls sill emplacement (e.g. Francis, 1982; Goulty, 2005) are brought into question (see section 1.1), as sills feeding other sills on multiple levels cannot be reconciled with this model (Thomson and Hutton, 2004; Thomson, 2007). Secondly the view that the sub-volcanic systems are dominated by dykes may be incorrect as the potential exists for magma to be moved from mid-crustal to shallow crustal level without the need for intervening sets of dykes (*see* Cartwright and Hansen, 2006).

2.1.5 Exploitation of pre-existing structure

Pre-existing basin structure and lithology exert a major influence on magma flow pathways through a basin by offering paths of least resistance to intruding magma (Valentine and Krogh, 2006; Gaffney et al., 2007). Commonly sills can be seen to deflect and climb faults planes to higher levels (Francis, 1982; Thomson, 2007; Thomson and Schofield, 2008).

This is highlighted in Figure 2.5 which shows a seismic line through the Judd Basin, NW European Atlantic Margin. Within the line, the sills are easily identifiable in the bottom half of the section as bright reflectors, which periodically transgress stratigraphy.

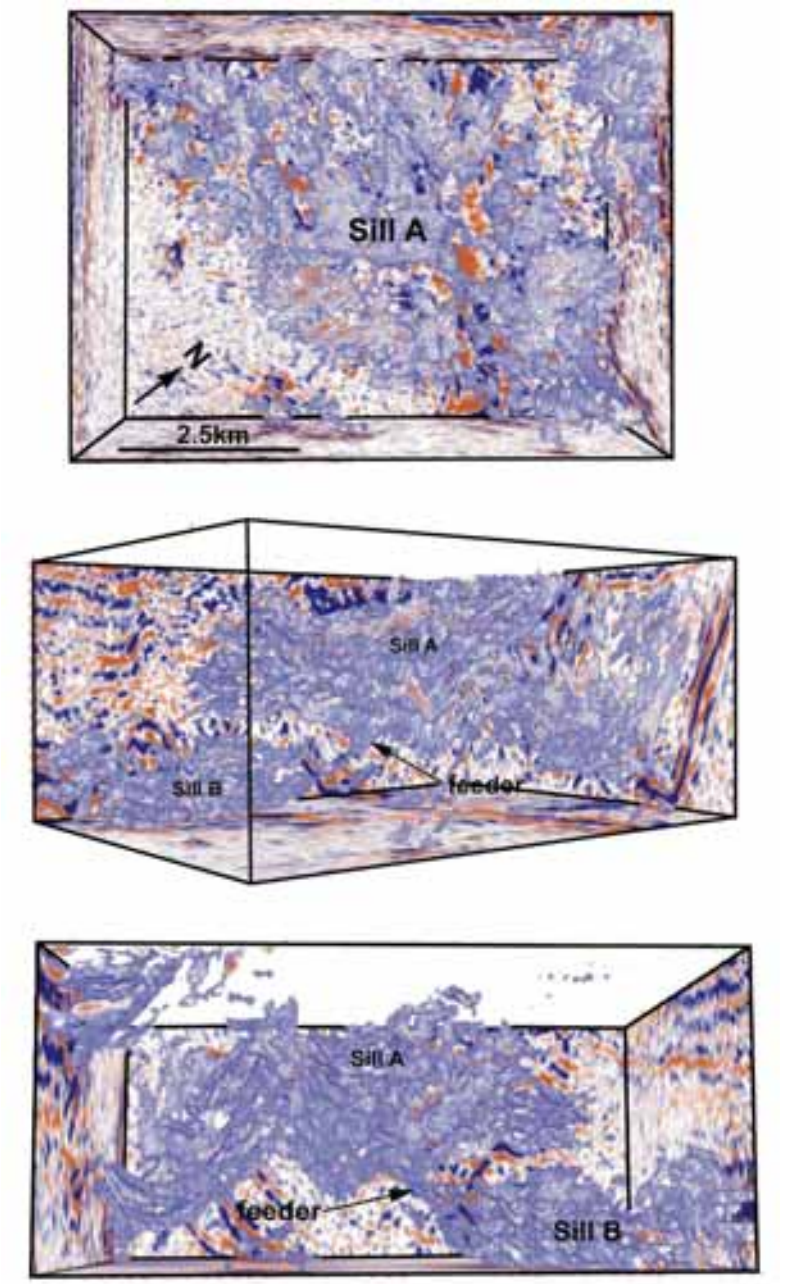

Fig. 2.3 – *Modified* from Thomson and Schofield (2008), showing opacity rendered sills from the NE Rockall trough. The outer rim of a sill (Sill B) can be seen to be feeding a stratigraphically higher sill (Sill A).

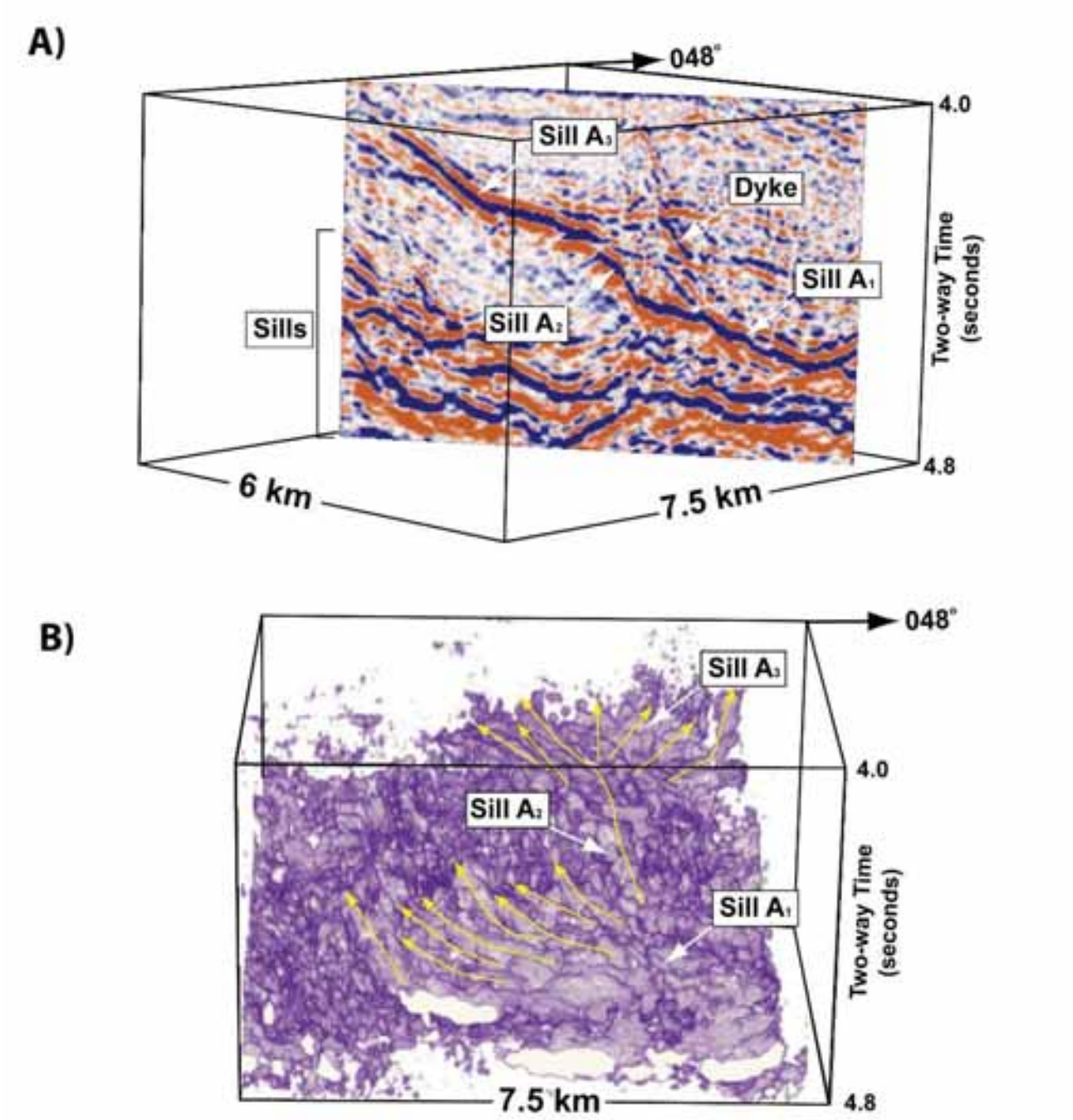

Fig. 2.4 – Modified from Thomson and Schofield (2008), showing an opacity rendered cube from the Flett Basin, UKCS. Sill (A1) can be seen feeding a stratigraphically higher sill (A3) through a 'finger-like' feeder (A2). Other finger-like forms can be seen, emanating away from the central saucer. These rendered features are effectively highlighting areas in which the sill is physically thinner and thicker.

Interestingly the sills can be seen to be exploiting fault planes of a series of tilted fault blocks. The sills are concentrated around the base of the post-rift sequence where they have exploited the synrift faults. Although several of the later generation post-rift faults appear to have been exploited by the sills, other post-rift faults cut the sills, suggesting that some faulting occurred contemporaneously with intrusion of the magma.

Thomson and Schofield (2008) made some key observations regarding the sills and influence of pre-existing basin structure;

- Saucer-Shaped morphology is still common despite pre-existing structure
- The presence of faults modifies this geometry
- Despite the inclined dip of the beds within the fault blocks, the sills do not exploit this and tend to independently cut stratigraphy climbing to higher stratigraphic levels.

These points are highlighted in Figure 2.6, in which the sills can be seen to possess a transgressive nature within the fault blocks. However on contact with faults the magma has exploited the fault, possibly acting as feeders to the overlying lavas (Thomson and Schofield, 2008).

2.2 Models of sill emplacement (Post 3D seismic)

The new information provided by 3D seismic data has led to a series of new models of sill emplacement (Fig. 2.7)

2.2.1 Thomson and Hutton (2004) and Bunger (1981)

Thomson and Hutton (2004) proposed a model of sill emplacement based on the laccolith emplacement model of Pollard and Johnson (1973) (Fig. 2.7a). Using opacity rendering to display relative thickness changes across saucer-shaped sills in the NE Rockall Trough, Thomson and Hutton (2004) defined lobe like features in the sills. By examining the branching patterns within these lobes, Thomson and Hutton (2004) were able to infer paleo-flow direction of the intruding magma.

Based on mapped out flow directions using these features they placed the feeder within the centre, or central axis of the saucer. Thomson and Hutton (2004) proposed that the saucer-shaped geometry was the result of inflation of the inner sill causing uplift in the roof rocks allowing peripheral fracturing and intrusion of dykes to occur. This in turn enabled the

magma to flow upwards and outwards away from the inner sill. Although the modified laccolith model of Johnson and Pollard (1973) fits reasonably well with observations of upward magma flow, it does not account for the formation of flat outer rims, as seen in some saucer-shaped sills. In addition, field examples of saucer-shaped sills show no apparent evidence of having dykes cutting up through strata above the inner-dish, as predicted by the model (*see* Chevalier and Woodford, 1999; Chapter 5).

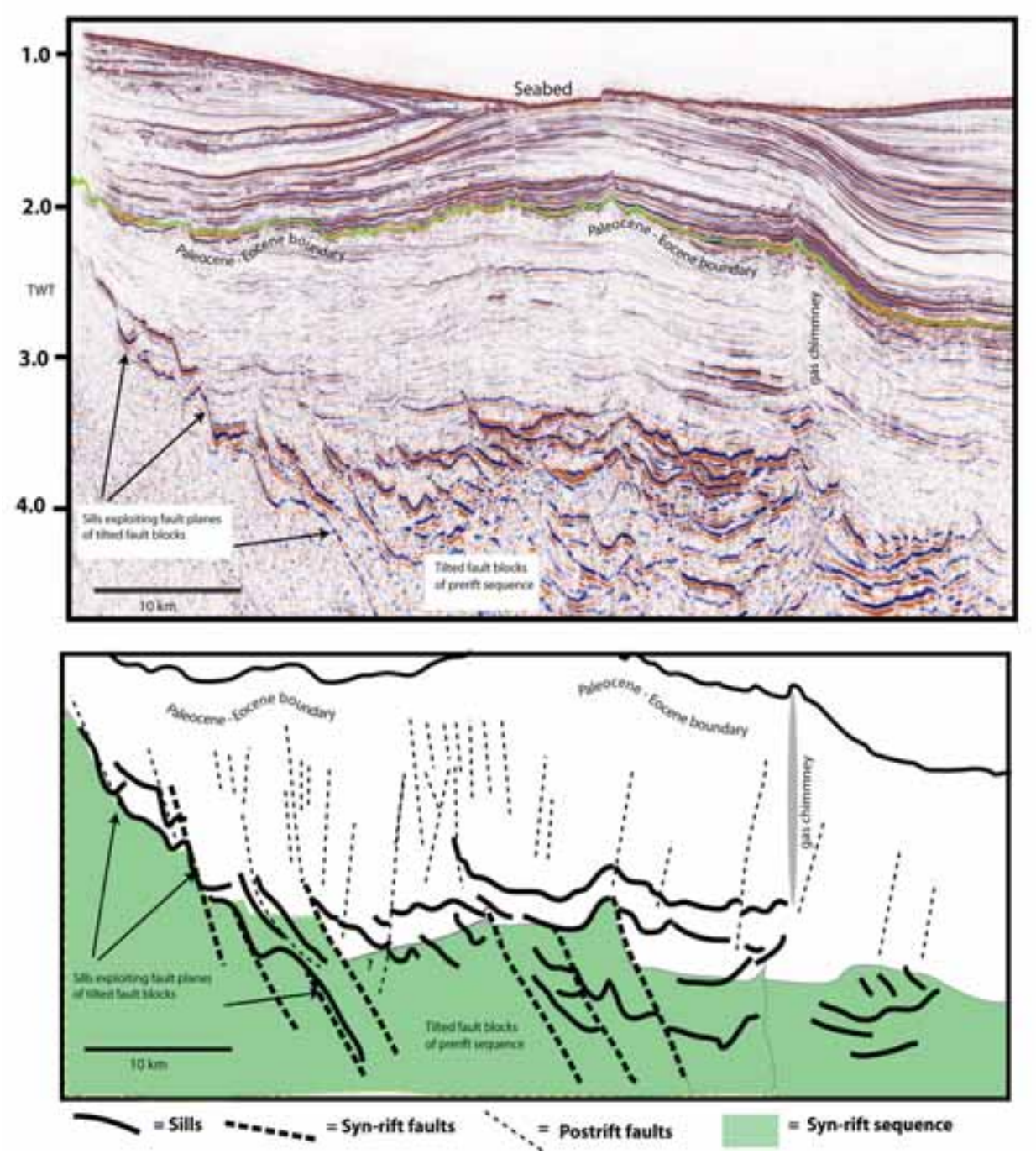

Fig. 2.5 – 2D seismic line from the Judd Basin, Faroe-Shetland Basin, NE Atlantic, showing sills exploiting fault planes to climb to higher stratigraphic levels. Note the high amplitude reflections of the sills.

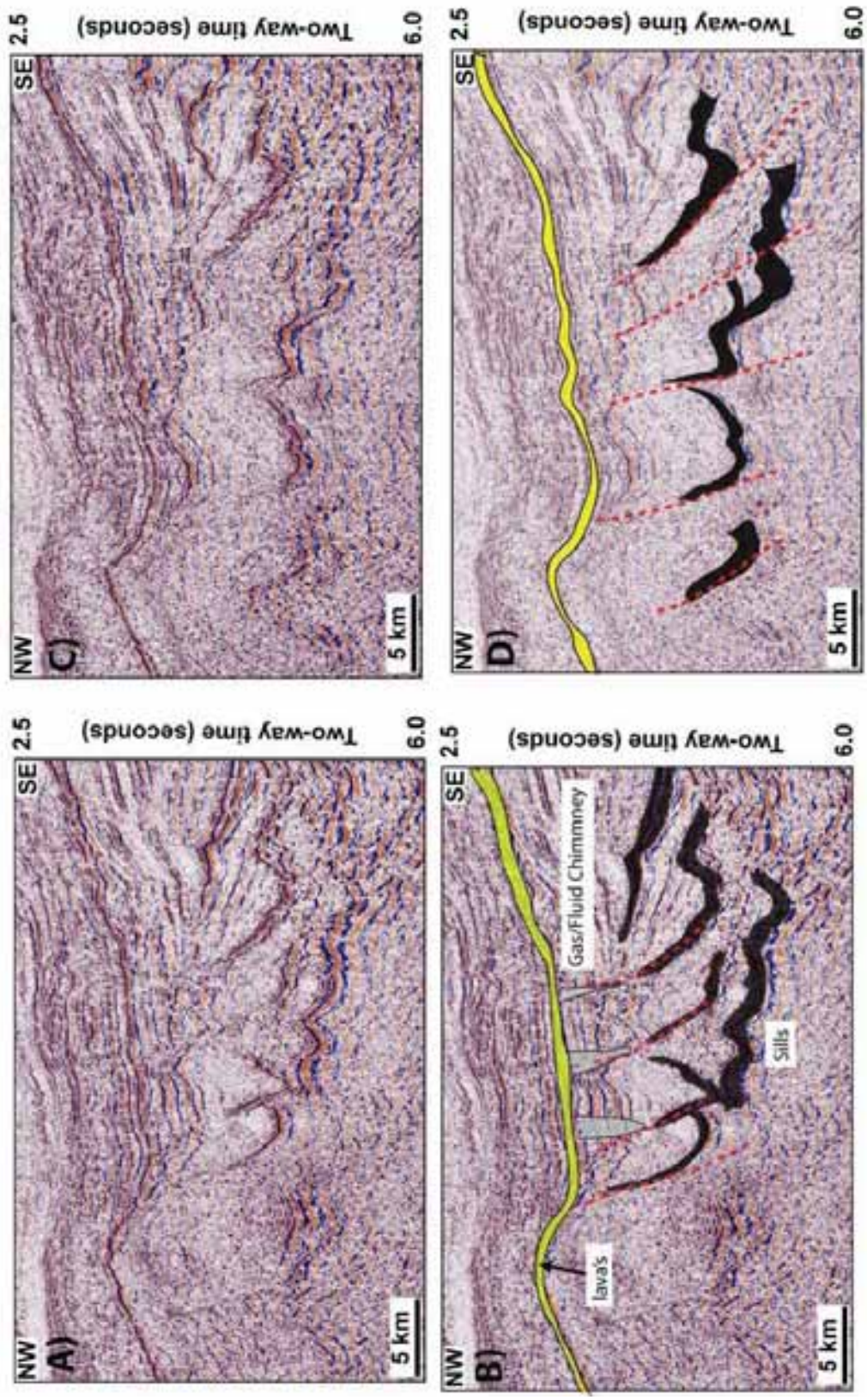

Fig. 2.6 – Modified from Thomson and Schofield (2008) showing sills exploiting faults in a series of normal fault blocks dipping in a SE direction. Although the faults have been exploited by the intruding magma, within the fault blocks the saucer-geometry is modified but still

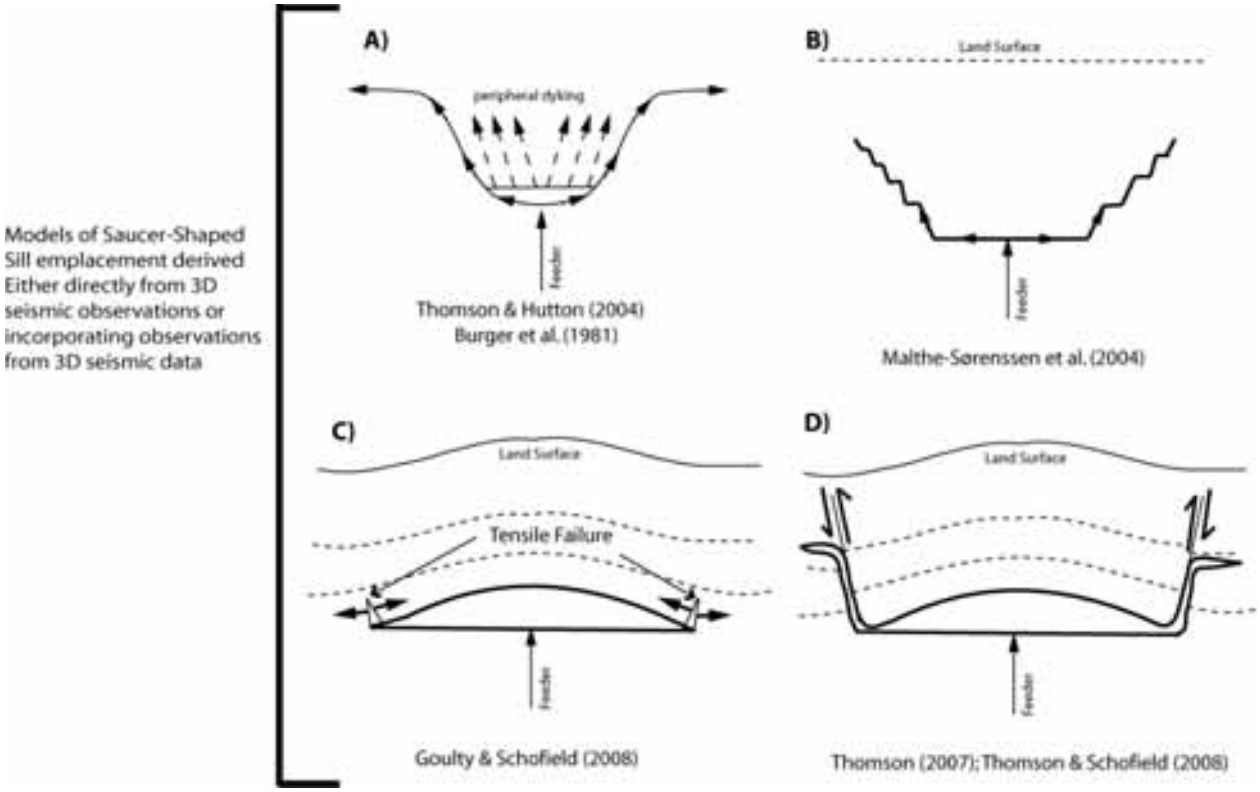

Fig. 2.7 – Sill emplacement models mostly derived from seismic data (with exception of Burger et al. (1981)). Note how the feeder is now placed beneath the centre of the base of the saucer, and not off to one side (see text for details).

2.2.2 Malthe-Sørenssen et al. (2004)

Malthe-Sørenssen et al. (2004) proposed a model of saucer-shaped sill intrusion based on 2D discrete element modelling (Fig. 2.7b). Within the model the sill began to propagate upwards at the point that the length of the sill equalled that of the overburden thickness due to re-orientation of the stress field at sill tips, as a result of inner sill inflation. The re-orientation of the stress field at the sill tip led to brittle fractures being opened at an angle of approximately 45° to the horizontal, thus enabling the sill to climb upwards. The model was based on a non-viscous fluid, representing the magma, injecting into a homogenous elastic medium, representing the host rocks of a sedimentary basin.

Within the Karoo basin, a general increase in inner sill diameter to the stratigraphically lower west region of the basin does occur (Chevalier and Woodford, 1999). This aspect is in agreement with the model of Malthe-Sørenssen et al. (2004) in that the inner sill needs to gain suitable diameter to allow rotation of the stress field at the tip of the sill. With increasing depth, the inner sill has to gain greater radius before the stress tips can re-orientate.

The model of Malthe-Sørenssen et al. (2004) predicts a step-stair nature to the inclined transgressive sheet of saucer-shaped sills (Fig 2.7b). This geometry is not ubiquitous across all saucer-shaped sills (*see* Thomson and Hutton, 2004; Hansen and Cartwright, 2006: Thomson, 2007; Thomson and Schofield, 2008; Smallwood, *in press*). Instead, in seismic and field observations (chapter 5), the sills generally have a transgressive arcuate rim characterised by a curved sheet with generally increasing dip.

2.2.3 Goulty and Schofield (2008)

Goulty and Schofield (2008) employed elastic plate theory to explain the formation of saucer-shaped sills (Fig. 2.7c) in a similar manner to Johnson and Pollard (1973) who applied the same approach to laccoliths. In this respect Goulty and Schofield (2008) derived a relationship to predict the maximum radius of the inner sill based on the excess magma pressure and emplacement depth.

$$R = 2h\sqrt{\frac{E\varepsilon_f}{3(1-\nu^2)\,\Delta p}}$$

R = Radius of Sill, h = Depth of emplacement, E = Young's modulus, ε_f = Radial tensile strain at failure, v = Poisson's Ration, p = magma pressure

In essence the relationship predicts that high tensile strains will develop at the sill periphery, and these will increase with increasing sill radius, so as the sill radius increases, eventually a point will be reached at the periphery were the tensile strain cannot be accommodated by the overburden, leading to failure. As a result increasing inner sill diameter will be expected with increasing sill depth, something which is seen in the Karoo basin (Chevalier and Woodford, 1999)

Although the model of Goulty and Schofield (2008) does agree with observation of an increase in inner sill diameter with depth, the model has limitations. Goulty and Schofield (2008) point out that the model is simplistic and only predicts up to the point of failure of the overburden, it makes no predictions in regard to the formation of the arcuate inclined sheet. In addition the fracture developed would initially be vertical, something which has not been documented in field or seismic data around the inner sill of saucer-shaped sills (*see* Thomson and Hutton, 2004; Hansen and Cartwright, 2006).

2.2.4 Thomson (2007) and Thomson and Schofield (2008)

Thomson (2007) and Thomson and Schofield (2008) extended the saucer-shaped sill emplacement model of Thomson and Hutton (2004) model giving a four stage saucer-shaped sill emplacement model (Fig. 2.8), which accounted for the occurrence of the flat outer rim in some saucer shaped sills. The four stages of sill emplacement summarised by Thomson (2007) and Thomson and Schofield (2008) are;

- Stage 1 – Sill initiation (Fig. 2.8a-c)
- Stage 2 – Sill lateral growth (forced folding, Fig. 2.8 b-d; roof faulting, Fig. 2.8b, c and j)
- Stage 3 – Sill Climbing (forced folding, Fig. 2.8 e-g; roof faulting, Fig. 2.8 k-m)
- Stage 4 – Sill Flattening (forced folding, Fig. 2.9 h and i; roof faulting, Fig. 2.9 n and o)

Sill initiation (Stage 1) ***after Thomson (2007) and Thomson and Schofield (2008)*** **-** On intrusion of magma in a dyke or sub-vertical feeder, for example, the edge of a saucer, sill initiation occurs when the intruding magma comes in contact with a suitable horizon e.g. an over-pressured shale horizon. In such a circumstance, the heating effect on confined pore-fluids within shale aids fracturing of the rock and allows magma intrusion to be initiated. The process may be augmented by fluidization of host rock (*see* Kokelaar, 1982; chapter 6 and 7).

Although Thomson (2007) and Thomson and Schofield (2008) proposed a lithological control on sill initiation, realising that in high level systems this factor cannot be ignored, other factors such as rigidity contrasts or discontinuities between rock layers could instigate lateral sill initiation. This been shown in analogue modelling (*see* Pollard, 1973; Kavanagh et al., 2008) and in dykes in Iceland, which appear to arrest at interfaces which possess large rigidity contrasts, e.g. tuff and lava (Gudmundsson, 2005).

Sill lateral growth (Stage 2) ***after Thomson (2007) and Thomson and Schofield (2008)***- After initiation, the inner sill will expand in an episodic manner, with the diameter of the inner radius being determined by the viscosity of magma and properties of country rock. This maximum radius will be governed by the ease at which the magma can propagate though host rock, governing this will be changes in host rock properties such as the ductility of host rock and/or its ability to fluidize.

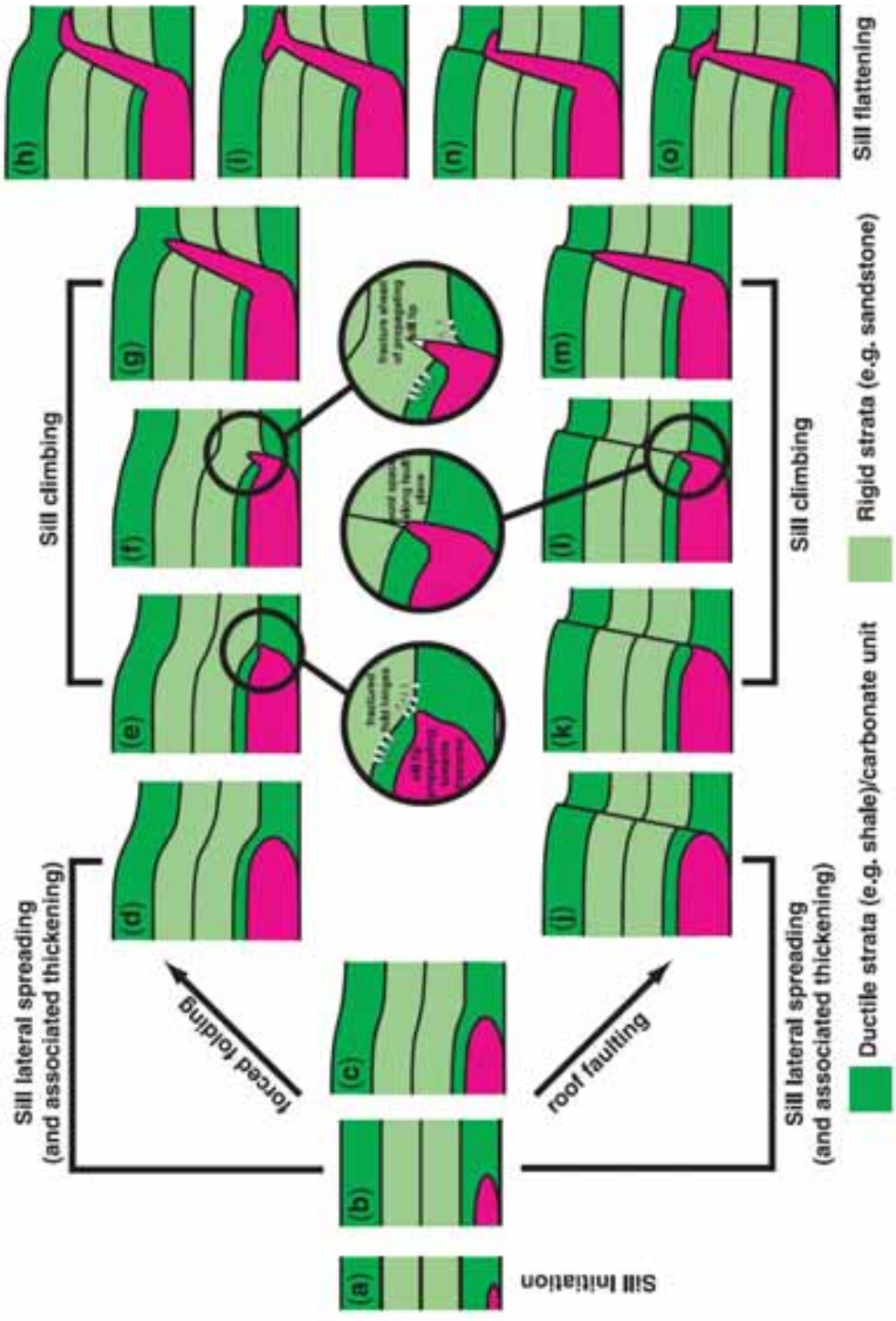

Fig. 2.8 – From Thomson (2007) and Thomson and Schofield (2008) showing model of saucer-shaped sill emplacement occurring in a series of steps, from sill initiation, through inflation, to failure of the overburden allowing transgression of the sill to higher levels (see text for details).

Sill climbing (Stage 3) ***after Thomson (2007) and Thomson and Schofield (2008)*** **–** During sill lateral growth, the inner sill will also inflate. This will result in forced folding at shallow emplacement levels (Trude, 2003; Hansen and Cartwright, 2006b) and fracturing of the overburden at deeper depths due to diminished flexural slip folding of beds with depth. At shallow emplacement depths fractures will develop in the fold hinge and dip towards the inner sill as the sill inflates. In deeper domains, reverse faults will dominate, again dipping towards the inner sill. In both of these circumstances, magma will be directed upwards along the plane of weakness, created by fracturing or faulting. The development of fractures in the roof rock, either as the result of force folding or faulting, is likely to occur in a stepwise, non-uniform fashion, leading to magma being tapped in a series of discrete events. This may lead to a series of flow pathways extending away from the inner sill, with some areas of the inner sill not forming an arcuate inclined sheet.

Sill flattening (Stage 4) ***after Thomson (2007) and Thomson and Schofield (2008)*** – Stage four essentially represents a re-introduction of stage 1 processes, in which the magma in the climbing inclined sheet encounters a suitable horizon into which it intrudes horizontally, forming a flat outer rim, or beginning of another saucer-shaped sill.

2.3 Summary of observations of sills from field and seismic data

- Sills tend to form saucer-shaped bodies (Francis, 1982; Thomson and Hutton, 2004).
- The morphology of saucer-shaped sills generally consists of an inner-sill and arcuate inclined sheet (Thomson and Hutton, 2004; Hansen and Cartwright, 2006). In some circumstances the arcuate inclined sheet can flatten to form a concordant ragged outer rim (Thomson and Hutton, 2004).
- The thickest portion of the sill generally corresponds to the inner sill (Francis, 1982; Smallwood *in press*).
- Saucer-shaped sills are generally fed from either a point, or line source, originating from the inner sill of the sill. When fed from a point source, the saucer tends to take a circular form (Thomson and Hutton, 2004), if the saucer is fed from a line source, the sill tends to take on an elliptical form (Goulty and Schofield, 2008).
- Large-scale features within sills related to flow, in the form of branching lobate features, analogous to lava flows but less dendritic, show the magma flow is generally

up and away from the inner sill (Thomson and Hutton, 2004; Hansen and Cartwright, 2006).

- Sills can feed other sills, without the need for intervening dykes (Thomson and Hutton, 2004; Cartwright and Hansen, 2006).

2.4 Discussion

Over the last 44 years various models of saucer-shaped sill emplacement have been proposed. Before the use of offshore 3D seismic data in the study of submerged and un-eroded sills and sill complexes, the majority of models of saucer-shaped sill emplacement placed the feeder for the saucer located away from the central axis of the saucer with magma flow directed down into its base (*see* Bradley, 1965; Francis, 1982; Chevalier and Woodford, 1999). With the use of 3D seismic data, the most significant in emplacement models for saucer-shaped sills is that the feeder for the sill has now been placed below the central portion of the sill. In addition, magma flow is directed up and away from the inner sill and no element of downwards magma flow has been inferred (*see* Thomson and Hutton, 2004; Malthe-Sørenssen et al., 2004; Thomson., 2007; Goulty and Schofield, 2008; Thomson and Schofield, 2008).

Work on 3D seismic data also showed that sills display a wide variety of structures and morphologies (see chapter 2), and also shows that sills can feed sills without the need for intervening dykes, potentially feeding magma around the system over large lateral distances (Cartwright and Hansen, 2006).

Chapter 3
Introduction to common structures seen within sills – Seismic and field based examples

Recently the increased use of 3D seismic data in the study of sill complexes has yielded a great deal of information regarding common structural elements seen within sills, however this has also led to some confusion within the literature regarding categorization of structures documented in sills within 3D seismic data and field data (Thomson and Hutton, 2004; Trude, 2004; Hansen and Cartwright, 2006). Therefore the following chapter attempts to clarify the common structures seen within sills and the relation, where possible, to structures seen within 3D seismic data.

3.1 Sill structure – Introduction

In considering common structural elements seen within sills, both in the field and in seismic data, it is important to classify features genetically rather than purely based on morphology as is common (Rickwood, 1990; Thomson & Hutton, 2004; Hansen & Cartwright, 2006).

Within this chapter, common structures within sills will be split into two categories. The first is structures which have their origin linked to brittle processes, the second are structures which have their origin linked to non-brittle processes. This process driven distinction has not been previously made within sill emplacement literature, but in the concluding chapters of this thesis it will become apparent that it is important to look at sill structures in this context and not purely based on morphology alone.

3.2 Structures related to brittle processes

3.2.1 Steps

Much of the current published literature dealing with structures within igneous sheet intrusions is focused on structures within dykes (e.g. Rickwood, 1990), however many structures seen with dykes also occur in sills. Steps are commonly seen features within dykes (Pollard et al. 1975; Rickwood, 1990) and result from a propagating sheet of magma segmenting along the direction of flow to occupy discrete planes. In sills, the same process operating results in a stepped appearance in cross section, with a series of sills interconnected by a vertical step of igneous rock (Fig. 3.1). The offset between horizontal sill segments

changes along the direction of flow, increasing in the flow direction, and decreasing in the up flow direction until absent (Rickwood, 1990).

Within seismic data, step-like features are commonly displayed on the outer rim of sills, which often leads to a ragged appearance to the outer edge of saucer shaped sills (Fig. 3.2) (Thomson and Hutton, 2004).

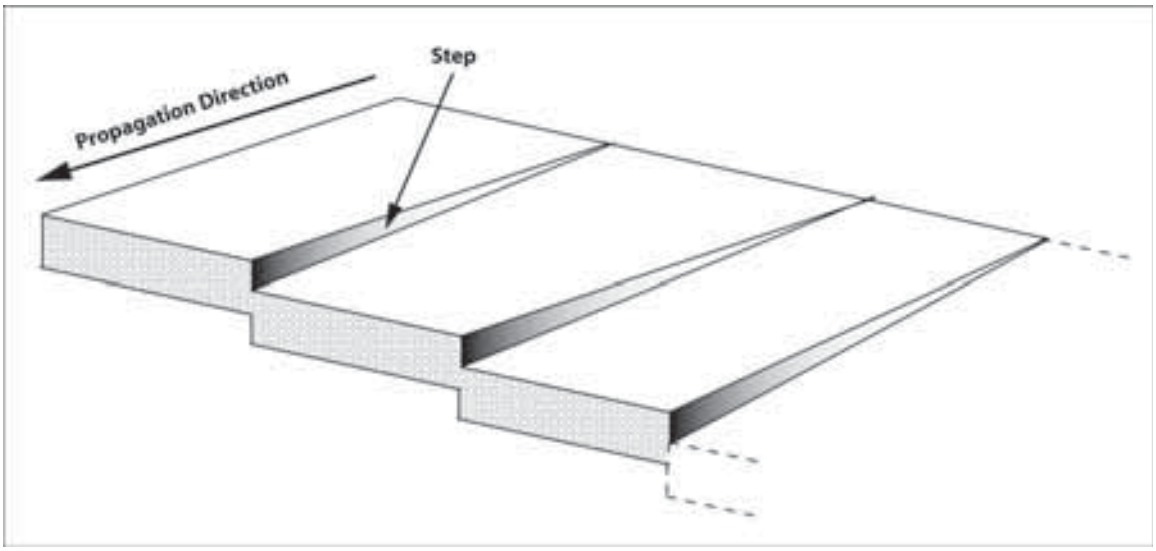

Fig. 3.1 – Re-drawn and modified from Rickwood (1990) illustrating the development of steps within a sill. Note the increase in offset between sill segments in a down flow direction.

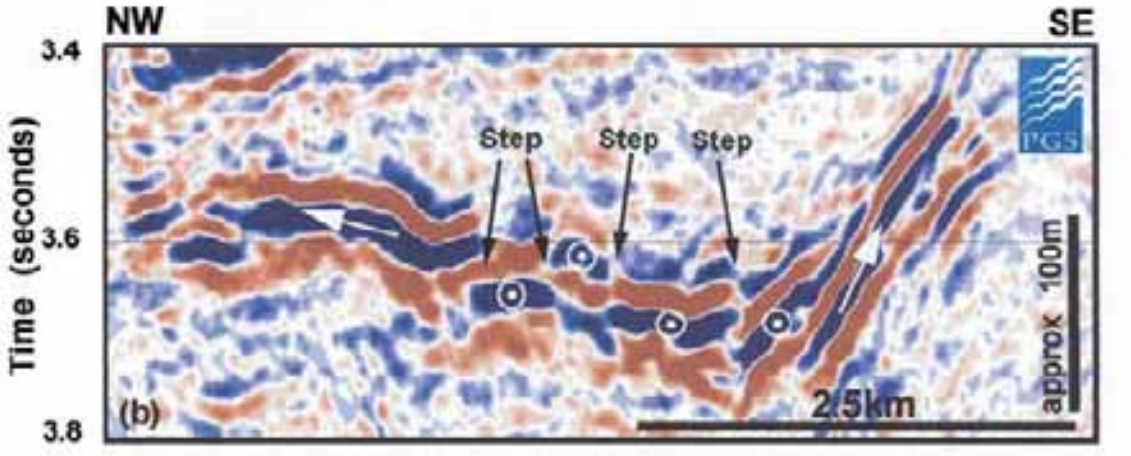

Fig. 3.2 – From Thomson and Hutton (2004) showing a 2D seismic line across a 'ragged' saucer shaped sill periphery with what are interpreted to be steps within the sill.

The reason for the abundance of these features on the often flat outer rim of saucer-shaped sills is not entirely clear. Goulty and Schofield (2008) link the occurrence of the flat outer rim in saucer-shaped sills to a drop in excess magma pressure, reducing flexural strain, causing magma to preferentially intrude along bedding planes of low tensile strength. It may be the

case that in such a situation steps are created at the outer rim of the sill due to the inability of magma to propagate through host rock as a result of reduced driving pressure, in this circumstance the sill may seek out and exploit preferential horizons for intrusion. Therefore, the occurrence of steps may be expected to occur with increasing frequency in a direction away from the magma source where for the sill to continue to propagate as magma supply wanes it must exploit preferential horizons.

Baer (1995) states that magma propagation under a brittle regime has three main processes: 1) propagation of the fracture ahead of the leading edge of magma 2) propagation of tip fluids and 3) magma flow within the body, with the overall final geometry of the body including segments and steps recording the propagation history of the initial fracture. An alternative method of formation of steps may therefore be related to the morphology of the fracture ahead of the sill tip. Step structures show a similarity in their form to hackle marks created on joint planes, which are thought to result from rapid propagation of a fracture through host rock under high stress intensity at a critical velocity (Hatcher, 1996; Frid et al., 2005) (Fig. 3.3). Therefore the formation of a stepped sheet may be the result of rapid crack propagation ahead of the intruding sill at a given point, causing a stepped facture, which is then infilled with magma invading into the crack.

This possible relationship has not been noticed before within the literature. In studies of the Wahatoya dyke, Spanish Peaks, Colorado, USA, Pollard et al. (1975) noted the stepped nature of a the dyke at outcrop (Fig. 3.4a and 3.4b) and re-constructed a schematic of the entire dyke showing offsets, which shows similarities to a plumose joint face containing stepped offsets (Fig. 3.4c).

Pollard et al. (1975) did not attribute the formation of the offsets as a result of fracture propagation but instead attributed their occurrence to the growth and coalescence of separate magma fingers (see section 3.3.2), in which host rock heterogeneities and/or changes in principal stresses caused separate fingers to propagate on different planes from one another, forming a stepped like nature to the dyke.

However, it is unclear if the formation of stepped sills is analogous to hackle formation on a propagating fracture. The generation of hackles as a result of rapid propagation ahead of a sill tip requires high stress intensities which seemingly contradict Goulty and Schofield (2008) who interpret the stepped outer rim of sills as a product of waning magma supply and lower pressure.

However the formation of a stepped fracture may explain some of the common features seen within stepped sills. In a stepped fracture, initially the offset in the fracture

surface across the hackle is small, but with increased distance from the origin of the fracture, the offset increases (Fig. 3.5a). If the same process operates ahead of the sill, initially it will be relatively easy for magma to occupy the step created by the hackle, but along the fracture, the offset will become greater, possibly reducing the ability of magma to occupy the hackle. In addition as magma propagates along the stepped fracture, mode 1 tensile fracture will operate ahead of the horizontal sill segments (Fig. 3.5a), however the step (hackle) between the two sill segments will undergo mode 2 fracture. The infilling of the fracture forming the step (hackle) with magma could therefore be inhibited compared to magma infilling the mode 1 fracture, which opens in the direction of magma flow ahead of the sill tip. This may explain why stepped sills sometimes show a vertical dyke-like step of magma connecting between separate sills segments, but in other cases do not, with only unconnected offset sill segments being visible (*see* Rickwood, 1990) (Fig. 3.5).

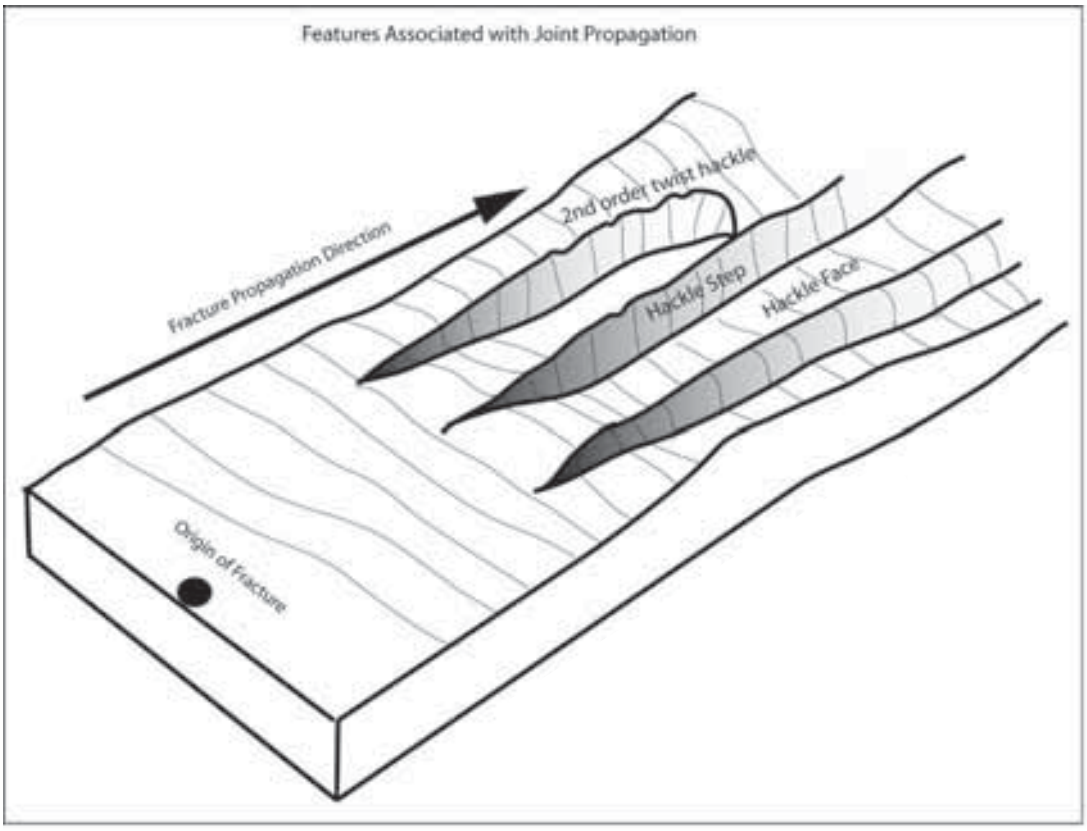

Fig. 3.3 – Re-drawn sketch of a joint plane showing development of hackle steps on joint surface. From Kulander et al. (1979), re-drawn from Hatcher (1996).

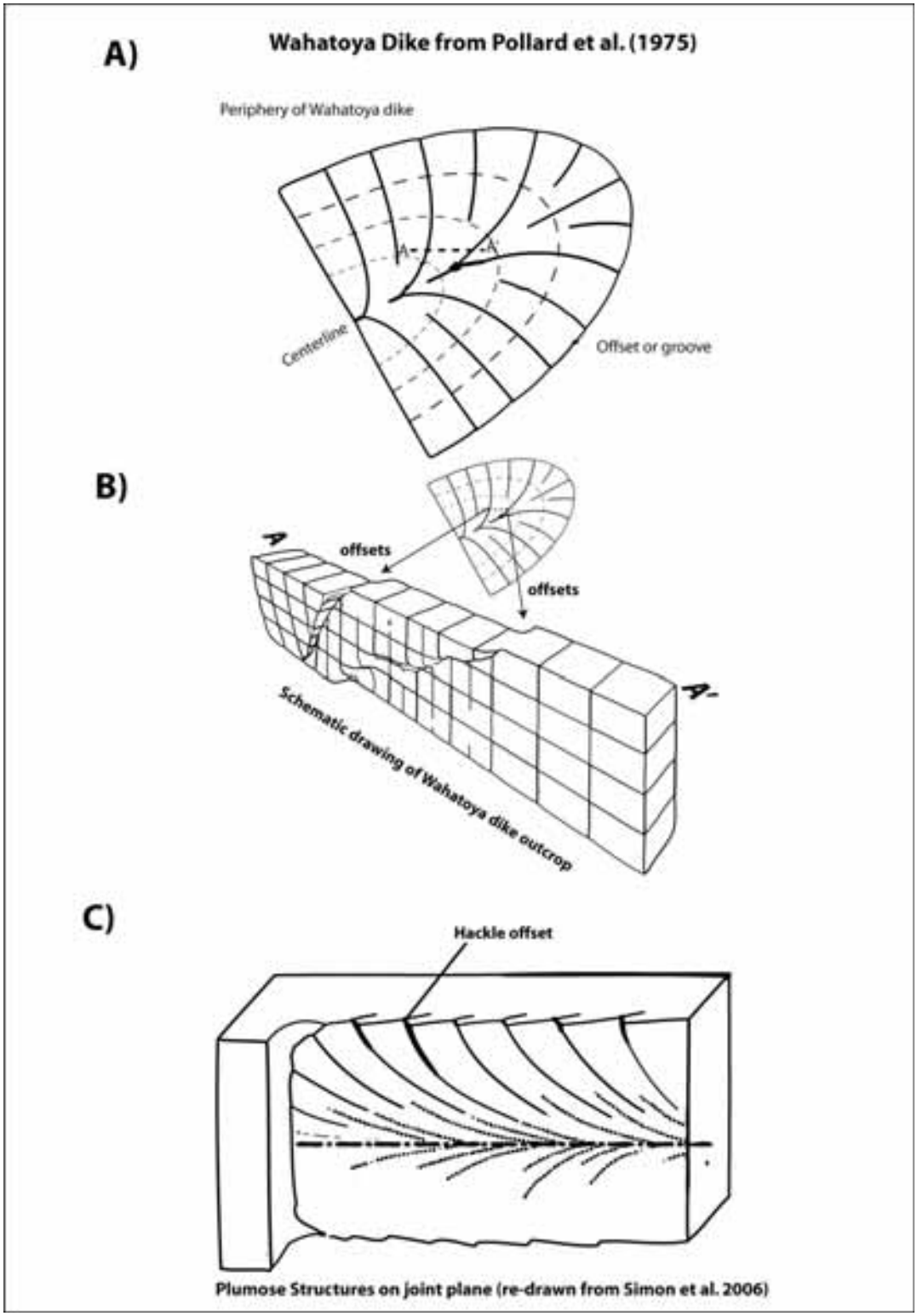

Fig. 3.4 – A) Overall structure of Wahatoya dyke (re-drawn from Pollard et al., 1975), showing occurrence of radial offsets emanating from a central axis B) Diagram of outcrop of Wahatoya dyke, showing offsets (steps) along the strike of the dyke C) Plumose joint face (re-drawn from Simon et al., 2006)

3.2.2 Broken Bridges

Broken bridge structures are well known features of dykes and intrusive veins (Delaney and Pollard, 1981), but have been rarely documented in sills (Liss, 2004; Thomson and Hutton, 2004; Nicholson, 1985; Nicholson and Pollard, 1985; Hutton, *in press*). They form when two separate sill segments or lobes of magma propagate contemporaneously on slightly offset horizons with each other (Fig. 3.6a) (Delaney and Pollard, 1985; Hutton, *in press*). Inflation of the individual sill segments will cause a bridge of strata between the two inflating bodies of magma to bend, resulting in longitudinal extension along the convex surfaces and contraction along the concave surface of the bridge. This will result in a series of tensile fractures opening perpendicular to the bridge axis in the zones of maximum flexure (Fig. 3.6b, Fig. 3.7, Fig. 3.8) (Hutton, *in press*). If inflation of sill segments continues, the tensile stress within the bridge will become too great for host rock to accommodate, eventually causing the bridge to undergo brittle failure, forming what is termed a 'broken bridge'. The final result of this process is a continuous, but stepped sheet of volcanic rock (Fig. 3.6c).

3.2.3 Broken Bridges within seismic data

Thomson and Hutton (2004) documented the occurrence of broken and partially broken bridges within seismic data (Fig. 3.9). Using 3D seismic interpretation in conjunction with 3D volume visualisation techniques, e.g. opacity rendering (see Thomson and Hutton, 2004), allows lobes of magma that propagated separately to be identified and their interactions to be studied in detail (Fig. 3.10). However the 2D lines of Thomson and Hutton (2004) do not show the equivalent 3D opacity render of the sill form and therefore the validity of their interpretation of broken and partial bridges is difficult to asses on the 2D lines alone.

Figure 3.10 shows the occurrence of broken bridges in relation to junctures between propagating lobes in a top down view of an opacity rendered sill that has climbed an inclined fault from the Judd Basin, NW European Continental Margin. The magma is interpreted as having propagated up the fault plane, in a series of separate lobes (Fig. 3.10a and 3.10b). A series of seismic lines orientated at right-angles across a contact zone of two magma lobes records the sequential development of a broken bridge (Fig. 3.10c and d).

At the distal end of the two lobes, the two separate magma lobes appear to be separate (Fig. 3.10d-i.), however in figure 3.10d-ii overlap in the two separate magma lobes appears to have occurred, and it is likely that a bridge of host rock exists between the two lobes. Further up-flow towards the base of the sheet, within figure 3.10d-iii, the two separate lobes appear to be fully interacting with the bridge being completely broken. Figure 3.10d-iv may represent a

situation in which the bridge has broken in two places leading to the complete detachment of the host rock bridge. The morphology of the 3D fence diagram, based solely on 2D lines can be seen in Fig. 3.11. Interestingly, it appears that the orientation of the broken bridge has reversed along the direction of flow (Fig. 3.11).

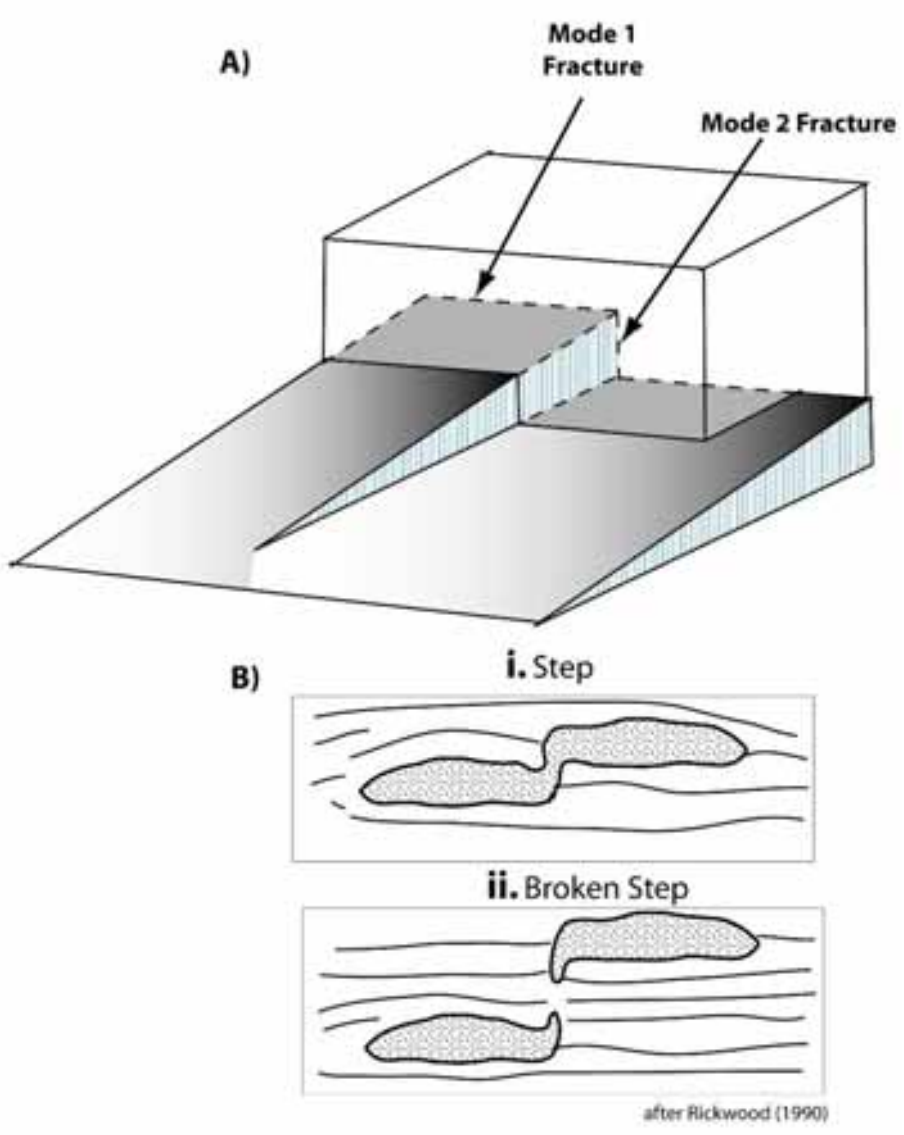

Fig. 3.5 – A) Schematic showing fracture modes associated with creation of a fracture step. On the horizontal portion of the fracture, the fracture is predominantly mode 1, opening in a tensile fashion in the direction of magma propagation. However the step interconnecting the two mode 1 fractures will be predominantly mode 2. Magma infilling into the fracture may find it easier to invade along the mode 1 fracture, compared to the mode 2 fracture forming the step B) After Rickwood (1990), illustrating the occurrence of interconnected stepped sills (B.i) and a sill with a non-connecting step (B. ii).

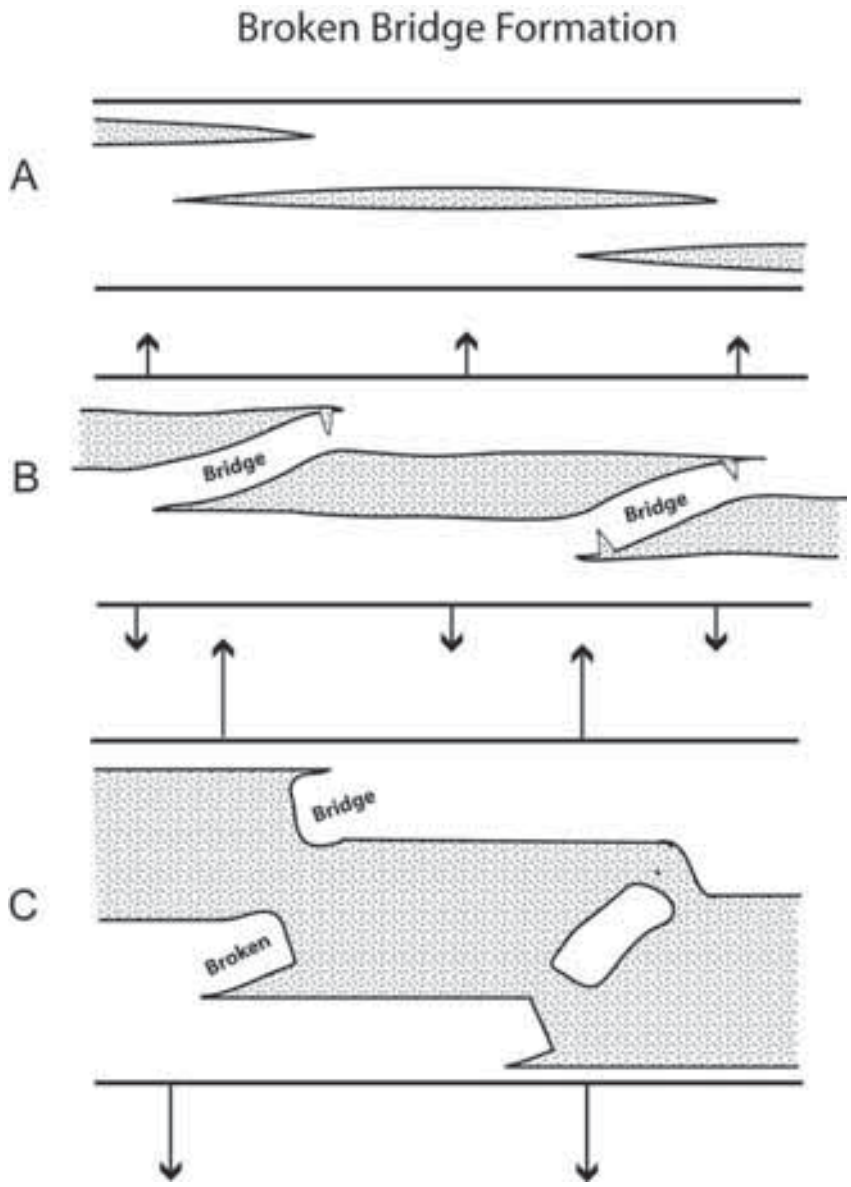

Fig. 3.6 – Modified from Nicholson and Pollard (1985) showing development of a broken bridge. A) Magma propagates as a series of offset bodies. B) As the bodies begin to inflate, the bridge of strata sandwiched between two sill segments begins to bend and deform. In zones where flexure of the bridge is at its maximum, tensile fractures form (see Fig. 3.7). C) If inflation continues, eventually one of the cross-fractures will dominate and cause failure in the bridge, leading to a 'broken bridge'. If failure occurs at both ends of the bridge, a raft of host rock strata can become fully detached from host rock.

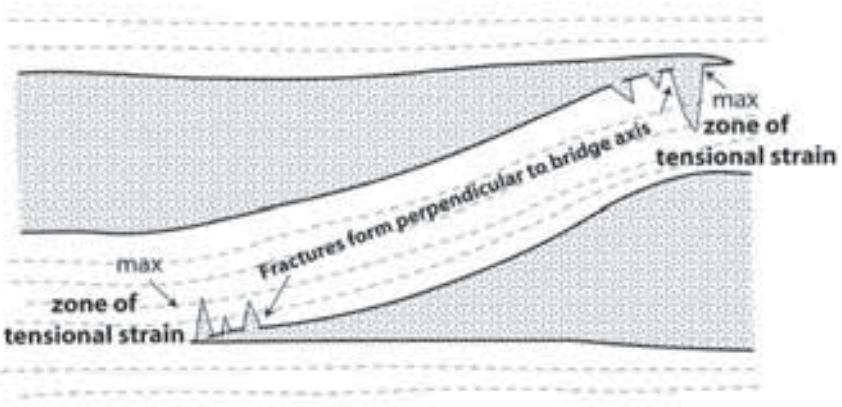

Fig. 3.7 – The initiation of tensile fracture at the points of maximum flexure in the bridge of strata.

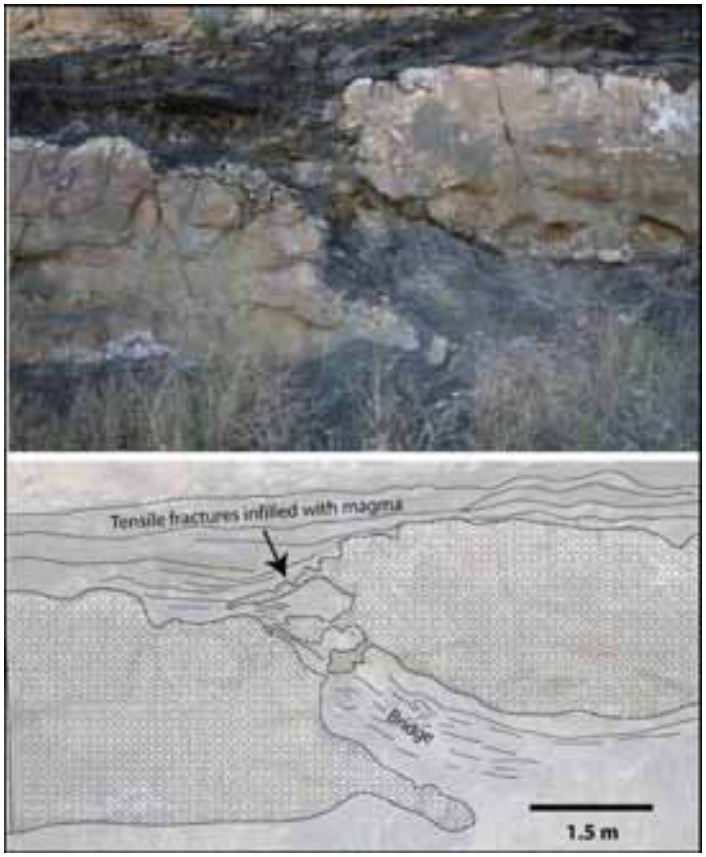

Fig. 3.8 – Field photo (Raton Basin, CO, USA) and diagram recording the middle stage of development in the formation of a broken bridge (equivalent to Fig. 3.6b). Note the tensile fractures which are in-filled with magma extending away from the sill segment on the left hand side cutting across approximately perpendicular to the bridge axis.

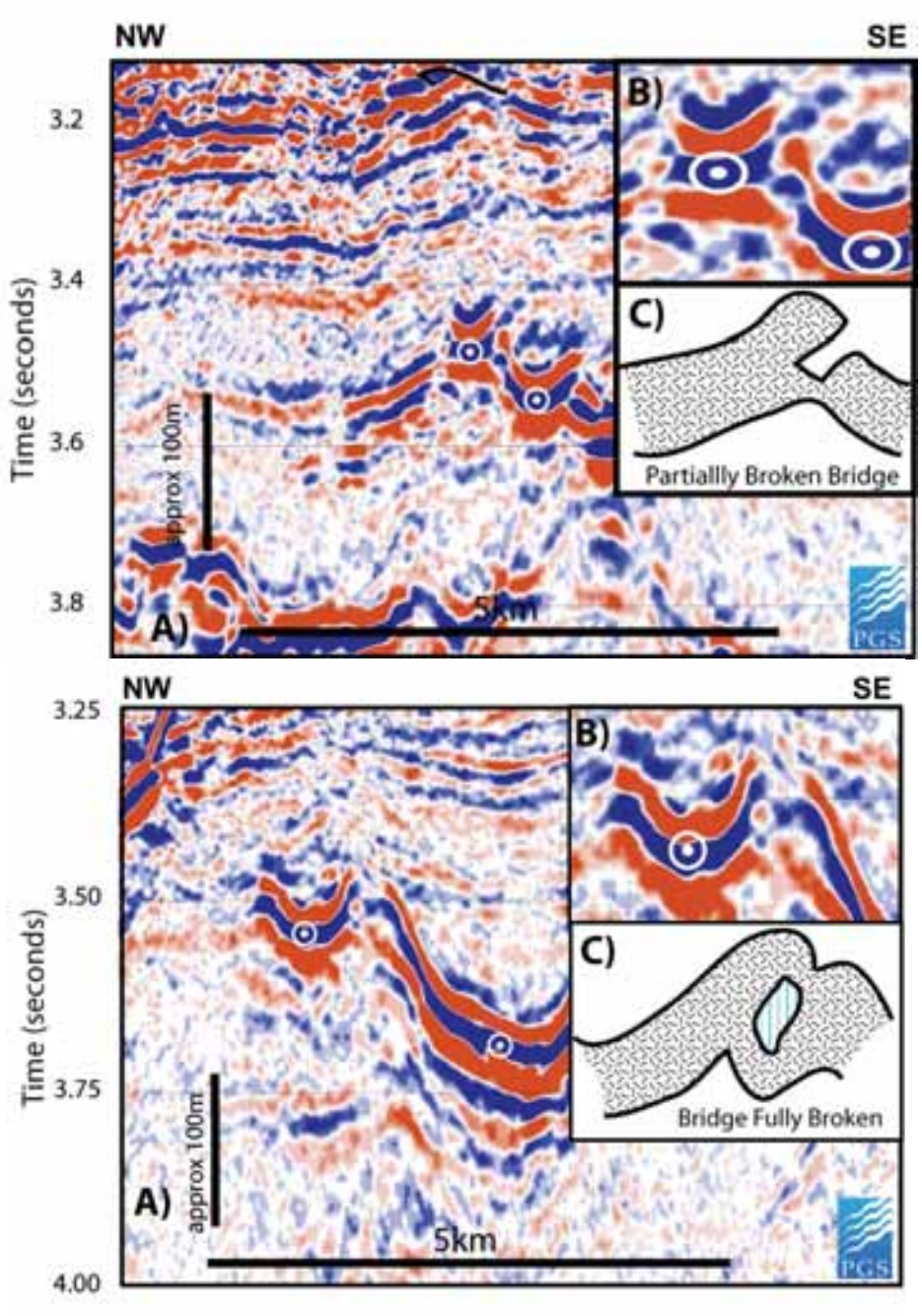

Fig 3.9. – Modified from Thomson and Hutton (2004) showing what are interpreted to be broken and partially broken bridges within seismic data.

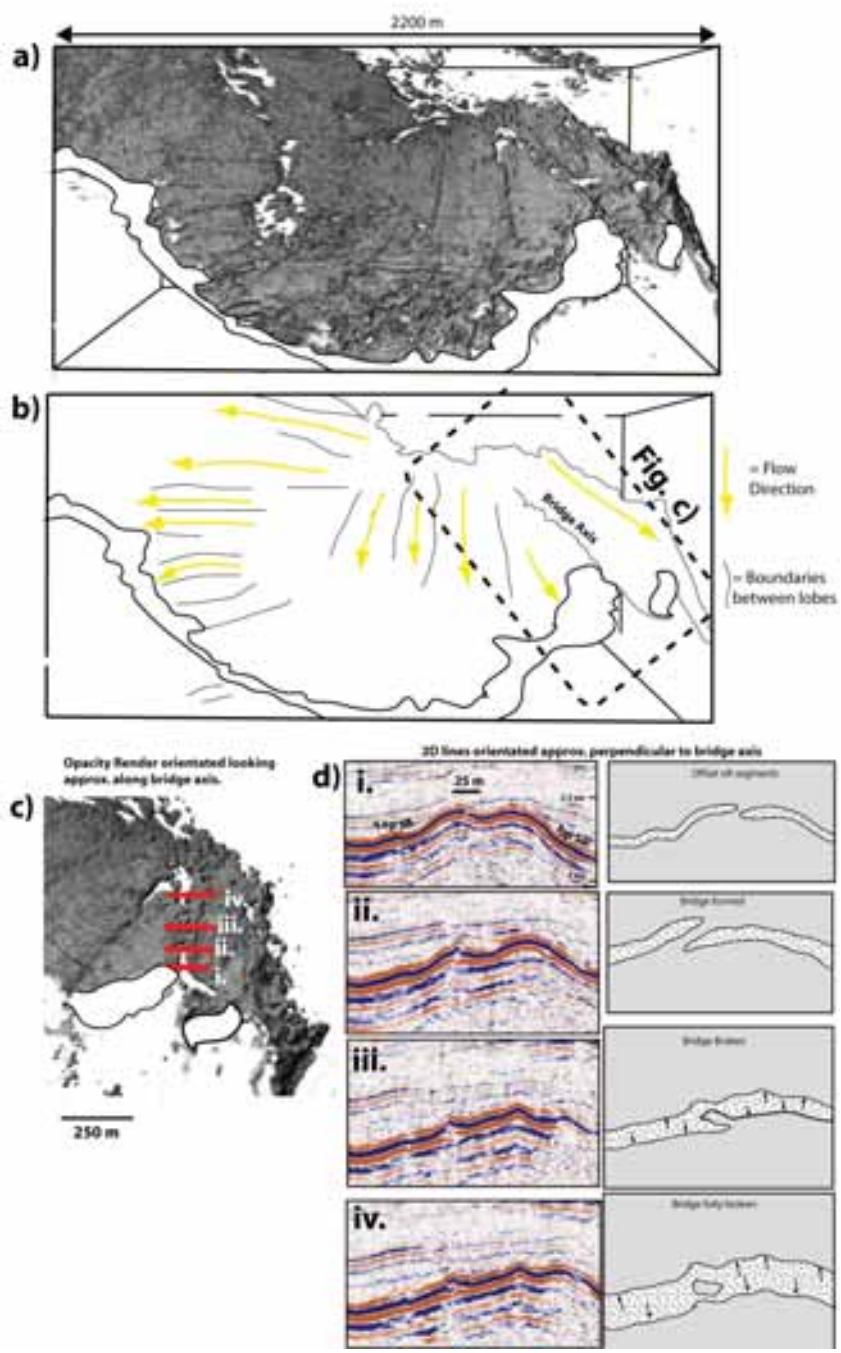

Fig. 3.10 – a) Top down view of an opacity rendered sill from Judd Basin, UKCS. The sill is climbing out of the page **b)** Sketch showing junctures between lobes seen in Fig. a, and the inferred flow directions. **c)** Shows a section of the opacity rendered sill (see Fig. a for location) re-orientated to look approximately along the axis of the juncture between two lobes. Red lines (i. – iv.) represent orientations of seismic lines seen in fig. d. **d)** Seismic lines (and accompanying interpretation) orientated approximately perpendicular to axis of juncture between two lobes showing sequential development of a broken bridge along axis of inferred flow (out of page). Note the reversal in the bridge orientation between line ii. and line iii. A 3D fence diagram reconstruction based on 2d lines (i. – iv.) can be seen in Fig. 3.11.

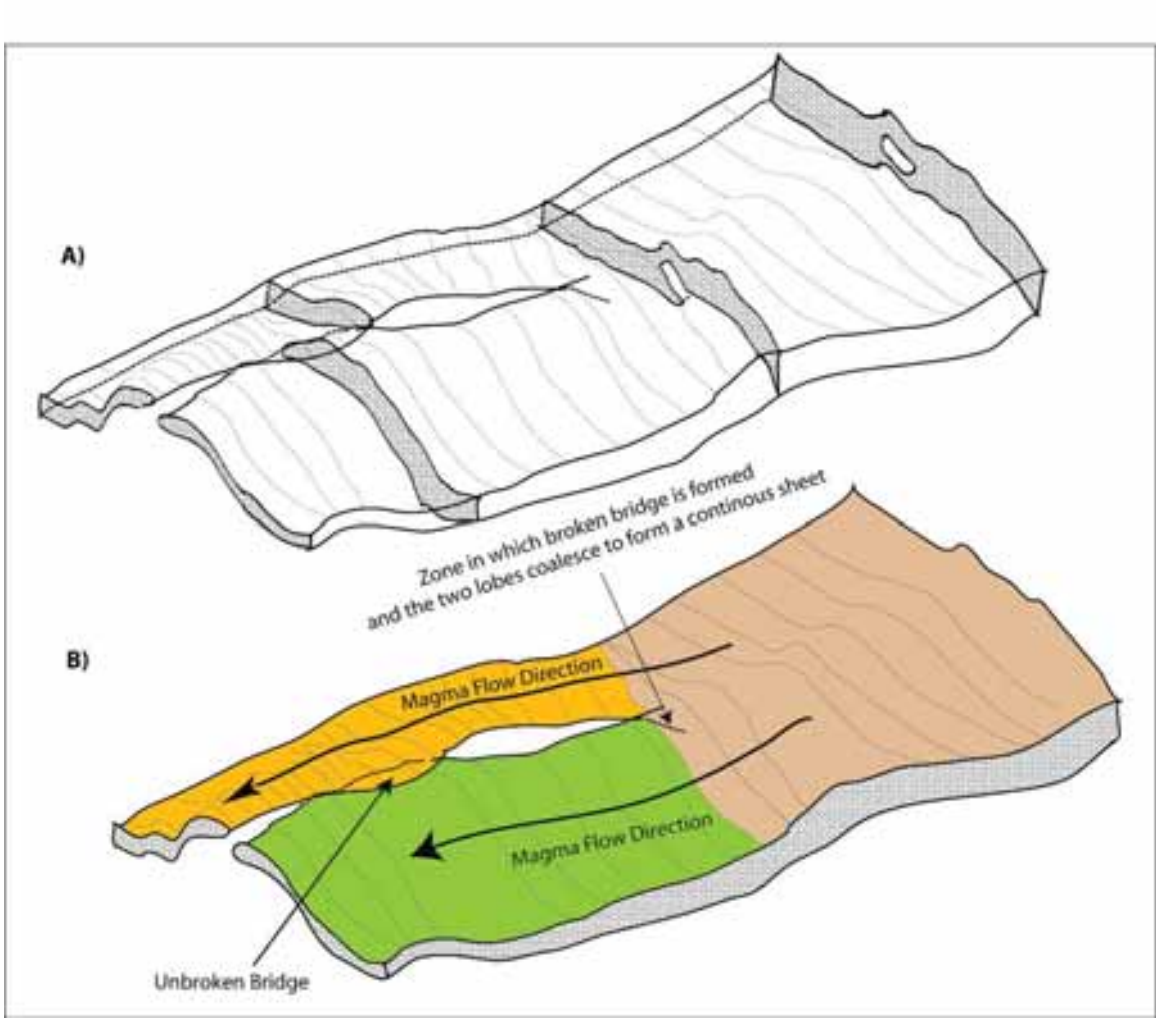

Fig. 3.11 – A) 3D fence-diagram reconstruction of sill lobes based on 2D seismic lines of Fig. 3.10d. **B)** The reversal of bridge orientation can be attributed to the two lobe segments changing orientation in respect to one another, i.e. the initially structurally lower lobes (orange), has climbed and overridden the initially structurally higher (green) lobe

3.2.4 Broken Bridges and Steps - A connection?

The occurrence of broken bridges and steps within a sill, although producing a similar stepped morphology in cross-section, have inherently different formation mechanisms to one another. For a broken bridge to form, two critical requirements exist, firstly an offset must exist between propagating sill segments and secondly the sill segments must overlap with one another. If no offset or overlap occurs, the sill segments will simply coalesce (Delaney and Pollard, 1981). Delaney and Pollard (1981) stated that during the process of coalescence of two overlapping but offset dyke segments, when the overlap between the two segments equalled that of the thickness of strata between them, the fracture at the tip of the dykes stopped propagating. Although this may explain the point at which two overlapping sill segments stop expanding laterally and begin to inflate vertically (instigating the first stage in

formation of a broken bridge), it does not explain why two sill segments are initially offset from one another.

The creation of two magma bodies propagating contemporaneously on two separate horizons to each other can occur for a variety of reasons, it may simply be the result of breakout of magma from a larger body of magma which crosses several stratigraphic horizons e.g. Shonkin Sag Sill, Montana, USA, (Pollard et al.,. 1975) or the result of breakout of thin proto-sills from a main body seeking out preferential horizons for intrusion on different stratigraphic levels (Hutton, *in press*). The formation of a stepped sill may play the pre-cursor role in creating a suitable offset in the propagating front of the sill required in the formation of a broken bridge *sensu* Nicholson and Pollard (1985) and Hutton (*in press*).

Figures 3.12 shows a schematic sketch, and series of cross-sections illustrating the evolution of a stepped sill, subsequent development of a broken bridge and possible relationship of each structure to one another. A stepped sill may result from exploitation of pre-existing joint planes. However, if initially the magma propagates as one continuous sheet (Fig. 3.12-**1)**, assuming brittle processes operating in host rock, propagation through host rock will mainly result due to the opening of a mode 1 fracture opening ahead of the sill tip (Kavanagh et al. 2008), it is proposed that at a given point, the fracture propagates rapidly through host rock at a critical velocity resulting in the formation of a hackly, stepped fracture. Magma then infilling into this fracture will begin to propagate on offset horizons forming two sill segments, still connected via a vertical sheet (Fig. 3.12-**2**). With further propagation, the offset between the two sill bodies increases (Fig. 3.12-**3**), eventually leading to a non-connecting vertical sheet segment (Fig. 3.12-**3** and Fig. 3.12-**4**). To form a broken bridge, the two separate sill segments (Fig. 3.12-**5**) must inflate laterally to overlap one another (Fig. 3.12-**6**), if this occurs and vertical inflation of the sills takes place, the creation of a bridge of host rock strata will occur (Fig. 3.12-**7**). If continued inflation of sill segments takes place the host rock bridge will eventually fail in a brittle fashion (Fig. 3.12-**8**).

3.3 Structures related to non-brittle processes

3.3.1 Lobes

One of the major advances in the understanding of sill emplacement arising from the increased use of 3D seismic data is the observation that saucer-shaped sills commonly display lobate features, ranging in size from hundreds of metres to kilometres in scale (Fig. 3.13) (Thomson and Hutton 2004; Hansen and Cartwright, 2006). Unlike lobes seen in lava flows where the term ‘lobe’ applies to the smallest discernable unit of flow (Self, 1998; Passey and

Bell, 2007), the term 'lobe' in sense of sill emplacement is purely a morphological term, to describe lobate protrusions which bud and expand away from the source region (Thomson and Hutton, 2004). Within saucer shaped sills, the lobes exhibit a branching pattern away from the inner sill (Fig. 3.13b) (Thomson and Hutton, 2004, Hansen and Cartwright, 2006). This aspect was used by Thomson and Hutton, (2004) and Hansen and Cartwright (2006) to infer direction of magma flow within the saucer to be up and away from the inner central dish. Other studies of sill emplacement (Hansen et al. 2004; Trude, 2004) had only inferred the direction of magma flow, by assuming that magma flow would be directed up and away from the inner sill.

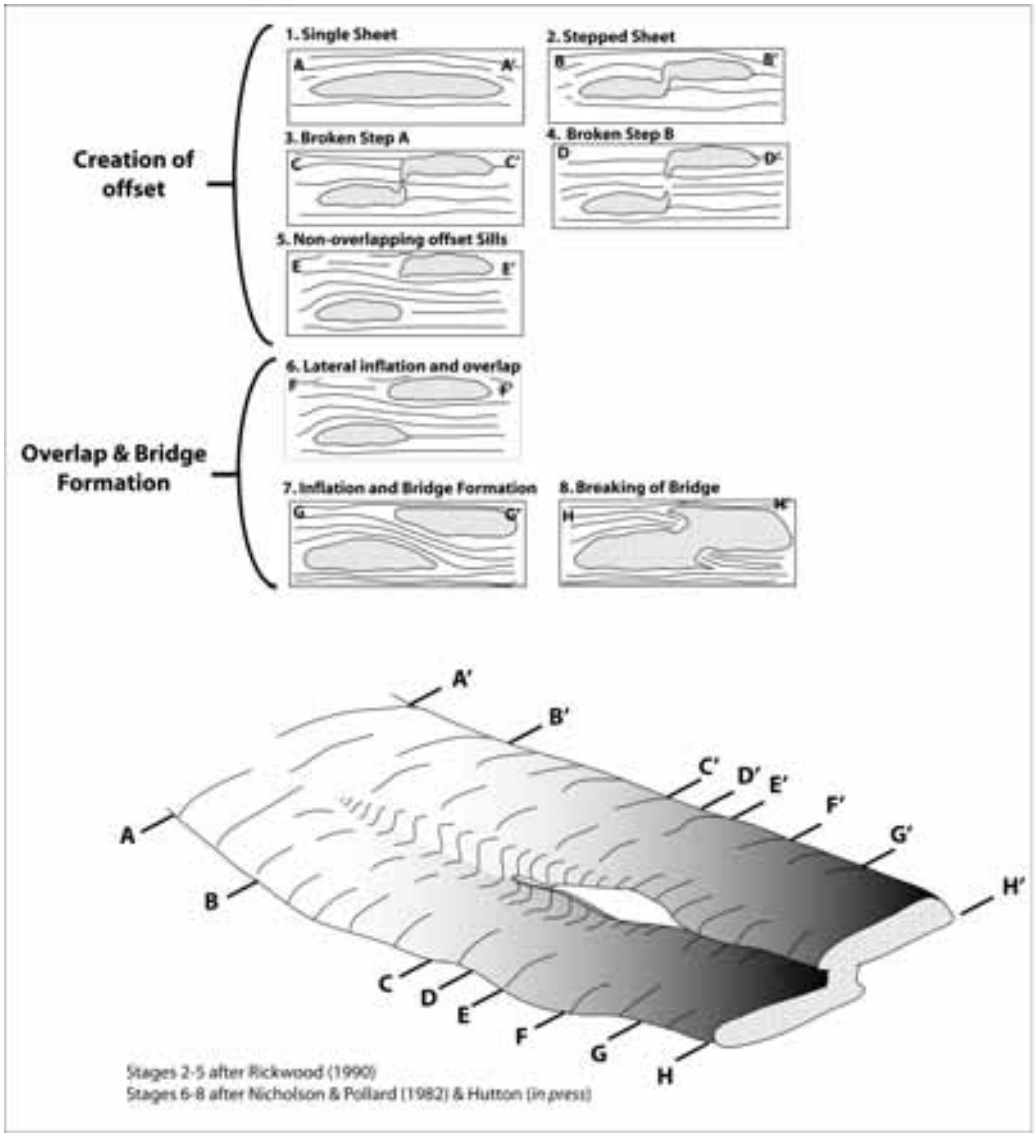

Fig. 3.12 – Schematic sketch and accompanying cross-sections illustrating possible relationship between steps (after Rickwood, 1990) and broken bridges (after Hutton, *in press*) (see text for details).

On 3D seismic data distinct lobes are generally restricted to the outer transgressive part of the saucer (Fig. 3.13c) (Thomson and Hutton, 2004; Thomson and Schofield, 2008). Thomson and Hutton (2004) proposed a hierarchy to lobe emplacement, with first and second order breakouts. Different orders of lobe-like features can be seen in Figure 3.13c, in which three constituent lobes appear to breakout from a centralised axis away from the inner sill. At the leading edge of the lobes, small, third order flow units can be identified. However as opacity rendering effectively shows relative thickness changes within a sill, and not absolute thickness, the exact nature of these features are difficult to reconcile from seismic data alone. Despite multiple seismic images of lobes presented by various workers (Thomson and Hutton, 2004; Hansen and Cartwright, 2006; Thomson and Schofield, 2009) field equivalents have not been documented.

In the study of lobate features in the Solsikke Sill, Norwegian Margin, Hansen and Cartwright (2006) drew analogies between lava flows and lobes, stating that the shallow inferred emplacement depth of the Solsikke Sill, Norwegian Margin coupled with the inferred poorly consolidated sediments at this level allowed the sill to inflate, causing breakouts away from the lobes. However, they go on to conclude that fracture segmentation (a brittle process), as modelled by Chang (2004) resulted in the lobate features seen within the Solsikke Sill.

The lobate features produced by Chang (2004) were formed by injecting gypsum slurry into a particulate host matter at very low confining pressures. The gypsum slurry then solidified and the host matter was removed to allow inspection. In this circumstance, despite the premise of Hansen and Cartwright (2006) and Chang (2004), the injecting slurry may have actually intruded by non-brittle deformation of the particulate matter around the intruding slurry and not via brittle fracture.

3.3.2 Fingered sill intrusion

Pollard et al. (1975) described the occurrence of a sill emanating from the Shonkin Sag Laccolith, Montana, USA, noting that the periphery of the sill appeared to possess a fingered appearance in cross-section, with fingers having roughly elliptical form and being in the region of 1-10m in width (Fig. 3.14a).

Pollard et al. 1975 noted evidence for lateral expansion of the finger structures, showing evidence of ductile deformation of shale adjacent to (Fig. 3.14b) and between fingers which had appeared to propagate towards one another (Fig. 3.14c). In certain areas the fingers also appeared to show signs of coalescence, leaving remnants of highly deformed shale above the juncture of two separate fingers (Fig. 3.14d). The finger structures appeared to be

restricted to one stratigraphic level composed of shale (Pollard et al. 1975). Pollard et al. (1975) argued that the formation of fingers at the leading edge of a sill was not mechanically beneficial for the propagating magma, due to the increased energy expended due to complex deformation of host rock between fingers, and hence hypothesised that the formation of fingers was analogous to the creation of a fingered instability between the propagation of one viscous fluid into another (Fig. 3.15) (Saffman and Taylor, 1958).

Pollard et al. (1975) provided no explanation of the actual mechanism for the formation of finger structures within host rock, conditions in which they might occur or other examples of their occurrence, noting that the fluid instability analogy of the Hele-Shaw cell of Saffman and Taylor used to explain the occurrence of fingers in the Shonkin Sag Sill (Fig. 3.15) was "not a fully understood mechanism for initiation of fingered intrusions". The formation of finger structures and its relationship to Pollard et al. (1975) fingers will be further dealt with in chapter 5 and 6.

Although the term 'magma fingers' *sensu* Pollard et al. (1975) has been applied in various senses to sill intrusion, often wrongly (see chapter 4 and 5; Thomson and Hutton, 2004; Hansen and Cartwright, 2006), there has been no attempt to understand the underlying process or mechanisms which underpin finger formation or properly categorize the structures involved.

3.3.3 Finger structures in seismic data

Finger-like structures have been imaged in opacity rendered sills (Thomson and Hutton, 2004; Thomson, 2007; Thomson and Schofield, 2008). They mostly occur in the arcuate inclined sheet of the sill, and are generally not present within the inner sill. The branching nature which some of the finger structures possess can be used to infer direction of magma flow (Thomson and Hutton, 2004). The finger structures imaged within seismic data (Fig. 3.16) occur on a 100's m to km scale in width, much larger then those documented by Pollard et al. (1975). Therefore it is difficult to ascertain from the seismic data alone if the two structures represent the same feature.

The genesis and form of 'Fingers' (*sensu* Pollard et al. 1975) and 'Steps' (*sensu* Rickwood, 1990) are inherently different, however in the 3D seismic study of sills by Thomson and Hutton (2004) they state that descriptions referring to steps (Francis, 1982 and Rickwood, 1990) and fingers (Pollard et al., 1975) within the literature refer to the same structures. This premise may be incorrect. The genesis of fingers is the result of viscous behaviour between the host rock and magma. They tend to form elliptical forms in cross-

section (Pollard et al. 1975) and form by either ductile deformation of host rock strata or fluidization of host rock (Baer, 1991; Chapter 6). They are often restricted to the same horizon relative to one another (Pollard et al. 1975). 'Steps' on the other hand probably form by brittle processes, with the stepped sheet often occurring over several separate stratigraphic horizons (Francis, 1982).

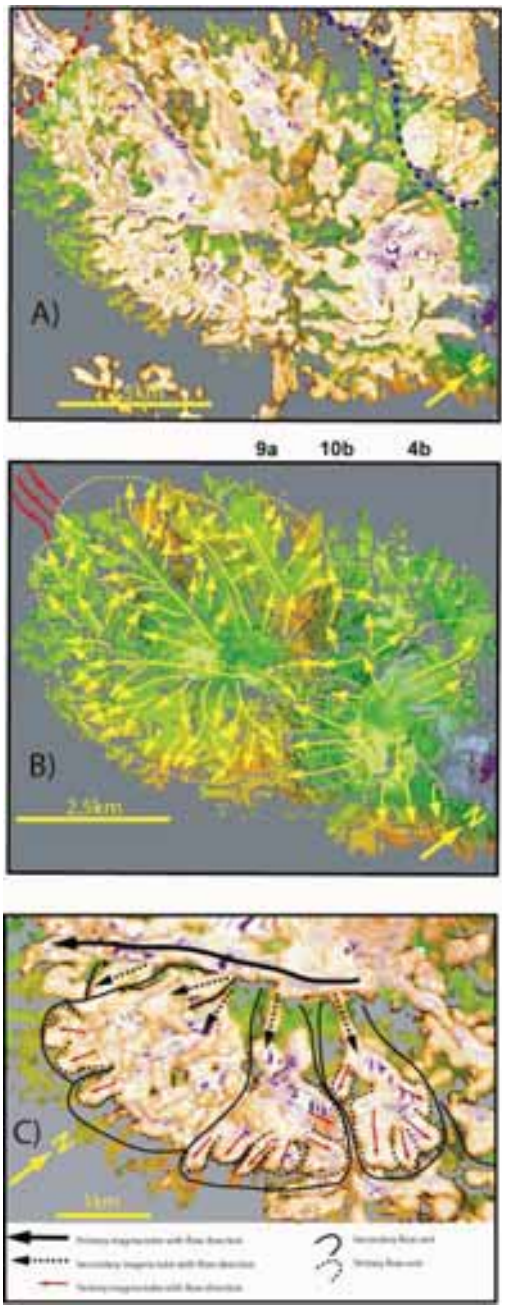

Fig. 3.13 – *From* Thomson and Hutton (2004) showing plan views of an opacity rendered sill from the NE Rockall trough. The sill displays an approximate elliptical saucer-shaped morphology with apparent branching patterns appearing to emanate from the centre of the saucer defining lobe like features. Note the 2nd and 3rd order breakouts from the lobes in Fig. 3.13C.

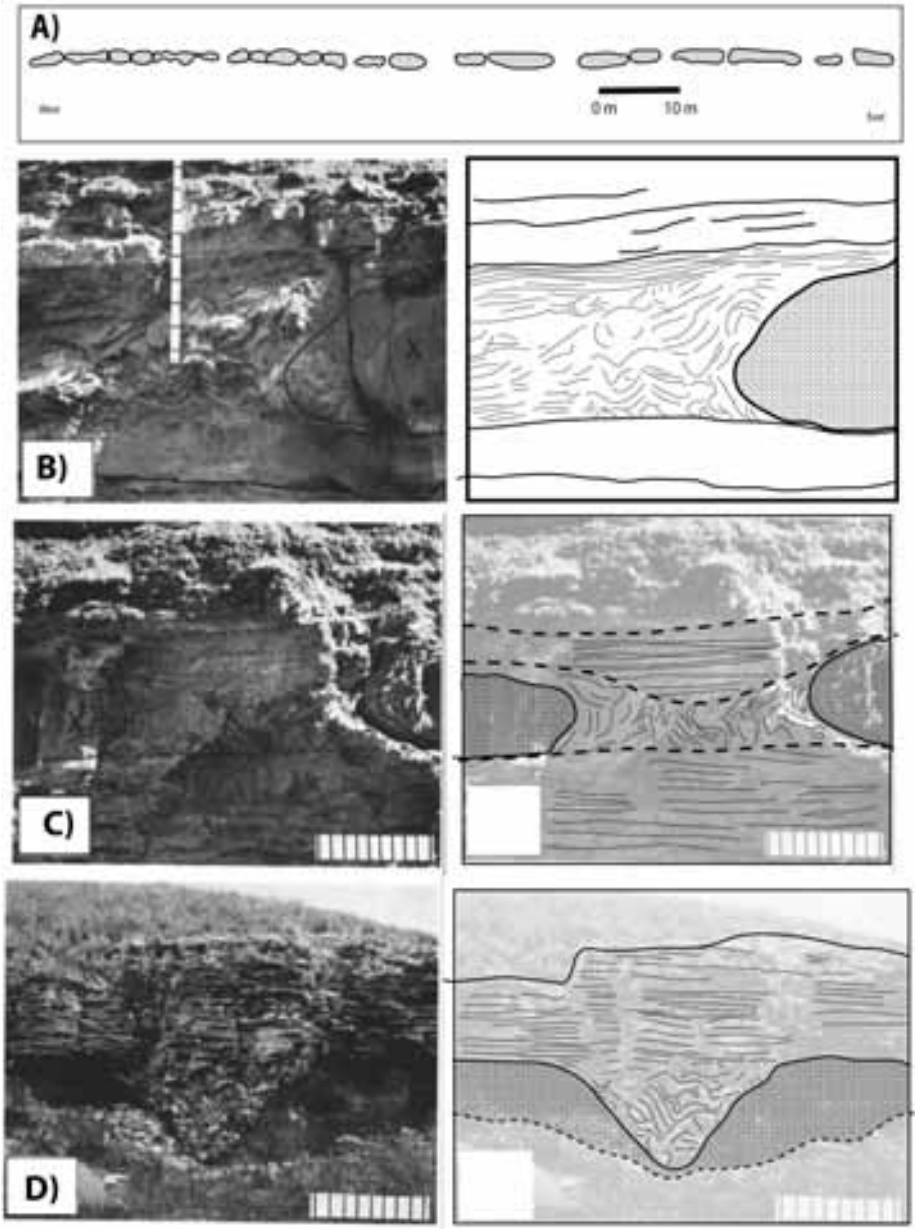

Fig. 3.14 – Re-drawn and modified from Pollard et al. (1975), showing the occurrence of magma fingers in the Shonkin Sag, Sill, Montana. a) The fingers, in cross section typically range in size from 1-10m in width. b) Shows ductile deformation within host rock as a result of lateral expansion of the finger (right of photo). c) Such deformation is also visible between two fingers, and eventually if fingers coalesce, a wedge of deformed sediments can be preserved at the juncture of the two fingers, Fig. D

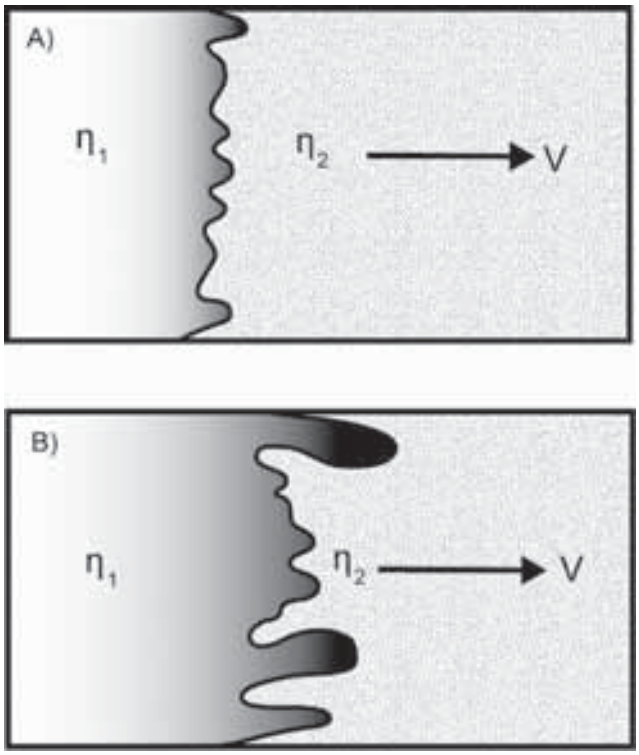

Fig. 3.15 – Fluid instability experiments of Saffman and Taylor (1958) (re-drawn from Pollard et al. 1975), showing the development of fingers as a result of propagation (at velocity V) of a lower viscosity medium (η_1) into a higher viscosity medium (η_2). Pollard et al. (1975) invoked the formation of fingers in the Shonkin sag sill to be the result of this mechanism based on conservation of energy arguments.

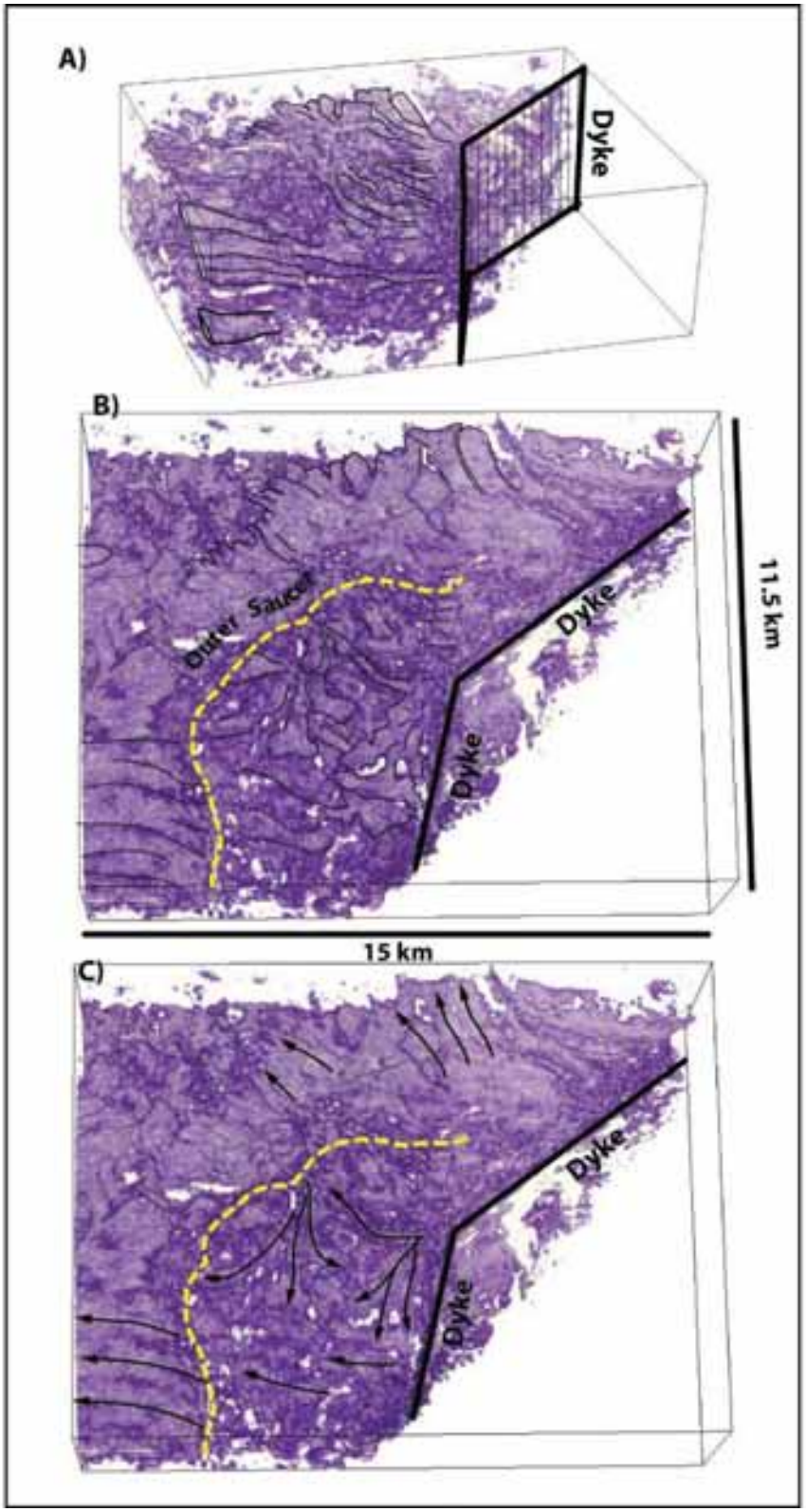

Fig. 3.16 – Structures possibly resembling fingers *sensu* Pollard et al. (1975) within an opacity rendered half-saucer shaped sill from the Flett Basin (modified from Thomson, 2007). The scale at which these features occurs is on the 100's – km scale, several magnitude bigger then fingers described by Pollard et al. (1975). However of note is that the development of the 'finger' structures appears to be best developed in the transgressive rim of the sill, with the inner sill being relatively devoid of well formed finger-like forms.

3.4 Discussion

Sills possess many structural elements, which can be identified to varying degrees in field and seismic data, these include steps (Rickwood, 1999), broken bridges (Thomson and Hutton, 2004) and fingers (Pollard et al. 1975). These can give important information regarding the emplacement mechanism and flow directions within a sill. The classification of these features is predominantly done in terms of morphology, e.g. lobes (Thomson and Hutton, 2004; Hansen and Cartwright, 2006), fingers (Pollard et al. 1975), steps (Rickwood, 1990; Thomson and Hutton, 2004).

A morphology driven classification means that structures are not classified in terms of their mechanism of formation and leads to confusion within the literature, with fingers *sensu* Pollard et al. (1975) being applied to understand the formation of lobes (Hansen and Cartwright, 2006) and steps and fingers being interpreted to represent the same structure (Thomson and Hutton, 2004). Although different sill structures may be morphologically similar, the process forming each structure is different and only by classifying the structures genetically, will it be possible to understand how final sill morphology is linked to the emplacement mechanism of the sill.

Chapter 4

The geometry and flow directions of the Trotternish Sill Complex, Trotternish peninsula, Isle of Skye

The Trotternish peninsula, Isle of Skye, contains an extensive suite of shallowly emplaced c.60Ma dolerite sills which intrude mainly Jurassic host rocks. The sill complex and country rock are well exposed on coastal sections, but inland exposure is extremely poor due to glacial drift and recent Pleistocene deposits.

Despite this, the Trotternish peninsula offers an excellent opportunity to study the emplacement of an extensive shallow level sill system in the BPIP (British Palaeogene igneous province) for comparison with similar sills imaged in offshore sedimentary basins of similar geology.

4.1 Geological summary

The BPIP cuts across several different structural terranes (Emeleus and Bell, 2005). Skye lies in the Hebridean Terrane which is bounded by two major structural lineaments: the Outer Hebrides fault zone (Minch Fault) to the NW and the Moine Thrust in the SE (Fig. 4.1). The basement rocks of the region consist of Lewisian Gneiss, which are thought to underlie most of the region (Emeleus and Bell, 2005) and form the majority of the Outer Hebrides landmass. Within Skye, the only exposure of Lewisian Basement occurs in the southern-most Sleat peninsula. Unconformably overlying the basement rocks are Mesoproterozoic to Neoproterozoic Torridonian sedimentary rocks; in Skye and to the north of Scotland these are unconformably overlain by Cambro-Ordovician shelf deposits which crop out on the foreland of the Caledonian orogen and within the Moine Thrust Belt. In SE Skye the Torridonian strata have been thrust over these younger rocks.

Major sedimentary basins were initiated towards the end of the Palaeozoic and continued to develop during the Mesozoic into the Cenozoic. During the Permian – Triassic thick sequences of desert and fluvial sandstone accumulated. The Jurassic period was characterised by shallow water sedimentation in the Inner Hebrides, consisting of deposition of shallow water sandstones, limestones and shales. However a progressive change from brackish water to deeper marine conditions is recorded in the middle Jurassic, with an abrupt

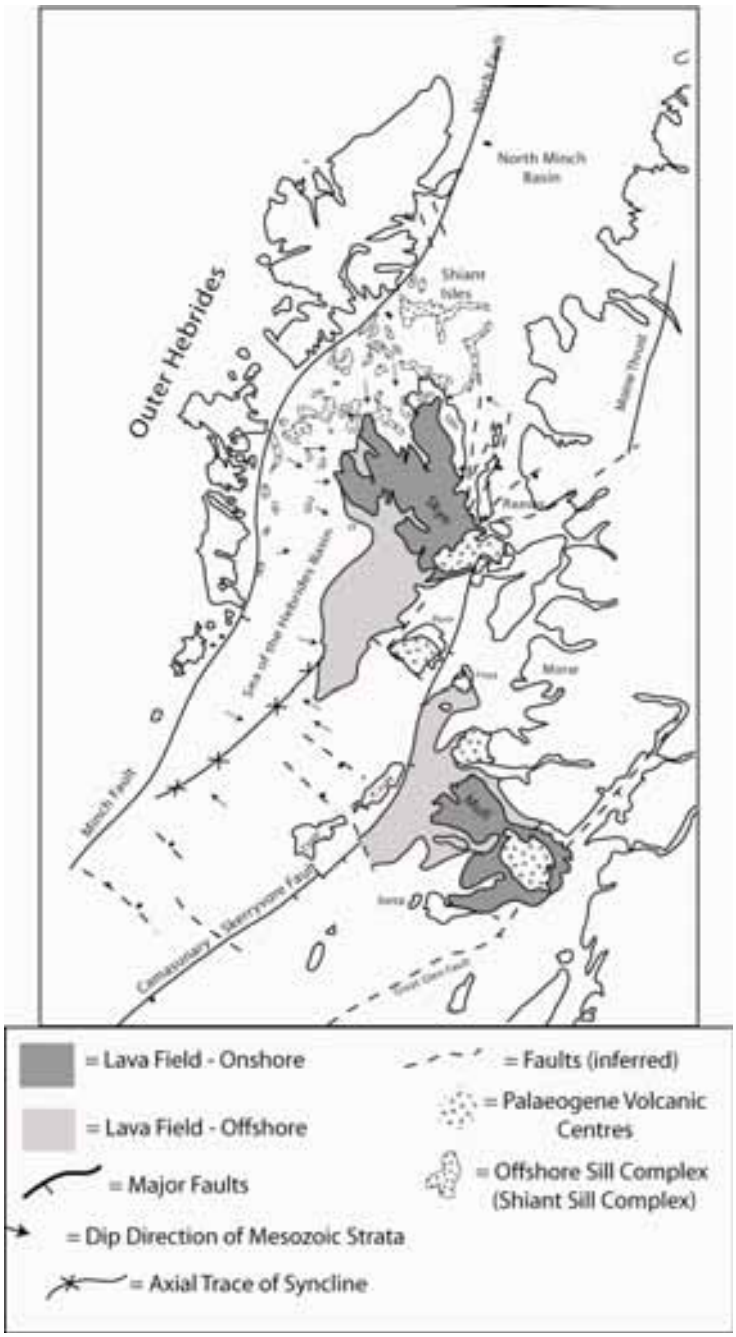

Fig 4.1 – Overview map of NW portion of the BPIP, note offshore aerial extend of the Shiant Isle Sill complex (Little Minch Sill complex), of which the sills of the Trotternish peninsula belong too. It should be noted that no 3D seismic data has been shot in the Sea of Hebrides basin at this current time (Map based on Binns et al., 1975; Butler and Hutton, 1994; Emeleus and Bell, 2005)

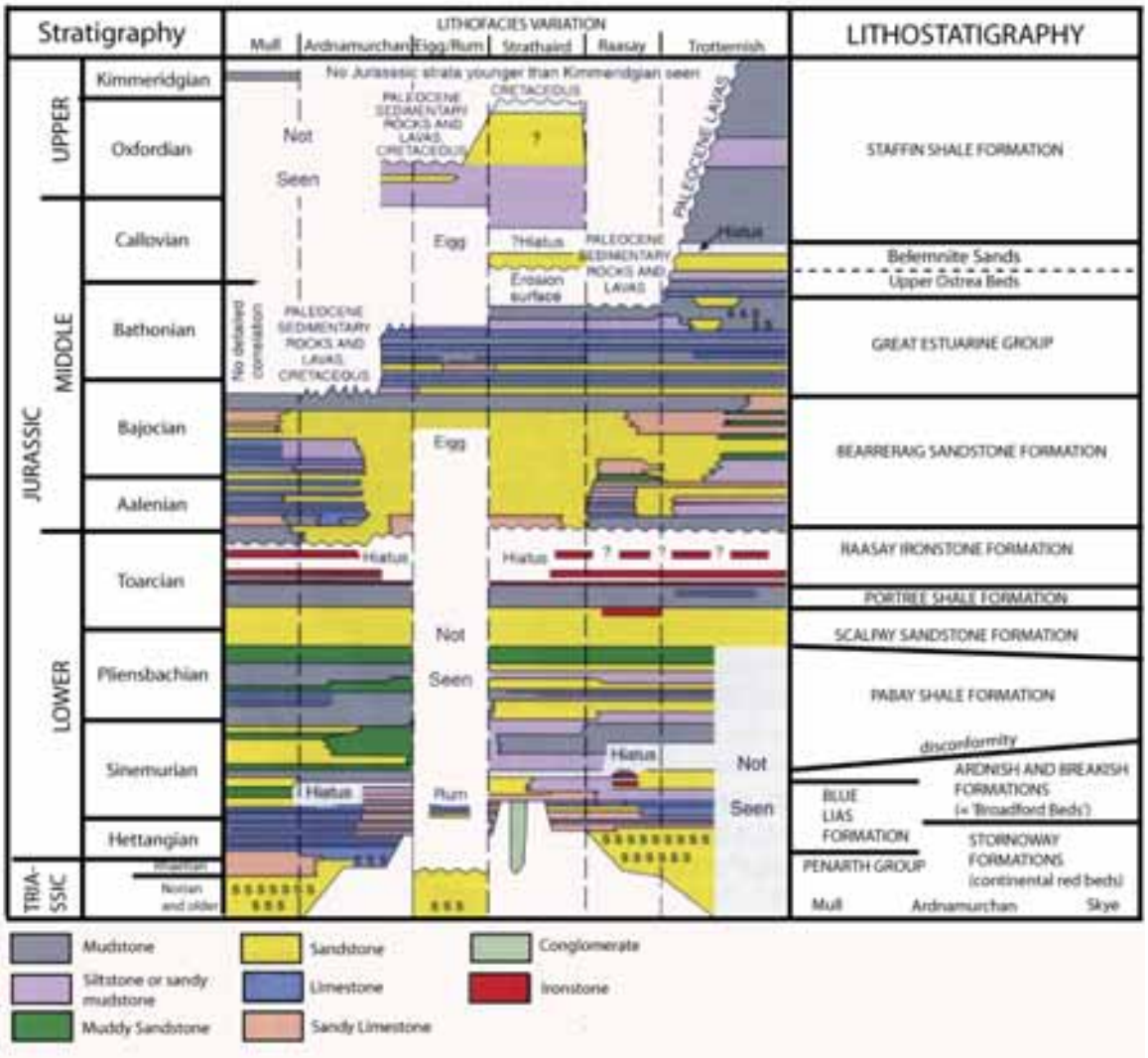

Fig. **4.2** - Re-drawn form Emeleus and Bell (2005) showing main lithologies and lithological variation within the Triassic and Jurassic sequences within the Inner Hebrides.

Formation	Lithology	Depositional Conditions
Staffin Shale Formation	mudstone, siltstone, sandy mudstone	fully marine, occasionaly anoxic
Belemnite Sands	sandy, occasionaly glauconitic, siderite nodules	offshore bar
Upper Ostrea Beds	wash-over sands, mudstone, siltsone	offshore marine, marine to brackish lagoon
Skudiburgh	mudstone, siltstone, channel-fill sandstones	fluvial and alluvial
Kilmaluag	calcareous mudstone, fissile limestone, dessication cracks	freshwater lagoon
Duntulm	fissile mudstone, limestone, nodular limestone and shell banks	marine to brackish lagoon
Valtos Sandstone	sandstone with carbonates concretions	fluvial delta
Lealt Shale	interbedded fissile mudstone and limestone, dessication cracks	brackish to marine lagoon

Fig. 4.3 - From Bell and Emeleus (2005) and Trewin (2002) showing main lithologies and depositional conditions of Jurassic sequences seen within the Trotternish Peninsula.

change from sandstone to mudstone dominated facies at the top of the Bearreraig sandstone formation, which corresponds to a widespread transgression seen across the Inner Hebrides (Fig. 4.2 and 4.3) (Emeleus and Bell, 2005).

Mesozoic sedimentation mainly occurred in a series of half-graben basins, controlled by two SW-NE trending westerly dipping faults; The Minch Fault and Camasunary-Skerryvore fault (Fig. 4.4) (Roberts and Holdsworth, 1999). This led to two large basins being created, the Sea of Hebrides Minch Basin and the Inner Hebrides Basin, separated by the SW-NE trending Skerryvore fault (Fig. 4.1). The main movement of the Camasunary - Skerryvore fault occurred prior to the eruption of the Paleocene lavas at c.58Ma. The northern extension of the fault across Skye is largely obscured and disturbed by the central complex of south Skye (Butler and Hutton, 1994), however it is thought that splays of the fault occur along the inner sound of Raasay, and cut Raasay in the form of the Screapadal fault, which offsets Lewisian strata against Triassic and Jurassic rocks (Binns et al., 1975; Butler and Hutton, 1994).

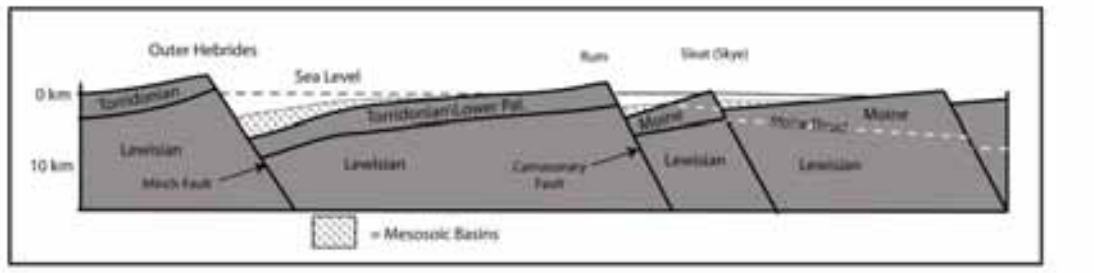

Fig 4.4 – Re-drawn from Roberts and Holdworth, (1999) showing half-graben structure of the west coast of Scotland

The BPIP experienced peak igneous activity from c. 63 to 59 Ma (Musset, 1986). The Palaeogene volcanic centre of Skye comprises of five principal units in order of oldest to youngest: Cuillins Centre gabbros and ultrabasic rocks, associated granitoid intrusions (Red hills, Beinn Dubhaich etc), the Skye main Lava series, Skye dyke swarm and finally the dolerite sill complex (Bell and Harris, 1986, Williamson and Bell, 1994; Emeleus and Bell, 2005, Bell and Williamson, 2002).

The main lava series erupted at ~ 60 Ma with radiometric ages and paleomagnetic studies indicating that the lava pile accumulated in little over one million years (Hamilton et al., 1998; Emeleus and Bell, 2005). The dolerite sills of the Little Minch Sill Complex, exposed extensively around the Trotternish peninsula locally cut the lavas at the base of the sequence, and are thought to post-date the eruption of the lava flows, but pre-date the last

generation of dykes which cross-cut the area (Anderson and Dunham, 1966; Emeleus and Bell, 2005). The chronological relationship of the sills to the lavas is corroborated by geochemical analysis of the sills which show that they are contaminated by upper crustal rocks, compared to the lava field which displays mostly lower crustal contamination, suggesting that the lavas and sill were fed from two separate magma sources (Kerr, 1993).

The sills pervasively intrude the Jurassic host rocks through out the peninsula, effectively isolating large rafts of Jurassic host rocks between separate sill units (Anderson and Dunham, 1966). Geochemical analysis of the sills indicate that the magma was derived from the lowermost lithosphere/uppermost asthenosphere and is thought to be related to a lithospheric thin spot over the c. 60 Ma proto-Icelandic mantle plume (Emeleus and Bell, 2005).

4.1.1 Faulting within the Trotternish peninsula

The Trotternish peninsula itself is cut by a series of generally NW-SE trending normal faults (Fig. 4.5), with the majority of post-Triassic and pre-Palaeogene movement thought to be restricted to the middle Jurassic (Binns et al., 1975). Many of the structures seen within the Inner Hebrides are inherited from Mesozoic and earlier times, with evidence for re-activation of some of these structures during Paleocene Volcanism (Emeleus and Bell, 2005). Detailed knowledge of pre-Palaeogene fault movement within the area is hindered by the extensive lava and intrusive pile both onshore and offshore, which prevents inspection of pre-Palaeogene structure on land (Anderson and Dunham, 1966), and further inhibits seismic imaging of structures within the Sea of Hebrides Basin (Binns et al., 1975). The exact origin of NW-SE trending faults seen within the Trotternish peninsula is unclear, but they are likely linked to the westerly dipping half graben basin structures initiated in the Mesozoic as a result of major movement along the Outer Minch fault and bounded by the inferred northern extension of the Camasunary fault (Binns et al., 1975; Roberts and Holdsworth, 1999).

Within the Trotternish peninsula, the lava field can be clearly seen to be cut by some faults, but not by others (Emeleus and Bell, 2005) (Map. 7), suggesting fault movement syn to post volcanism.

4.1.2 Previous work on Little Minch Sill Complex – Gibson and Jones (1991)

The sills of the North Trotternish peninsula, Raasay and the Shiant Isles represent a small on-land exposure of the much bigger, mainly submarine, Little Minch Sill Complex

(sometimes referred to as the Shiant Isle sill complex) which covers an area of ~ 4000 km^2 (Gibson and Jones, 1991) (Fig. 4.1).

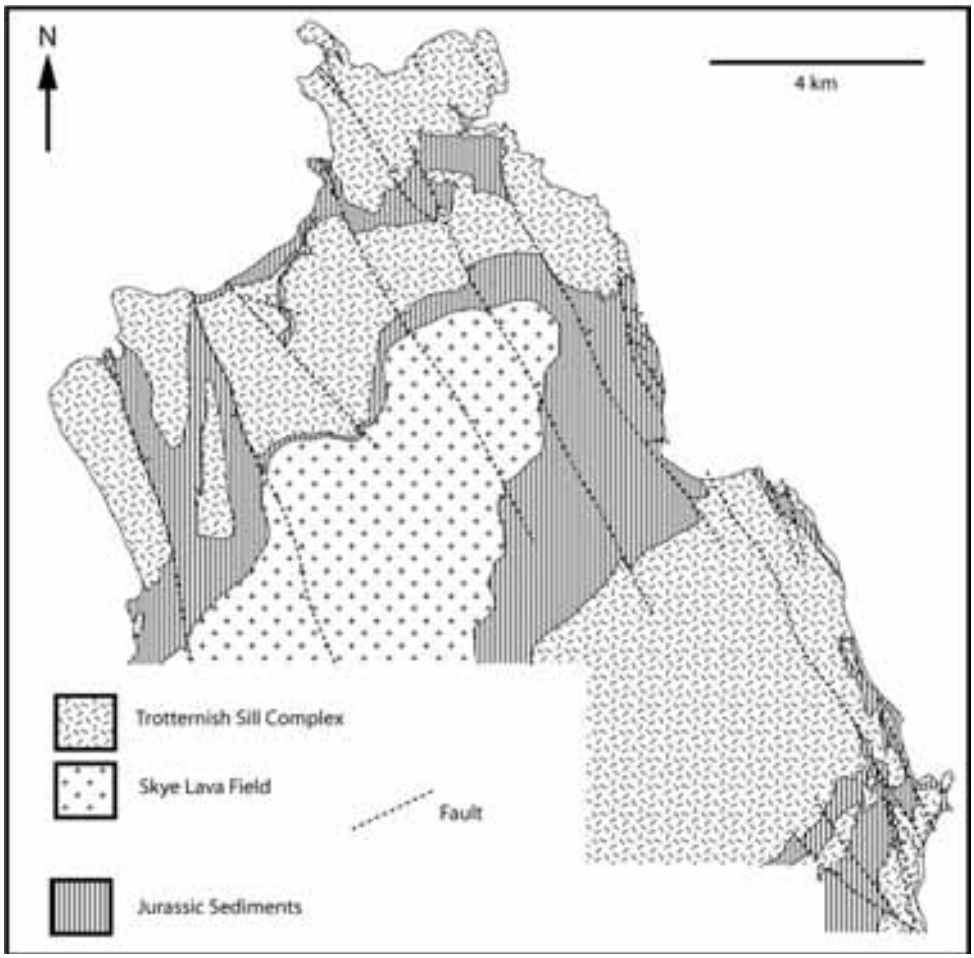

Fig. 4.5 – Simplified geological map of the Trotternish Peninsula (based on 1:50:000 BGS solid geology map)

The complex which is generally exposed at or just below the sea bed extends into the NW portion of the Sea of Hebrides Basin and SW portion of the North Minch Basin. The sills of the Trotternish peninsula form the largest single on-land expression of the Little Minch Sill Complex with individual sills ranging in thickness from 10 – 120m (Emeleus and Bell, 2005), with the thickest sill occurring in the sheer cliff face of Meall Tuath in the north of the peninsula.

The sill complex as a whole is both structurally and petrographically complicated. Previous studies have been predominantly concerned with field relationships, petrography and geochemistry of the sill complex (Anderson and Dunham, 1966; Gibson and Jones, 1990; Emeleus and Bell, 2005). Gibson and Jones (1991) to date provide the only comprehensive

petrographic and geochemical investigation of sills of the Trotternish peninsula. Using vertical sections through the sills, Gibson and Jones (1991) proposed an igneous stratigraphy consisting of three petrographically distinct compositions, picrite (40-60% Olivine), picrodolerite (10-20% Olivine) and crinanite (< 5% Olivine).

A given section through a single sill can be formed from one or more of these compositions (Fig. 4.6). The three types are considered to have been created from fractionation of an alkali olivine basaltic magma at shallow depth (Gibson and Jones, 1991). Gibson and Jones (1991) produced a composite profile of geochemical variations through the sills within the northwest of the peninsula (Fig 4.7), which showed that the sills show a marked increase in MgO and other trace elements towards the centre of the picrite units, which may suggest that some flow differentiation has occurred (Gibson and Jones, 1991).

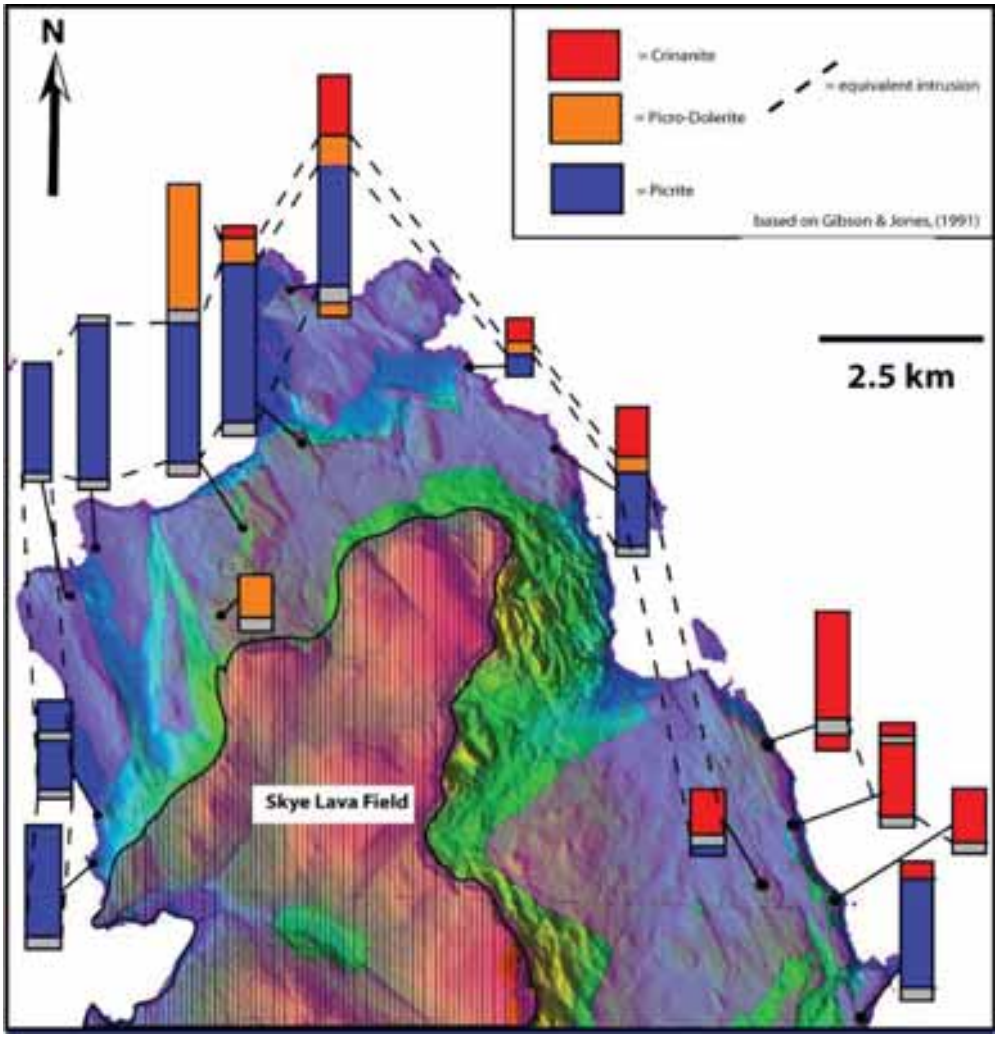

Fig 4.6 – Re-drawn from Gibson and Jones (1991) showing series of vertical sections through sills, which can be composed of crinanite, picrodolerite or picrite, or a combination of the three.

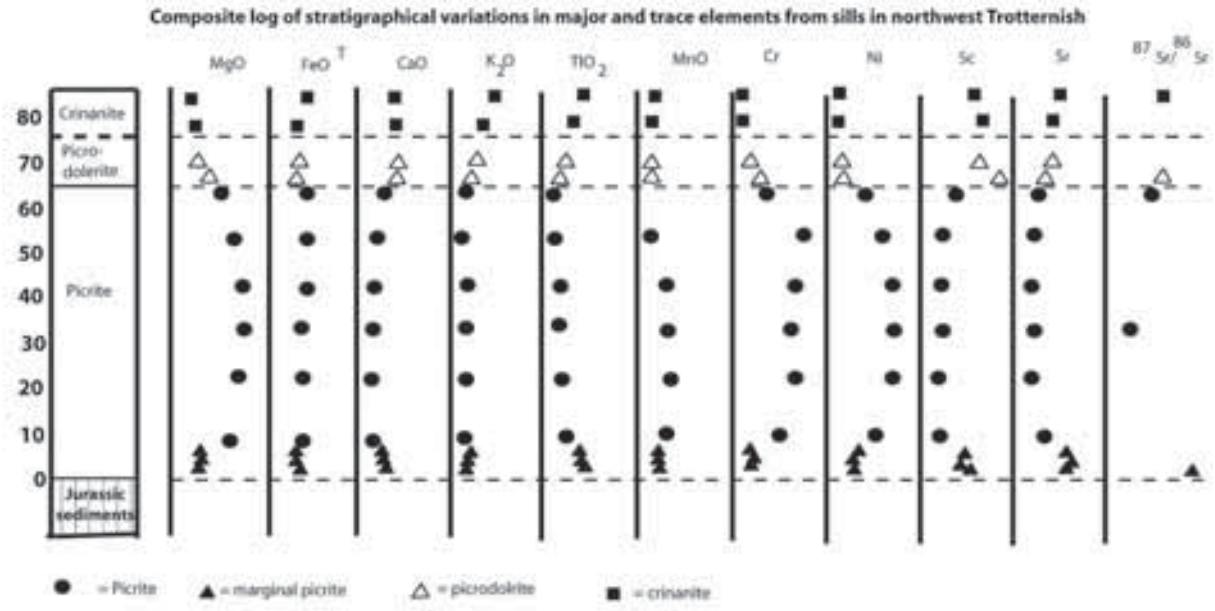

Fig. 4.7 – Composite log showing stratigraphic variations in major and trace element abundance from sills from northwest Trotternish (re-drawn from Gibson and Jones, 1991). It should be noted that highest concentrations of MgO (a function of olivine content) occur towards the centre of the picrite unit before gradually decreasing to the edges.

Previous work on the peninsula had proposed that the picrite and crinanite sills were formed by in-situ fractionation or flow differentiation (e.g. Walker, 1930). However, Gibson and Jones (1991) argued that flow differentiation alone could not account for the presence of internal chills, the multiple lithologies and marked change in petrographic textures and mineral composition between different units. Gibson and Jones (1991) proposed that similar compositions seen in the olivine in both crinanite and picrite units across the peninsula, combined with systematic variations in mineral chemistry suggests a single compositionally zoned magma chamber as the source for the sills.

Gibson and Jones (1991) acknowledge that the field relationships cannot be easily explained as a result of periodic tapping of a compositionally zoned magma chamber, and instead require a more complicated emplacement model.

Based on the work of Murata and Richter (1976), who found a correlation between discharge rate (eruption rate) and olivine content in lava flows in Hawaii, Gibson and Jones (1991) proposed that during the emplacement of the Trotternish sill complex the variation in sill composition could be explained by a similar process operating. Gibson and Jones (1991) proposed that the olivine-poor crinanite sills seen across the peninsula were the result of low discharge rates from the magma chamber, in which only olivine-poor upper regions of the

source chamber were tapped, conversely, the olivine-rich picrite sills were the result of high discharge rates tapping deeper olivine-rich levels in the chamber. Gibson and Jones (1991) note that Sr isotope ratios show a continuous correlation, with no evidence of magma replenishment, which would suggest that the differences in olivine content within the Trotternish sill complex cannot be explained by periodic replenishment in the source magma chamber by an olivine rich magma.

4.2 Aims and methodology

Although the petrology and geochemistry of the Trotternish Sill Complex have been heavily investigated (Gibson and Jones, 1991; Emeleus and Bell, 2005), the flow directions and emplacement mechanisms of the sills have not been studied in detail. The conflicting petrological variations in sills and field relationships led Anderson and Dunham (1966) to conclude that the intrusion of magma may have intruded along a series of separate fissures.

The sills within the Trotternish peninsula are well exposed within cliff-sections surrounding the peninsula, but poorly exposed inland. This chapter will adopt the stratigraphy proposed by Gibson and Jones (1991) for ease of comparison with previous works, but given the conflicting stratigraphic relationships and lack of knowledge regarding emplacement direction of the sill complex, mapping of the sill complex focused on two aims: 1) establishing broad sill stratigraphy from coastal sections within a view to extending inland, 2) identifying indicators of flow in an attempt to establish emplacement direction/feeder source of the sills.

These two aims were accomplished by use of field observations, including work on coastal sections from boats, combined with interpretation of high quality aerial photographs in conjunction with the NEXT map™ digital terrain model and radar images of the peninsula.

Composite sills were identified in the field by the presence of internal contacts, with crinanite and picrite components displaying different weathering colours and/or change in nature of cooling joints. However it was found that picrodolerite was indistinguishable within cliff sections laterally, with little evidence of internal chills being visible, suggesting it was emplaced contemporaneously with the picrite and may not actually represent a separate distinct sub-unit, but simply a modal variation of olivine within the picrite. This point appears to be indirectly acknowledged by Gibson and Jones (1991) whose descriptions of field relationships of sill stratigraphy refer to the internal contacts of picrite with crinanite as “picrite/picrodolerite”.

The NEXT map™ data archive was originally commissioned by the UK insurance firm Norwich Union to aid in flood risk mitigation. The data-set was subsequently acquired by the BGS and made available through the NERC Earth Observation Data Centre (NEODC) to NERC funded projects, including PhD studentships, in 2004.

The data itself was gathered using Interferometric Synthetic Aperture Radar (IFSAR), giving a cell size of approximately 5m across the entire of the United Kingdom. The data is provided in two forms, the basic unprocessed DSM (Digital Surface Model) and DTM (Digital Terrain Model). The DSM encompasses all height data shot, including man-made objects, trees, crops and vegetation. To produce a DTM, also referred to as a 'bare-earth' model, algorithms are applied to the data to remove height data that is not a primary function of the terrain (Downman et al*.,* 2003). The DTM has the advantage of being a representative model of the true terrain of the earths surface (Dowman et al*.,* 2003), thus allowing landform features to be more readily identified. All terrain data used within this chapter are of the latter DTM type.

Sampling for AMS (anisotropic magnetic analysis) was carried out as part of the mapping of a previous study of the dolerites in the Trotternish Peninsula (Hutton and Owens, unpublished report). However, it was found that the AMS results were anomalous, possibly the result of secondary hydrothermal alteration to the sills (Kerr, 1993; Owens, personal communication). On this basis, it was therefore decided not to carry out further AMS analysis as part of this study.

4.2.1 Pullout descriptions

Throughout this chapter reference will be made to a series of pullouts, consisting of maps and coastal cliff sections.

Pullout 1 and 2 – Large figures, mostly cliff sections and interpretation which are key to relationships discussed in this chapter. When referred to in the text, e.g. (Fig. P1.3), this refers to pullout 1, figure 3.

Map 1 – Aerial photograph of the mapped area.

Map 2 – Slope shaded DTM of the peninsula with place names.

Map 3 – Aerial photograph rendered with slope shaded NEXT map™ DTM to highlight change in slope features.

Map 4 – General location map.

Map 5 - 1:50000 Edina Digimap BGS solid rock geology overlain on 1:50000 Edina Digimap Ordnance Survey map and aerial photograph.

Map 6 – 1:50000 Edina Digimap BGS solid rock geology overlain on 1:50000 Edina Digimap Ordnance Survey map and aerial photograph overlaid on slope shaded DTM showing the correlation of DTM with solid rock geology.

Map 7 – Same as map 6, but highlighting the non-topographic expression of faults across the peninsula.

Map 8 – Sill Stratigraphy and flow directions of the Little Minch/Trotternish Sill Complex.

Map 9 - Same as map 8, but with inferred large scale flow directions across the peninsula.

4.3 Key features of the Trotternish Sill Complex

Before the detailed stratigraphy of the Trotternish Sill Complex is covered, it is important to outline some key aspects of the peninsula which are fundamental in understanding the intrusion history of the sills.

4.3.1 General Form

The sills within the Trotternish Sill Complex do not possess a saucer-shaped morphology such as those imaged in offshore seismic data (Thomson and Hutton, 2004) or seen in the Karoo Basin, South Africa (Chapter 5). Although local transgressions of the sills do occur, most notably at Kilt Rock (see section 4.5.2), the sills are generally tabular in nature, being approximately concordant with the Jurassic host rocks.

Aside from the lava pile the sills within the Trotternish peninsula generally form the highest topographic points. Contacts with country rock are rarely exposed, apart from on coastal sections, but may be followed inland as sharp changes in slope between the more

easily eroded Jurassic country rocks (forming the low ground) and the more resilient dolerite (generally forming the high ground) (Map. 1-6). Within the dolerite sheets, distinctive finger-like features can be seen (e.g. Staffin Harbour and Camas Mor) (Map. 1-6).

4.3.2 Columnar Jointing

In general columnar joints form perpendicular to and increase in width away from a cooling surface (Grossenbacher and McDuffie, 1995). The orientation of the joints can be used to construct the original orientation of the contact of the country rocks, if this is not exposed or has been removed by subsequent erosion, and secondly the decrease in spacing of joints towards a cooling surface can be used to discern chronology of intrusion, especially in sill units that consist of discrete chronologically distinct intrusion events (e.g. sub-pulses; Goto and Tsuchiya, 2004).

In sub-horizontal sill intrusions the columns are typically sub-vertical. Anderson and Dunham (1966) noted that in the North Trotternish peninsula this is not always the case; but did not expand on its significance (Hutton and Owens, unpublished report). In the following discussion, columnar jointing is used to ascertain the timing of sill intrusion.

4.3.3 Sill Morphology – Convex-up tops

In cross-section the crinanite sills commonly have a corrugated top surface, for instance at Staffin the features have a wavelength of ~ 200m (peak to peak) and are approximately 75 m in thickness (Fig. 4.4). These convex-up profiles are preserved inland, and can be traced by changes in slope on aerial photographs and the DTM (fig 4.8; Map. 4) some 800m in a SSE orientation, forming tapering finger-like landforms (Fig. 4.8 and 4.9).

As extensive erosion and glaciation has occurred in the area, coupled with faulting, which appears to coincide with these structures (Fig. 4.9), it is tempting to attribute the landforms to faulting and/or glacial processes. However several lines of evidence exist which indicate that these features may have a primary origin related to the intrusion of the sill.

4.3.4 Origin of finger structures – Erosion, glacial or magma flow?

Since cessation of volcanic activity at ~ 59 Ma, the landscape of the Trotternish peninsula has undergone heavy erosion and glaciation dominated by uplift and erosion resulting in deposition of extensive clastic sequences offshore (Anderson and Dunham, 1966, Emeleus and Bell, 2005). Removal of at least 1200m of overlying lava's (Emeleus and Bell, 2005)

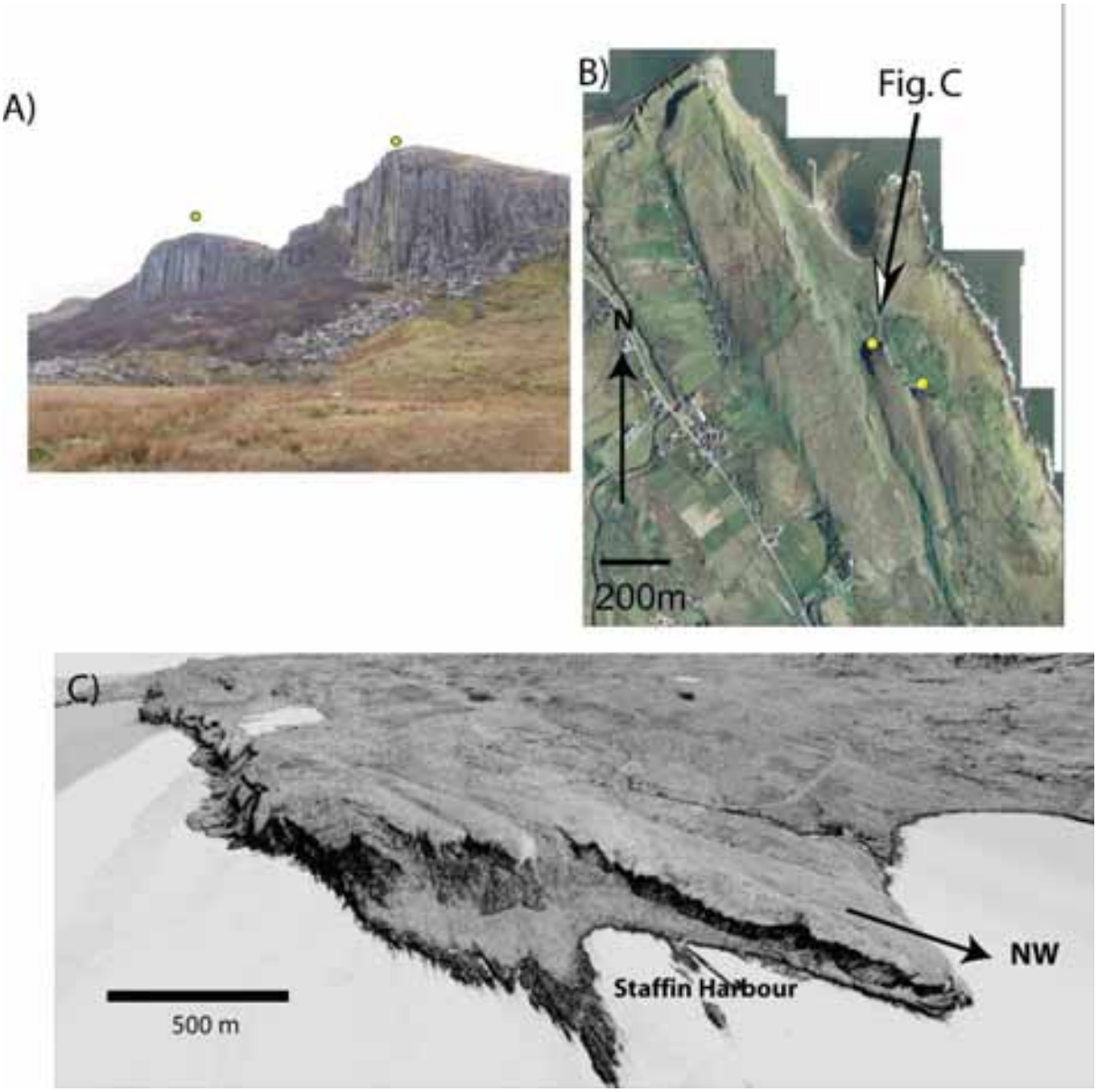

Fig. 4.8 – A) Corrugated cliff tops of the upper dolerite sill at Staffin harbour. B) Aerial photography showing the convex-up landform features forming finger-like structures extending ~ 800 m inland. C) Oblique view of radar image draped over NEXT map™ DTM showing topographic expression of finger structures. The view within Fig. C is looking in a south-easterly direction, along the approximate direction of inferred ice-flow over the area. Note that this is at an oblique angle to the axis of the finger structures.

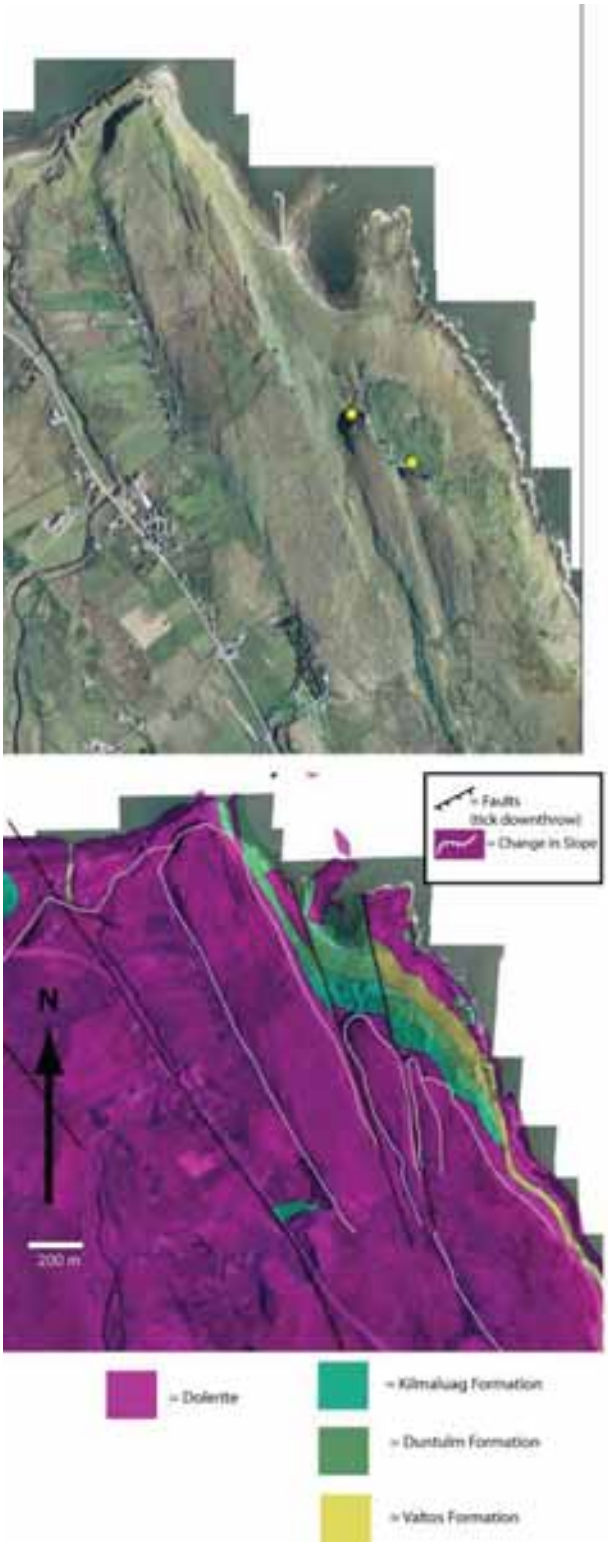

Fig. 4.9 – Aerial photograph and aerial photograph draped with BGS 1:50000 solid rock geology map. The BGS interpretation places faults coinciding with the troughs between the finger structures at Staffin. No evidence of faulting can be seen within the fore-shore area of the harbour and no apparent offset occurs in the top surface of the dolerite forming the fingers.

has taken place across the peninsula exposing the underlying Trotternish/Little Minch sill complex which now forms the prominent landscape of the peninsula.

From approximately 1.8 million years to 10,000 BP, several periods of glaciation have taken place. The last major glaciation, within the late Devensian, which ended approximately 10,000 year B.P, covered most of Britain in a thick ice-sheet creating glacial features seen throughout the west coast of Scotland (Bennett and Boulton, 1993; Ballantyne et al., 1998; Emeleus and Bell, 2005). During this glaciation, the ice sheet over the Trotternish was between 450 – 600 m thick being predominantly directed away from the Cuillins in a SW to NE orientation over the peninsula (Benn, 1997).

The gouging action of ice-sheets across the area during the main Devensian glaciation (Emeleus and Bell, 2005) could have plausibly led to the creation of the convex-up finger like features. It is clear that the Trotternish peninsula has been heavily influenced by erosion and glaciation; for the sub-basalt network of sills to be exposed, a thickness of approximately 1200 m of the overlying lava pile has had to be removed. However from the work of Benn (1997) the palaeo flow direction of the ice over the peninsula was shown to be predominantly from a SSW-NNE direction (Fig. 4.10), as the finger structures seen have a predominantly SE – NW and N-S orientation, this would suggest that the features seen at Staffin are not related to ice-flow over the area, and do not represent gouged features as a result of ice movement (C.K. Ballantyne, pers. comm.).

In addition the exposures on the top surface of the convex-up fingers the dolerite possesses a chilled facies, in the form of small scale cubic jointing patterns and decrease crystal size, suggesting that the exposed sill top approximates its configuration at the time of intrusion (Fig. 4.11).

Figure 4.5 shows the BGS 1:50,000 colour solid rock geology raster overlain onto an aerial photograph of Staffin harbour. Inferred normal fault traces extend in a SSE direction into the valleys between the convex-up finger structures. Evidence of faulting within the dolerite sheet is lacking in the field, mainly due to poor exposure, but no discernible offset can be observed between the top surfaces of both finger structures upon crossing the fault. As the tops of the sills approximate to that of the original intrusion, this would suggest that the faults do not necessarily cut the dolerite sheet.

4.3.5 Flow indicators Staffin Harbour

The top contact of the lower sill is extensively exposed forming the harbour and fore-shore

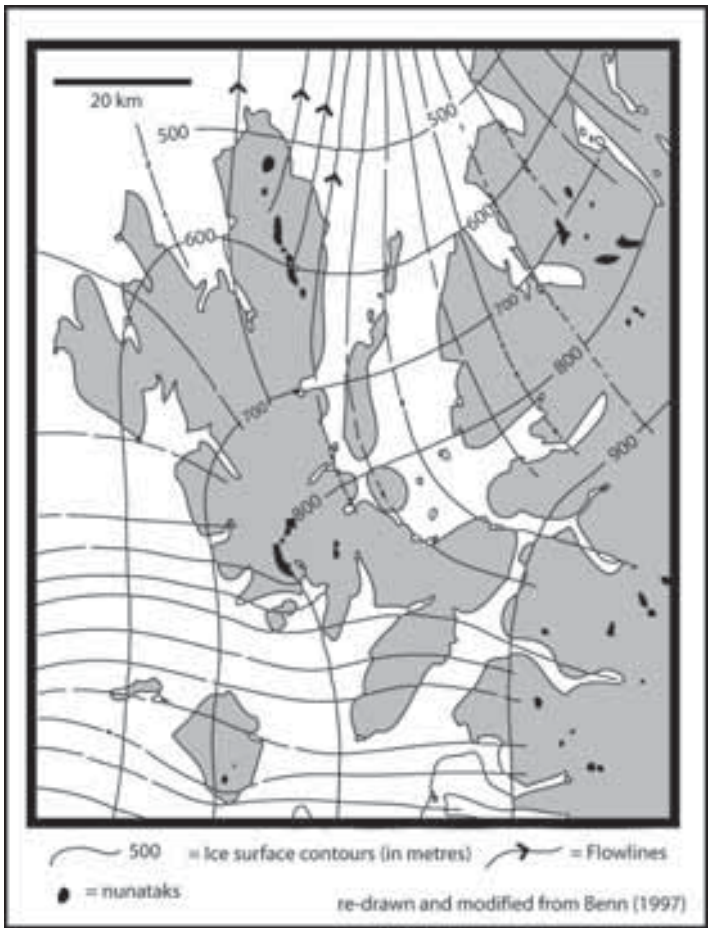

Fig 4.10 – Devensian ice sheet reconstruction over Skye. Note in the region of Staffin harbour the flow directions are in a predominantly SSW to NNE direction.

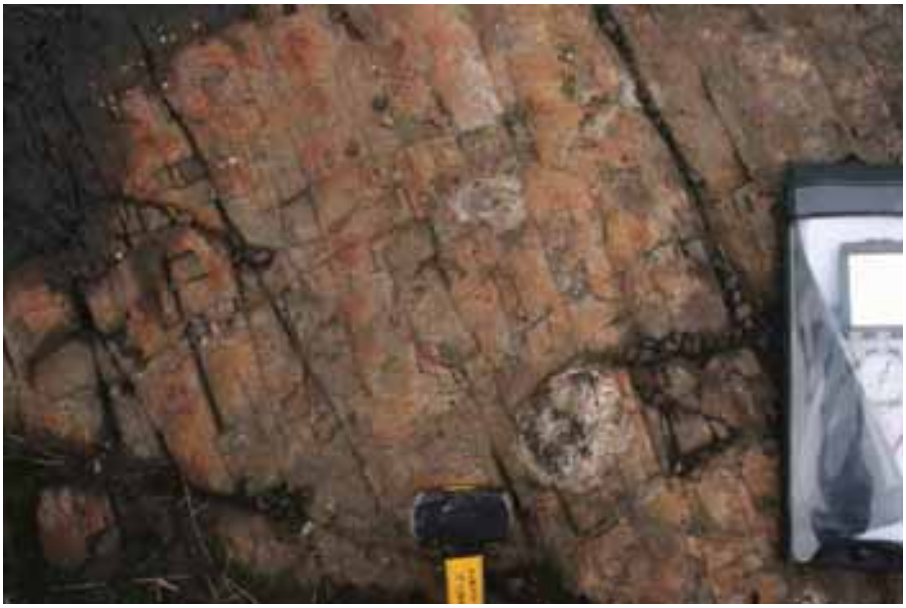

Fig 4.11 – Field photograph of isolated outcrop on top of finger structure, showing closely spaced jointing patterns and vesicles, indicative of a chilled top contact. Hammer head ~ 6 cm in width.

area. Upon its top surfaces flow indicators in the form of aligned vesicles and ropy flow structures can be found in abundance, such features can be successfully used to infer both the axis of magma flow (aligned vesicles; Rickwood, 1990) and direction of flow (ropy flows; Liss et al*.,* 2002). Figure 4.8b shows a ropy flow structure from South Staffin. The abundance of flow indicators at this locality, in particular ropy flow structures, compared to the rest of the peninsula, seems to be a combination of extensive exposure of the roof contact by erosion due to wave action and the nature of the host rocks into which the sill intruded. Ropy flow structures form as a result of a free-surface of gas being created at the interface between magma and host rock (Liss et al*.,* 2002). The roof rock to the sill is Jurassic aged limestone, and it is possibly the heating and contact metamorphism of the overlying limestone which created a film of gas at the top contact of the sill, allowing the formation of ropy flow structures as the magma was emplaced. However, the ropy flow structures described in the Whin sill by Liss et al. (2002) differ from those occurring at Staffin, as the Whin Sill, the ropy flow structures occurred in eye-shaped gas vugs within the sill (Liss et al*.,* 2002) (Fig. 4.12a), whereas the Staffin are more widespread, occurring over large swathes of the top surface of the sill (Fig. 4.12b). In the ropy flow structures described by Liss et al*.* (2002), the flow ridges were orientated approximately perpendicular to the direction of flow (Fig. 4.12a). At Staffin the roof contact of the dolerite with limestone country rock is uneven which led to pendants of limestone protruding into the underlying magma as it flowed. Where two roof pendants occur adjacent to each other, the flow ridges form parallel to the local direction of flow, where magma has flowed between pendants (Fig. 4.12b, Fig.4.12c, Fig. 4.14 rose diagram **v.**), unlike the ropy flow structures described by Liss et al*.* (2002). In areas were a single roof pendant occurs, the flow ridges drape around the roof pendants indicating the direction of flow (Fig. 4.13; Fig. 4.14 rose diagram i. and iii.)

In North Staffin, the flow direction is predominantly S – N, further SE along the foreshore the orientation of aligned vesicles and ropy flow structures is seen to re-orientate to ~ SW-NE, suggesting some divergence in the flow of the sheet has occurred (Fig. 4.14). This is not necessarily surprising, as Thomson & Hutton (2004) showed divergence in flow direction within individual lobes within saucer-shaped sills. However of note is that the direction of flow of magma in North Staffin appears approximately coincident with the axis of the convex-up finger structures when traced inland (Fig. 4.14).

Although the flow indicators occur within the lower tier of dolerite, and not the upper tier of dolerite, where the convex-up undulatory features are preserved it is proposed that

convex-up finger structures at Staffin are a function of flow, whose axis is orientated parallel to the direction of flow. Additional weight is given to this interpretation as morphologically similar convex-up finger like features can be seen to occur within the saucer-shaped sills within the Golden Valley Sill, Karoo Basin, South Africa, as described in Chapter 5, and can be confidently attributed to flow (Polteau et al*.,* 2008).

4.3.6 Camas Mor

The outcropping sills at Camas Mor possess a similar finger-like morphology to Staffin Harbour, however rather then being convex-up their tops appear relatively planar due to

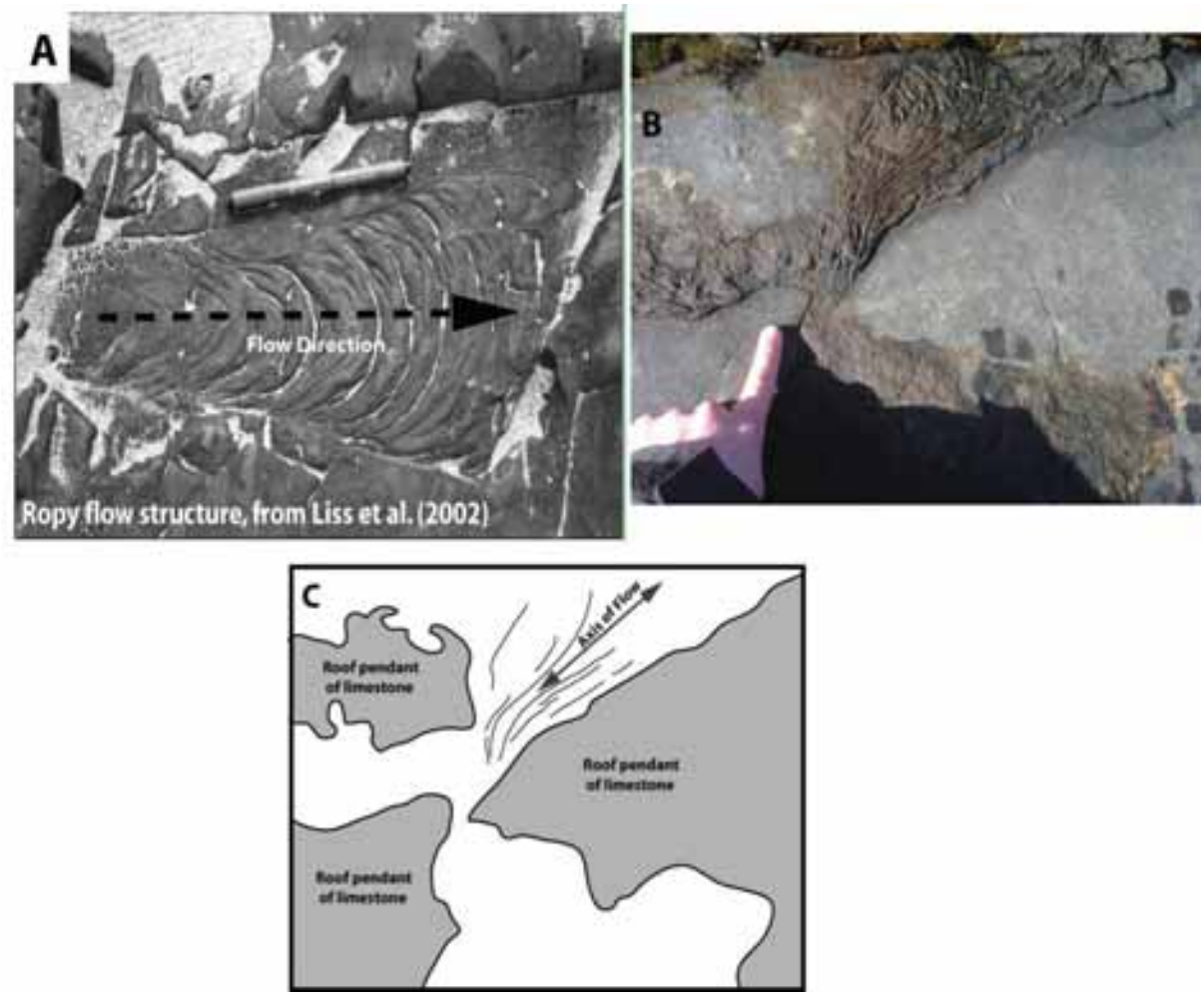

Fig 4.12 – A) Ropy flow structure within a gas vug from Liss et al. (2002). B) Roof contact of lower tier sill at Staffin showing channelling of flow between two roof pendants (Fig. c).

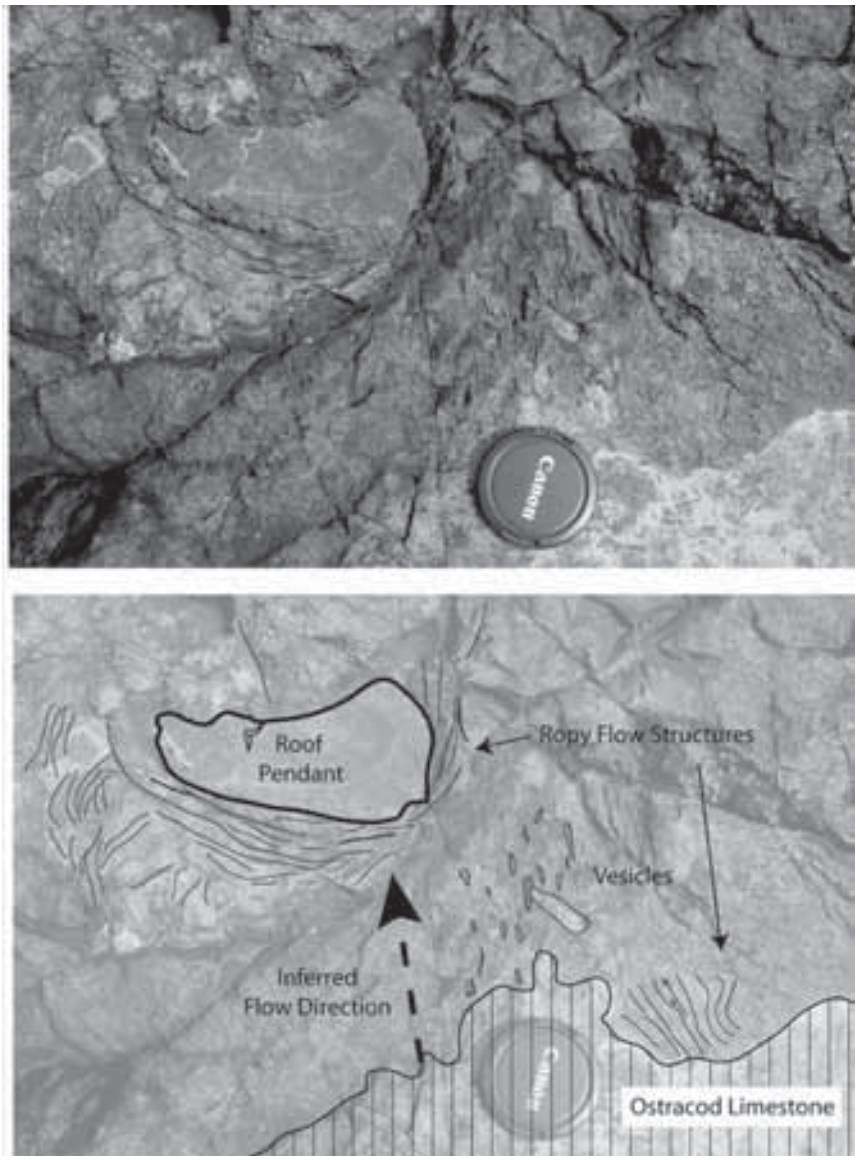

Fig 4.13 – Ropy flow pendant structure on top surface of lower tier sill, Staffin harbour, caused by draping of ropy flow around a roof pendant of limestone (arrow pointing ~ NE). Note the alignment in the vesicles whose orientation is in agreement with the flow direction inferred from the draping of ropy flows around the roof pendant of limestone (top right).

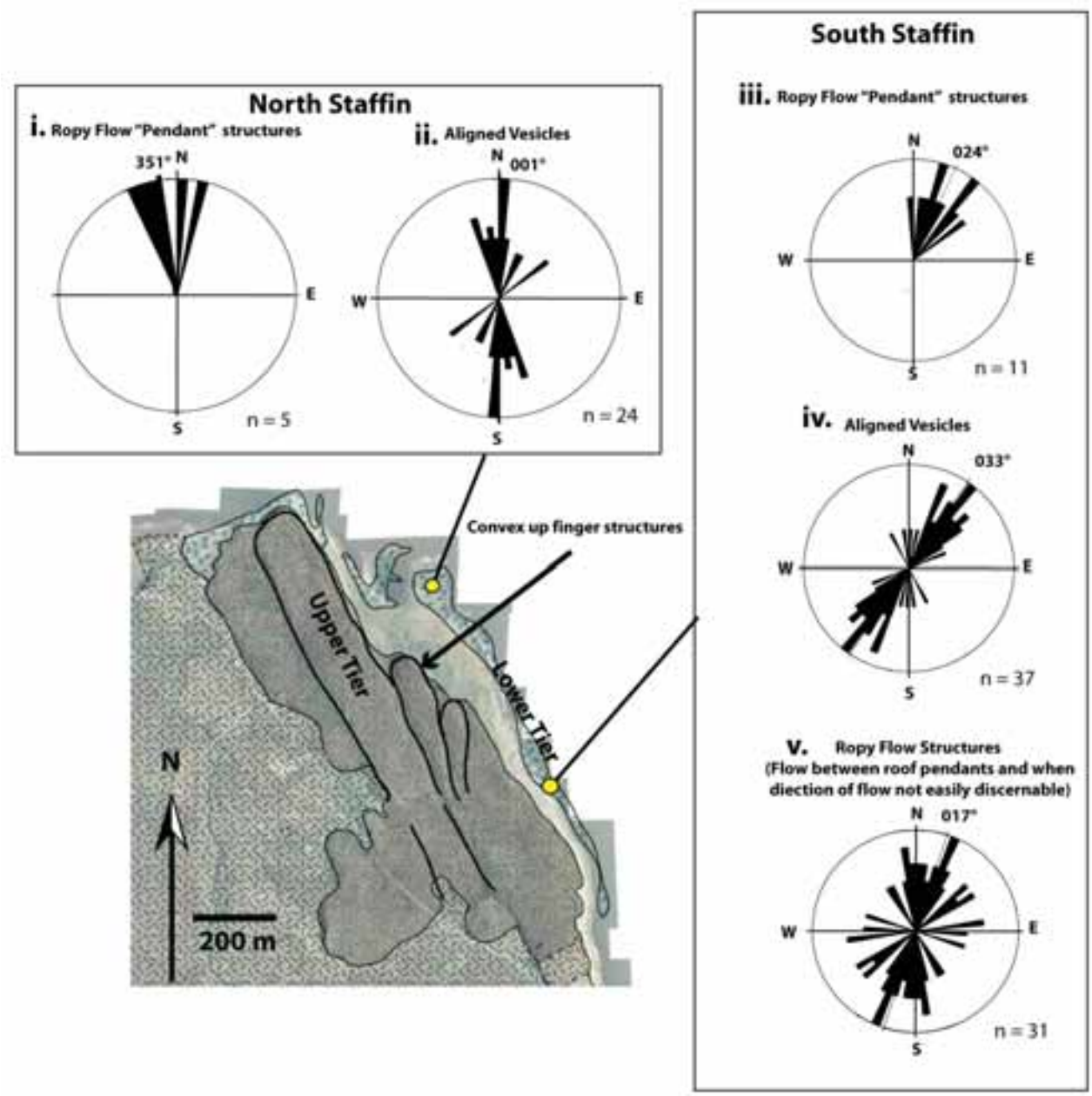

Fig 4.14 – Rose diagrams of ropy flows, ropy flow 'pendant' structures and aligned vesicle orientations (re-drawn from Hutton and Owens, unpublished report) from the lower tier dolerites of Staffin harbour. The outline of the finger structures (marked by thick black lines) can be seen to have their axis coincident with flow within the lower sheet.

erosion of the overlying crinanite layer (Fig. 4.15). The finger structures, as at Staffin harbour, are defined inland by the presence of shallow valleys running in an approximate SE-NW orientation. The four finger structures of Camas Mor have a wavelength of ~ 500 m and lie between to normal faults. It is hard to determine if the finger structures at Camas Mor are a product of sill emplacement or a function of one or more of faulting, erosion or glaciation, due to the erosion of the overlying crinanite, poor exposure and lack of flow indicators. However there is no evidence of faulting in the form of linear valleys on the fore-shore north of the fingers.

Two of the fingers at this location show evidence of tapering in a SE direction. If indeed the fingers are related to flow, this would suggest that the flow direction is in a SE – NW direction (Schofield et al., *in press*), matching the inferred flow direction seen at North Staffin.

4.4 Igneous stratigraphy and emplacement

Sill emplacement in the Trotternish peninsula area did not occur as a single intrusive event Gibson and Jones, (1991). The following sections outline the igneous stratigraphy of the sills across the Trotternish peninsula. The sills have been split into three zones across the peninsula, the south eastern dolerites, central dolerites and northern dolerites (Fig. 4.16; Map. 8 and 9). For detail of localities see Map. 4.

4.5 South eastern dolerites

4.5.1 Invertote and Rub nam Brathairean

Invertote offers the most easily accessible locality to study the sill stratigraphy in detail (Gibson and Jones, 1999) (Fig. 4.17). Invertote quarry (NG 519 606) shows a typical sill stratigraphy of crinanite sitting structurally above picrite (Fig. 4.17), and as noted by Gibson and Jones, (1991), the base of the crinanite displays evidence of cooling texture against underlying picrite suggesting the picritic unit emplaced prior to the crinanite. The contact between the two units is sharp and is easily traceable easily traced onto the adjoining cliff sections (Fig. P1.1). The lower picrite layer within the coastal cliff section takes on a segmented and layered appearance.

Compositional layering within the picrite units across the peninsula is common (Gibson and Jones, 1991; Emeleus and Bell, 2005). However the segmented and blocky

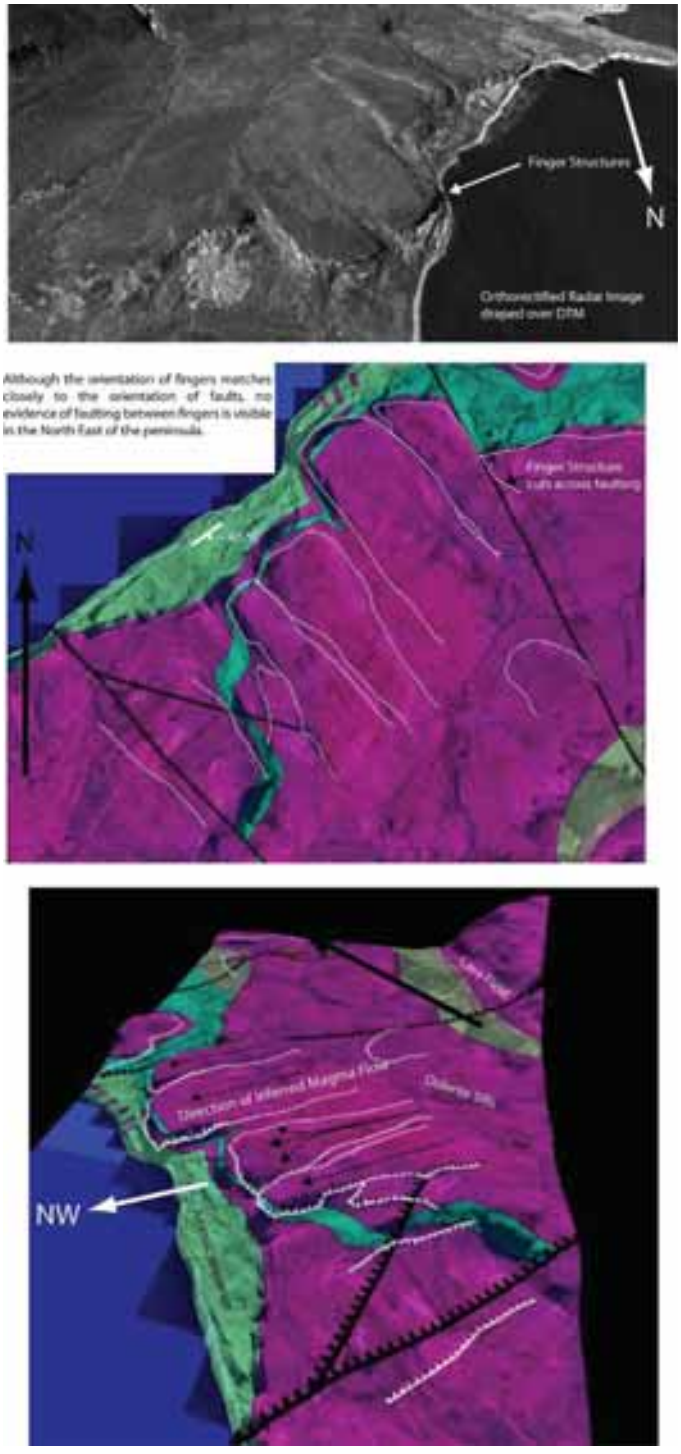

Fig. 4.15 – DTM showing the Camas Mor finger structures at the leading edge of dolerite on the NE coast of the Trotternish peninsula (top) and with BGS 1:50000 solid geology map draped over (middle and bottom). The finger structures (white) within dolerite (purple) can be seen to have an axis coincident with the orientation of inferred fault traces as mapped by the BGS.

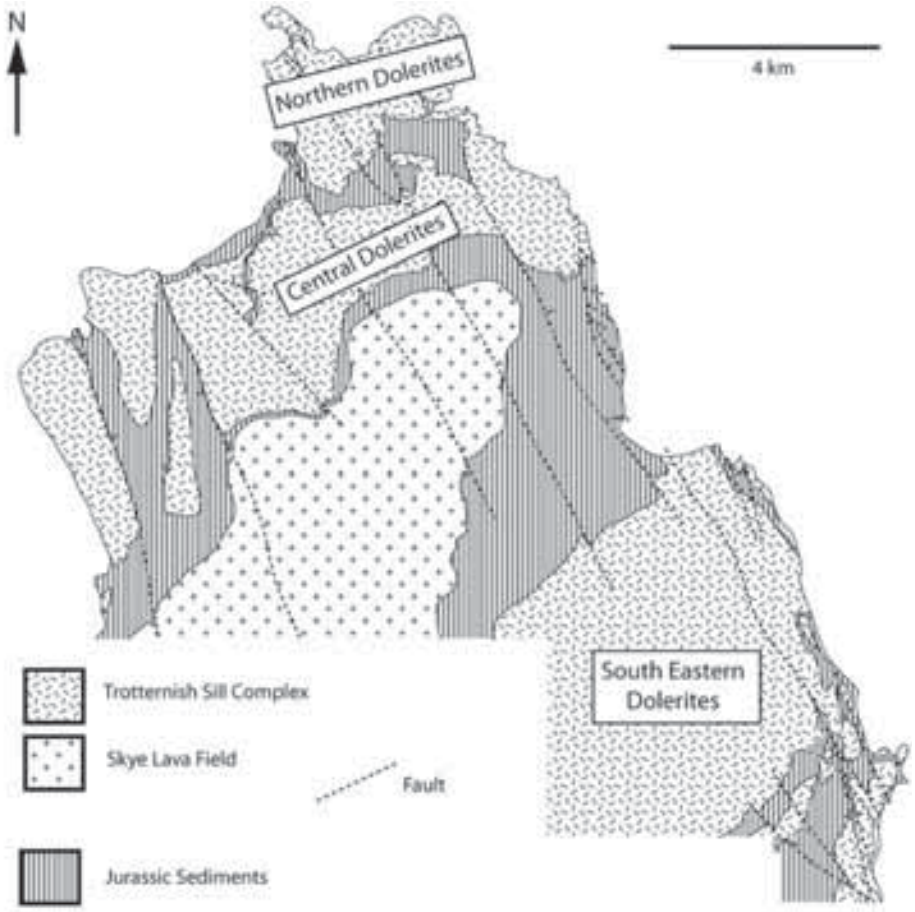

Fig 4.16 – The three divisions of the Trotternish sill complex for ease of description and orientation.

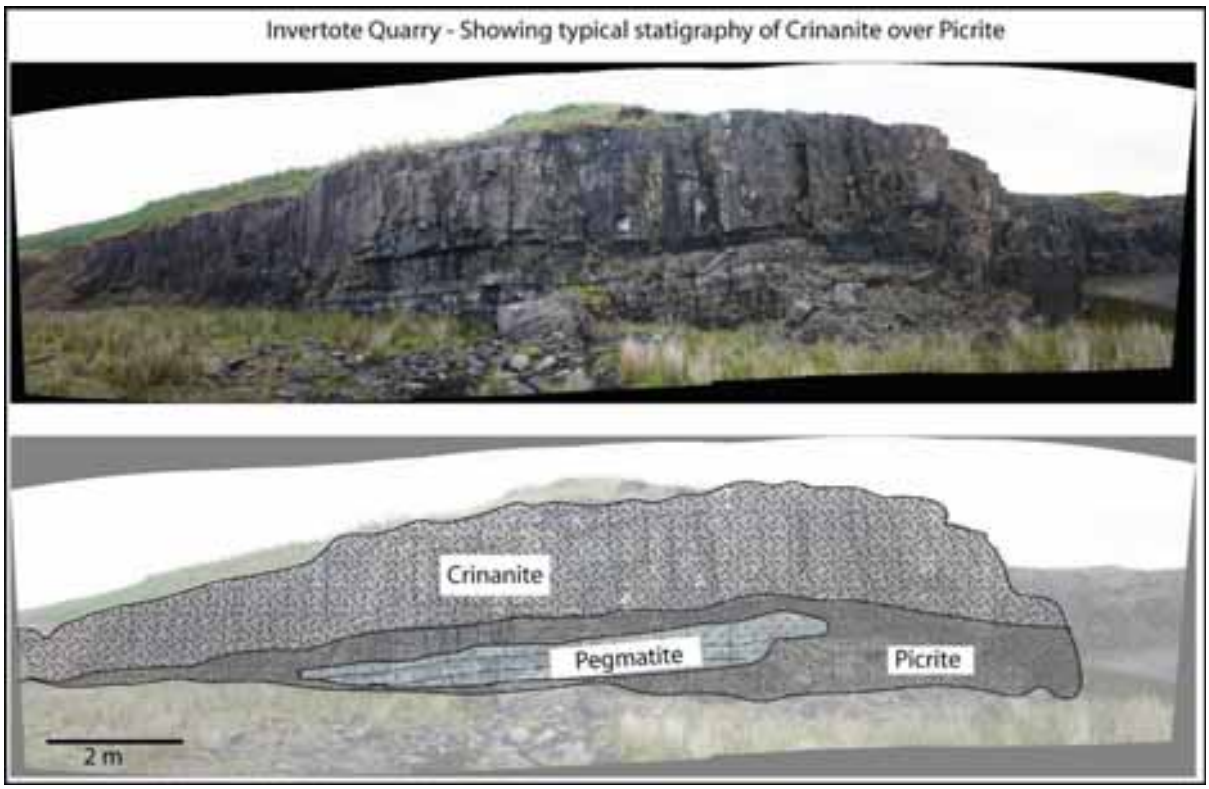

Fig 4.17 – Invertote quarry showing quarry face exposing contact between crinanite and picrite, the crinanite post dates the picrite. Note the sharp nature of the contact between crinanite and picrite.

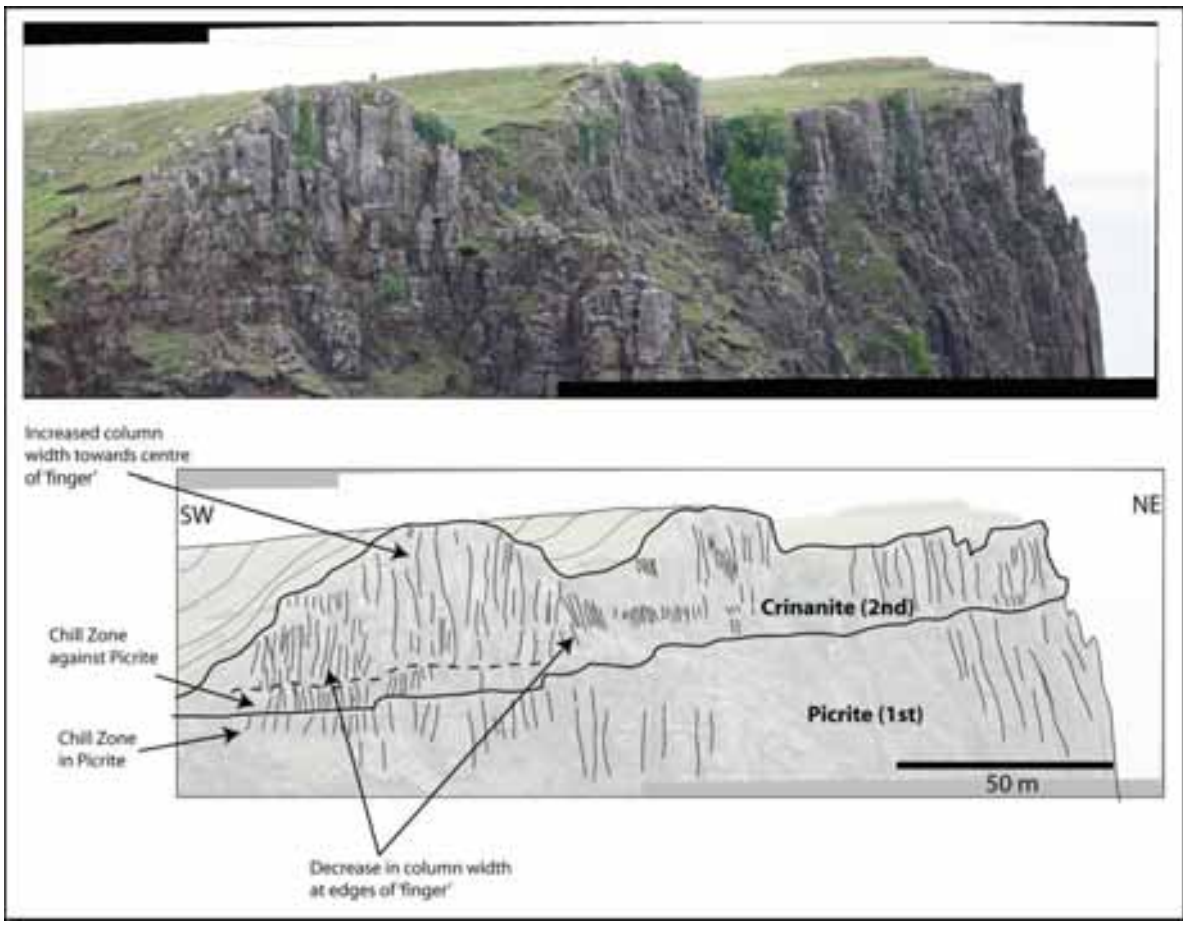

Fig 4.18 – Figure showing cliff section of crinanite at Invertote displaying convex-up profile, note decrease in columnar joint width towards troughs of the undulations.

nature to the columnar joints within the picritic unit (Fig. 4.18) resembles that more closely related to the formation (and breakdown) of horizontal jointing patterns across columnar joints (Bermudez and Delpino, 2008) rather than that developed by mineral layering alone.

The top surface of the crinanite shows a distinctive undulating nature to its surface, similar to the convex-up finger features preserved at Staffin, but on a smaller scale (Fig. 4.18). Interestingly columnar joint width can be seen to decrease within the troughs of the undulations but increase in width towards the peaks of the undulations. This would suggest that columns now seen within the troughs underwent faster cooling compared to the peaks of the undulations (Grossenbacher and McDuffie, 1995) suggesting that the now exposed top surface corresponds approximately to that of the original intrusion surface, i.e. ridges representing thicker parts of the units, and troughs thinner.

The convex-up tops to the crinanite can be traced inland using changes in slope (Fig. 4.19), until obscured by thickening Pleistocene deposits. The convex-up profiles visible within the cliff section appear to amalgamate inland into one broad convex-up landform profile approximately 125 m away from the cliff edge (Fig. 4.19b). Interpreting these features as analogous to the convex-up features at Staffin, and therefore related to flow, the amalgamation of the unit in a NW direction away from the cliff face would imply that the flow is bifurcating in a SE orientation, and therefore the flow direction of the top crinanite unit at this location is in a NW to SE trend.

Along the cliff section from Invertote to Rub' nam Brathairean (Fig. P1.2), the picrite unit maintains a fairly constant thickness along the cliff section before thinning towards the NE of the section and the Rubha Nam Brathairean headland. The top crinanite unit can be seen to change in apparent thickness along section, however this is likely the result of erosion instead of actual true thickness changes in the sheet, as evidence of a chilled top cannot be observed. The section has been considerably dissected by faults, although most post-date the sills, some appear to pre-date the intrusions.

Indicators of flow direction, or flow axis, are sparse, however at Rubha nam Brathairean (Fig. 4.20), several indicators occur in the crinanite sills exposed on the foreshore. Here inclined rafts of shale can be seen separating bodies of dolerite (Fig. 4.20a and 4.20b). These rafts of shale represent the eroded remains of a broken bridge, with the axis of the bridges being traceable along the fore-shore (Fig. 4.20a). Taking the bridge axis to be orientated along the axis of magma flow (Hutton, in press), the axis of magma flow within the sheets of the Rub nam Brathairean foreshore is approximately NE – SW. Figure 4.21 shows a

bottom chilled contact of a dolerite sheet, within the chilled margin, small finger-like forms in the region of 1-2 cm in diameter appear to bud and branch, in a eastwards orientation. These features would seem analogous to those describe by Baer (1991) occurring in the chilled contacts of dykes, produced by ductile deformation of host rock during intrusion. The branching and budding of the features would suggest a flow direction of magma in a eastward direction, which agrees with the axis of magma flow as given by broken bridge structures.

A map showing sill units and inferred flow directions is shown in Figure 4.22. The thinning of the picrite unit towards the headland of Rub nam Brathairean, although not a reliable indicator of magma flow direction, suggests that the source for the picrite was located in a easterly to south easterly direction, suggesting possible separate feeder locations for the picrite (emplaced first) and the crinanite (emplaced second). The flow directions of the structurally lowest exposed crinanite sheet (Green, Fig. 4.22) suggest flow within the crinanite predominantly occurred in a SW to NE direction.

4.5.2 Dun Dearg, Lough Mealt and Kilt Rock

The cliff section from north of Rubha Nam Brathairean to South Staffin provides some of the most spectacular cliff sections around the Trotternish peninsula, including the tourist viewpoint of Kilt Rock (P1.3).

The section is characterised by multiple intrusions of sills (Fig. P1.4); Gibson and Jones (1991) showed the composition of the sills within the section are all crinanitic in composition. However, evidence for multiple intrusions or pulses can be seen within the sills (Fig. P1.4). This illustrates that although the petrographic distinction of sill units as proposed by Gibson and Jones (1991) is broadly correct, the petrology alone cannot differentiate the multiple pulses which can be identified from internal contacts within the sills.

The section is dominated by two sills of dolerite (Fig. P1.4), with the lower sill being cut by the upper sill. The upper tier dolerite sheet forms a broad open synformal structure, locally stepping up stratigraphy e.g. Kilt Rock. The broad open synformal structure formed by the dolerite sheet appears to be more a function of gentle folding of the Jurassic strata prior to intrusion of the dolerite, which has been preferentially exploited by the dolerite sheet intruding along the Duntulm Formation (lower Ostrea beds), rather than a primary function of the dolerite sheet stepping up stratigraphy. The thickness of the dolerite is fairly uniform at ~ 40-50m in thickness, except in the structurally lowest area of the sill at Lough Mealt were the

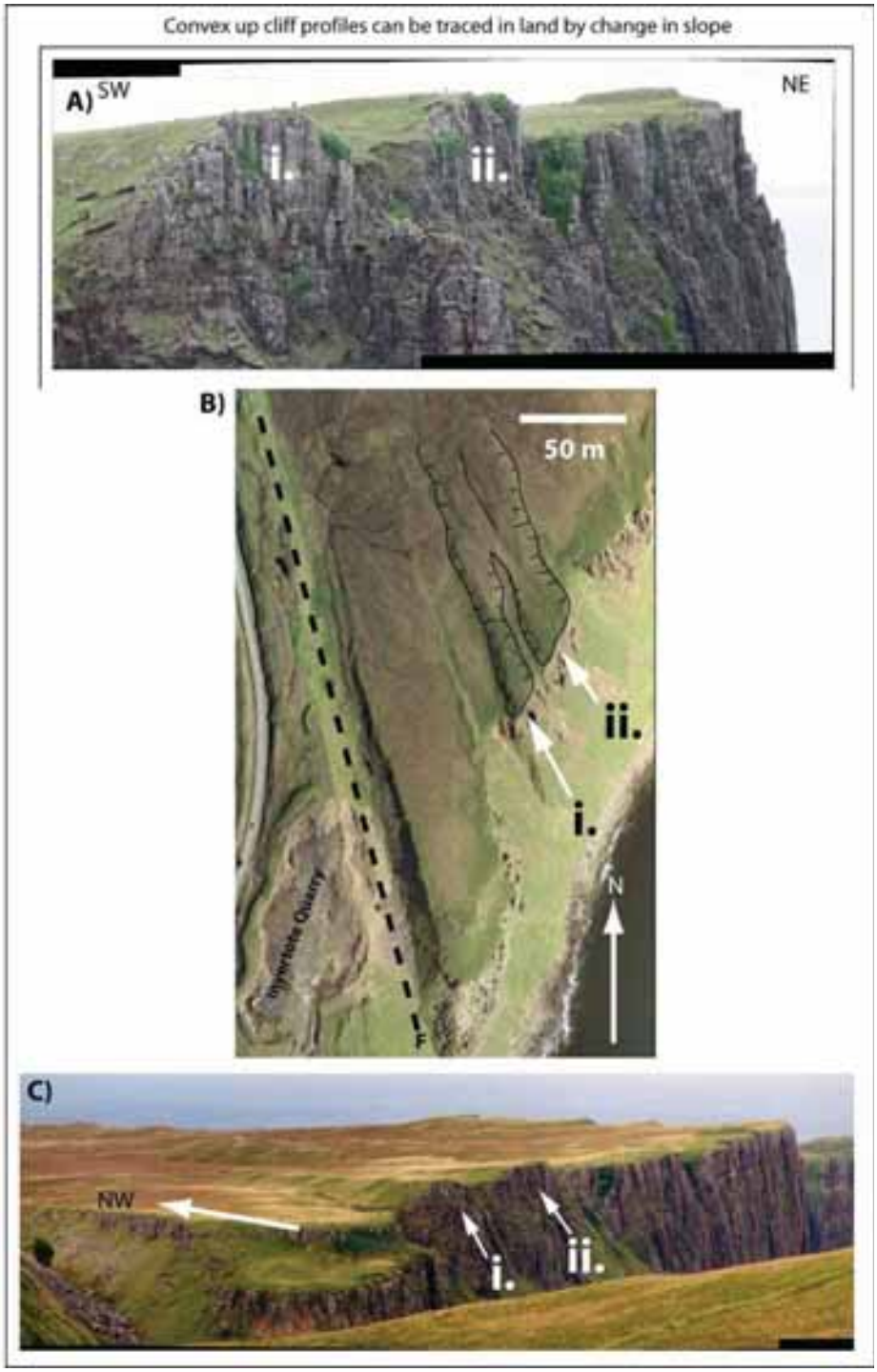

Fig 4.19 – Inland expression of convex-up cliff profiles as seen in Fig. 4.14. Inland the two convex-up cliff profiles (fig. a, i. and ii.) are defined by two corrugation structures extending ~ 125 m in a NW direction away from the cliff edge (fig. b and c).

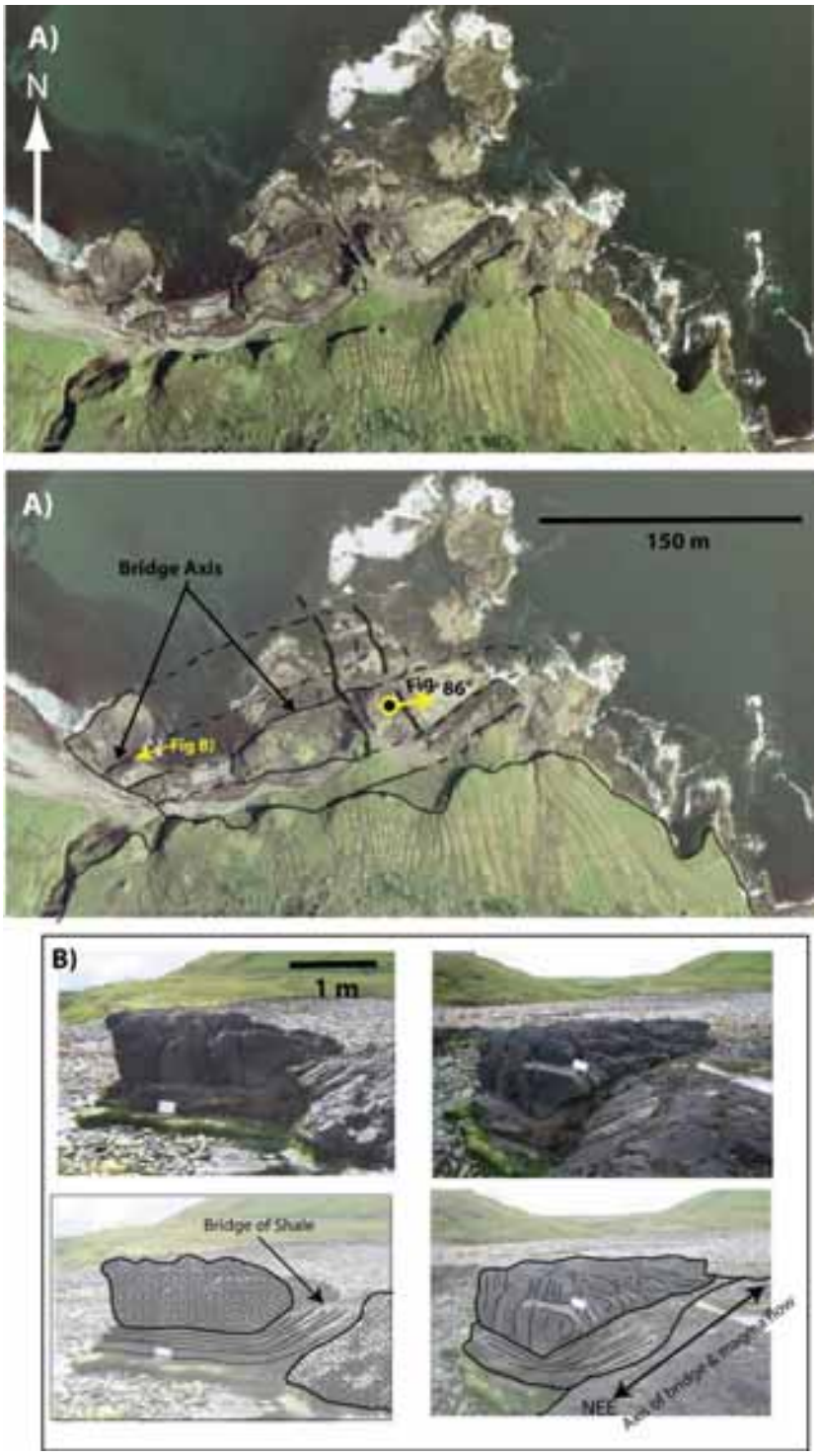

Fig 4.20 – Fore-shore of Rub nam Brathairean, which contains the remnants of eroded broken bridges within the dolerite sheets on the fore-shore. A) Bridges axis orientations as traced along the fore-shore. Two dykes (solid black) strike across the sheets in a SE-NW orientation. B) Eroded remnant of broken bridge, and preserved bridge of shale between two sheets of dolerite, axis of bridge and magma flow marked.

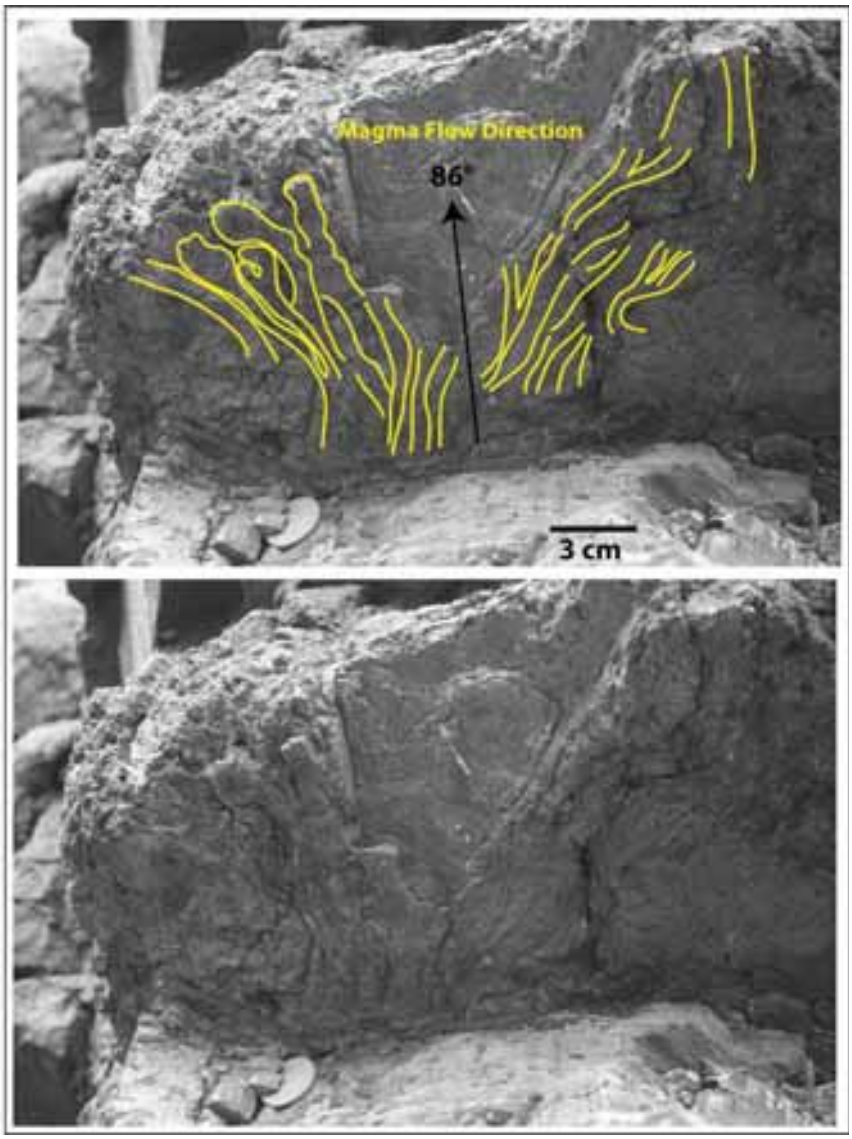

Fig 4.21 – Budding and branching finger structures on bottom contact of sill at Run nam Brathairean (see text for details). Photo taken looking up at bottom contact.

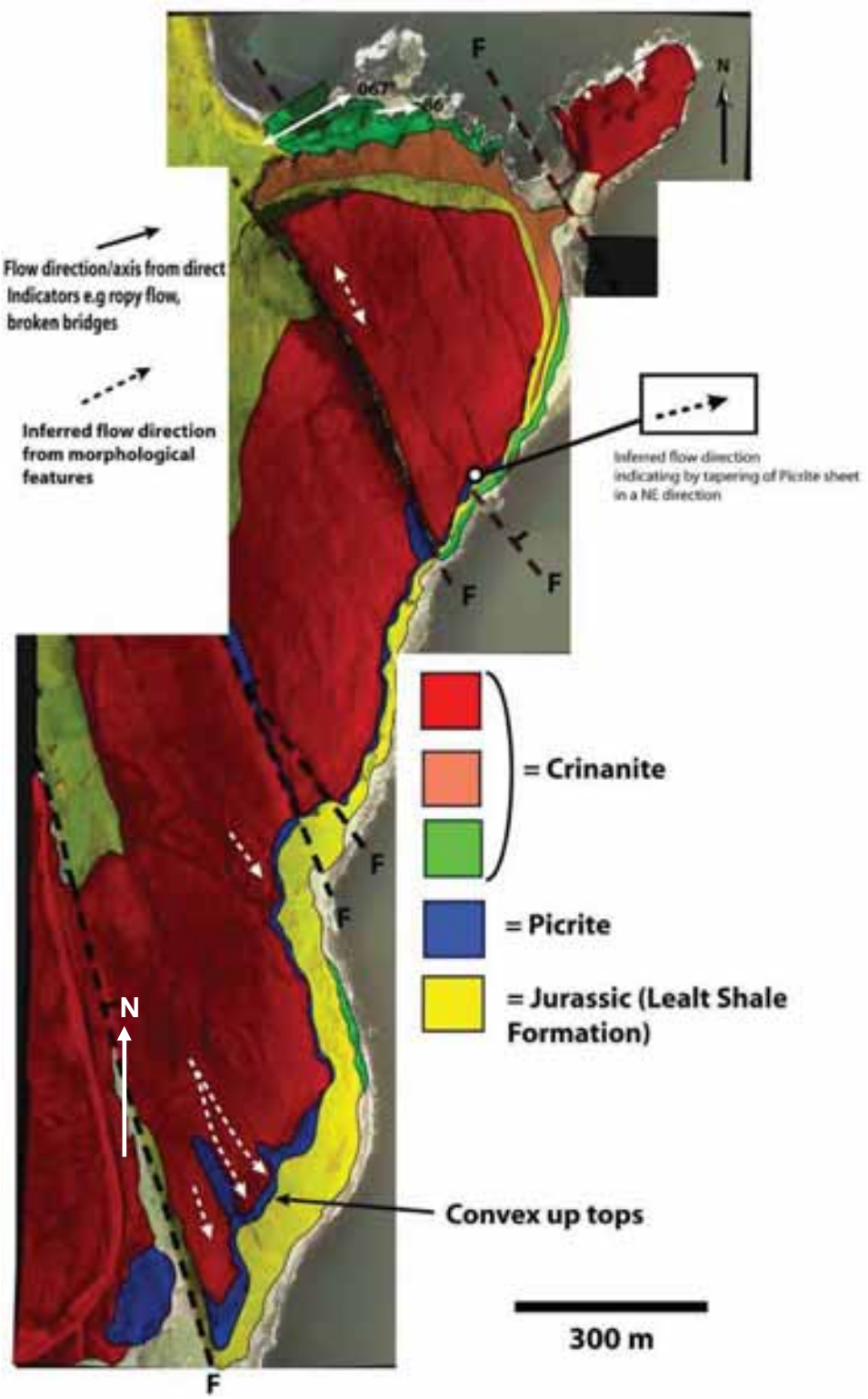

Fig 4.22 – Map showing sill stratigraphy and flow direction of Invertote section (see text for details).

sill thickness is in the region of 80m. The lower tier of dolerite outcrops mainly at sea-level, and occurs almost exclusively within the Valtos Formation (concretionary sandstone).

4.5.3 Dun Dearg – Structural features related to emplacement

Unlike the cliff sections at Invertote, the cliff section of south Staffin possesses many structural features which give indications of flow orientation. The exposure occurs as sheer cliff faces which extend from south Staffin to Dun Dearg. Within the concretionary sandstones (Valtos Fm) of Dun Dearg, the lower tier of dolerite has been emplaced approximately parallel to the bedding. The section contains several structural features in the forms of steps, offset sill segments, un-broken and broken bridges (Fig. P1.5). The prevalence of such features along strike within the cliff face suggests that the current orientation of the cliff face is orientated approximately perpendicular to the sense of the axis of magma flow, approximately ENE-WSW (Map 8).

4.5.4 Lough Mealt – Structural features related to emplacement

South of Lough Mealt, a major broken bridge structure occurs in the upper tier of dolerite, within the structure rafts of Jurassic strata are isolated and inclined to an angle of approximately 35 – 40° from horizontal between two bodies of dolerite forming the upper tier and lower tier (Fig P1.6).

Although the inflation of a sill segment can occur in an effectively continuous manner (Hutton, in press), in the structurally lower sill forming the broken bridge at Lough Mealt, the inflation appears to have occurred in a stepwise fashion by the intrusion of series of pulses of crinanite magma (Fig. P1.6). The first pulse, occurring adjacent to the bridge has poorly formed columnar joints, possibly suggesting rapid cooling of the unit. The second pulse, shows evidence for chill against the first pulse, appears to have emplaced only slightly before the third pulse (see Fig. P1.6). Close to the broken bridge, columnar joint width of the third pulse can be seen to decrease towards the second pulse indicating that the second pulse was acting as a cooling surface, however northwards along section, the columnar joints can be seen to be continuous through the units, suggesting that both the second and third pulse underwent the same cooling regime at this location.

North of Lough Mealt, the sill can be seen to transgress stratigraphy cutting across the lower tier dolerites in the process (Fig. P1.7). Within the upper sill several internal contacts indicated by discontinuous cooling joint sets, suggest that the sill was amalgamated by several

different pulses of magma. However the internal contacts are not laterally continuous suggesting that the separate pulses emplaced contemporaneously with each other and essentially underwent the same cooling regime.

Several steps and broken bridge stubs can be seen within the lower tier sill indicating the magma flow axis was approximately NE-E (Fig. 4.23). For instance just above the shoreline in the northern end of the section, near Kilt Rock, two stubs of country rock caused by vertical inflation of the sill, can be seen in the lower dolerite (Fig. 4.23).

4.5.5 Lough Mealt sheet and Staffin Harbour sheet juncture

Approximately 50m south of the headland forming Kilt Rock, a major sill junction can be seen within the cliff face between the crinanite sill forming the Lough Mealt section and the crinanite sill forming the Staffin harbour section (Fig. 4.24).

The exact nature of the junction is difficult to assess due to vegetation, however differences in columnar joint orientation suggest that the lower Lough Mealt sheet, which can be seen to climb and cut up stratigraphy, is overridden, or cross-cut by the Staffin Harbour sheet.

4.6 Central dolerites

In the South Eastern dolerites of the Trotternish/Little Minch sill complex intrusion of picrite was followed by crinanite. In contrast, within the northern and central dolerites of the Trotternish peninsula, the crinanite pre-dates the intrusion of picrite, although the crinanite still overlies the picrite.

4.6.1 Galta Mor section (Flodigarry-Balmaqueen)

The Galta Mor section consists of sheer, north facing cliffs of dolerite over 100m high that to the foreshores of Balmaqueen (see Fig. P2.1c).

The picrite unit along section shows a well-developed colonnade with columns being ~ 2m in diameter, narrowing and curving into the contact with the overlying crinanite (Fig. 4.25), indicating that the picrite post-dates the intrusion of the crinanite.

Within the southern end of the section at Flodigarry, the dolerite can be seen to step up (Fig. P2.1). Discontinuities and kinked columnar joints within the picrite as seen on the cliff section suggest that the picrite was emplaced in at least two separate pulses, one now exposed above and another one occurs below sea level, the latter only exposed in the step-up structure.

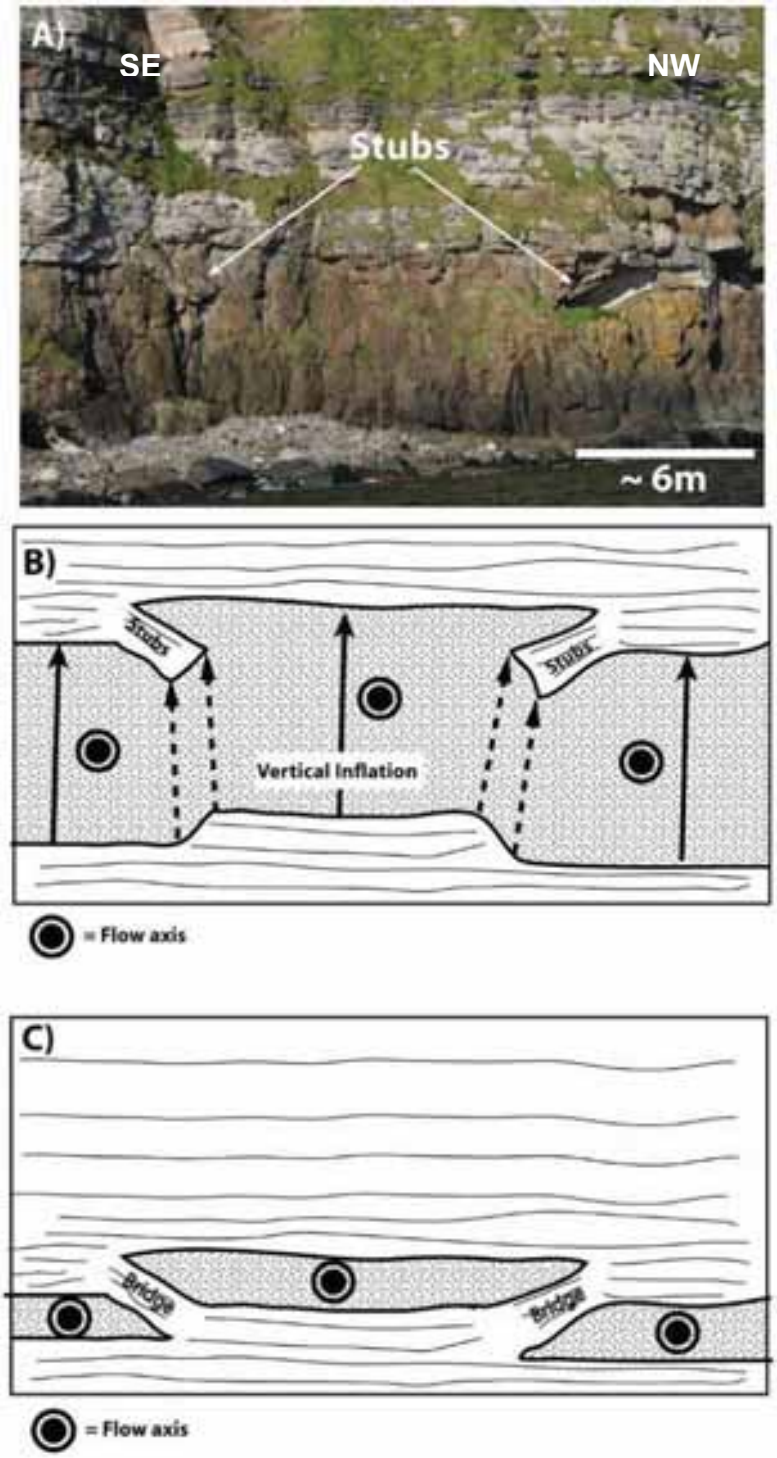

Fig. 4.23 – A) Stub structures in lower tier sill just below Kilt Rock, caused by vertical inflation of offset, but overlapping sill segments (Fig. B and C).

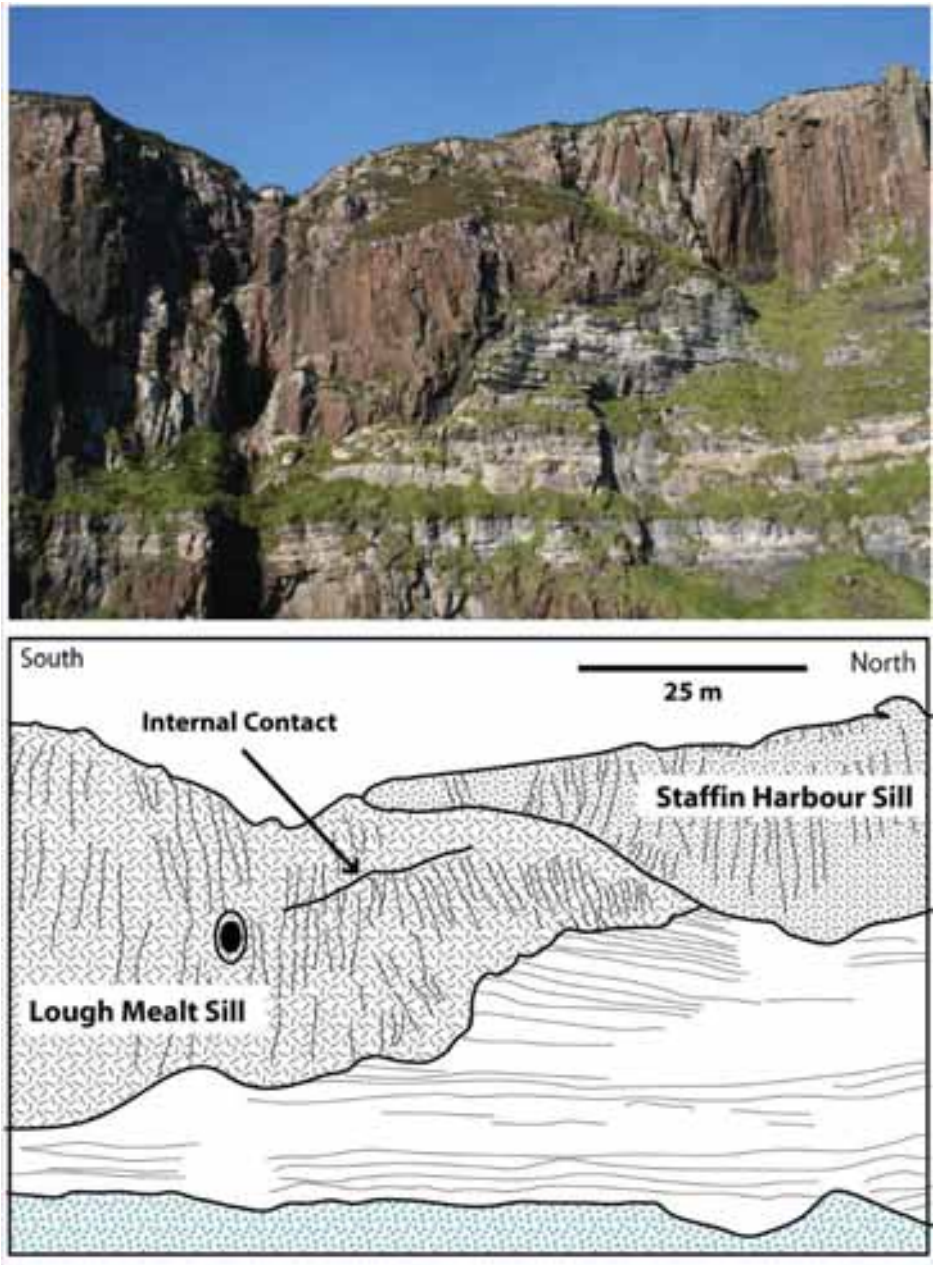

Fig. 4.24– Juncture between Lough Mealt sill and Staffin Harbour sill. Cooling joints within the Staffin Harbour sill are orientated away from the contact with the Lough Mealt sill, suggesting the Staffin Harbour sill cooled against the Lough Mealt sill and was therefore emplaced after the Lough Mealt sill.

The aerial photograph of the step-up structure reveals the presence of finger like structures with convex-up tops, similar to those seen at Staffin Harbour (Fig. 4.26 and P2.3). These structures appear to be primary and no evidence for faulting can be seen offsetting the lowest sill unit at sea-level, suggesting that the junctures between the finger structures are primary morphological features related to emplacement.

4.6.2 Rubh' a' Chairn Leith (RCL)

The sills of Rubh' a' Chairn Leith (RCL) form the westernmost expression of sills exposed within the Trotternish peninsula. Gibson and Jones (1991) showed that the sills of RCL were composed entirely of picrite, however mapping of coastal and inland sections shows that the sills are composed of separate pulses of picrite. Figure P2.3 shows the coastal cliff section of RCL with mapped out internal contacts. Most of the section consists of sheer vertical faces of dolerite, making outcrop inspection of the internal contacts difficult, but such a contact is accessible towards the west of the section. Although cooling joints are pervasive throughout the picrite, two separate layers of picrite can be identified (Fig. P2.4). A heavily altered glassy margin can be traced laterally along the section forming a discontinuity between the two units (Fig. 4.28). This discontinuity can be traced inland by change in slope (Fig. P2.4b, Fig. 4.29).Other internal contacts across the section can also be traced in inland and illustrate the multiple pulses of picrite which have taken place to form the RCL headland as a whole (Fig. 4.30).

4.7 Northern dolerites

The sills within the northern section preserve the same stratigraphic relationship as the rest of the peninsula i.e. crinanite structurally above picrite. However the relative timing of the two units is not as clear as in the rest of the peninsula. The dolerite forming sills the northern section were emplaced structurally below the sills forming the central dolerites (Fig. 4.31).

The sills of the northern section are the thickest of any sills preserved around the peninsula, with the sill forming the headland of Meall Tuath having a total thickness of approx. 120 m. The presence of chilled tops, as displayed on the cliff section, and columnar joints orientated perpendicular to the current top surface of the dolerite (Fig. P2.6) suggest that the sill thickness is close to the true thickness at time of intrusion, although no evidence for a chilled top can be seen at Meal Tuath, implying some erosion has occurred and that aggregate thickness of the sill at this location could have been greater at time of emplacement.

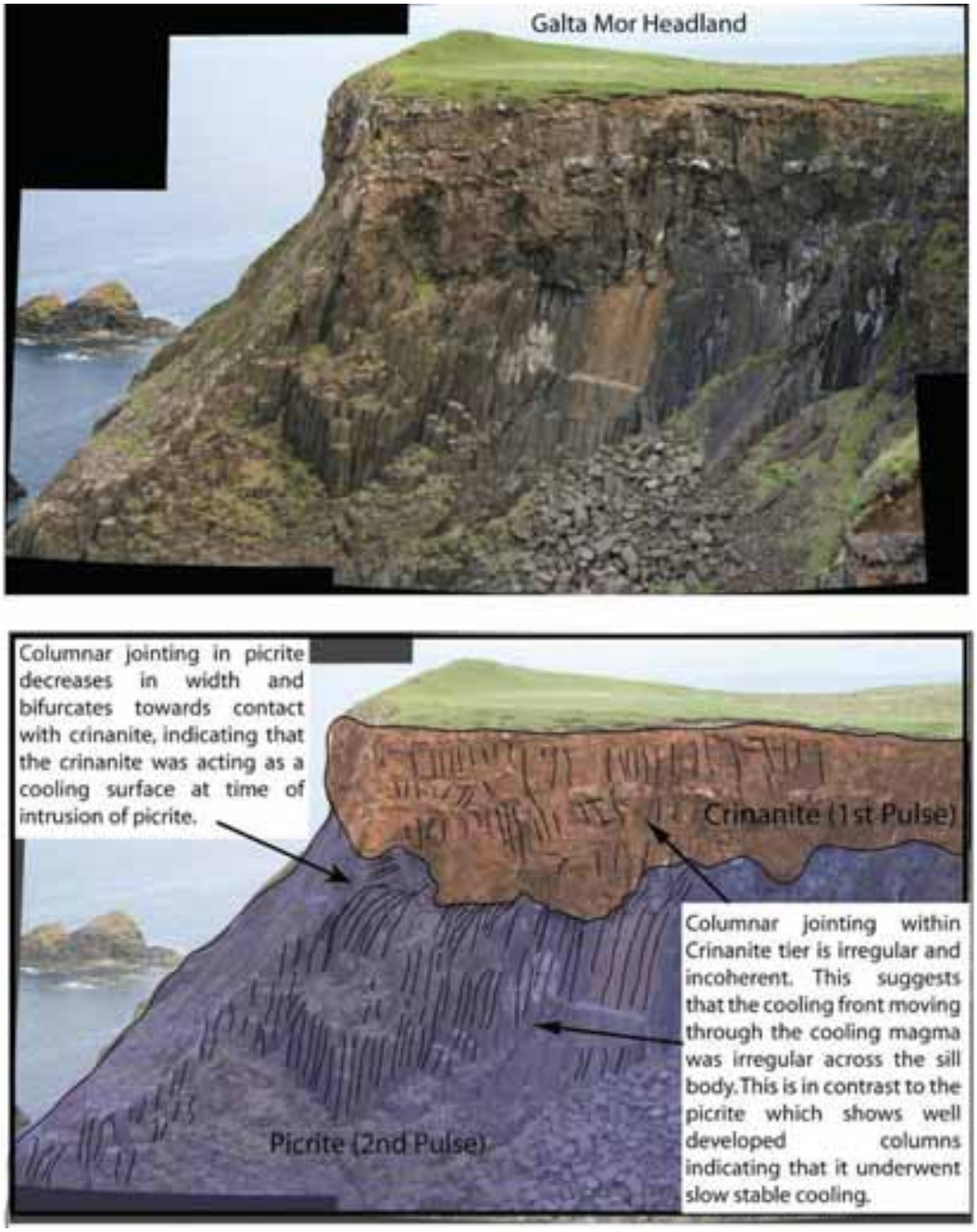

Fig. 4.25 – Cliff section and interpretation showing cooling joints in lower picrite unit decreasing in width and curving towards overlying crinanite, suggesting overlying crinanite layer acted as a cooling surface and therefore pre-dated the intrusion of picrite. Photo looking south-east.

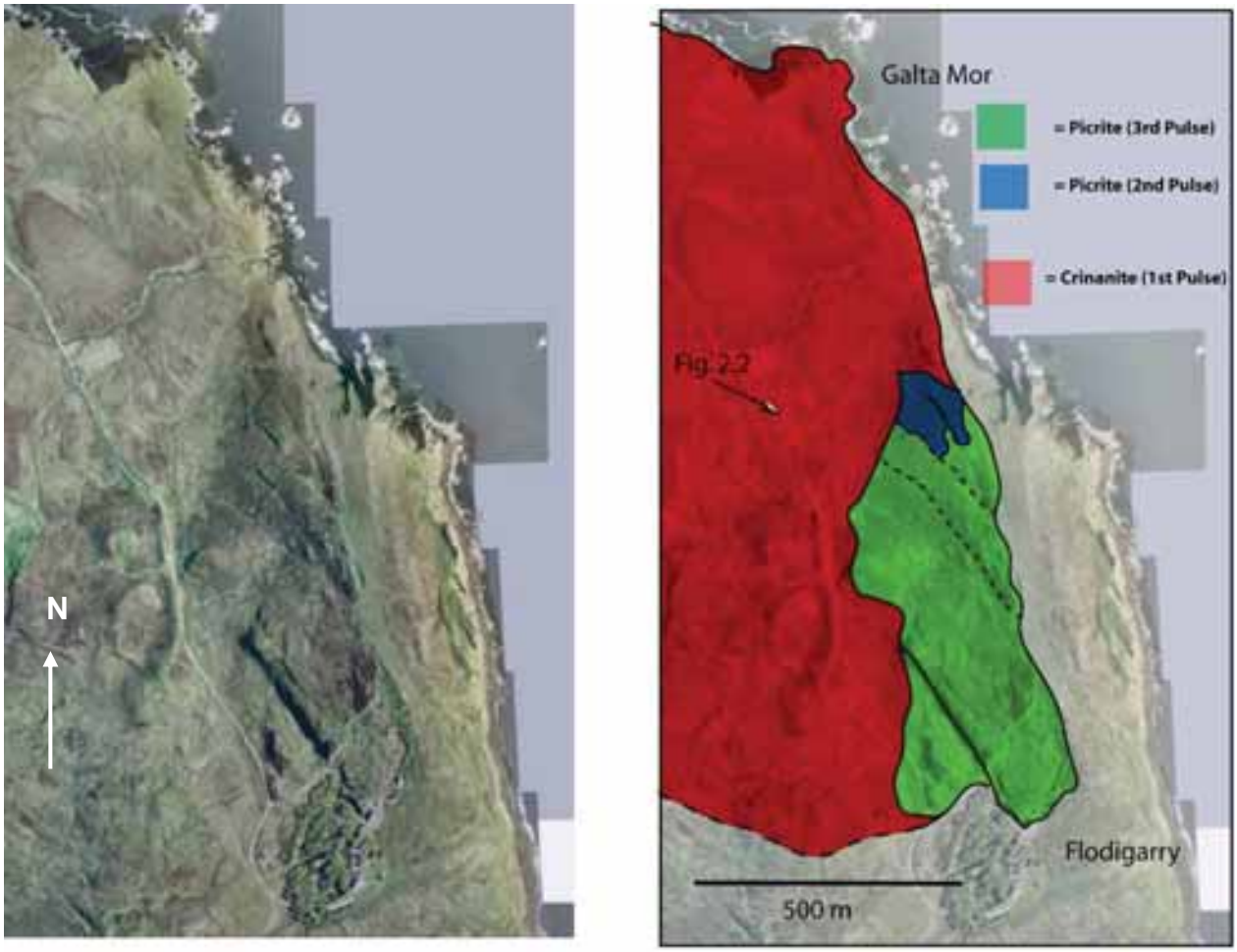

Fig. 4.26 – Aerial Photograph and map showing finger structures and sill stratigraphy as defined in coastal sections (Fig. P2.2).

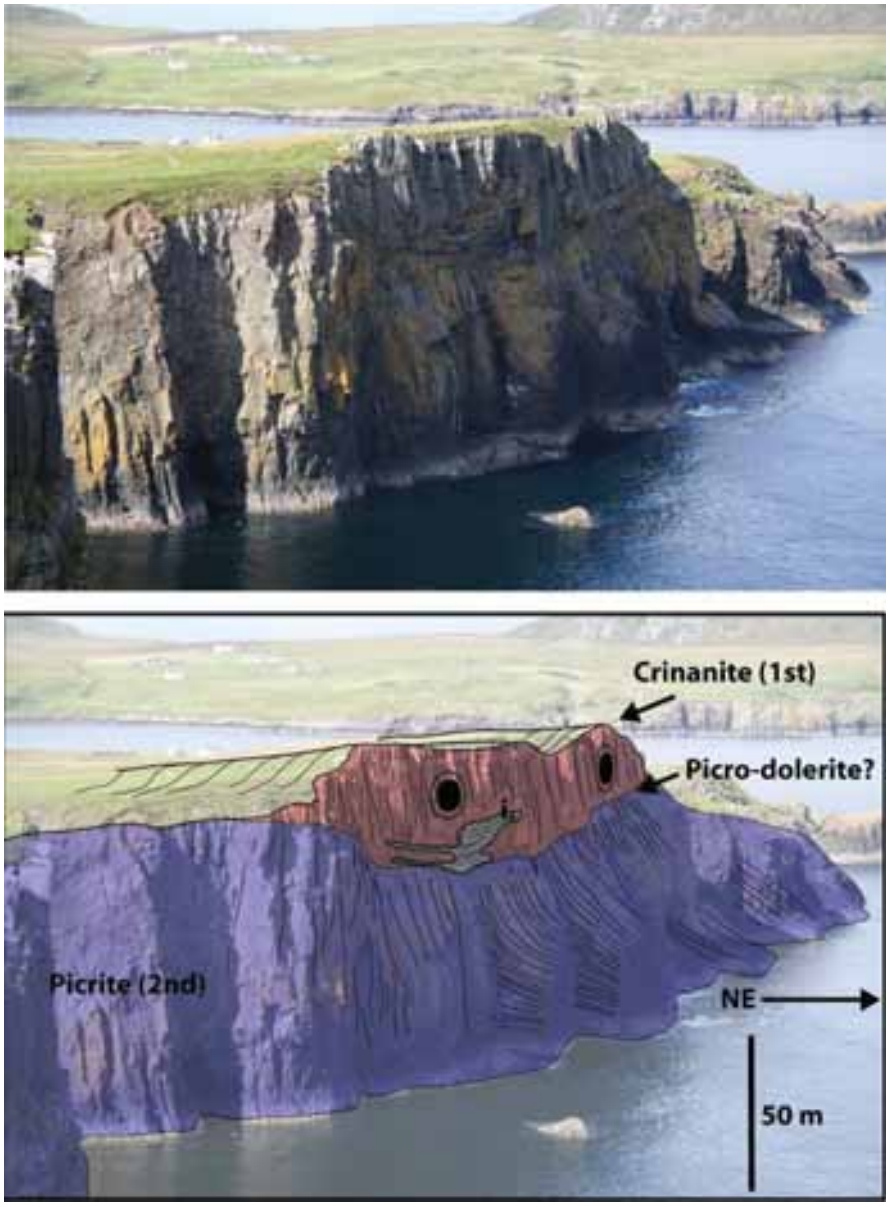

Fig. 4.27 – Finger structure bending up at Balmaqueen, with picrite cooling away from contact with crinanite. See Fig. P2.1 for location.

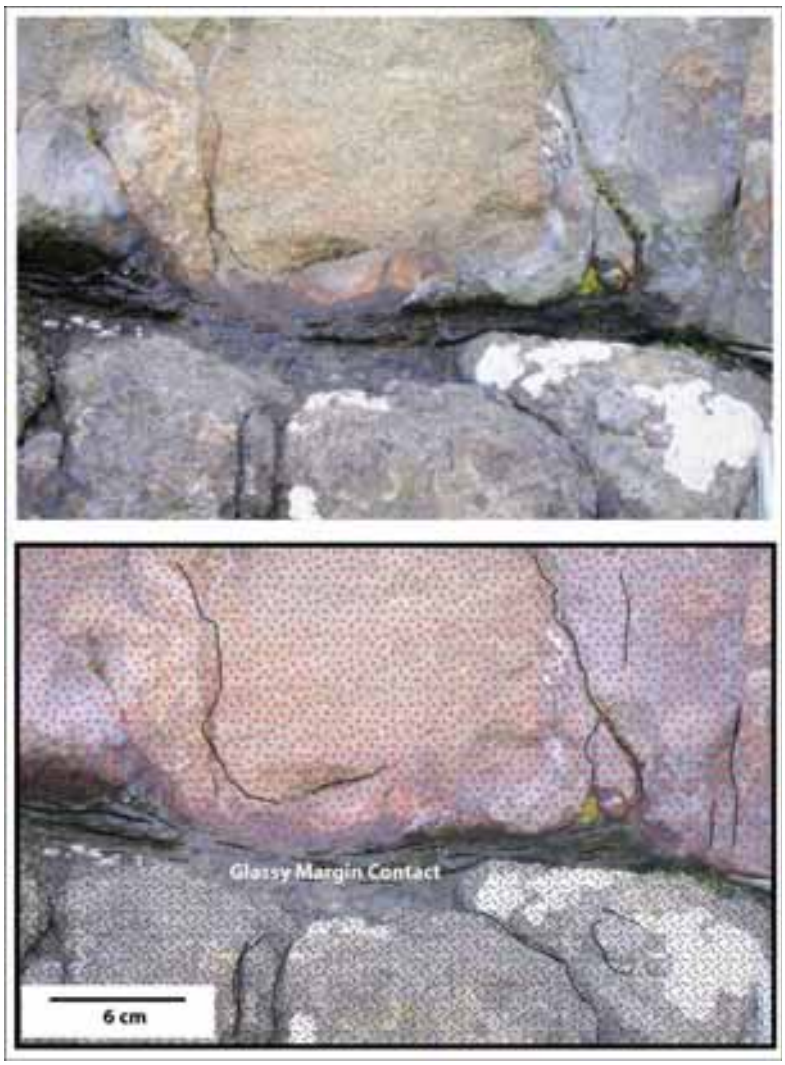

Fig. 4.28 - Glassy margin preserved between picritic units.

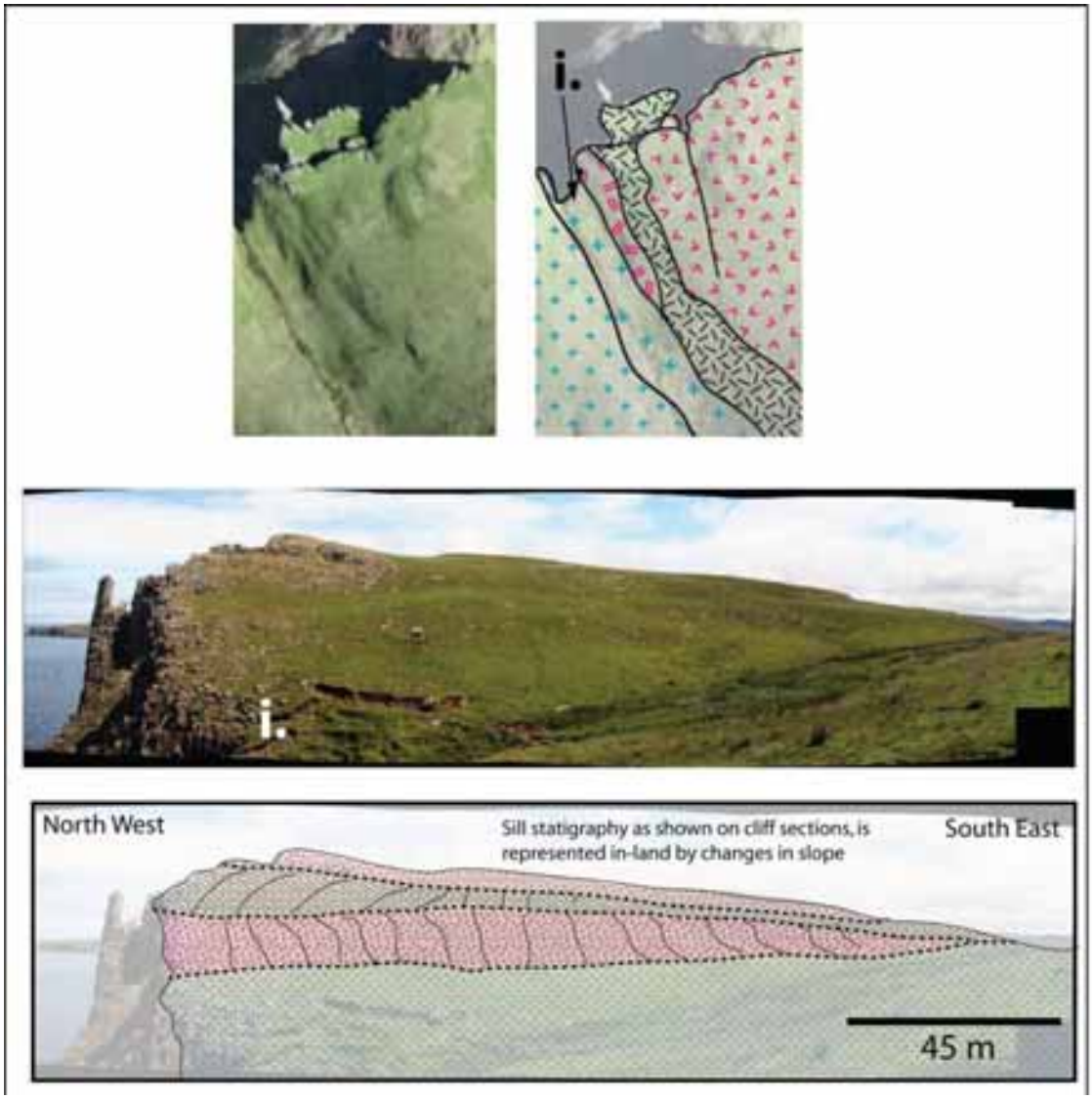

Fig. 4.29 – Change in slope expression of sill stratigraphy exposed on coastal sections.

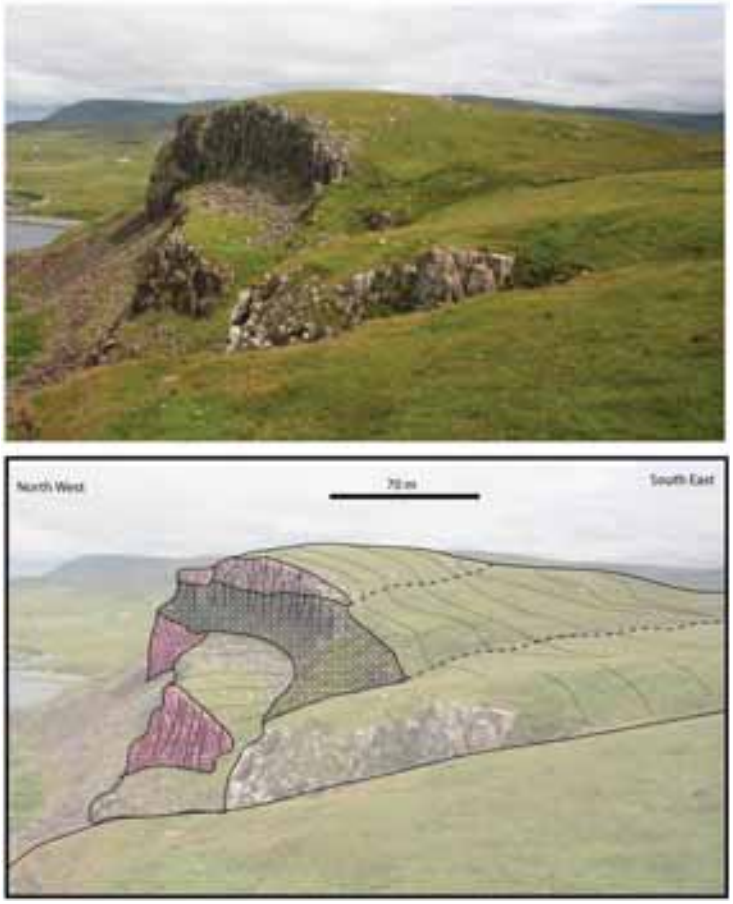

Fig. 4.30 – Oblique view of RCL cliff face, showing how separate sill units, as defined within the cliff face can be traced inland by changes in slope.

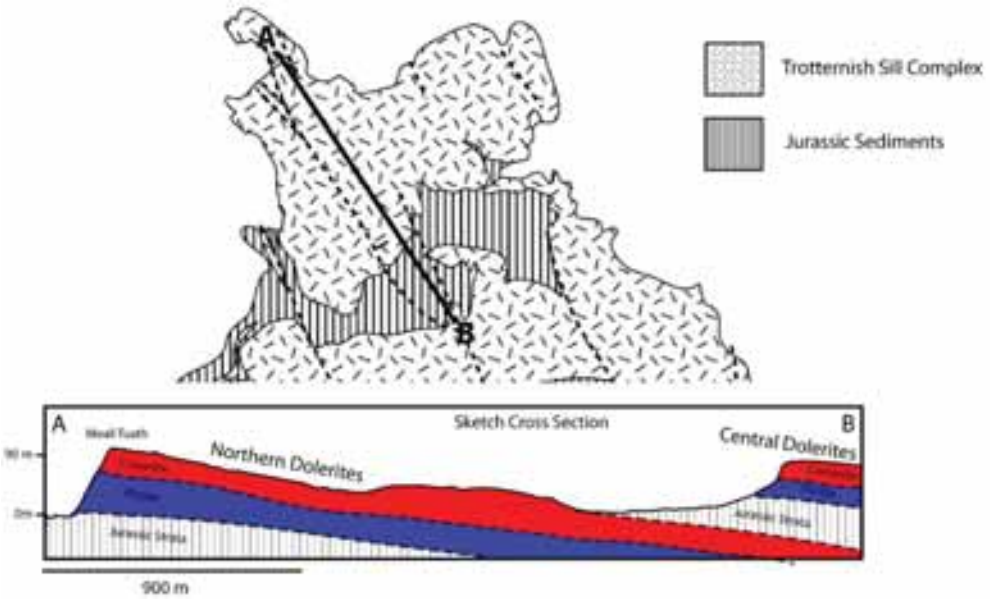

Fig. 4.31 – Sketch cross-section across peninsula. The sills forming the northern dolerite sills can be seen to have intruded at a lower stratigraphic level when compared to the central dolerite sills.

4.7.1 Timing of intrusion of picrite and crinanite

Within the northern section, the relative timing the crinanite and picrite units in respect to one another is not as clear as in other areas of the peninsula. At Meall Tuath, adjacent to the fault zone cutting the cliff face, the picrite unit is seen to post-date the intrusion of the crinanite unit (Fig. 4.32).

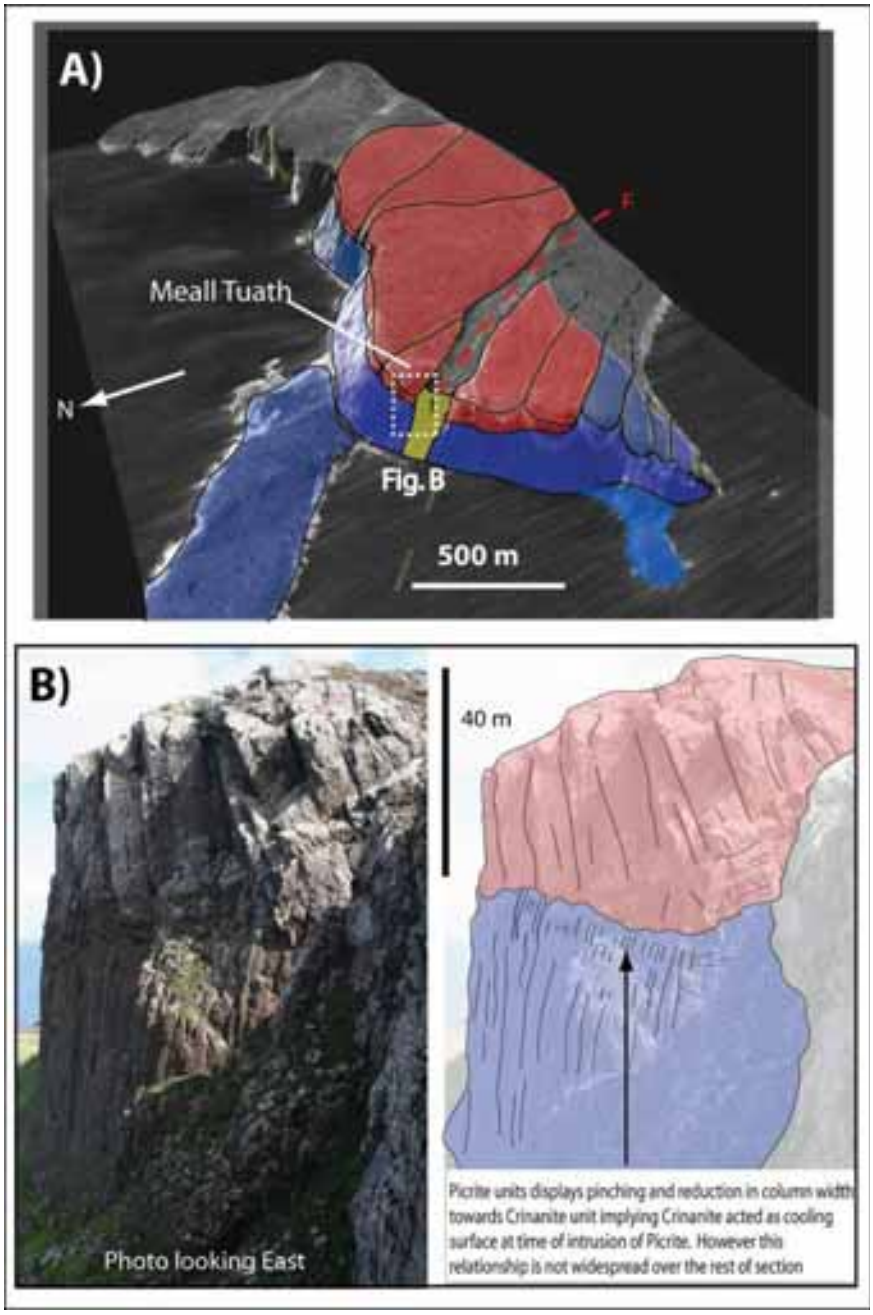

Fig. 4.32 – A) Oblique view of DTM with crinanite (red) and picrite (blue) shown B) Blocky jointed crinanite with underlying picrite appearing to have cooled against the contact with the overlying crinanite (see text for details).

At this locality the overlying crinanite unit has a blocky appearance as a result of large width in cooling joints. The zone of blocky jointed crinanite extends from west of the fault zone, to approximately 50 m east of the fault zone where columnar joints reduce in width until the joints become pervasive through both crinanite and picrite units (Fig. P2.6, Fig. P2.7)

The relationship as seen at Meall Tuath is somewhat contradictory. Within the blocky crinanite, the large column width would imply that the crinanite sheet has undergone slow cooling (Ryan, 1978). However the underlying picrite, shows evidence to suggest it cooled against the overlying crinanite, which implies that the blocky crinanite must have cooled sufficiently to act as a cooling surface before intrusion of picrite. The blocky nature within the crinanite may be result of a second period of sustained flow within the sheet (magma channels; Polteau et al*.,* 2008), but if this is the case is unclear.

As with RCL, the sill stratigraphy exposed on the cliff section can be traced and inland (Fig. P2.8).

4.8 Discussion

4.8.1 Recognition of sill outcrops and faulting across the peninsula.

The inland exposure of the sill complex and Jurassic country rock is extremely poor, but the sill complex, in general can be easily differentiated inland from Jurassic host rocks by marked changes in slope (e.g. Map. 6). Also faulting, which clearly affects both Jurassic and dolerite units e.g. the fault at Meall Tuath can be easily picked out on the bare-earth DTM (Map 2-6).

However, examination of the DTM raises questions with regard to the current published BGS interpretation of the area, in particular to the faulting. Across the Trotternish peninsula, it is clear from the DTM that within the northern and central dolerites some of the faults have clear topographic expression through the dolerite sills (Map. 6 and 7), indicating that they cut the dolerite sheets (e.g. Meall Tuath). However many of the faults which clearly cut the Skye lava field do not show any sign of topographic expression within the dolerite sheets. It could be argued that lack of topographic expression of the faults is the result of thick Pleistocene deposits, but within other areas of the peninsula, which also have overlying Pleistocene deposits the faults can be seen to have a topographic expression across the dolerite sheets (Map. 7). In addition topographic features within the dolerite sheet, such as at Balmacqueen, are not offset along inferred faults traces, suggesting that the faults do not cut the dolerite sheets (Map. 7).

On this basis Map 8 and 9 represents the re-interpretation of faulting and sill outcrops within the peninsula. Inferred fault traces cutting the dolerite sheets have been restricted to areas were a topographic expression is visible, or an offset of sill features occurs.

The main implication of this interpretation is that some of the faults cutting the peninsula occurred post-eruption of lava and pre-intrusion of the sills. This would be in agreement with the eruptive history of the lavas, which pre-date the intrusion of the sills (Emeleus and Bell, 2005).

Studies of other sill complexes have shown that sill emplacement is influenced by the existence of pre-existing structure, e.g. in the form of faults (Carter Krogh and Valentine, 1986; Thomson, 2007; Thomson and Schofield, 2008). In such circumstances the presence of faults can act as pathways to magma movement (Thomson and Schofield, 2008) or as barriers by offsetting preferential horizons of magma propagation within host rock, effectively preventing magma intrusion occurring across faults (Francis, 1982).

Anderson and Dunham (1966) noted the sills of the Trotternish peninsula maintain a fairly uniform level of emplacement, attributing this to the sills following an isobaric level, i.e. where magma pressure equals that of the lithostatic pressure (Bradley, 1965). Sills are known to preferentially exploit shale and limestone horizons (Liss, 2004) and it would seem that the fairly uniform level of emplacement of the sills of the Trotternish peninsula is more likely the result of preferential exploitation the Kilmaluag, Duntulm and Valtos Formation of the Great Estuarine series by the intruding magma (Hutton and Owens, Unpublished Report) (Fig. 4.33).

These formations are mostly composed of interbedded limestone, shale and sandstone horizons and it is suggested that particular horizons within these formations acted as preferential beds for intrusion of magma (Fig. 4.34a). Therefore it is proposed that the offset of these sequences by faulting prior to intrusion of the sills lead to preferential intrusion of specific horizons within fault blocks, thus effectively channelling magma along the NW – SE axis of the fault blocks (Fig. 4.34b).

4.8.2 Magma flow directions and sill stratigraphy of the Trotternish Sill complex

All the pulses forming the sills of the south eastern dolerites can be seen to have flow directions which are approximately in a NE direction. However some divergence in the flow direction is apparent. At Invertote the finger structures give a direction as predominantly

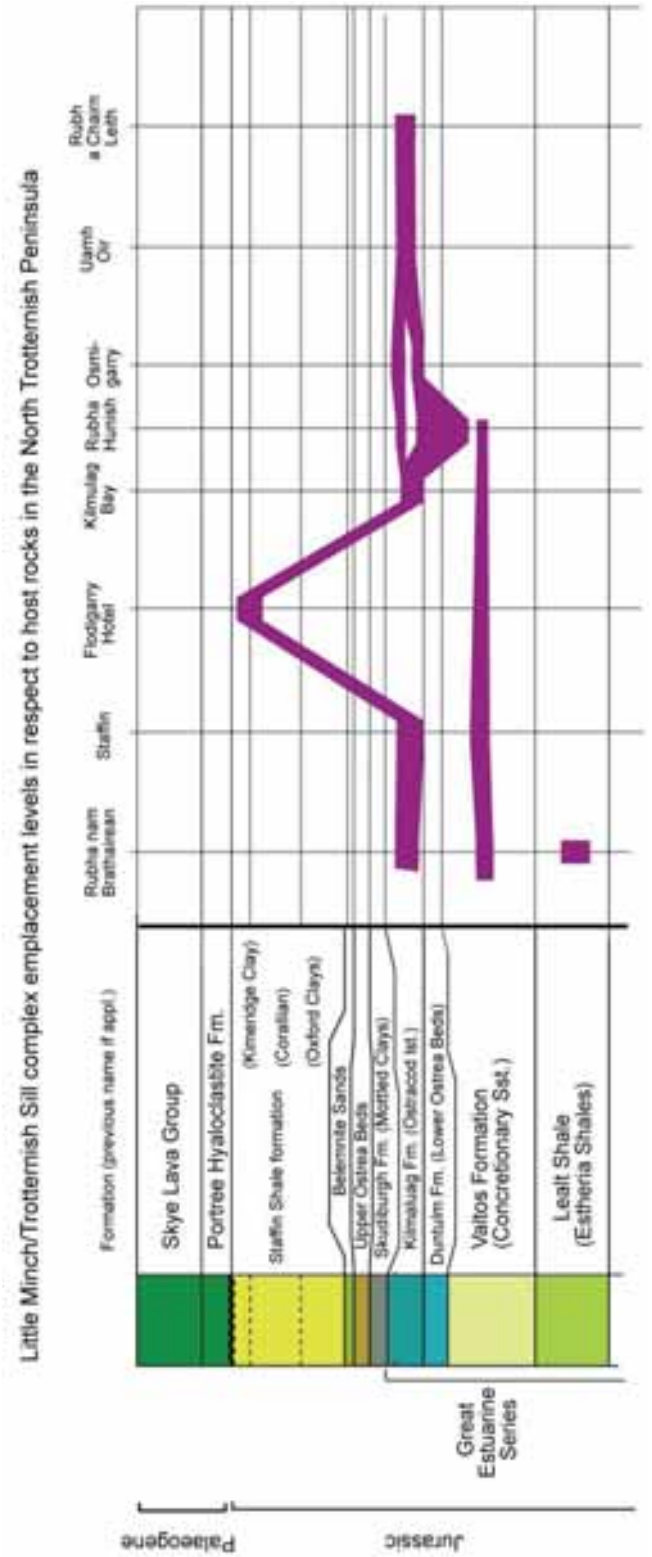

Fig. 4.33 – Emplacement level of the Trotternish Sill Complex (re-drawn and modified from Hutton and Owens, unpublished report)

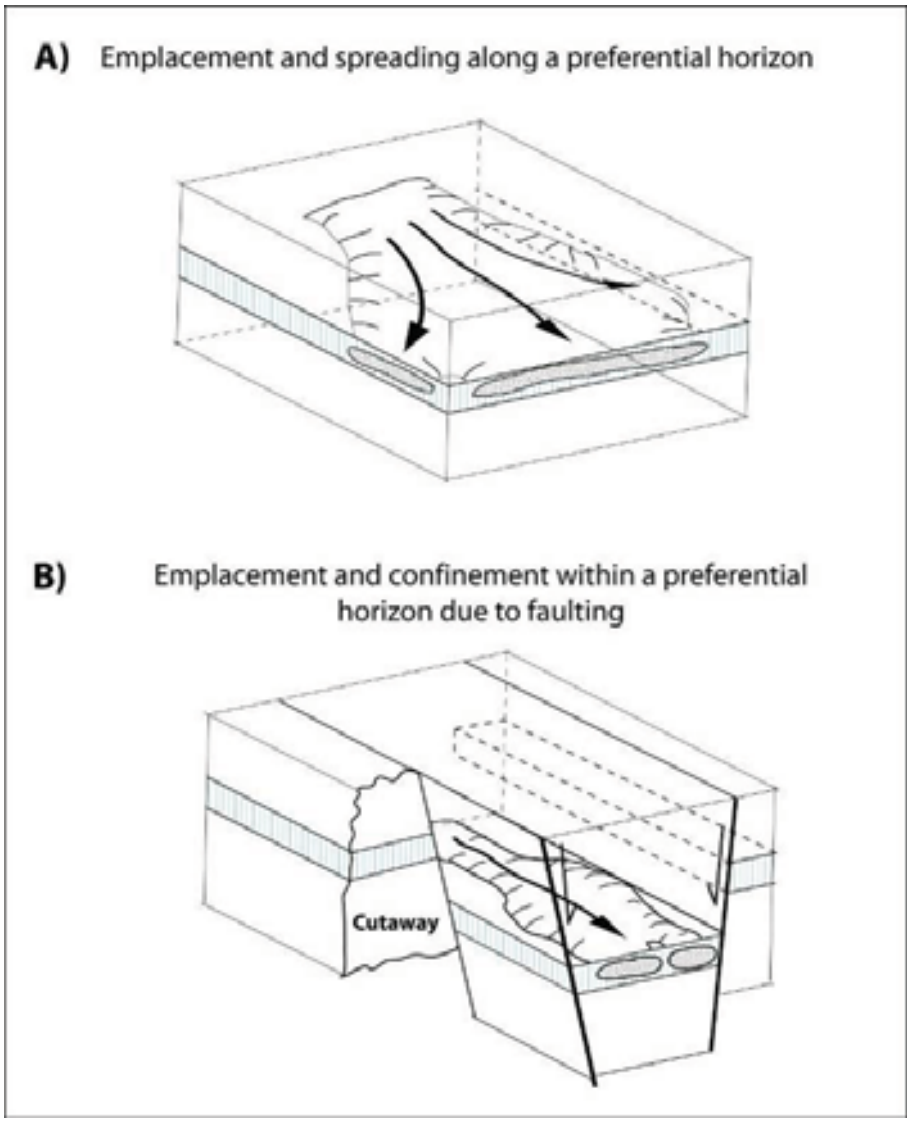

Fig. 4.34 – Schematic illustrating possible effects of faulting on channelling of magma. A) The magma follows and spreads out along preferential horizon. B) Faulting causes magma to be confined within preferential horizons within the fault block, channelling the magma along the axis of the fault block.

south, whereas the magma flow direction at Staffin harbour diverges from northwards to north-eastwards moving south along the coast.

In the north, although unambiguous flow directions in the form of magma flow indicators such as aligned vesicles, broken bridges and steps are lacking, the inferred magma flow appears to be orientated predominantly in a NW direction over most of the northern and central dolerite, suggesting that although the northern dolerites were emplaced structurally below the central dolerites, they were in fact fed from the same source area. Divergence does occur along the Galta Mor section, were divergence in flow appears to occur eastwards and southwards as indicated by the finger structures at Flodigarry and Balmaqueen. Anderson and

Dunham (1966) suggested that the sills of the Trotternish peninsula had been fed from separate source regions, based on the complicated field relationships they encountered, however this would be disagreement with the work of Gibson and Jones (1991) who propose a common source for the sills.

Gibson and Jones (1991) proposed that the emplacement of LMSC occurred by sequential withdrawal of magma from a fractionated and compositionally zoned alkali dolerite magma chamber. In addition, Gibson and Jones (1991) stratigraphically linked the picritic units occurring in the south-eastern dolerites to the picritic units within the central and northern dolerites. The cooling relationships interpreted from columnar joints show that the central dolerites are characterised by the relationship of crinanite followed by picrite, whereas as the southern dolerites consistently show picrite followed by crinanite. This difference in relative timing would suggest that the stratigraphic linking of the sill units of the northern and central dolerites with those in the south east by Gibson and Jones (1991) may be incorrect.

4.8.3 New emplacement model for Trotternish Sill Complex

Petrographic and geochemical data of Gibson and Jones (1991) are combined with the stratigraphic and flow direction study presented in this chapter, to generate a new emplacement model for the Trotternish sill complex. Several key points are considered;

- Gibson and Jones (1991) proposed that the sills of the Trotternish peninsula were sourced from one compositionally zoned magma chamber.
- The model of Gibson and Jones (1991) proposed that the different petrological compositions of the sills in the Trotternish peninsula can be explained by varying discharge rates from the source magma chamber. In the model Gibson and Jones (1991) they proposed that the olivine-poor crinanite sills seen across the peninsula were the result of low discharge rates from the magma chamber, whereas the olivine-rich picrite sills were the result of high discharge rates tapping deeper olivine-rich levels in the chamber.
- Faulting within the peninsula may have occurred contemporaneously with emplacement of the sills. It should be noted that in the south eastern dolerites, the sills appear to be heavily affected by the NE-SW trending faults cutting the peninsula, whereas no expression of faulting is visible in some of the sills in the northern and central dolerites.

- Mappable pulses of magma occurring in crinanite and picrite units are more readily identified in coastal sections within the crinanite sills in the south eastern dolerites. Mappable pulses are less identifiable in the picrite units across the peninsula, except at RCL.
- The exact timing between the northern and central dolerites and south eastern dolerites is unknown. However opposite age relationship between the crinanite and picrite units in the northern and central dolerites compared to the south eastern dolerites, plus the change in general flow direction may suggest that the dolerites of these two areas were emplaced at different times. Therefore the stratigraphic linking of the areas by Gibson and Jones (1991) may be incorrect.

The discharge rate model of Gibson and Jones (1991) is difficult to confirm from field data alone. However, assuming that discharge rate equates approximately to emplacement rate (thus low discharge rates led to slower emplacement rates), it might be expected that the crinanite sills emplaced at slower rates during periods of low discharge from the source magma chamber (*sensu* Gibson and Jones, 1991). It therefore follows that crinanite sills may show greater evidence of internal contacts at outcrop, as within picrite sills emplaced under high discharge rates, pulses even if present may be less easily differentiated, due to the short time period between separate pulses suppressing the development of significant cooling surfaces at contacts. This is supported by evidence that the highest concentration of mappable pulses occurs within the 3rd crinanite unit in the south eastern dolerites around Lough Mealt which forms the last intrusive episode forming the sills in this region of the peninsula (Map 8).

The integration of the work of Gibson and Jones (1991) with the data in this chapter, is shown in figure 4.35. Within figure 4.35 the south eastern dolerites are placed at the beginning of the emplacement episode of sills in the peninsula. Although the northern and central dolerites appear to have been emplaced in a separate intrusive event from the south eastern dolerites, no clear field evidence exists within the peninsula to indicate relative timing of each area to one another. However, in section 4.8.1 it was proposed that at least some of the SW-NE trending faults cutting the peninsula may have initiated contemporaneously with emplacement of the sill complex, possibly acting to channel magma along fault blocks. If such faulting initiated after the emplacement of the south eastern dolerites, then this may

explain the change in emplacement area for the magma from south east area of the peninsula to the north of the area by channelling of magma along the NW-SE trending fault blocks.

4.9 Conclusions

4.9.1 Stratigraphy and emplacement history

The Little Minch/Trotternish Sill complex was emplaced in two discrete events, but from one single zoned magma source, which did not undergo replenishment during the emplacement of the complex.

The northern and central dolerites are characterised by two main intrusions of magma forming the sills, crinanite followed by picrite. Within the picrite, pulses can be identified on coastal sections close to Flodigarry. The picrite sill forming the headland of Rubh' a' chairn Leith is composed of approximately eight identifiable pulses of magma although the relative timing of these pulses is unknown. Within the northern headland of the peninsula, the relative timing of the crinanite and picrite units to one another is also uncertain, with columnar joints being generally pervasive through both units, indicating identical cooling conditions. However given the relationship of the central dolerites, it is suggested that the emplacement of the picrite post-dated the emplacement of the crinanite unit.

The south-eastern dolerites are characterised by three main pulses of magma, the first picrite, followed by two separate pulses of crinanite, which can be seen to cut one another (see Lough Mealt, Fig. P1.4). Within the final intrusion of crinanite, up to three pulses of magma can be differentiated by the presence of internal contacts within the host rock.

4.9.2 Corrugated sill tops

A common feature seen within the crinanite units across the peninsula is presence of convex tops to the sills which can be traced inland, often for several hundreds of metres to kilometres, forming finger-like features in the region of 50 – 500 m in width. The presence of chilled facies on these features can be identified in places e.g. Staffin Harbour, suggesting the tops of some of these features are close to the original tops of the sills prior to erosion.

Attributing the convex-up finger like features to glacial processes can be discounted as Devensian ice-flow across the peninsula occurred oblique to the axis of the features suggesting that the two are not related.

Magma flow indicators in the form of ropy flow structures and aligned vesicles at Staffin harbour indicate that magma flow within other sills in the region of where the fingers

are present was orientated approximately along the axis of the fingers. The primary morphology of these features, coupled with the magma flow indicators infer that the finger structures seen across the peninsula are possibly related to magma flow.

The convex-up features seen within the peninsula have not been previously identified in the published literature on Skye, possibly because the features were dismissed as a result of glaciation and erosion. Similar convex-tops to sills can be seen to be a common feature of sills as will be shown in the following chapter.

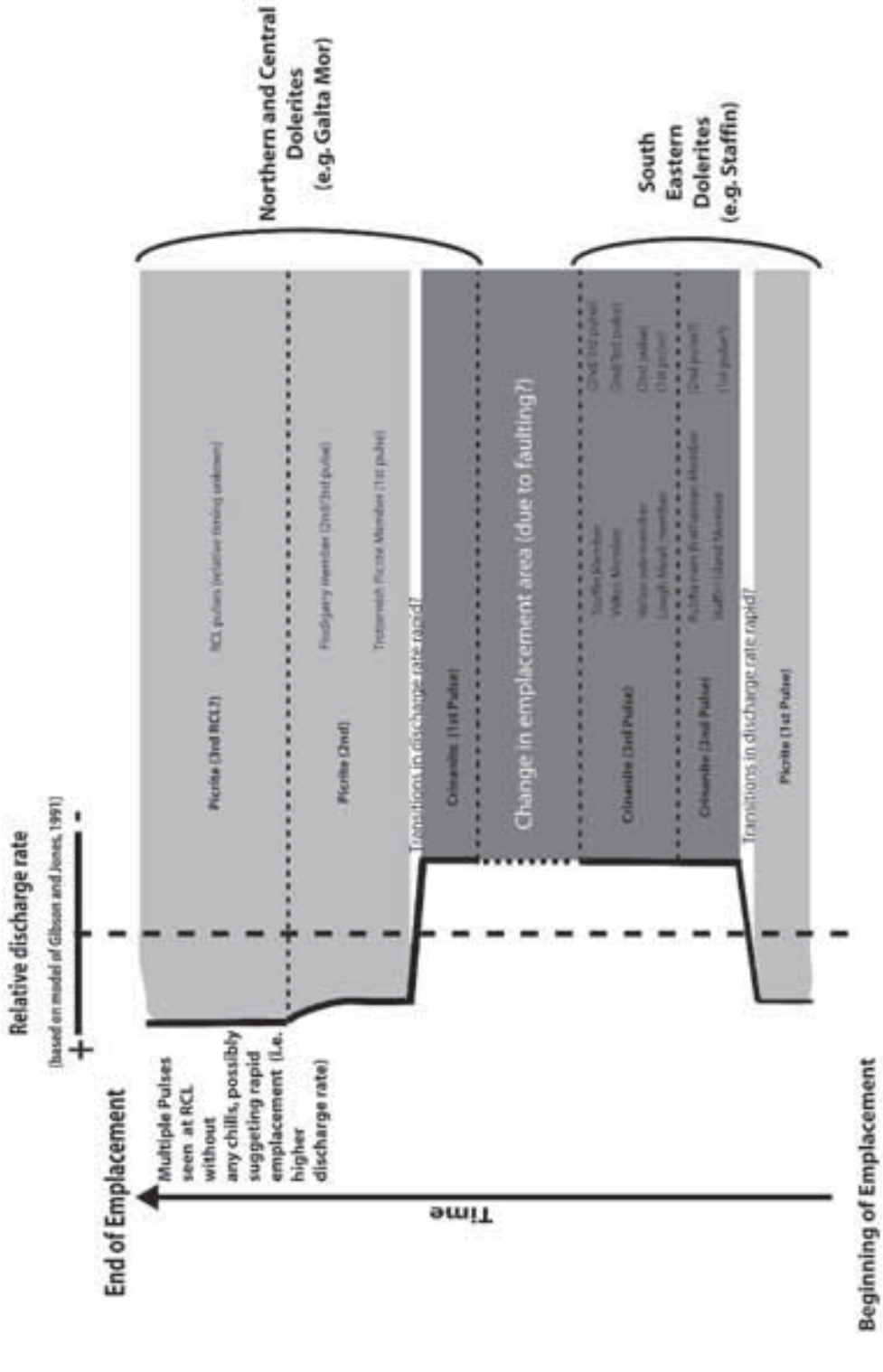

Figure 4.35 – Figure showing integration of data presented in this chapter with the model of Gibson and Jones (1991) which relates discharge rate of magma to magma composition. It should be noted that duration of each intrusive event in the emplacement of the Trotternish sill complex is unknown.

Chapter 5
Karoo Basin, South Africa -
Seismic scale field examples of saucer-shaped sills

Introduction

Some of the most significant advances in the understanding of the sub-volcanic systems have come about due to the increasing availability of petroleum industry offshore 3D seismic data sets. A key observation from this work has been that the geometry of sills in sedimentary basins is usually saucer-shaped, circular or elliptical in plan view with an inner flat dish surrounded by an inward dipping arcuate rim (see Chapter 2 for details). Such saucer-shaped sill complexes have been imaged on the NW Australian Shelf (Symonds et al*.,* 1998), offshore Senegal (Rocchi et al*.,* 2007), along the NE Atlantic margin in the Vøring and Møre basins (Planke et al*.,* 2005; Hansen and Cartwright, 2006), the Faroe-Shetland area (Bell and Butcher, 2002; Davies et al*., 2002;* Smallwood and Maresh, 2002; Hansen et al*.,* 2004; Thomson, 2007), and the Rockall Trough (Thomson and Hutton, 2004; Thomson and Schofield, 2008).

Although many of these studies have elucidated gross relationships of the sub-volcanic system, giving insights into morphology and structure of such systems, the limitation of 3D seismic data has meant that mechanisms and controls governing saucer-shaped sill emplacement are difficult to put in context from seismic data alone. This chapter will present observations from sills within the Karoo Basin, South Africa, which displays one of the most spectacular and readily exposed saucer-shaped sill complexes in the world (Fig. 5.1).

5.1 Geological summary of the Karoo Basin and occurrence of sills

The Karoo Basin, South Africa, initiated at the end of the Carboniferous at ~ 300Ma, in response to the Gondwanide orogeny (Cape fold belt) along the southern margin of Gondwana (Visser et al., 1999). The main Karoo sedimentation, which forms the Karoo Supergroup, continued through the Permo-Triassic into the early Mesozoic before being capped by the large scale eruption of continental flood basalts, and associated intrusions at ~ 183Ma (Visser et al., 1998, Eales et al., 1984). The sediment pile forms a 6 km thickness of mostly layer cake stratigraphy, consisting from base to top of the Dwyka, Ecca, Beaufort, Molteno, Elliot and the Clarens formations (Fig. 5.2).

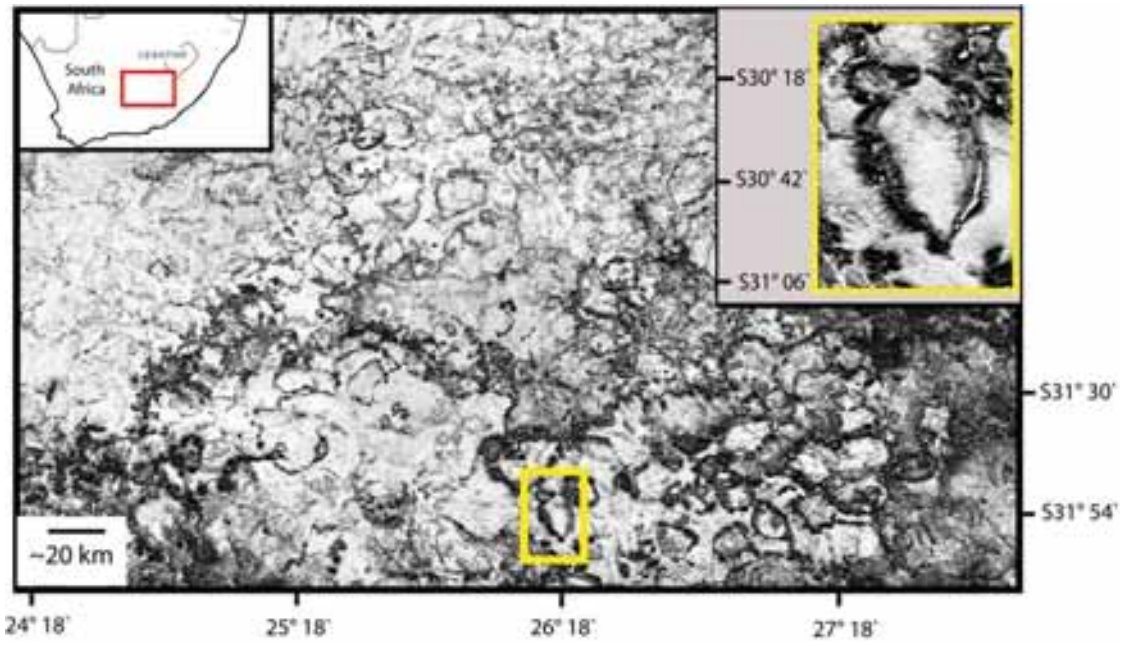

Fig. 5.1 – SRTM-90 (Shuttle Radar Tomography Mission) data rendered as a dip map showing pervasive nature of saucer-shaped sills (note scale) within the Karoo Basin, Golden valley sill is highlighted in yellow and shown inset.

The magmatic event at 183Ma which preceded the breakup of Gondwana, forms part of the Karoo-Ferrar Large Igneous Province (Riley et al., 2006) and was caused by an inferred mantle plume located off the eastern seaboard of South Africa (Cox, 1989; Elliot and Fleming, 2000). The episode gave rise to extensive sequences of both intrusive and extrusive mafic igneous rocks. Lesotho preserves the only large scale remnant of the continental flood basalts associated with this event (Fig. 5.3), but isolated outcrops of Karoo lavas extend to the north of Zimbabwe (Fig. 5.3) indicating that large areas of the sub-Saharan continent were covered with flood basalts at this time.

The subsequent erosion of the region, and in particular of the Karoo Basin, has exposed the sub-volcanic plumbing system, which is dominated by the presence of saucer-shaped sills (see Fig. 5.1). Du Toit (1920) first described the intrusive ring-like structures that characterize this basin, identifying the concave up geometry of individual intrusions. The saucer-like intrusions are predominantly circular or elliptical in plan view and range from a few kilometers to over 30 km in diameter in the western part of the Karoo Basin (Chevalier and Woodford, 1999). In general, the diameter of the intrusions appears to be related to the depth of emplacement within the Karoo Supergroup; larger diameter saucer-shaped sills occur in the lower sequence and smaller diameter sills towards the top of the sequence (Chevalier and Woodford, 1999).

Based on fieldwork and electrical resistivity soundings van Zijl (2006) proposed a three zone model for the emplacement of distinct morphologies of sills within the Karoo basin (Fig. 5.4).

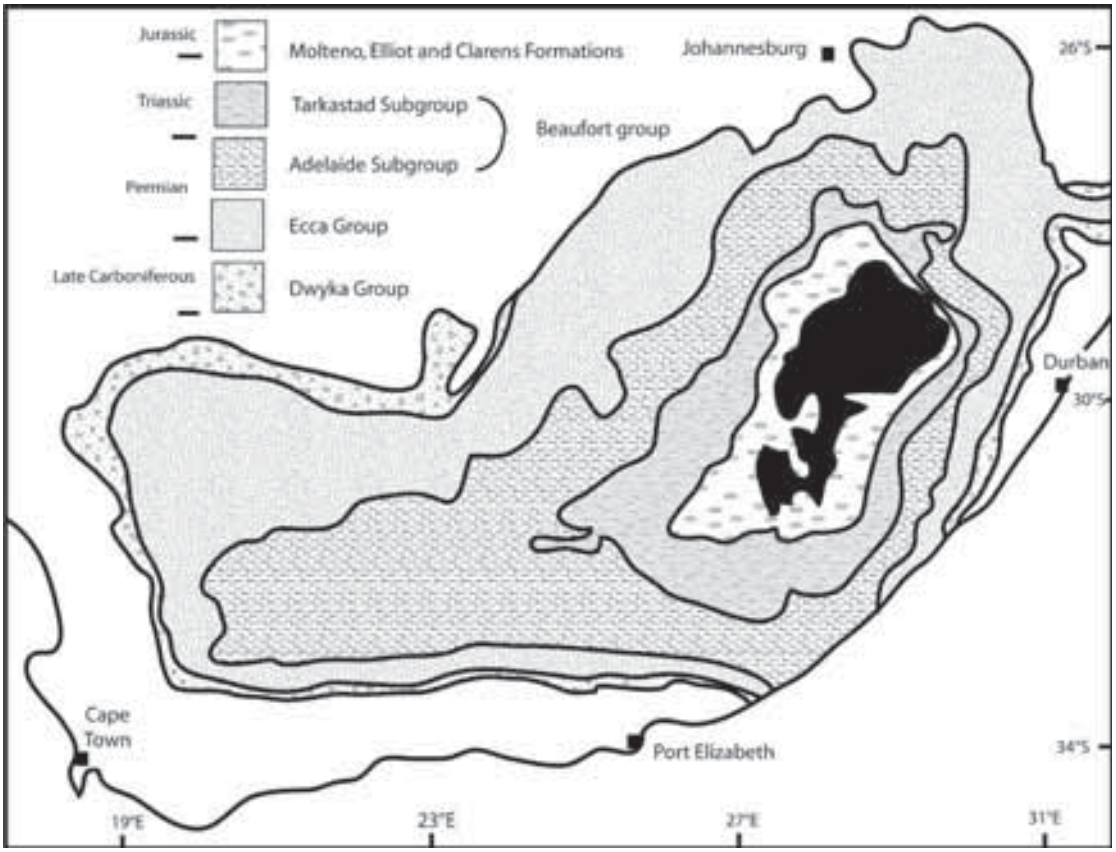

Fig. 5.2 – Redrawn from Visser et al. (1999) showing main division of sediments within the Karoo Basin, which form a layer cake stratigraphy across the basin.

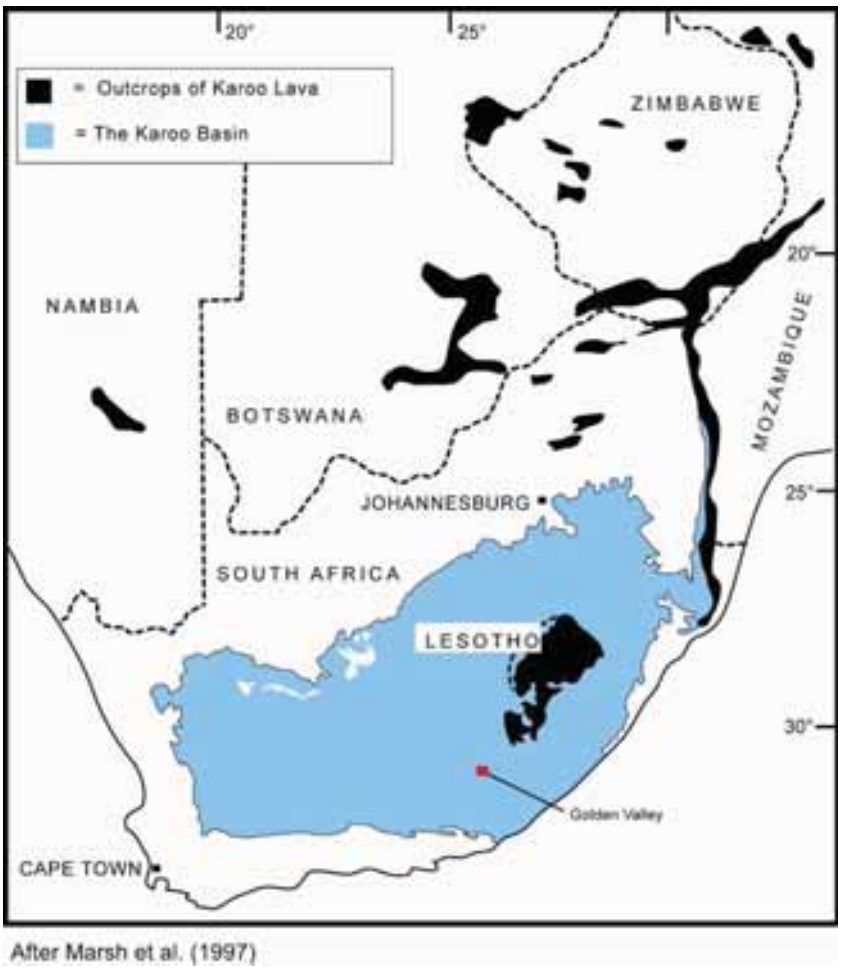

Fig. 5.3 – Showing the extent of the Karoo Basin, and current outcrops of Karoo lava, which indicates much of the sub-Saharan continent was covered with flood basalts related to the Karoo magmatism.

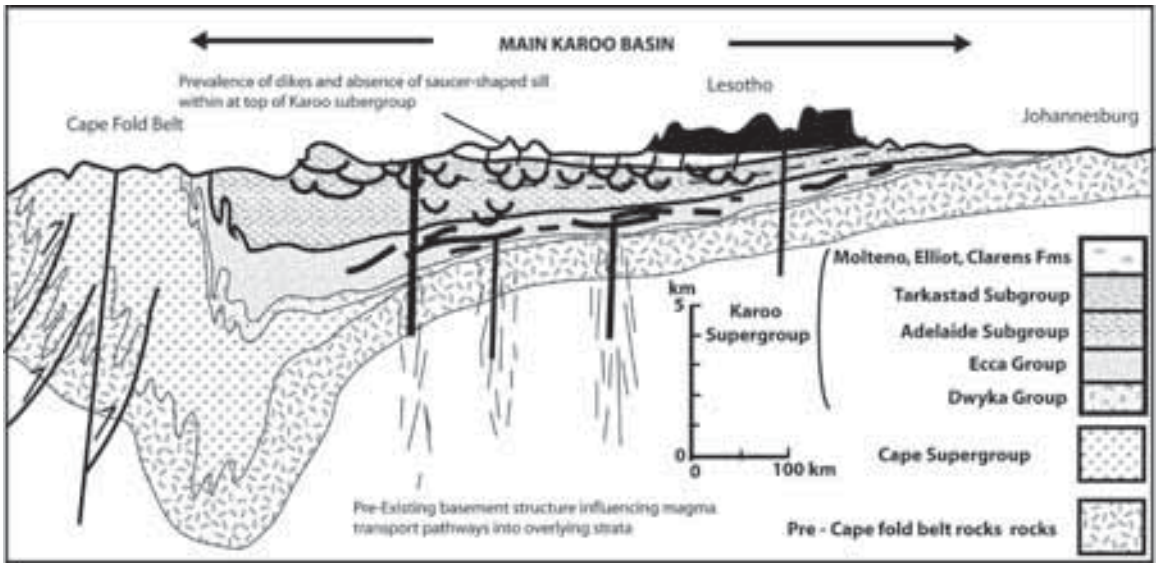

Fig 5.4 – Redrawn from Visser et al. (1999), with physical characteristics of intrusions throughout the basin marked based on work of Van Zijl (2006), see text for details. Note saucer shaped intrusions are more abundant in upper parts of the Karoo Supergroup.

Zone 3 dolerites are dominated by laterally continuous, approximately planar, relatively low density sills, which intrude into the well laminated, and relatively homogenous shales of the Ecca subgroup. Zone 2 dolerites, the highest abundance of sills within the basin, form a dense series of saucers. They are intruded into mainly interbedded, relatively homogenous sandstones and mudstones of the Beaufort formation. In general, the diameter of the saucers is considerably larger than the thickness of overburden at the time of intrusion (Van Zijl, 2006). Zone 1, which consists of the upper 700m of the volcanic sequence, below the lavas, is generally absent of sills, with the little dolerite present (0.5% of the sequence) occurring in steeply dipping sheets or in dykes. Van Zijl (2006) states that paleomagnetic studies of the dolerites in zone 1, which are reverse magnetized, suggest that they represent the only feeders to the overlying flood basalts, as most of the other dolerites are normally magnetized. Van Zijl (2006) also notes that the upper 900m of the Drankensberg lavas are normally magnetized, which would suggest they were fed by the underlying normally magnetized intrusions. This is confirmed in part by Galerne et al. (2008) who showed geochemical affiliations between the magma forming the Golden Valley Sill Complex and the main Lesotho lava, suggesting that the two emplaced at the same time and that the Golden Valley Sill complex may have formed part of the sub-volcanic complex feeding the overlying lavas.

5.1.1 Structural elements of the Karoo Basin and underlying basement

The movement of magma through the crust is governed to a high degree by the presence of pre-existing heterogeneities, and on a large scale by regional stress fields (Delaney et al., 1986). Pre-existing discontinuities in highly strained tectonic terranes may act to control dyke geometry (England, 1988), and therefore although dykes may provide some constraints to infer paleostress regimes, they do not necessarily lie perpendicular to the direction of least compressive stress (Delaney et al., 1986). Two of the main factors controlling the intrusion of dykes and sills in the high level crust is stratigraphic and structural controls (Francis, 1982; Thomson and Schofield, 2008). The Karoo Basin, given its enormous extent, is relatively unstructured, with the major structural elements being mainly confined to the south of the basin and the Cape Fold belt, which initiated in the Permian and continued into the Triassic (Halbich, 1992). However, the underlying metamorphic cratons, such as the Namaqua Natal Belt, and Kaapvaal Craton, have undergone a long history of complex tectonic activity and therefore the underlying discontinuities and structure have to be assessed in an attempt to understand what has controlled the distribution of igneous activity in the Karoo (Eales et al., 1984).

Reactivation of the crustal weaknesses created during previous tectonic events, although no doubt on a minor scale, seem likely to have played a role in focusing igneous activity within the Karoo Basin and southern Africa (Eales et al., 1984). The sediments of the Karoo Basin obscure the basement geology, but along the east coast of Africa, the Limpopo monocline, acts as a focused site for the intrusion of dyke swarms and ring complexes (Eales et al., 1984).

A structural control on the orientation and emplacement of dykes across the southern Karoo Basin, where a dominant NNW-SSE orientation of dykes can be observed in the central Karoo basin (Figure 5.5). Chevalier and Woodford (1999) suggest that the pronounced E-W trend of dykes, is the result of a right-lateral shear zone within basement rocks which extends from the Eastern Cape to the Atlantic. Figure 5.5 shows dykes and general dyke orientations overlain on the inferred boundaries between various metamorphic belts, which underlie southern Africa. The dykes cutting the Karoo sedimentary pile which overlies the Namaqua Natal belt show a distinct conjugate style, with a strong E-W and NNW-SSE component. Given that the Karoo Basin is unstructured, and shows no structures matching an E-W and NNW-SSE trend, this would suggest that the pattern of dykes seen in the Karoo sedimentary pile may be inherited from the underlying basement structures beneath. This assumption is further supported by the trajectory of the curved dykes which emanate from the Eastern Cape in an approximate E-W orientation and then periodically rotate to a N-S trajectory. The final N-S trajectory of the dykes appears to be stopped at the approximate boundary between the Namaqua Natal Belt, and southern Kaapvaal Craton, where the dykes possess a general E-W trajectory, thus suggesting that the presence of this major crustal boundary is affecting the dyke emplacement pathways to a considerable degree.

The role the dyke network across the Karoo Basin has had in feeding the saucer-shaped sill complex is not entirely clear. Galerne et al. (2008) showed that dykes surrounding the Golden Valley Sill (GVS) have a different geochemistry to the GVS, and therefore concluded they did not feed the sill complex, implying that magma may have been sourced from sill to sill, and not from dyke to sill. Goulty and Schofield (2008) showed that elliptical saucer-shaped sills were probably fed by an underlying source running along the long-axis of the ellipse of the saucer, in the form of a dyke.

While elliptical saucer-shaped sills could also be fed from the outer periphery of another sill, the similarity between the orientation of elliptical sills and the orientation of dyke swarms as mapped by Chevalier and Woodford (1999) suggests that some saucer shaped sills are probably fed by dykes.

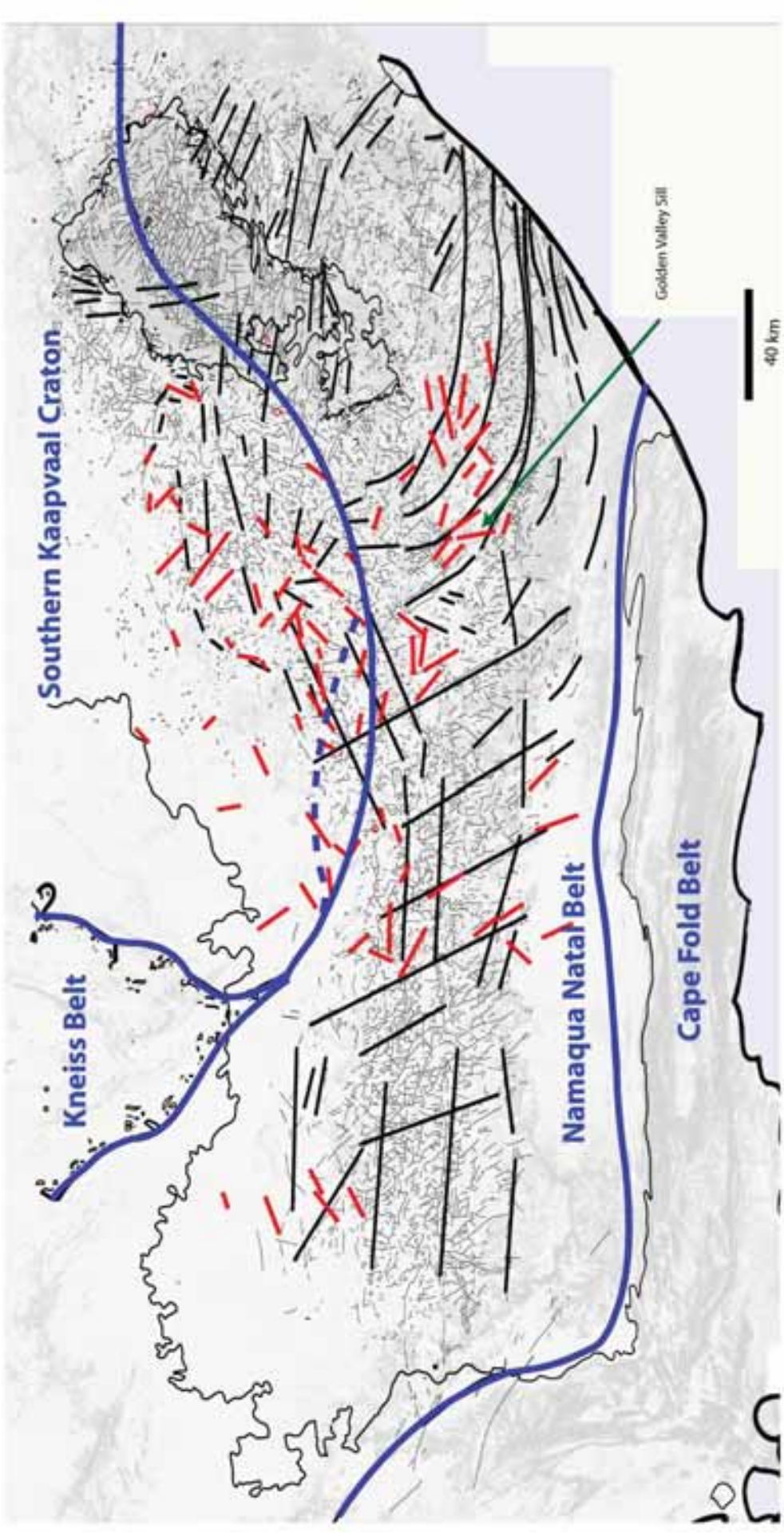

Fig. 5.5 - Figure showing mapped out dikes (thin solid black lines) and general trend of dikes (thick black) based on Chevallier and Woodford, (1999). Underlying basement terranes are marked based on Jourdan, (2006). Red lines represent the orientation of the long axis of elliptical saucer shaped sills identified on SRTM-90 Data. Of note within the figures is the changed in dike orientations between the Namaqua Natal belt and southern portion of the Kaapvaal Craton. This suggest that the basement fabric imparted a control on magma pathways into the overlying Karoo sedimentary pile. Interestingly, the orientation of the elliptical saucer shaped sills also changes between the two basement terranes and appear to correspond to dike orientations.

5.2 Golden Valley Sill

5.2.1 Geological setting of the Golden Valley Sill

The Golden Valley Sill (GVS) is a well-exposed example of a saucer-shaped sill, comparable in size to those seen in seismic data offshore Scotland (Thomson, 2007). It is located in the south eastern Karoo Basin, approximately 250km south west of the Karoo Lava sequence in Lesotho.

The GVS is intruded into the Tarkastad Subgroup, which forms the upper division of the Permo-Triassic rocks of the Beaufort Group which is the most extensive sedimentary sequence within the Karoo basin covering an area of approximately 200,000 km^2 and making up 20% of the total surface area of South Africa (Visser et al., 1992: Catuneanu et al., 2005). The Beaufort Group attains a cumulative thickness of ~ 7000m within the Karoo foredeep, and thins rapidly to the north (Johnson et al., 1996). The Tarkastad sub-group records a sudden change in depositional environment, caused by rapid tectonic uplift of the source region to the south east, and the end-Permian warming event (Catuneanu et al., 2005). Deposition began at the Permo-Triassic boundary and is composed mainly of terrestrial deposited interbedded arenaceous and argillaceous sediments, which were most likely deposited in a fluvial mud-flat type environment, drained by sluggish meandering rivers (Catuneanu et al., 2005).

The GVS intrusion is dated as ~ 183±0.5 Ma (Galerne et al., 2008), and is chronologically linked to the main phase of Karoo Volcanism which began at approximately c.182 Ma (Riley and Knight, 2001). The dolerite from the GVS is typically medium grained, consisting of plagioclase, clinopyroxene and orthopyroxene (Galerne et al., 2008), the rocks also contains Fe oxides, in particular magnetite, sufficient to deflect a compass needle (considerably) up to a metre away from the rock surface.

5.2.2 Structure of the Golden Valley Sill

The sill takes the form of an elliptical concave up saucer 10 km (east-west) × 19 km (north-south) (Fig. 5.6). The central portion of the saucer is concordant with the country rock and dips <5° northeast. Around this inner flat sill is an arcuate rim of transgressive dolerite, which cuts up stratigraphy for 2 km at an inclination of ~ 20 – 35° (Fig. 5,6). The dolerite forming the GVS's arcuate rim shows a curved trajectory that steepens in dip towards the edge of the dolerite sheet. No ramp-flat geometry is visible, such as that predicted in the saucer-shaped emplacement model of Malthe-Sørensen (2004), which has the saucer-shape of the sill being formed by a series of steps within the dolerite as it climbs.

The transition between the approximately planar inner sill and the peripheral transgressive arcuate outer sill is sharp, and only occurs over a very short distance, approximately 50 – 80 m (Fig. 5.7). This suggests that transition of the magma from the horizontal plane to a transgressive trajectory was not incremental, but abrupt.

The thickness of the dolerite varies between 10 – 70m. No faulting of the arcuate inclined sheet is visible. Within the inner sill, the limited exposure, and horizontal layer cake stratigraphy makes the identification of any faults difficult. However, no sudden breaks in slope can be identified within inner sill on aerial and satellite imagery, suggesting there are no significant faults.

5.3 Sill morphology

5.3.1 Large scale radial undulations

The top surface of the arcuate transgressive rim of the Golden Valley Sill displays regular undulations at wavelengths which generally range from 50 – 100m (Fig. 5.8), but a wavelength of 500 m exists in the NW sector of the sill. The axis of these linear bodies define broad convex up finger like structures of dolerite that trend radially away from a central North-South trending axis. In detail they are characterized by broad long wavelength undulations (peak-peak) and sharp troughs, (Fig. 5.8) with a peak-trough amplitude of ~ 25 – 30m. Within the troughs, a chilled facies of fine grained dolerite is visible often in association with vestiges of roof rock (Fig. 5.9, Fig. 5.10, Fig. 5.11). Figures 5.12 and 5.13 show the extent of chilled facies and the inferred original sill geometry. Erosion of sill material has generally been concentrated over the topographically higher points of the sill formed by the convex-up finger-like structures removing the chilled facies at these locations.

Within the thickest parts of the sill, which occur in conjunction with the peaks of the undulations, the width of dolerite columns are larger, in the region of 3 – 4m across, in contrast to the troughs, in which the columns are usually in the region of 1 – 2 m (Fig. 5.12). This suggests that magma within the troughs cooled quicker than the peaks, a point additionally noted by Polteau et al. (2008). This would correspond to the troughs and peaks now preserved within the GVS being representative of the original intrusion morphology i.e. The preserved troughs, represent the thinnest parts of the sill during intrusion and cooled the quickest. This morphology and structural relationship matches that of the convex-up features seen in the Trotternish Peninsula, Isle of Skye (see chapter 4, Fig. 4.14).

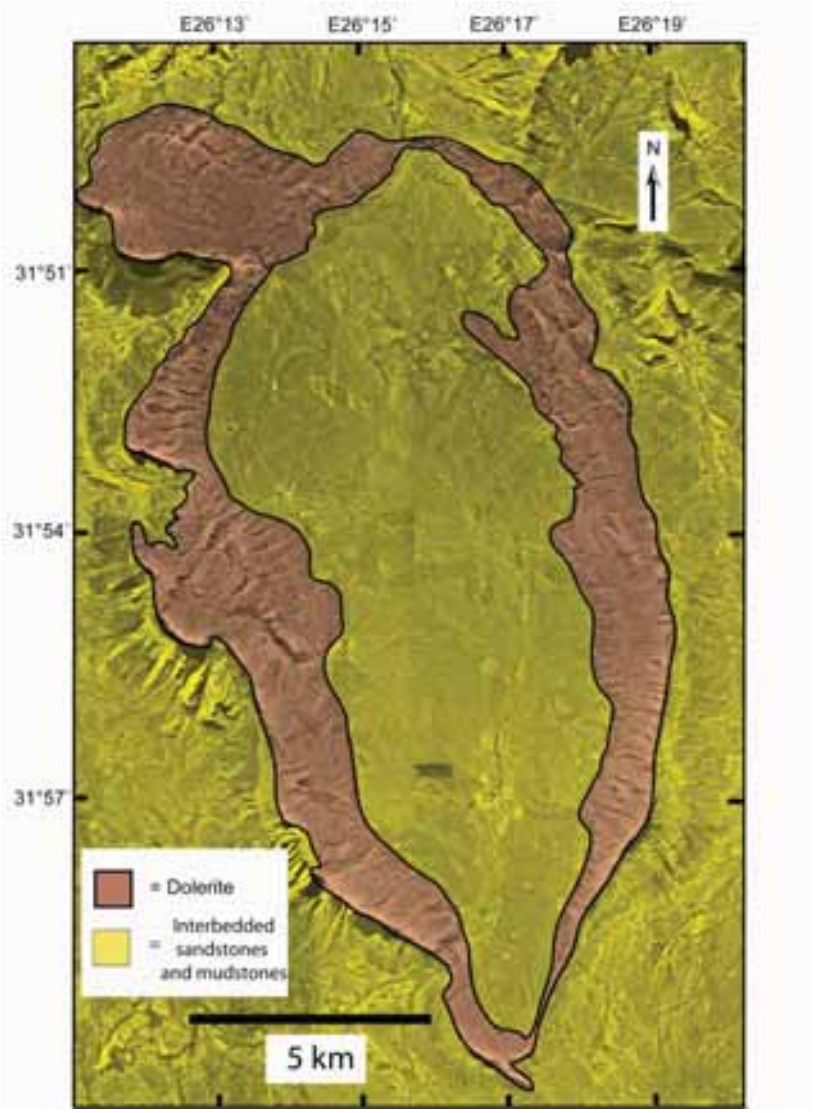

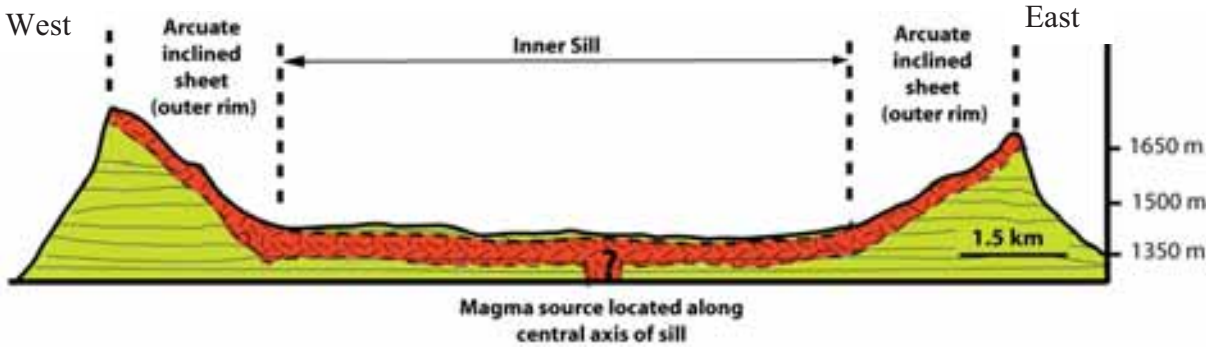

Fig 5.6 – Aerial photograph showing the outcrop of the Golden Valley Sill and sketch cross-section. Note the eye-like elliptical shape in plan view (Modified from Goulty and Schofield, 2008)

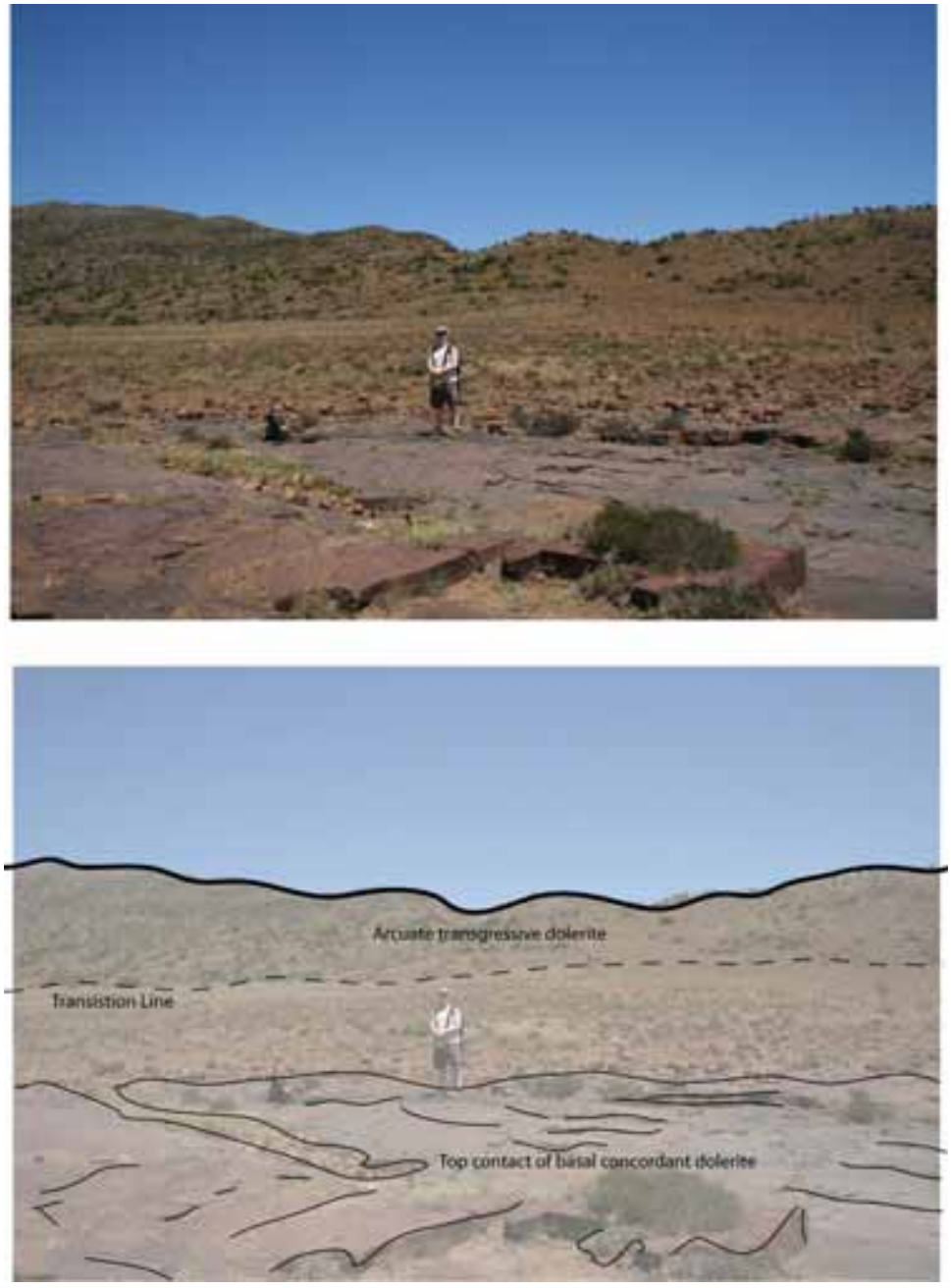

Fig 5.7 – Roof contact of inner sill, with transgressive arcuate inclined sheet in background. Photo looking south.

Polteau et al. (2006) and Polteau et al. (2008) reported the occurrence of undulations with a wavelength of ~ 5m occurring on the top surface of the dolerite sill that are superimposed upon the long wavelength undulations around the arcuate inclined sheet, giving a 'wrinkled' appearance to the top surface of the sill (Fig. 5.14). However, the wrinkles were examined in the field and on aerial photographs appear to be the result of prominent cooling joints across the dolerite surface. The joint sets, which can be identified on cliff faces (Fig. 5.14), extend over the top surface of the arcuate saucer (Fig. 5.14 and 5.15). Upon exposure, preferential erosion has taken place along the joints, creating a domed appearance to the dolerite between joint sets and a 'wrinkled' appearance.

Figure 5.17 shows the orientation of finger-like structures in the Golden Valley identified from fieldwork and air photo interpretation. The radial nature of the undulations is apparent, with the focus of the undulations appearing to be the long axis of the saucer (Fig. 5.16 and 5.17). Figure 5.19 shows feldspar alignments recorded around the saucer and which show a general alignment with the undulose features. The radial nature of the undulations about the saucer together with the parallelism of undulation axes with phenocryst alignments (Fig. 5.18 and Fig. 5.19) suggests that they are related to flow, additionally confirmed by AMS measurements of Polteau et al. (2008). Polteau et al. (2008) drew little conclusion regarding the undulations, aside from referring to them as 'magma channels', similar to those imaged by Thomson and Hutton, (2004). The genesis of these features will be described later in the chapter, but for descriptive purposes, the undulose features will be described as magma fingers from this point onwards within the chapter.

Although exposure of the inner sill is limited, no evidence for the existence of fingers in the inner sill exists, either from exposures, or as a surface expression in the overburden. This is particularly apparent in the bottom SE portion of the sill, in which the overlying host rock has been eroded away exposing the roof contact of the inner sill, which can be seen to be planar in nature (see Fig. 5.7). It is unclear if this relationship exists over the rest of the sill, but it is assumed to be the case.

5.3.2 North west lobe

This zone contains the most convincing evidence that the sill formed from multiple intrusions of magma. Two separate units of magma fingers can be identified, which extend radially away from the central axis of the sill. In general, the first unit sits structurally below the second unit of magma fingers (Fig. 5.22), although on occasions both units intrude on the same stratigraphic level. The first unit is characterized by broad magma fingers which posses

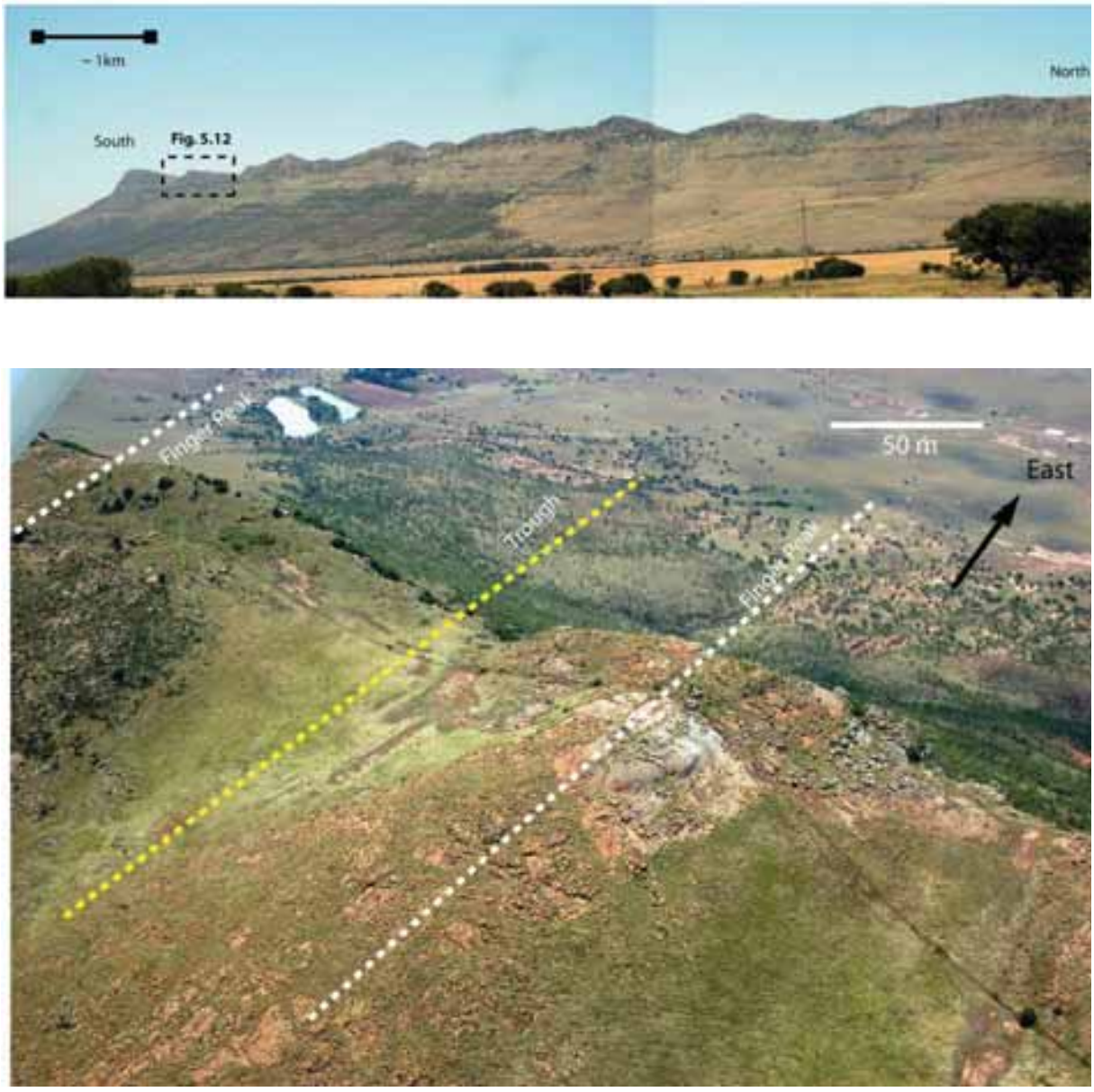

Fig 5.8 – Showing the peaks and troughs of fingers

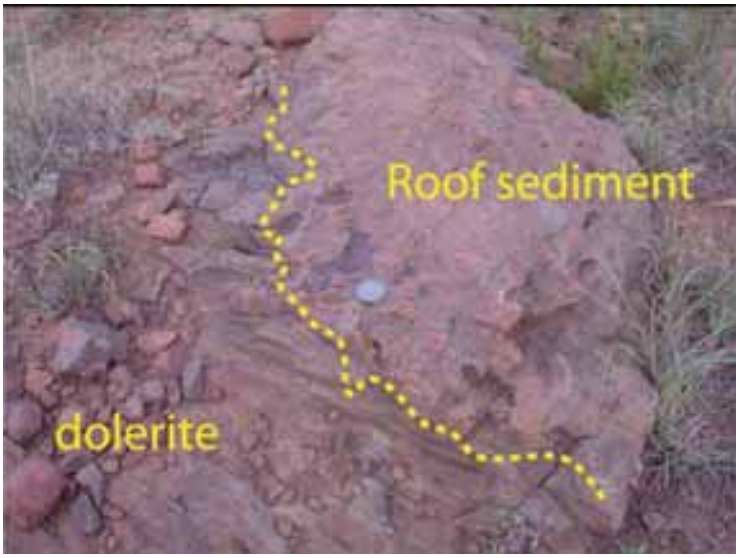

Fig. 5.9 – Roof contact between dolerite and sediment.

Fig. 5.10 – Chilled facies on top surface of dolerite within trough between peaks.

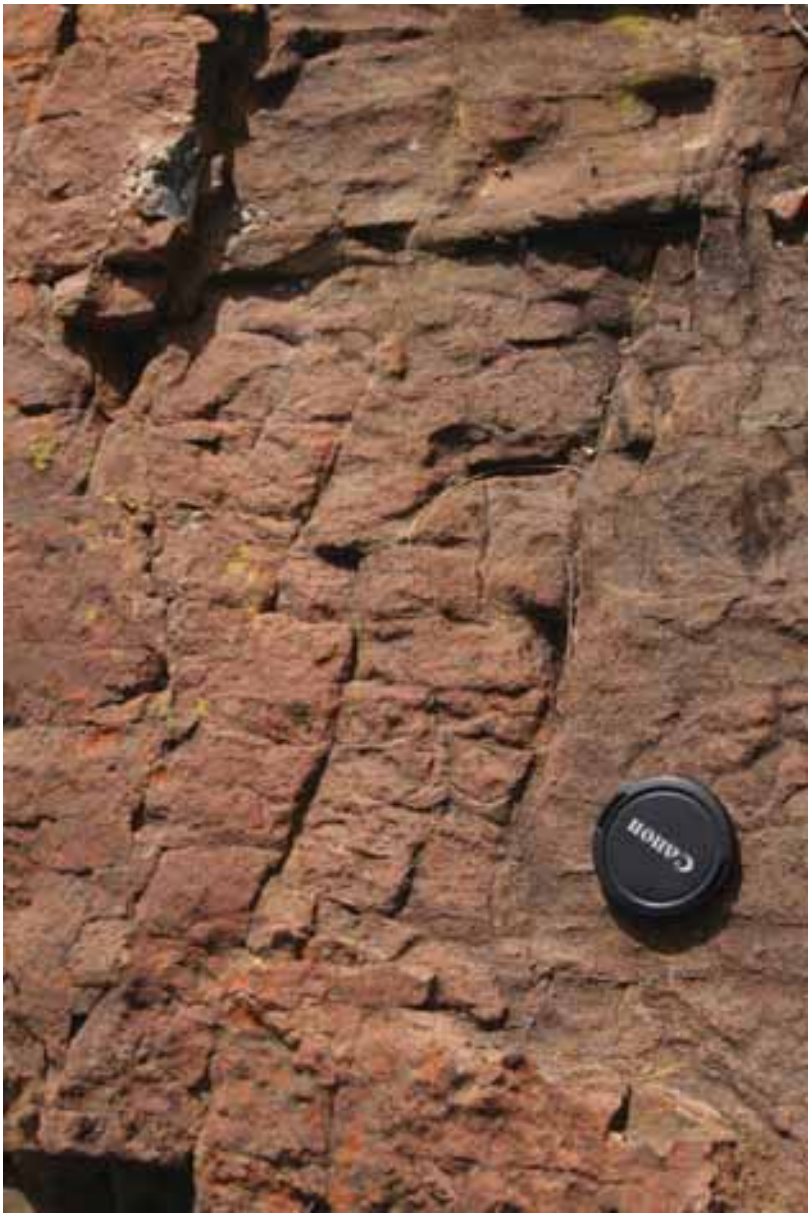

Fig. 5.11 – Chilled facies on top surface of dolerite within a trough between two peaks. Note the small-scale cooling joint patterns.

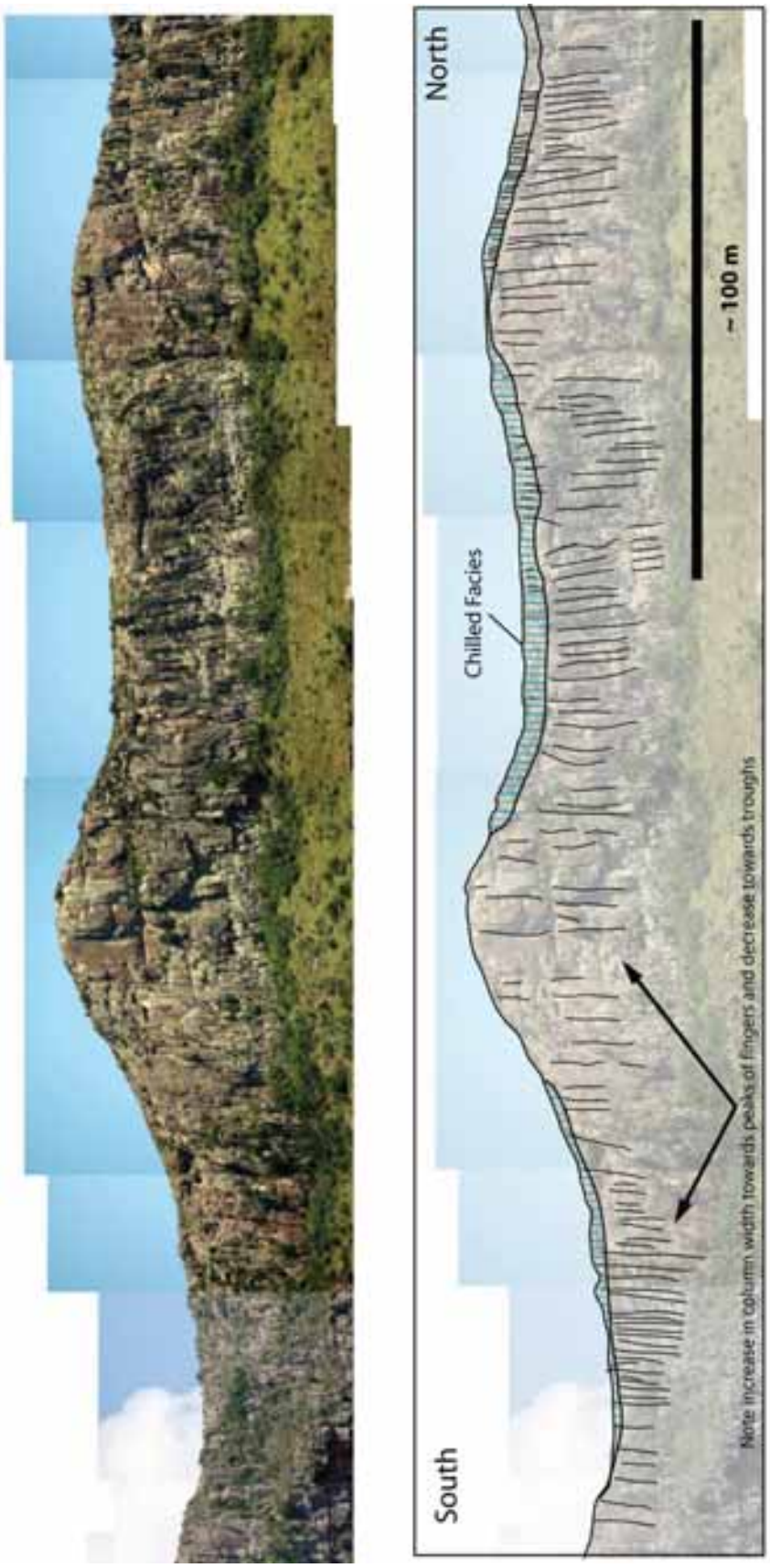

Fig. 5.12 - Composite photo of portion of eastern cliff section of the Golden Valley Sill

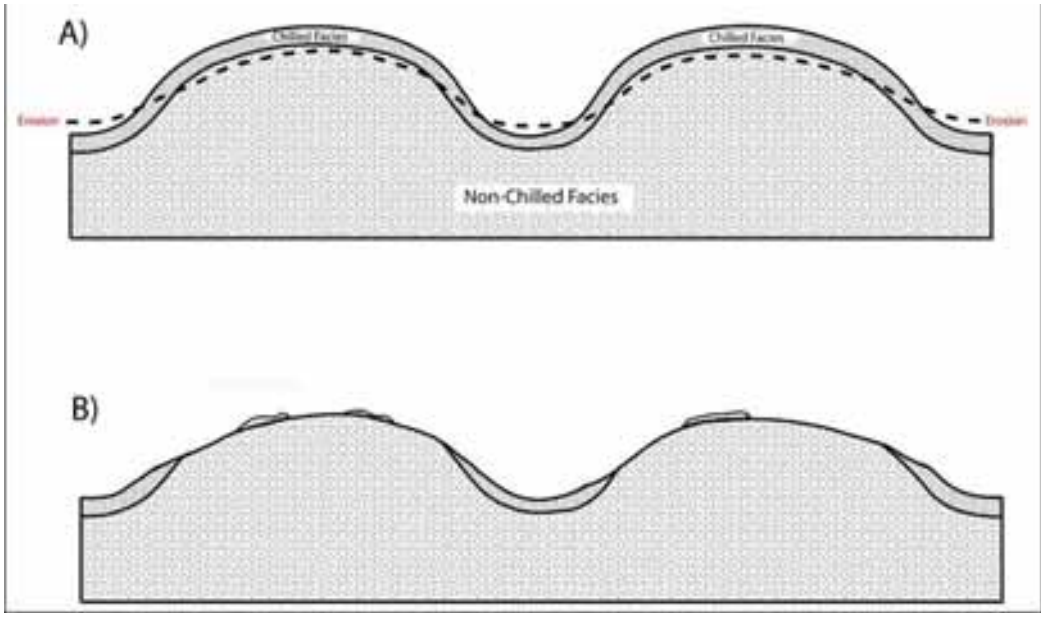

Fig. 5.13 – Schematic sketch showing approximate configuration of chilled margin at time of intrusion (A) and present day configuration due to erosion (B).

Fig. 5.14 – Field photographs taken from light aircraft showing undulose "wrinkle" structures described by Polteau et al. (2008). Features can be attributed to preferential erosion of joint sets, visible on cliff face extending along the top surface of the sill.

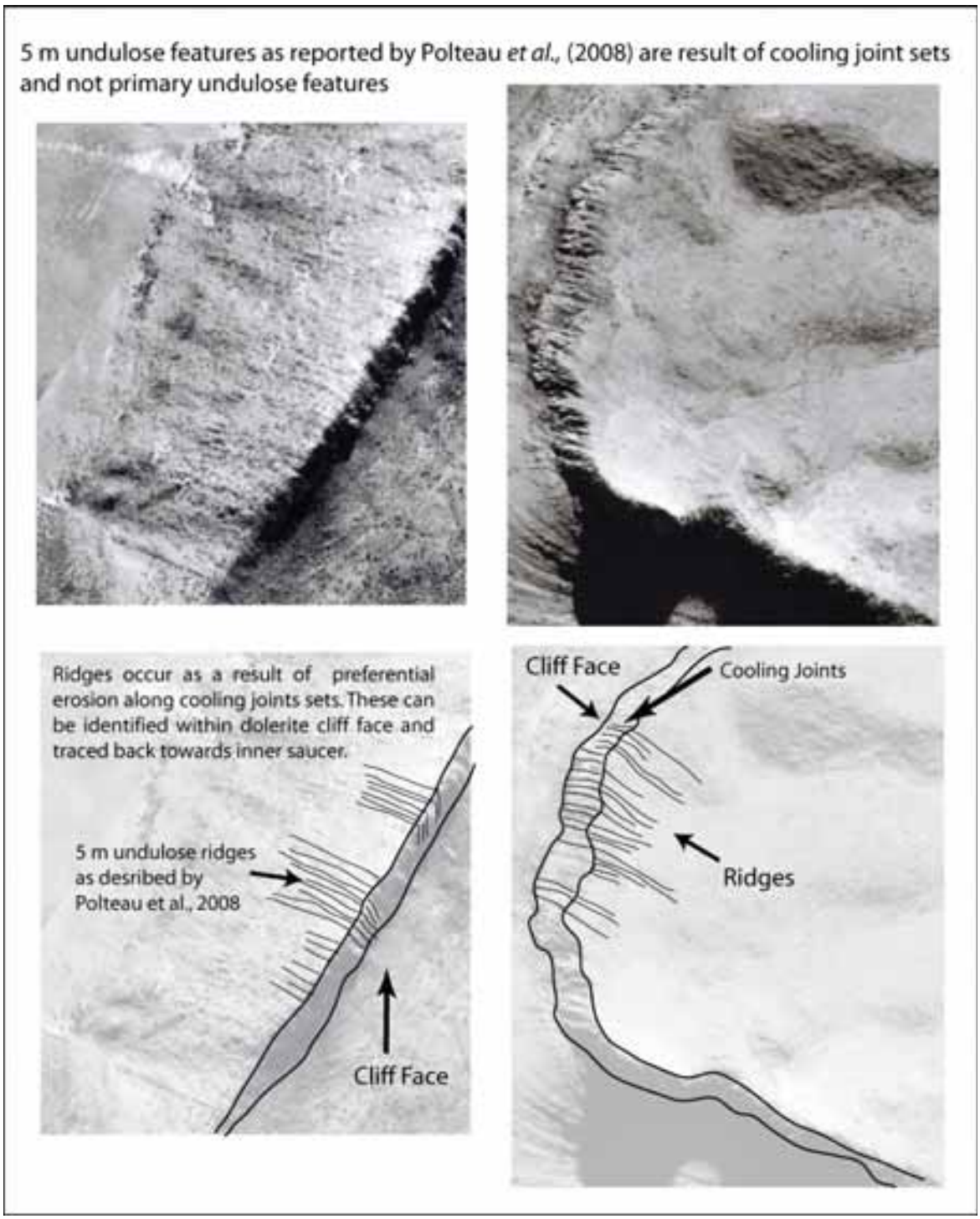

Fig. 5.15 - Illustrating the occurrence of small wavelength (~5) undulations in top surface of dolerite, attributed by Polteau et al. 2008, to be the result of 'wrinkling' caused by cooling in the top surface of the sill. However the features can be attributed to preferential erosion of cooling joint sets which can be seen within cliff faces and traced back along the top surface of sill.

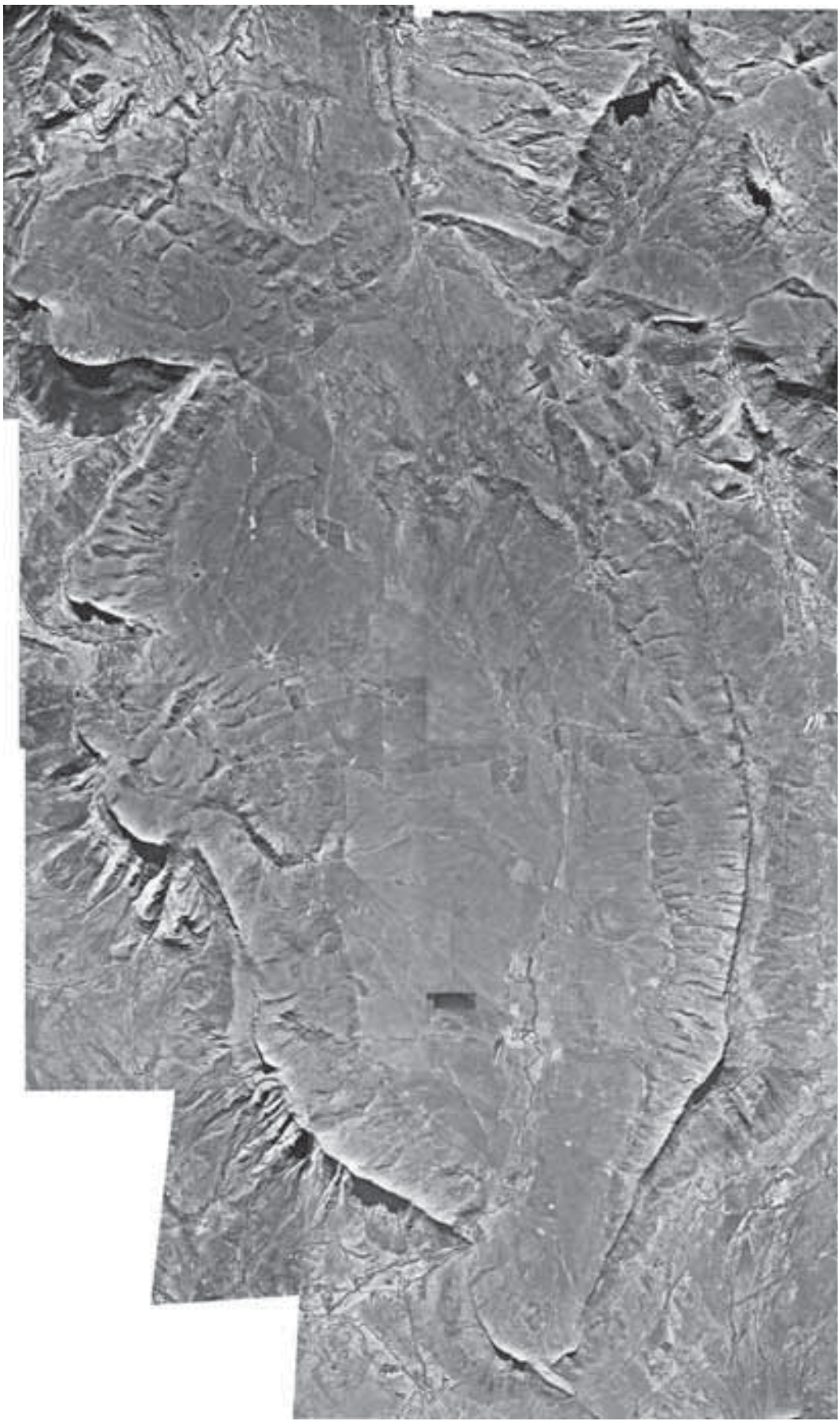

Fig. 5.16 – Aerial photograph of Golden Valley Sill.

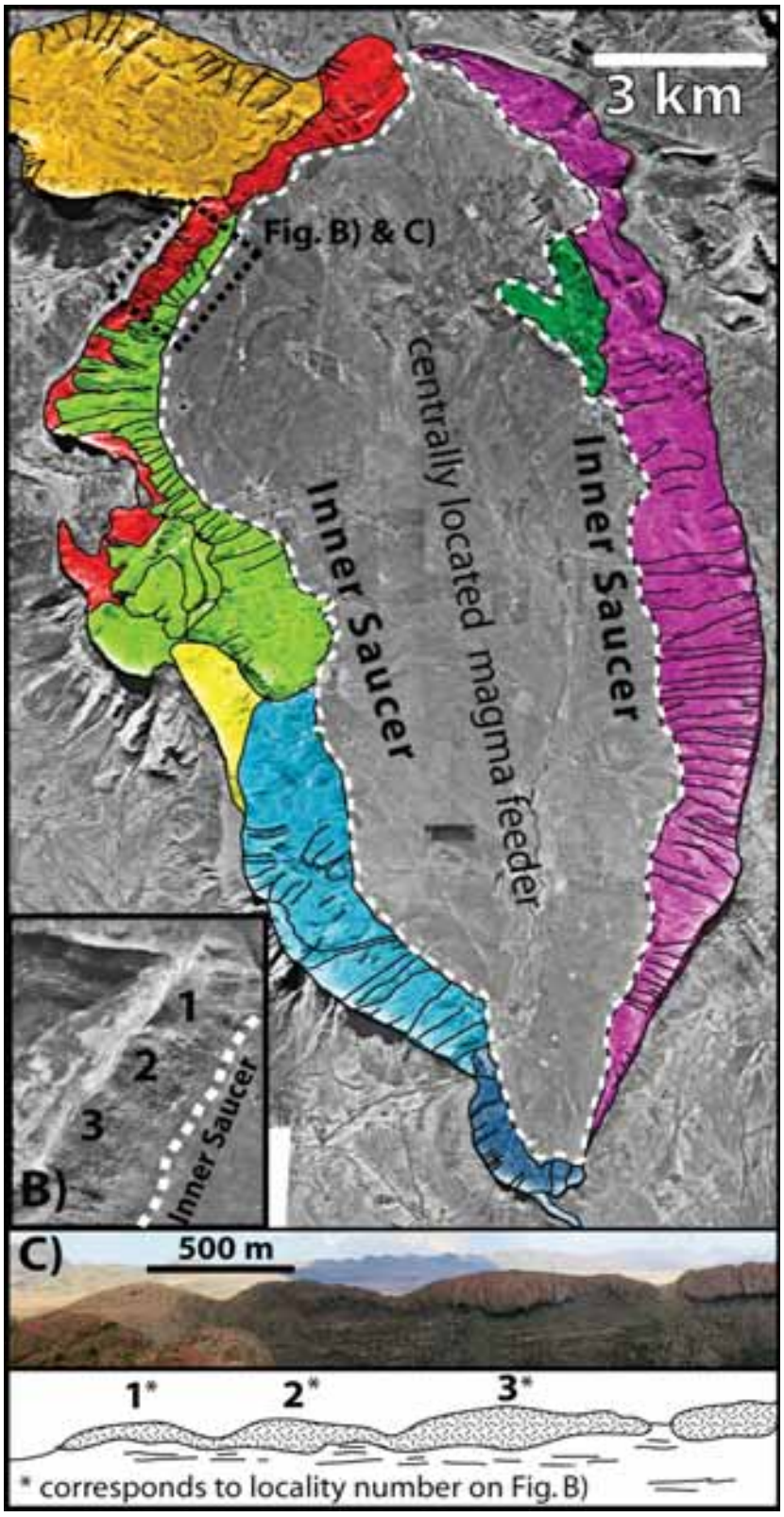

Fig. 5.17 - Aerial photograph of Golden valley sill, with finger orientations overlain (from Schofield et al., *in press)*. Magma fingers on the arcuate transgressive rim of the sill extend radially away from the broadly concordant inner sill of the saucer. Different colours on the map represent inferred pulses or lobes of magma. This is particularly the case in the western part of the intrusion, where multiple tiers of magma fingers, some overlapping, can be identified.

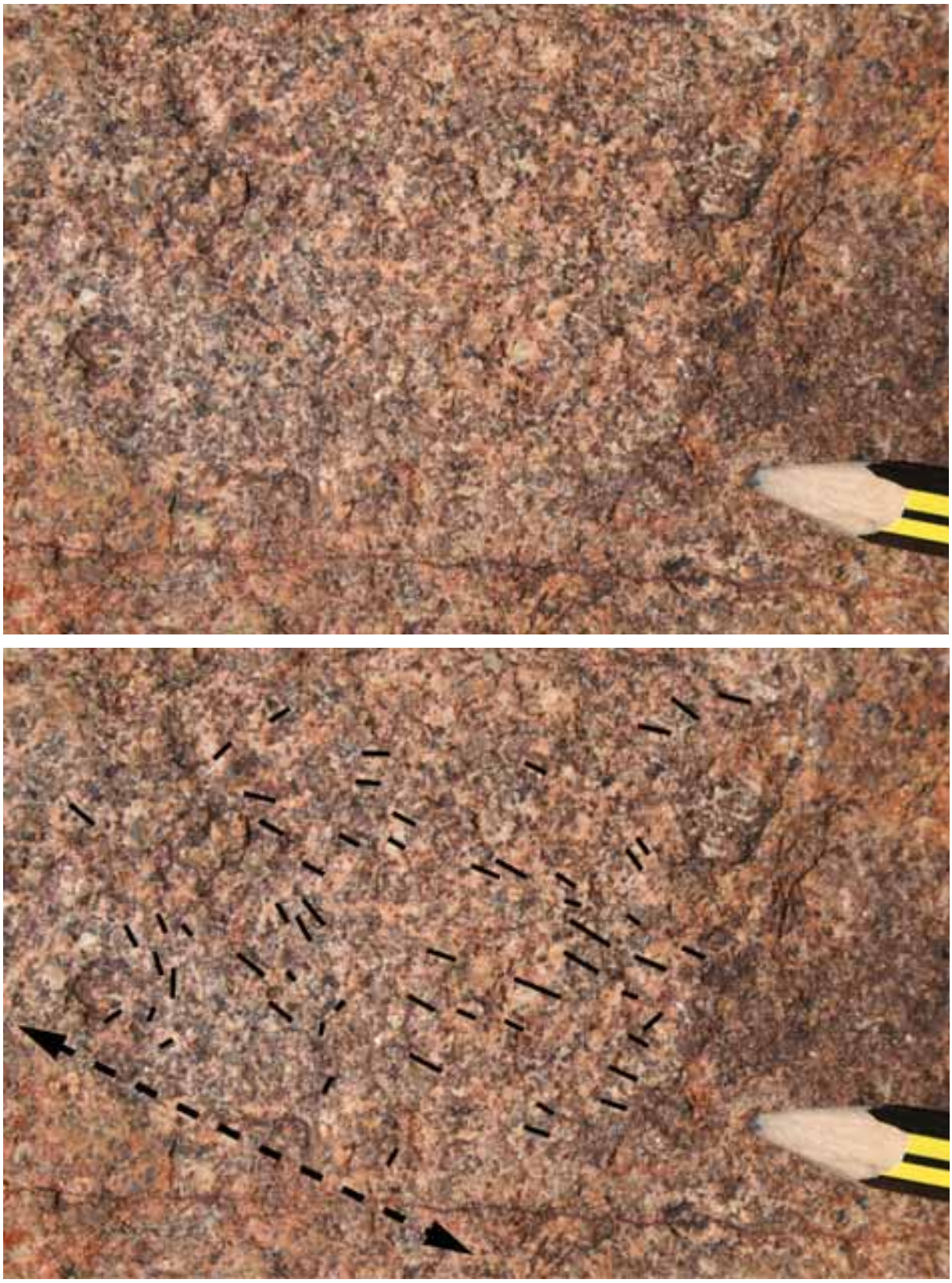

Fig. 5.18 – Top surface of convex-up top showing alignment of feldspar crystals

Fig. 5.19 – Feldspar phenocryst alignments around GVS (red lines).

a long wavelength peak to peak (~ 500m), these are best exposed within the cliff face close to the a smaller saucer-shaped sill that appears to form an offshoot of the main sill (see section 5.3.4), where three conjoined convex up finger structures can be identified (Fig. 5.20).

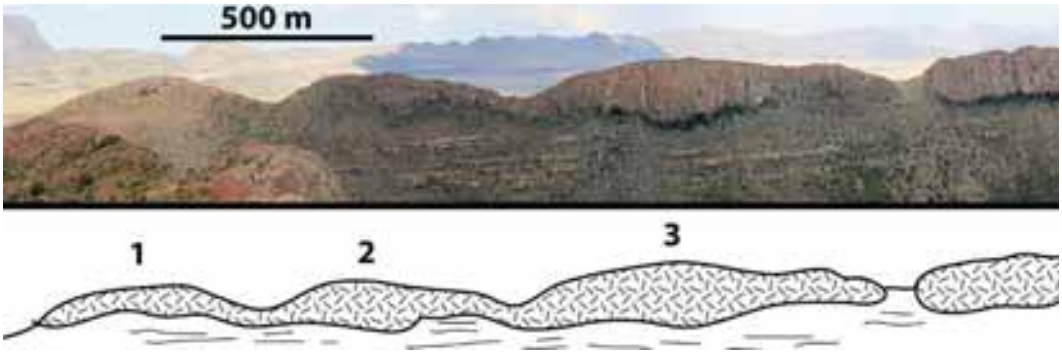

Fig. 5.20 – Long wavelength fingers, NW lobe, GVS.

At the northern end of the NW lobe the second tier of magma fingers can be seen to extend only a short distance away from the inner sill, only slightly overlapping the first tier of fingers, but to the south, the fingers overlap and extend much further (Fig. 5.21, Fig. 5.22, Fig. 5.23). The magma fingers of the second unit have shorter wavelength fingers of ~ 60 – 80m peak-peak compared to those in the first unit (Fig. 5.24). Towards the cliff face forming the edge of the transgressive sheet, it can be identified on stereo aerial photographs that the first unit fingers appear to cut stratigraphy at a steeper angle, leading to an intersection of the first unit magma fingers with second unit magma fingers at the same stratigraphic level (Fig. 5.25). No discernable internal contacts between magma fingers of the first and second units can be identified in the form of a change in style or orientation of columnar joints within the cliff face in the field. This suggests that the two tiers underwent the same cooling regime and although they were emplaced as separate pulses, they have done so in a short time frame relative to one another.

5.3.3 Eastern lobe

The eastern lobe of the GVS comprises the entire eastern half of the GVS. It is characterized by a single unit of dolerite, possessing a well-developed corrugated upper surface (Fig. 5.26). Within the south eastern sector of the sill the dip of the dolerite rapidly increases, until it takes a dyke-like form, cutting host rock at at ~ 75-80° (Fig. 5.27). Northwards, towards the middle sector of the sill, the dip lessens and maintains a fairly constant dip of 25-30° through the minor axis of the ellipse (widest part of the inner sill in an E-W direction). However towards the north of the sill, the dolerite steepens in dip once more to between 30 – 45°.

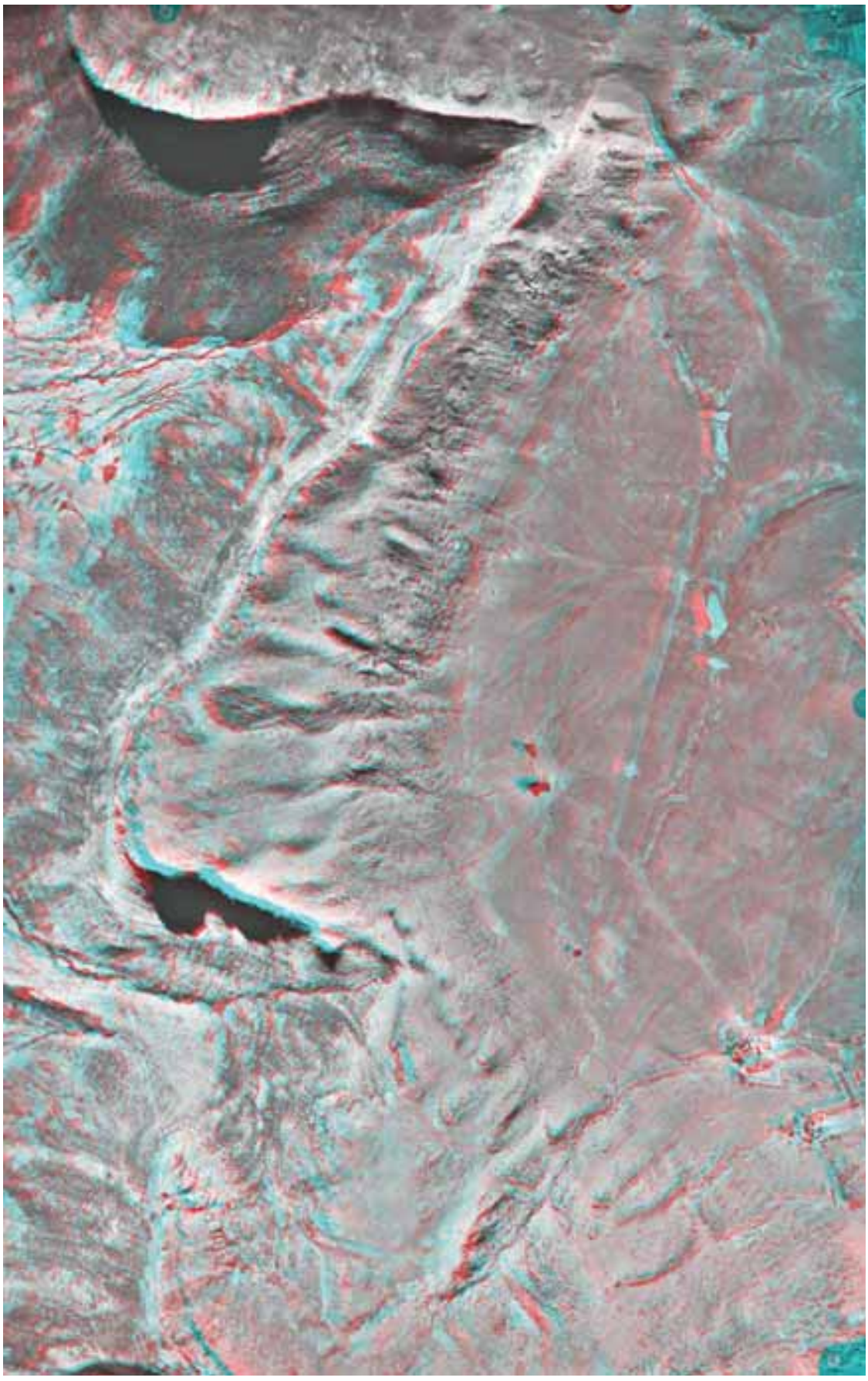

Fig 5.21 – 3D red/cyan anaglyph of NW portion of Golden Valley (3D glasses in pouch).

Fig 5.22 – Geological interpretation of 1st (red) and 2nd (blue) tiers of fingers within the NW lobe, thin solid lines represent orientation of dominant joint sets on top surface of sill

Fig. 5.23 – Oblique Google Earth ™ image of the NW lobe.

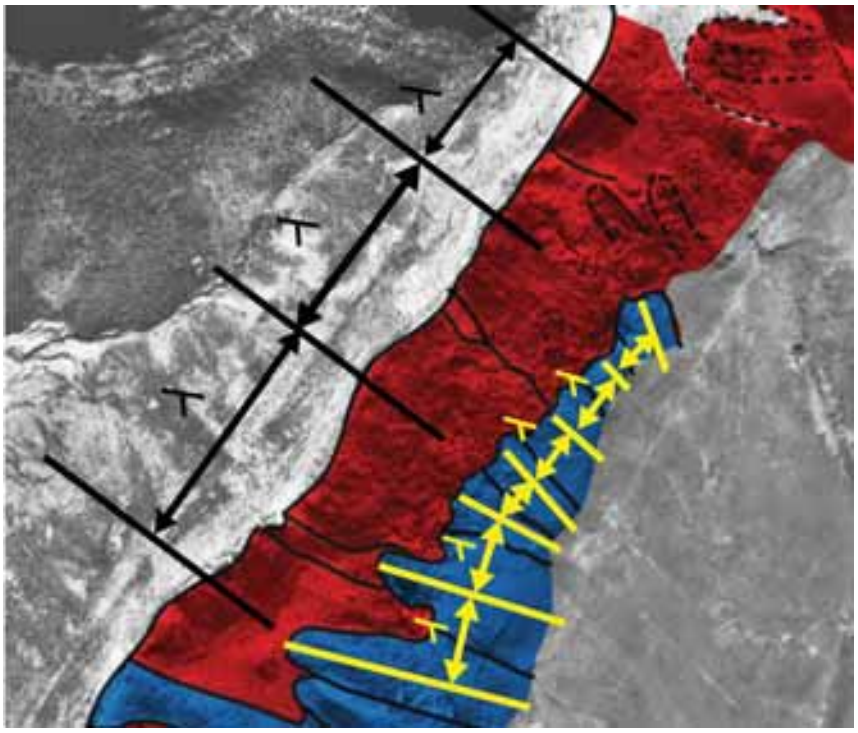

Fig 5.24 – Illustrating the uniform, but different wavelength peak-peak of fingers of the 1st and 2nd tier (outlined by solid black lines). Dashed lines represent landform features whose origin is not easily identified from stereo photo interpretation.

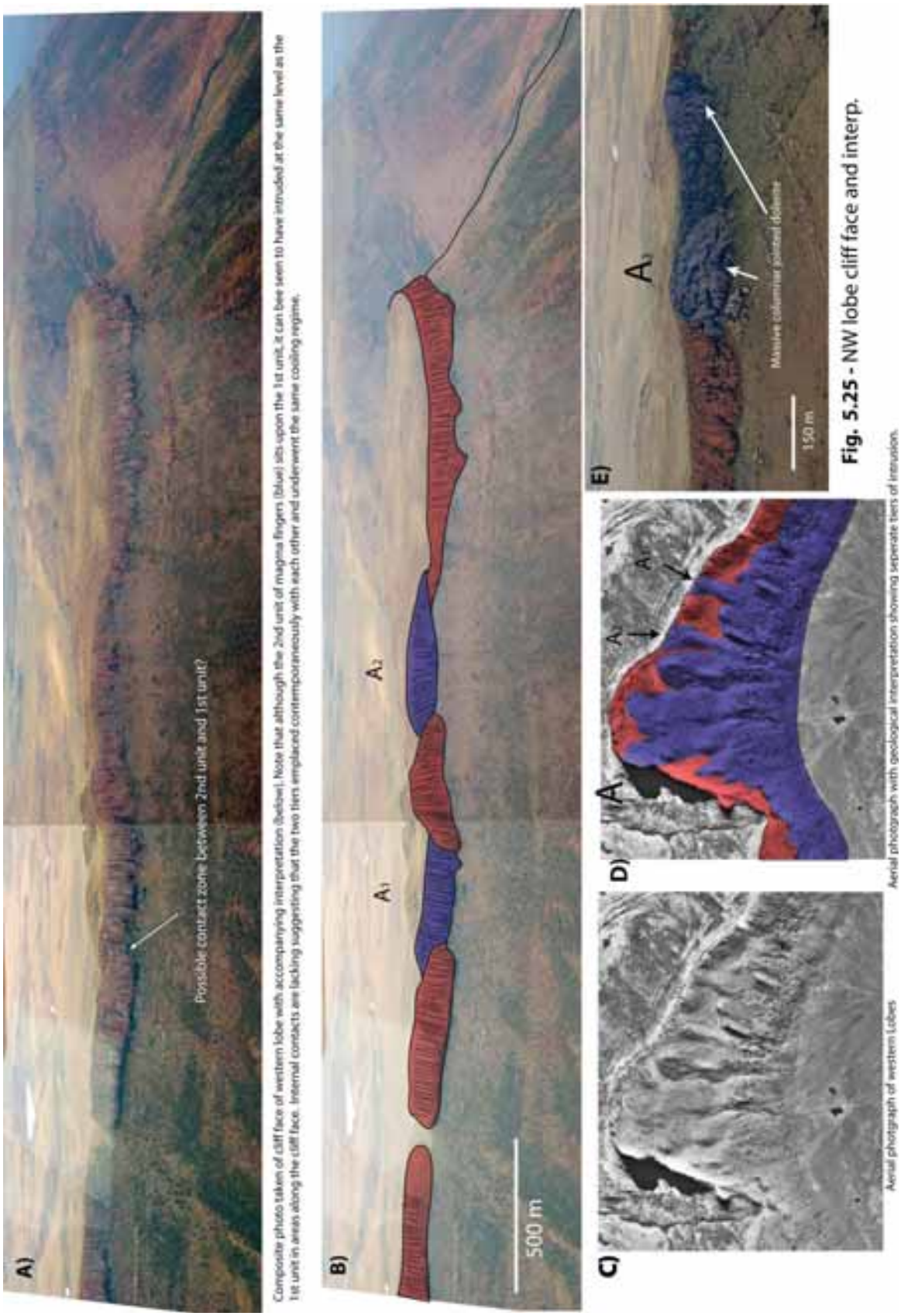

Composite photo taken of cliff face of western lobe with accompanying interpretation (below). Note that although the 2nd unit of magma fingers (blue) sits upon the 1st unit it can bee seen to have intruded at the same level as the 1st unit in areas along the cliff face. Internal contacts are lacking suggesting that the two tiers emplaced contemporaneously with each other and underwent the same cooling regime.

Fig. 5.25 - NW lobe cliff face and interp.

.

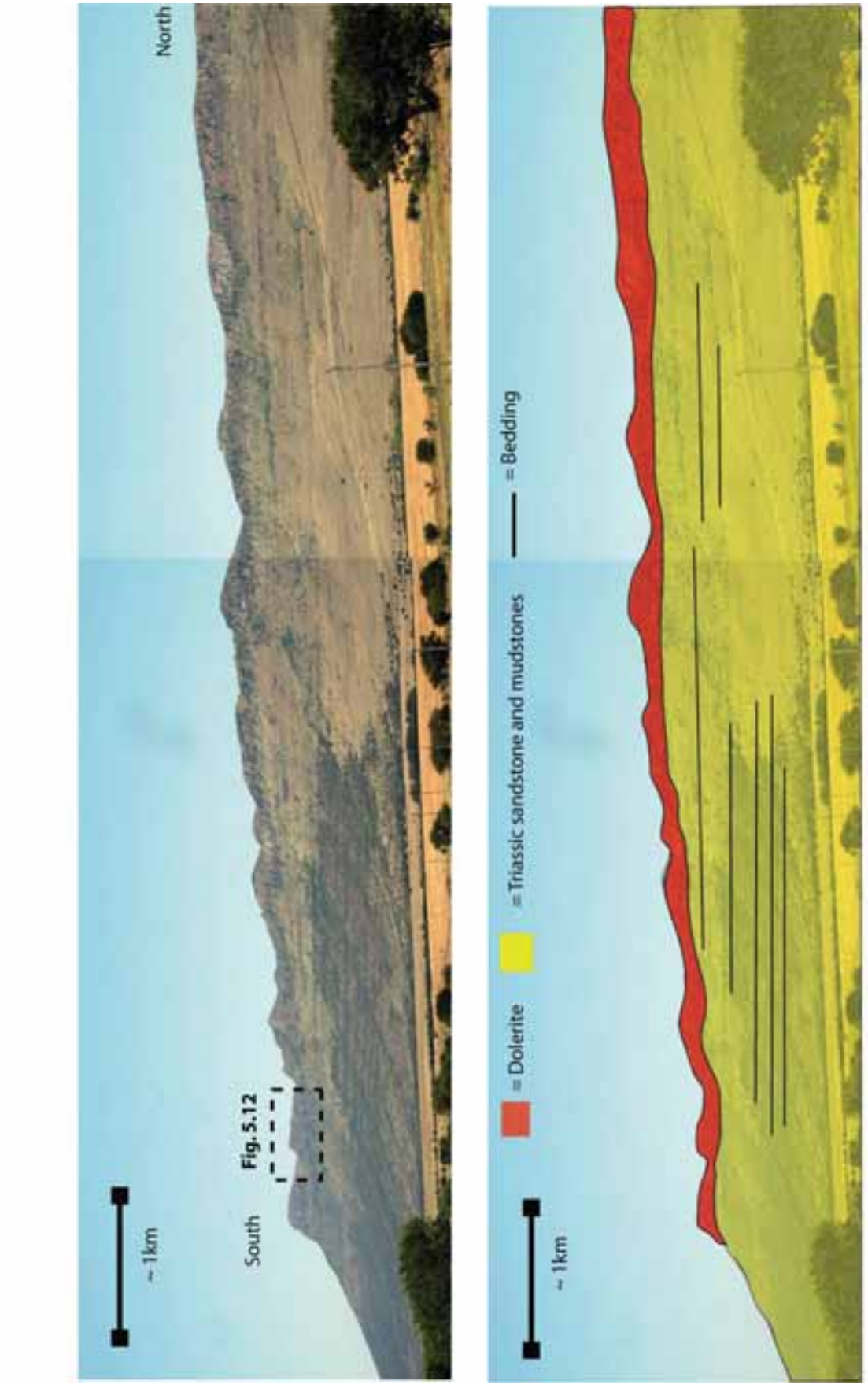

Fig 5.26 - Showing the broad peaks and troughs of the Eastern ridge of dolerite GVS. Note the layer cake laterally continuous strata

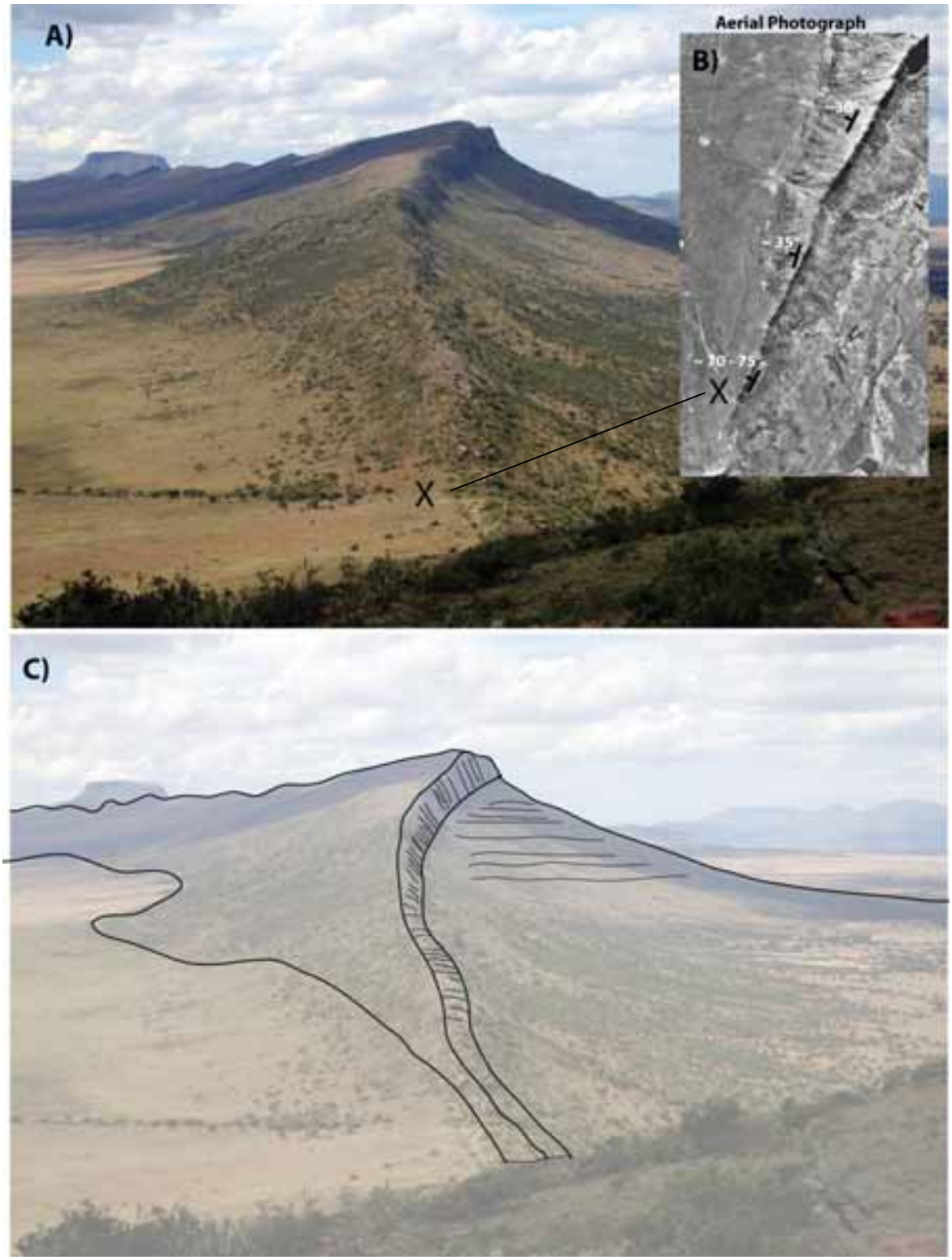

Fig. 5.27 – Photo looking NNE, showing the rapid increase in dip of the arcuate inclined sheet along the eastern sector of the GVS toward the south.

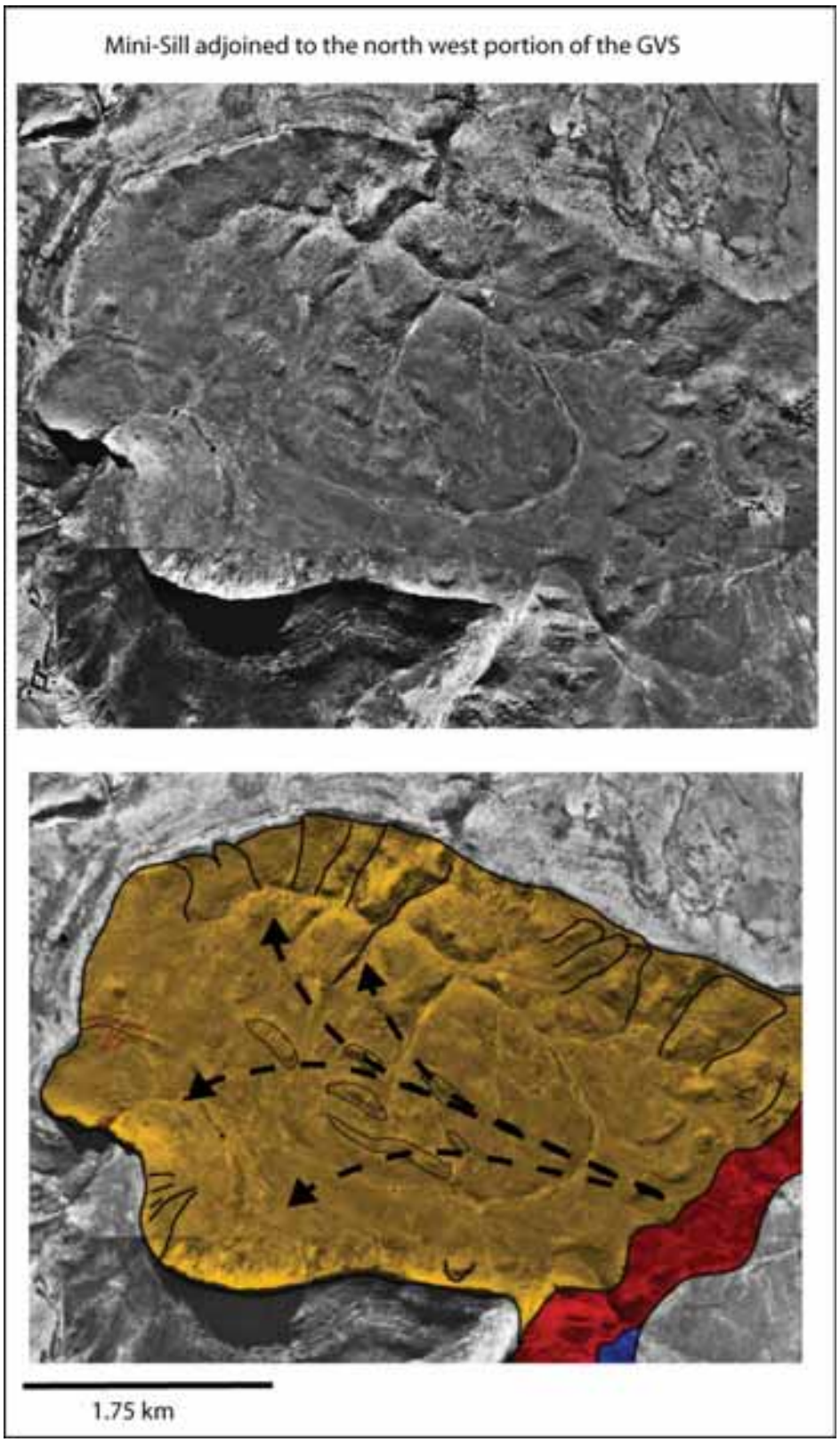

Fig. 5.28 – Parasitic saucer-shaped sill which adjoins the main Golden Valley Sill. Convex up finger-like features are shown (solid black lines black). Interpreted Flow directions are based on feldspar alignments (Fig. 5.19) and geochemical studies of Galerne et al. (2008), which showed that the dolerite forming parasitic sill was geochemically identical to the dolerite of the main GVS and therefore likely a offshoot from the main sill.

Interestingly where the dip of the eastern lobe increases, i.e. at the north and south tips of the sill (long axis of the ellipse), magma finger structures are poorly developed, compared to shallowly inclined sectors of the sill which are adjacent to the short axis, which show well-developed magma finger structures.

5.3.4 Parasitic Saucer-Shaped Sill

One prominent feature of the GVS is the outgrowth of a small saucer-shaped sill from its north west rim. This smaller saucer-shaped sill is a roughly circular saucer-shaped sill with a diameter of 3.5km and appears to be connected to the main Golden Valley Sill. (Fig. 5.28).

The sill, contains features similar to those seen in the Golden Valley Sill, albeit on a smaller scale. Finger-like structures can be identified on the inclined sheet of the outer sill, and trend radially around the outer sill with a locus which extends towards a centrally located axis running approximately SE – NW along the axis of the saucer (Fig. 5.28). This suggests that the sill is fed from a centrally located source. Galerne et al. (2008) found the geochemistry of the mini-saucer exactly matched that of the main saucer of the GVS, suggesting that the mini-saucer was sourced directly as an offshoot from the Golden Valley Sill.

5.4 Interpretation of convex-up undulations (Magma fingers)

The radial nature of the magma-fingers and observed weak alignment of phenocrysts along the axes of undulations suggests some genetic connection between the magma-fingers and magma transport (flow), this was confirmed by Polteau et al. (2008), in which AMS analysis and field observation of ropy flow folds showed flow fabrics orientated away from the central axis of the saucer. Polteau et al. (2008) drew no conclusions about the finger structures' genesis aside from referring to the features as 'magma channels'.

Given their primary nature, there are two possible explanations for these "magma channels": flow localisation or magma fingers (Fig. 5.29).

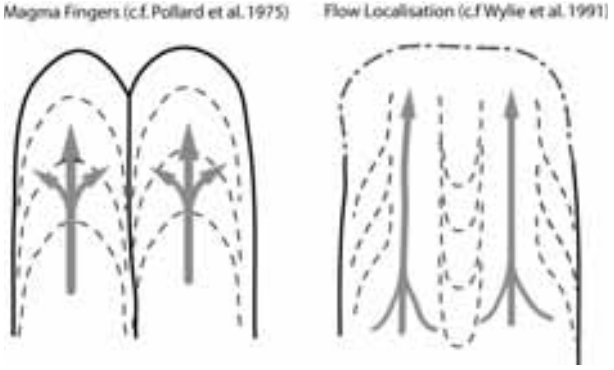

Fig 5.29 – Showing conceptual models of flow within fingers (Pollard et al., 1975) and flow within a sheet undergoing flow localisation (Wylie et al., 1999).

Flow localisation (Wylie et al., 1999), develops as a consequence of uneven cooling across a sheet, focusing flow into channels similar to lava tubes. To occur, the sheet must undergo a period of sustained flow (Holness and Humphreys, 2002), meaning that the process is unrelated to primary sill propagation at the tip of the intruding sheet. In the circumstance that flow localisation did form the fingers seen within the GVS, one would expect the tip of the sill, if exposed, to be linear.

Magma fingers - The second possibility is that the radiating undulations represent magma fingers (Pollard et al., 1975) where the tip of the sill has propagated as a series of separate tube-like fingers, which accelerate ahead of the main sheet and then inflate vertically and laterally to coalesce to form a continuous sheet. As magma fingers will not advance through host rock at a uniform rate, tips of fingers should be visible, if suitable exposure exists and subsequent erosion has not altered the form of the fingers.

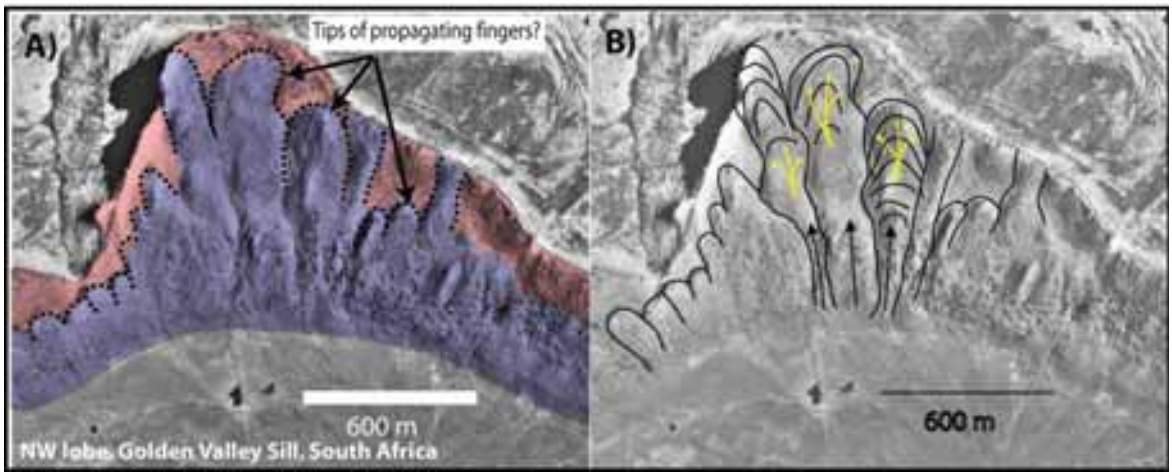

Fig. 5.30 – A) Showing Aerial photographs of the NW lobe illustrating tips of fingers, which also posses a bulbous nature B) Sketch of expected flow regime within finger during formation

Within the North West lobe of the GVS, finger-like structures can be mapped out along the front of the upper sill unit. Clear evidence of tips to the finger-like structures can be seen (Fig. 5.30). In addition, the finger-like structures typically have bulbous terminations, suggesting that they propagated as separate finger-like features, and subsequently inflated laterally towards each other (Fig. 5.30b).

These observations would suggest that the features seen within the GVS are finger structures *sensu* Pollard et al. (1975) and not the result of flow localisation (*sensu* Wylie et al., 1999) forming lava like 'magma channels', as suggested by Polteau et al. (2008).

Pollard et al. (1975) proposed that finger formation was the result of viscous fingering, caused by propagation of one viscous fluid into another (Saffman and Taylor, 1958). Finger

formation and the emplacement model of the Golden Valley Sill will be dealt with in Chapter 6, however as noted by Pollard et al. (1975), the process of viscous fingering results in fingers possessing a regular wavelength peak-peak. Of note is that within the GVS, although the wavelengths of fingers developed in the upper and lower sill units vary, the finger structures within an individual sill display a remarkably uniform wavelength (peak-peak), this is particularly obvious in the eastern lobe of the GVS (see Fig. 5.17)

5.4.1 Finger structures in other Saucer-Shaped Sills

Several geochemically identical saucer-shaped sills formed in immediate proximity to the GVS (Fig. 5.31), and were probably fed from the same source of magma (Galerne et al., 2008).

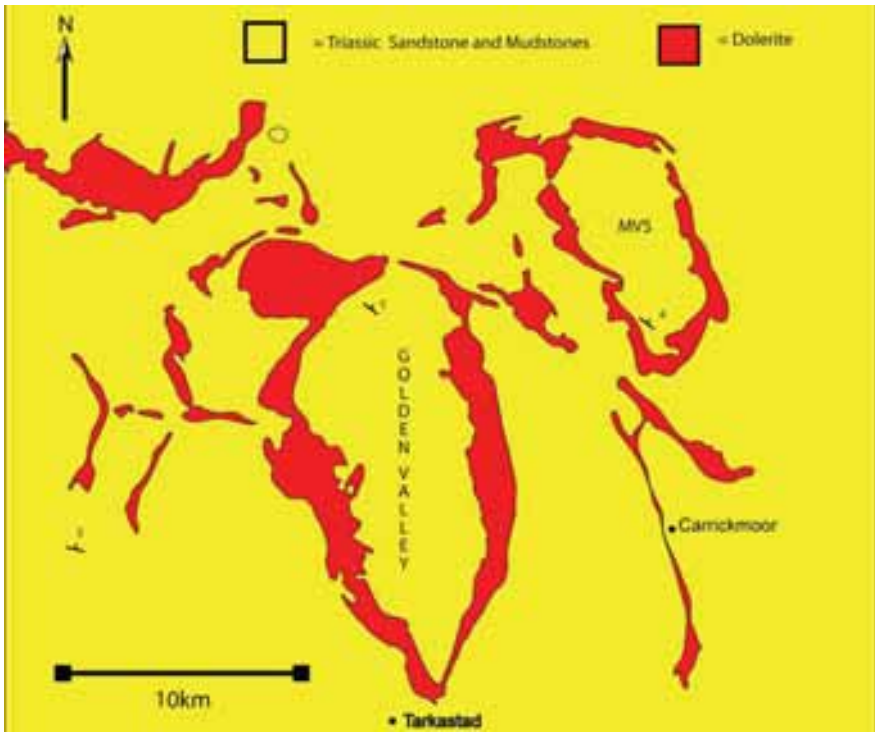

Fig. 5.31 – Showing Golden Valley Sill and Morning Valley Sill, top right

Similar finger-like structures, to those seen within the GVS can additionally be identified within the Morning Valley Sill (MVS), which is an elliptical saucer-shaped sill, 10 × 4km in scale (Fig. 5.31 and Fig. 5.32). The outline of the sill is less symmetrical that that of the GVS with the sill outcrops of dolerite showing a complicated segmented outcrop pattern within the MVS (Fig 5.33).

5.4.1.1 Lobes and fingers

In the eastern transgressive rim of the MVS, finger-like structures, analogous to those in the

GVS were identified, extending upward and away from the inner sill. Although the form of the finger-like structures is not as well preserved as that within the GVS, with no finger-tips being readily identifiable, splaying of fingers can be identified within the dolerite, particularly in the SE sector of the sill (Fig. 5.32 and Fig. 5.33).

The finger-like structures define broad zones of dolerite, which appear to constitute separate lobes (Fig. 5.34). The occurrence of separate lobes is further supported by a region in the NE corner of the sill, where one lobe of dolerite sits structurally atop another (Fig. 5.35 inset), confirming the separate emplacement of dolerite associated with each lobe.

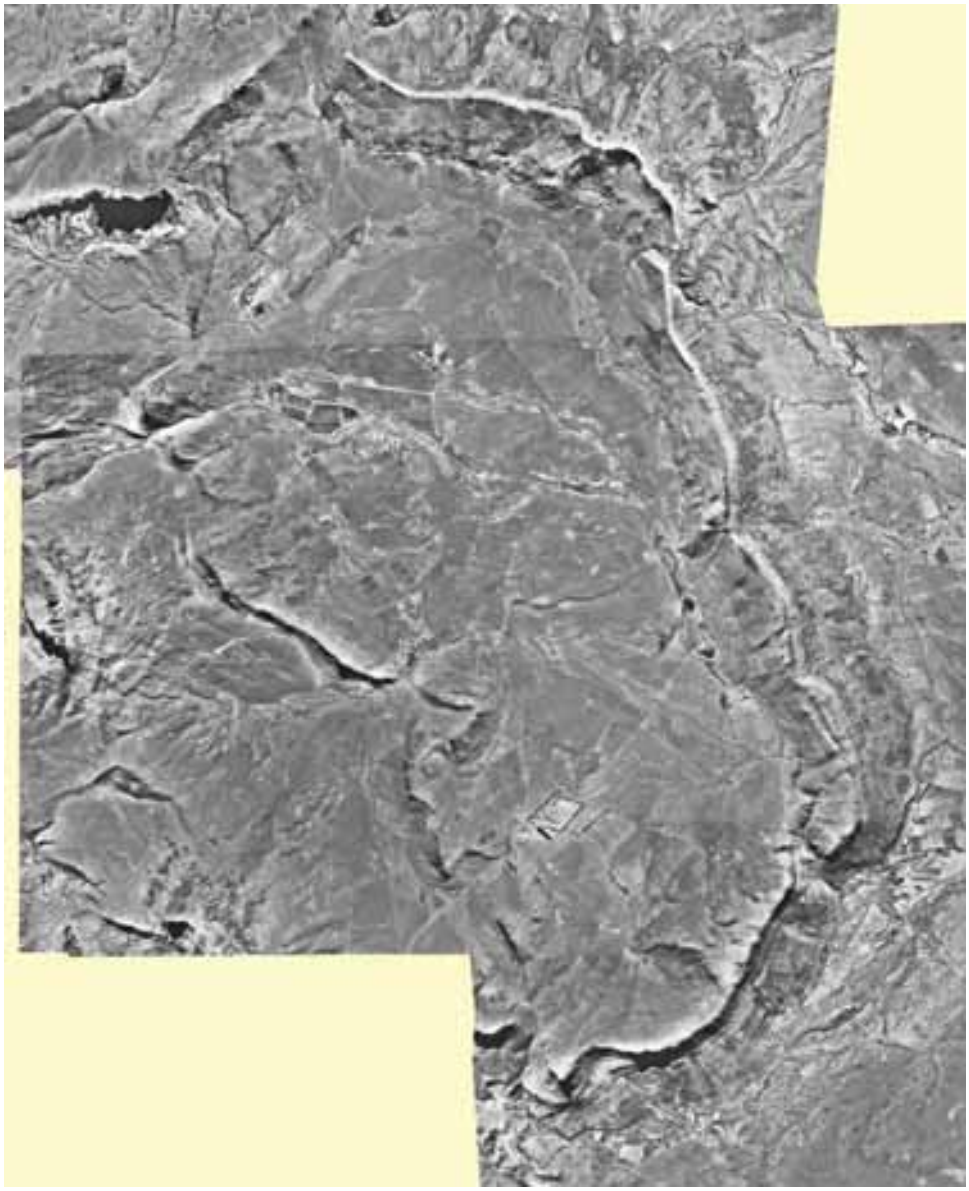

Fig. 5.32 – Aerial photograph of MVS Sill. Note the segmented nature to the dolerite outcrops forming the prominent cliff faces.

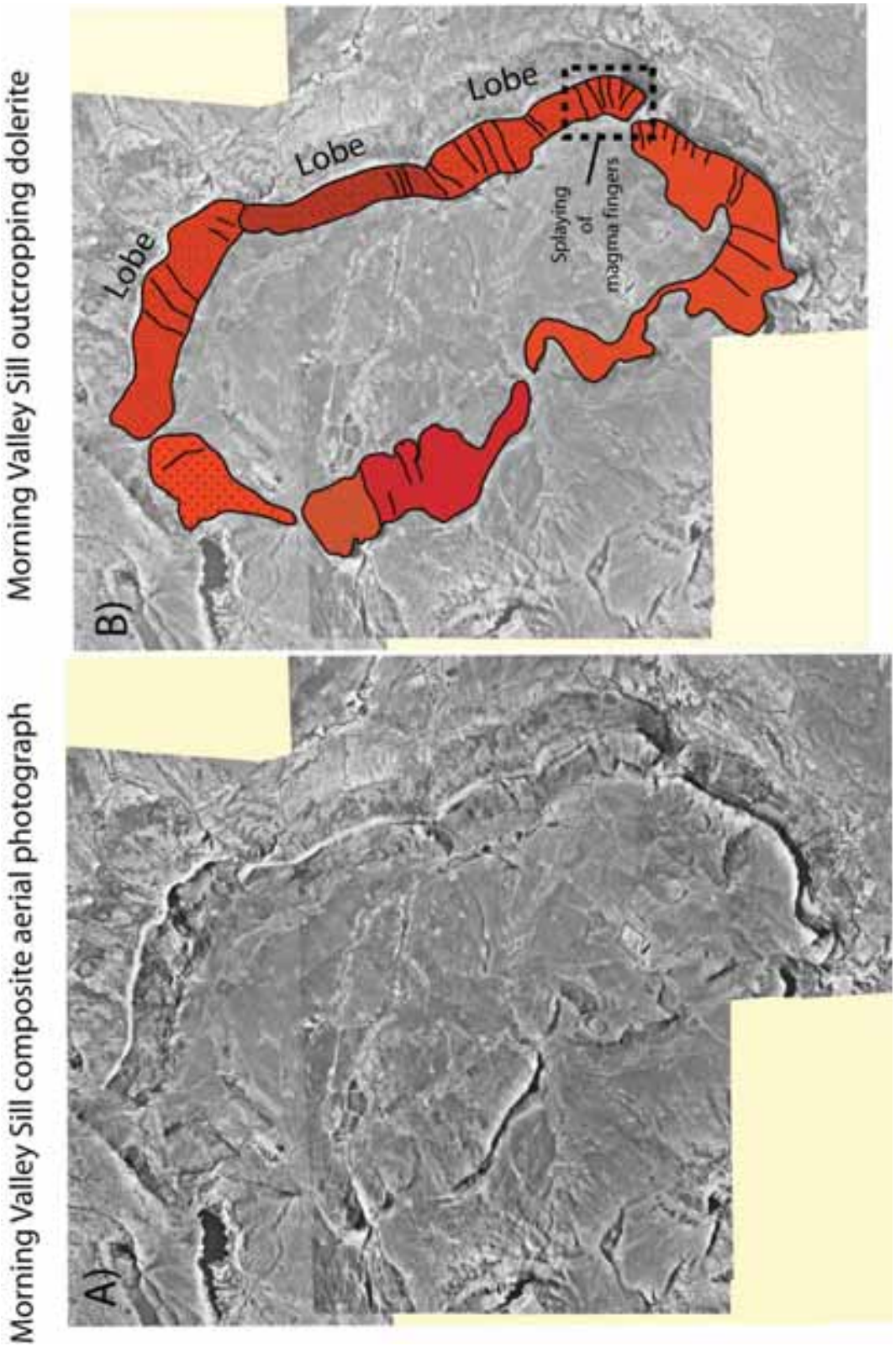

Fig. 5.33 – Figure showing segmented nature of the dolerite outcrops forming the arcuate inclined sheet of the sill.

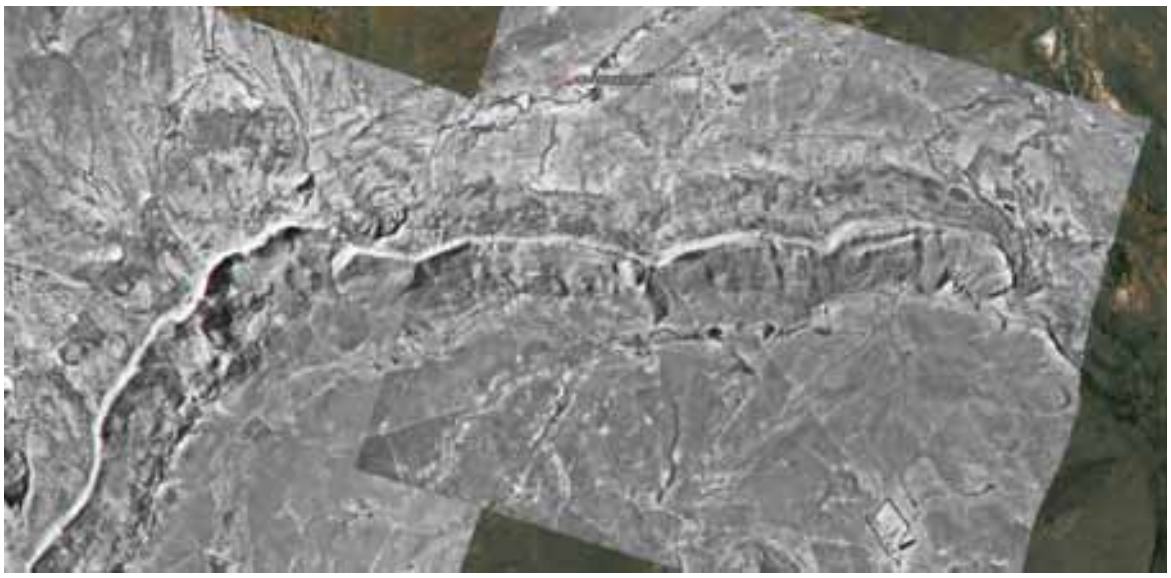

Fig. 5.34 – Eastern Segment of MVS, illustrating finger structures, which splay through approximately 80° (East to south) in the right hand portion of the image (south of the sill)

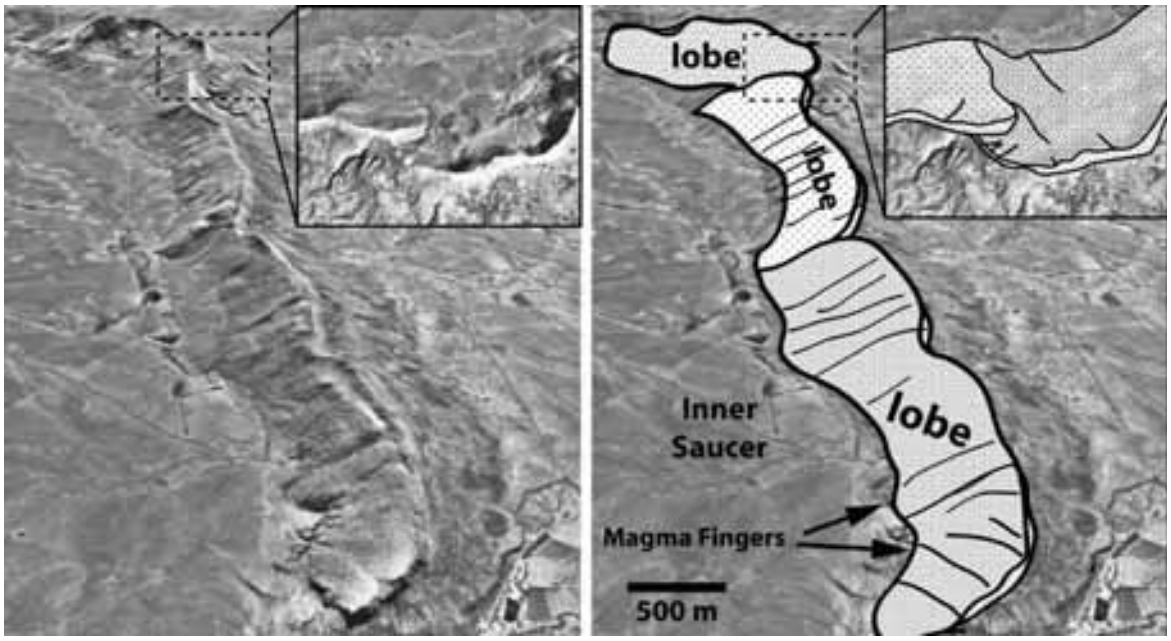

Fig. 5.35 – Figure showing oblique view of the eastern arcuate rim of the MVS, as seen in Fig. 5.33, showing the presence of finger-like structures, but illustrating that the finger structures define lobe like features.

5.5 Discussion

The key observations from the GVS and MVS are:

- The Golden Valley Sill has large-scale undulatory finger structures over 80% of its arcuate inclined sheet, which are primary in origin.

- The convex-up undulatory finger structures within the GVS resemble the convex-up finger structures seen within the sills of Trotternish Peninsula. They therefore may have a common origin.
- The magma fingers display a regular wavelength from peak-peak and are characterized by having broad humps interspersed with narrow troughs.
- The magma fingers extend radially away from the inner sill, which itself displays no evidence of fingers.
- Spatially associated sets of magma fingers can be mapped out, which appear to denote broad lobe like zones.
- The NW zone of the sill displays two tiers of magma fingers, the first is characterized by large wavelength fingers of ~ 500 m (Peak-Peak), with the second tier displaying smaller scale fingers of approximately 50 – 100m.
- Smaller 'wrinkle' features are visible in areas of the sill, but are the result of erosion along cooling joint sets. They are not the result of 'wrinkling' of the top surface of the sill under cooling, as proposed by Polteau et al. (2006) and Polteau et al. (2008).
- The exposed tips and bulbous terminations of fingers discount the formation of the features as a result of flow localisation (Wylie et al., 1999), but instead suggest they can be regarded as magma fingers (Pollard et al., 1975).
- Finger-like structures are exposed in the adjacent MVS, which equally show radiating patterns around a centrally located axis running along the long axis of the sill and are interpreted to represent magma fingers.
- Magma fingers within the GVS and MVS appear to form a fundamental part of lobe construction, i.e. that sills are formed from lobes, and lobes are formed from fingers.

5.5.1 Fingers within seismic data – a comparison with the GVS

From the work of Thomson and Hutton, (2004), it was found that saucer-shaped sills are either fed away from a centrally located source, or along a lateral (dyke) source, located in the lower most point of the inner sill. In each example Thomson and Hutton, (2004), noted the presence of lobes, and suggested that lobes may be constructed from smaller structures, suggesting a hierarchy with first order, second order etc. Although lobes within seismic data have been readily identified (Thomson and Hutton, 2004; Hansen and Cartwright, 2006), confirming the presence of smaller units has proved difficult to accomplish. Although seismic images produced in Thomson and Hutton (2004) and Thomson and Schofield (2008) show 'finger-like' structures (Fig. 5.36), the limitation of seismic resolution and opacity rendering makes it difficult to assess if these features are real.

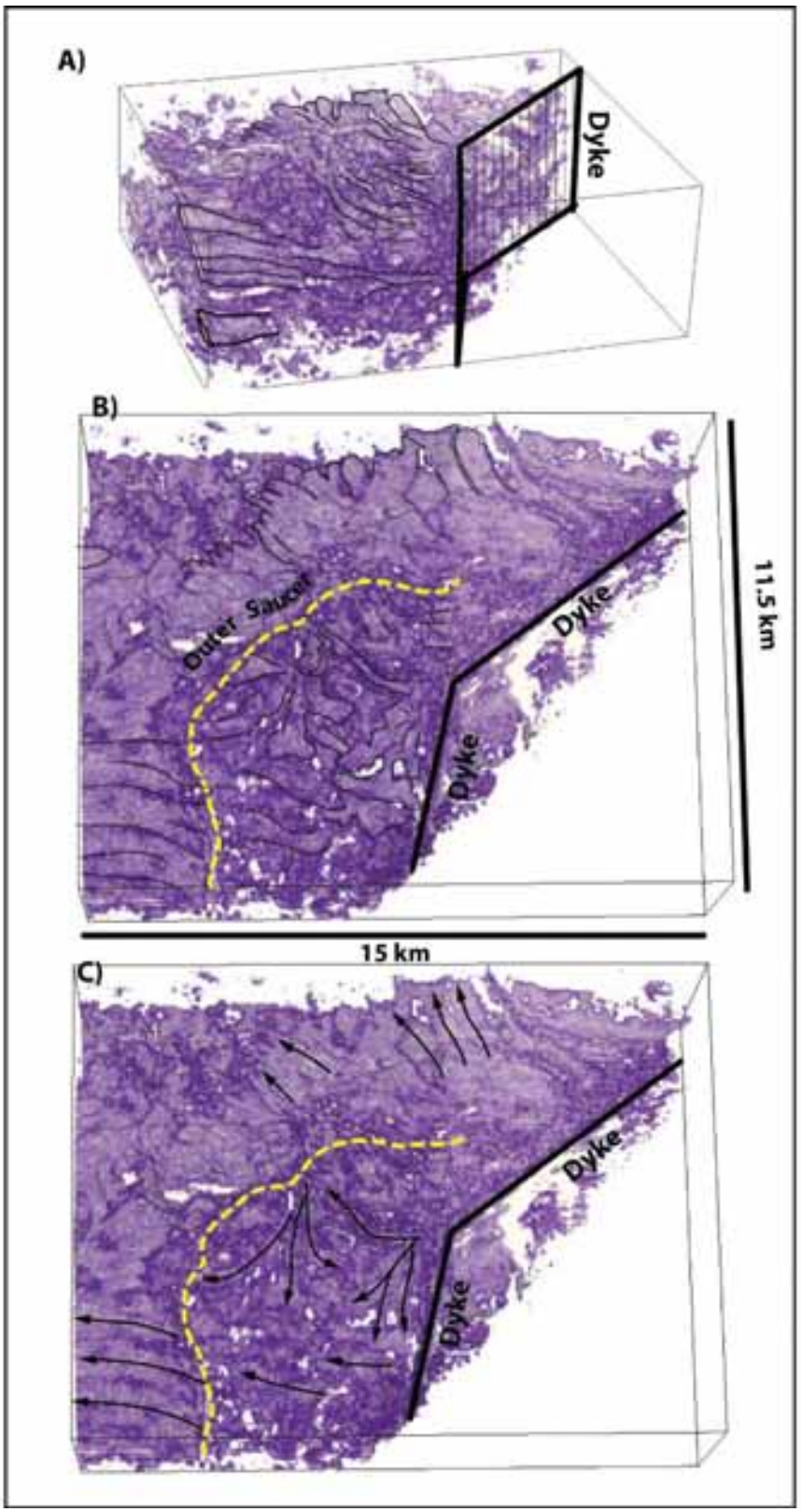

Fig. 5.36 – Modified from Thomson, 2007, shows half of a saucer-shaped sill from the Flett Basin, UKCS, being fed from a dyke source. A) Shows an oblique view, illustrating the presence of finger structures B) and C) Illustrates the occurrence of finger structures in the arcuate inclined sheet, and the complicated lobate structures seen in the approximately concordant inner sill. Interpreted flow directions are shown as black arrows.

The undulations seen within the GVS and MVS may represent this sub-unit (*sensu* hierarchy of units; Thomson and Hutton, 2004). Their occurrence and scale matches that of finger-like features imaged on 3D seismic data within the inclined sheet of saucer-shaped sills (Fig. 5.37)

5.5.2 Definition of fingers and lobes - A case for confusion

In extrusive terminology, a lobe is classified as the smallest discernable unit of 'flow', and may be several 10s centimeters to several meters in size with a series of lobes forming a single (lava) flow (Self et al*.,* 1998). In sub-volcanic emplacement a series of lobes comprise a single sill, however these structures are identified from seismic data based on morphology where the limiting factor is seismic resolution (in the order of 10s meters laterally) (e.g. Hansen and Cartwright, 2006; Thomson and Hutton, 2004). Therefore, the smallest discernable unit (a lobe *sensu lato*) is at least an order of magnitude bigger. What is clear from observations presented here, from both the GVS and MVS, is that a lobe (sensu Thomson and Hutton, 2004; Hansen and Cartwright, 2006; Figure. 5.38) is constructed from finger structures, which define the lobe (detailed emplacement model in Chapter 6). To maintain consistency with previous work on sills from seismic data, a lobe (*sensu* Hansen and Cartwright, 2006; Thomson and Hutton, 2004; Figure. 5.38) can be determined as a fundamental component of a sill, and a finger (*sensu* Pollard et al*.,* 1975) as a fundamental component of a lobe.

Hansen and Cartwright (2006) allude to the model of magma finger formation *sensu* Pollard et al. (1975) to explain the possible formation of lobate features, with second and third order breakouts in the Solsikke Lobate Sill, imaged on 3D seismic data within the Norwegian Margin (Fig. 5.38a and 5.38b). However within some of the breakouts Hansen and Cartwright (2006) show the presence of what they term 'discontinuities' on a scale below the lobate features (Fig. 5.38b) that are similar in scale to the finger structures seen in the GVS (Fig. 5.38d). These may represent finger structures constructing the lobes, however more importantly it highlights that lobes and fingers are not the same structure, and that the emplacement mechanism of fingers (sensu Pollard et al., 1975) cannot be invoked in the formation of lobes, as done so by Hansen and Cartwright (2006) unless finger structures have been clearly identified forming the lobes.

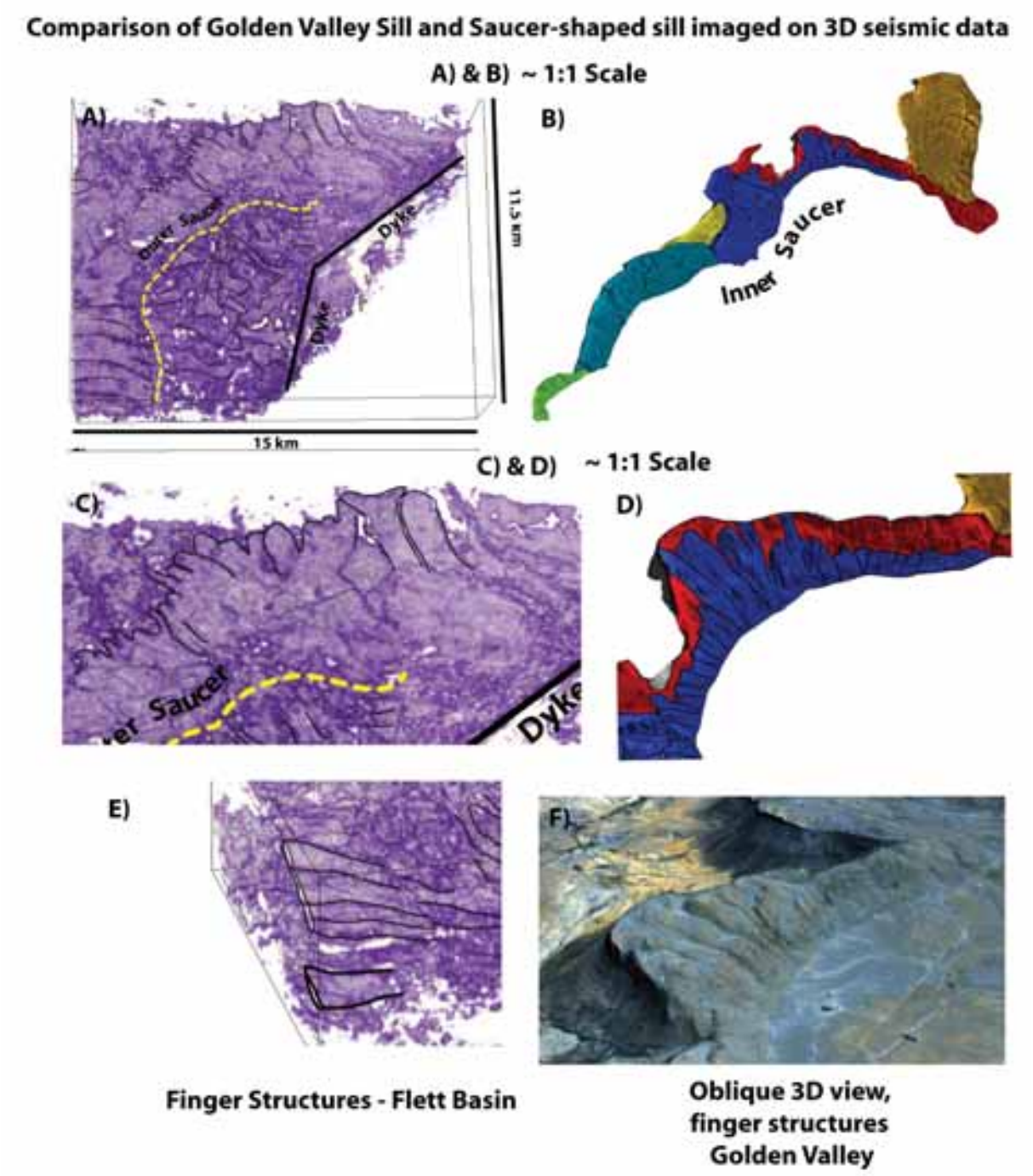

Fig 5.37 – An opacity rendered sill (modified from Thomson, 2007) at 1:1 scale with diagrams of the Golden Valley Sill (Fig. A & B, Fig. C & D). What is firstly apparent is the comparable scale between the field example of the Golden Valley Sill and those imaged within seismic data. Fig. E shows a zoomed oblique view of the fig. A, illustrating occurrence of finger structures. An oblique view of the NW lobe of the golden valley sill is shown for comparison (Fig. F).

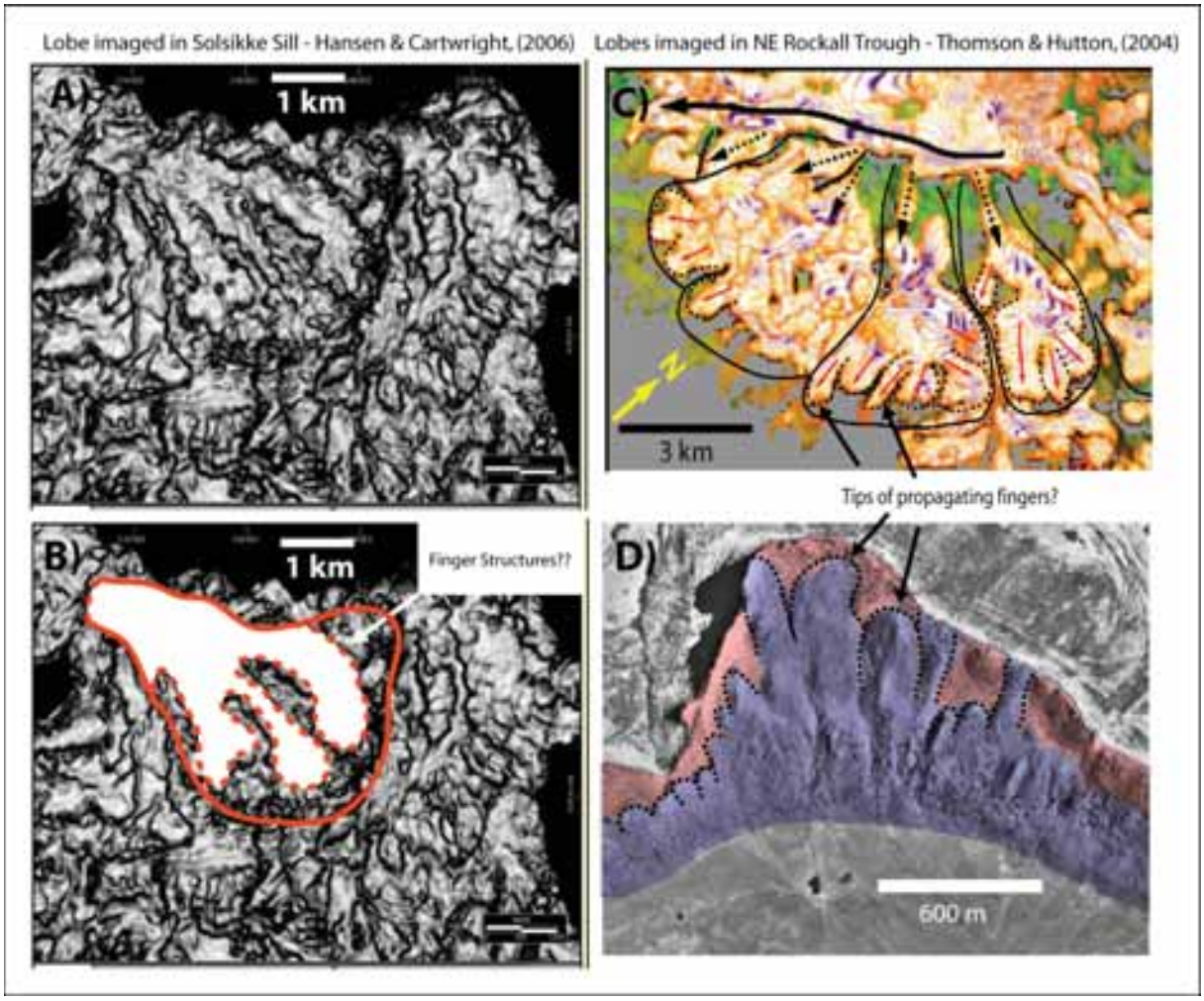

Fig. 5.38 – A) and B) Taken from Hansen and Cartwright, 2007, showing a lobate feature, with internal discontinuities. C) Taken from Thomson and Hutton, 2004, showing lobate features and possible evidence of fingers D) GVS North West lobe for comparison

Chapter 6
Magma finger formation and the emplacement model Of the Golden Valley Sill

The Golden Valley Sill (GVS) exhibits magma fingers with unprecedented access to 3D exposure. Since Pollard et al. (1975) first detailed the occurrence of magma fingers, little work has been done in understanding the actual mechanisms which govern their formation.

This chapter will explore some of the possible mechanisms of magma finger formation and then apply this to the overall emplacement model of the GVS, which in turn may be applicable to the emplacement of other saucer-shaped sills.

Throughout this chapter the term 'host rock' will be applied in sense of the host medium into which the magma intrudes, the term is not intended to make any allusion to state of consolidation.

6.1 Magma finger formation - Introduction

The first full description of the occurrence of magma fingers in relation to sills was made by Pollard et al. (1975). To explain their formation Pollard et al. (1975) used the analogy of viscous fingering described by Saffman and Taylor (1958), in which a fingered interface forms as a result of the propagation of a lower viscosity fluid into a high viscosity fluid.

The assumption that the same process operated in the formation of magma fingers is based solely on the argument that magma finger formation is a mechanically inefficient process (Pollard et al., 1975). Pollard et al. (1975) argued that compared to the intrusion of a planar sheet of magma, the formation of magma fingers would expend more energy due to increased viscous drag forces operating around the magma fingers and deformation of country rock needed as a magma finger propagated through host rock. Pollard et al. (1975) therefore proposed that viscous magma fingers must operate to effectively override the minimum energy argument.

Pollard et al. (1975) did not explore the mechanism in which magma fingers were triggered in any more detail, or explore their occurrence in other sills, stating that the formation of viscous magma fingers was "as yet not a fully understood mechanism for the initiation of fingered intrusion".

The use of the term 'magma magma fingers' has become commonplace in sill

emplacement literature, in particular due to the recent advances in the use of 3D seismic data to elucidate large-scale morphologies of sill complexes. Thomson and Hutton (2004) employ the term 'magma finger' *sensu* Pollard et al (1975) to refer to the stepped edges of saucer-shaped dolerite sheets (see chapter 3), stating that the staircase morphology of sills reported by Francis (1982) and Rickwood (1990) are the same as the magma fingers proposed by Pollard et al. (1975). Hansen and Cartwright (2006) applied the observations of Pollard et al. (1975) on magma fingers to explain the formation of lobate sills on the Norwegian Margin.

Both the work of Thomson and Hutton (2004) and Hansen and Cartwright (2006) demonstrate the current misuse of the term 'magma fingers' in the published literature due to the limitations of resolution in seismic data. The staircase morphology as reported by Francis (1982) and Rickwood (1990), are not magma fingers. As explored in Chapter 5, lobes are not the same as magma fingers, as assumed by Hansen and Cartwright (2006), given that saucer-shaped sills within field examples which possess lobate morphology often contain lobes which are formed from magma fingers.

Morever, the classification of features within the literature as magma fingers *sensu sticto* Pollard et al. (1975), sometimes incorrectly (Thomson and Hutton, 2004; Hansen and Cartwright, 2008), is done so without the ability to examine the mechanisms underlying magma finger formation.

6.2 Magma finger formation: Non-brittle behaviour of host rocks

Magma finger formation is incompatible with normal brittle fracture (Pollard et al., 1975; Baer, 1991) as the host rock must act in a viscous state. Magma finger formation will always occur where a viscosity contrast exists between two fluids (Saffman and Taylor, 1958). For host rocks to behave in a purely viscous manner is an idealized situation, but a pseudo viscous-viscous relationship can be established between magma and host rock in two circumstances;

- **Primary non-brittle behaviour** - Host rock can behave in a viscous fashion if it possesses no mechanical strength, so on intrusion of magma, the low shear modulus of the host rock renders it incapable of taking a brittle fracture. In this circumstance viscous deformation of an un-consolidated host rock will occur at the propagating front of the intrusion, in effect mimicking a fluid-fluid interface between host rock and intruding magma, which will subsequently become unstable.

This type of situation is likely to occur where magma has intruded into host rocks which have little or no cohesion between grains. Such a situation would be analogous to intrusion of magma into unconsolidated host rocks at shallow crustal levels (*see* Duffield et al., 1986). In this scenario, as the magma propagates the host rock particles will be displaced around the intruding front of the magma, and not behave in a brittle fashion.

- **Secondary triggered non-brittle behaviour** – If host rock contains some coherent strength, if it is to behave in a viscous manner during intrusion of magma a secondary process must operate which degrades the mechanical strength and coherency between particles. Such a secondary process can be defined as a process which only operates as a result of intrusion of magma, and is not an inherent property of the host rock

  A widely accepted process in triggering host rock to behave in a viscous-like fashion is fluidization (Kokelaar, 1982). Fluidization can occur if rapid expansion of heated pore-fluid/vapour occurs at such a velocity that it causes disaggregation of host rock by effectively suspending particles of the host rock within a buoyant fluid/gas matrix, causing the host rock to act as a fluid-like mass. The process can equally operate in unconsolidated sediments, enhancing the fluid-like behaviour of the rock, but can also act on partially consolidated rock, which contains some inherent mechanical strength, by breaking apart the rock matrix and triggering it to behave in a fluid-like state.

6.2.1 Fluidization after Kokelaar (1982)

If magma contacts water-saturated host rocks vapour can be generated under a wide range of temperature and pressure conditions (Kokelaar, 1982). The mechanisms of fluidization of host rock are complicated and varied, in an attempt to understand fluidization Kokelaar (1982) placed a series of theoretical constraints based on the specific volume of water under a range of temperature and pressure conditions.

Kokelaar (1982) gave four example pathways (Fig. 6.1), showing the possible effect of heating and pressure drop in pore-fluid;

Pathway A is representative of heating at a uniform pressure, Kokelaar (1982) hypothesised that on crossing the phase boundary, an explosive expansion of water will occur causing a momentary fluidizing flow of vapour and instigating fluidization of host rock.

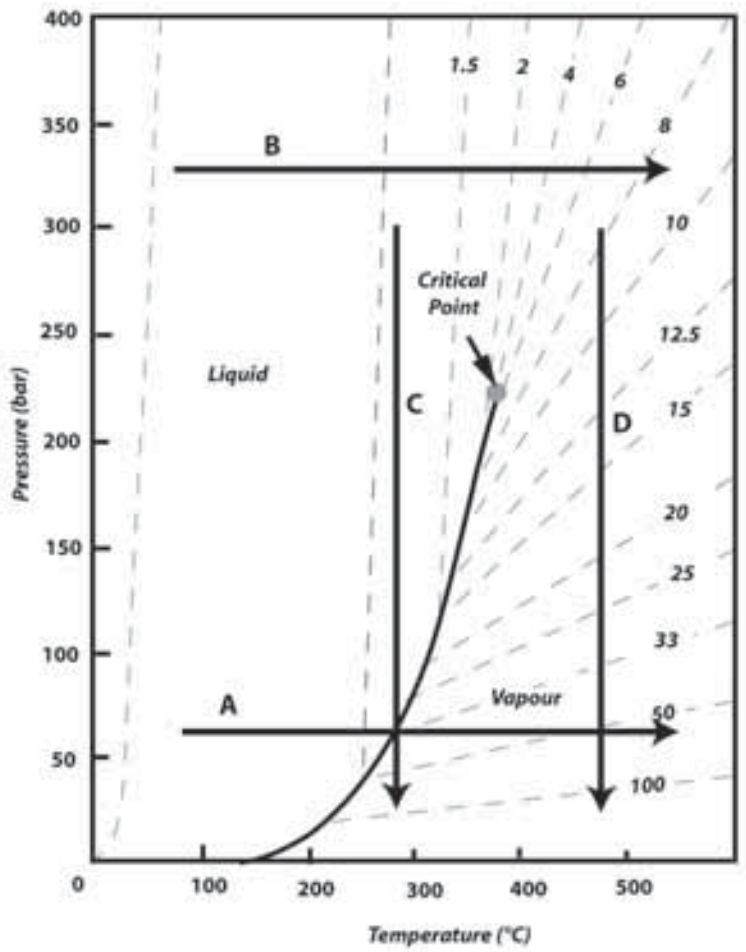

Fig 6.1 –Re-drawn from Kokelaar (1982) showing variations in specific volume of water with temperature and pressure. See text for details

Pathway B is representative of heating above the critical point, although moderate expansion occurs in the non-distinct transition of liquid to vapour, Kokelaar (1982) argues that this expansion may be mainly accommodated by inter-granular fluid flow.

Pathway C is representative of a heated pore-fluid, in a liquid state, undergoing rapid pressure drop, which causes it to rapidly cross the phase boundary, causing a rapid expansion in vapour.

Pathway D is representative of supercritical fluid undergoing a rapid pressure drop, causing a rapid transition from a super-critical liquid phase to a vapour phase accompanied by a subsequent expansion in vapour volume. Such an effect may occur due to opening of a fracture (Kokelaar, 1982; Curtis and Riley, 2003).

Kokelaar (1982) concluded that fluidization was only likely to occur in Pathways A, C and D.

The model of Kokelaar (1982) in which fluidization occurs, and applied by others without further investigation (Busby-Spera and White, 1982; McPhie, 1992, Thomson and Hutton, 2004; Thomson, 2007; Thomson and Schofield, 2008) was based solely on the phase relationships of water determined by experiments of Kennedy and Holser (1966), conducted by heating of water in a confined pressure vessel. Kokelaar (1982) took no account of host rock properties, i.e. porosity, permeability and host rock strength and made no attempt to understand the effect of expanding pore-fluid on these properties and ultimately on the process of fluidization. Delaney (1982) showed that in heated shallow level host rocks with low permeability and high porosities, pore-pressures could develop which were higher then lithostatic pressure, thus triggering failure in the host rock. Therefore it is important to try and understand the process of fluidization in context of host rock properties and its applicability to the emplacement mechanisms of magma.

Busby-Spera and White (1987) concluded that host rock sediment character played a major role in controlling magma-sediment interaction. They noted that in high permeability sediments, the peperitic structures produced tended to be blocky peperites, due to the inability of host rocks to maintain a vapour film, whereas in fine-grained, well sorted sediments, with low permeability, fluidal peperites could form due to the maintenance of a vapour film, allowing the rock as a whole to act in fluid-like fashion.

The heating effect of an igneous intrusion will tend to drive pore-fluid away from intruding magma (McPhie, 1992), depending on permeability and pore space connectivity (Francis, 1982b). In the case of a highly permeable rock, pore-fluid will travel away from the heat source through permeable pathways, leaving the pre-intrusion porosity of the host rock relatively unchanged (Francis, 1982b). However if a rock is highly impermeable, with low pore space connectivity, the pore-fluid will remain in place, and the heating effect of the intruding magma would cause thermal expansion of the pore-fluid and increase in fluid pressure (Francis, 1982b; Hanson, 1995). If pore-fluid pressures becomes high enough, disaggregation of the sediment matrix and opening of small micro-fracture act to increase porosity and permeability, at least temporally, thus allowing pore-fluids to escape (Francis, 1982b; Kokelaar, 1982). The ability for fluidization to operate will be dependant on the speed at which pore-fluid expansion takes place and the mechanical strength of the host rock.

6.3 Classification of fluidization

Within this chapter, the mechanism of fluidization will be examined in terms of two separate process driven classifications; Thermal Fluidization and Triggered Fluidization (Schofield et al., *in press*). Kokelaar et al. (1982) did not act to classify fluidization, however it is important to make this distinction as the mechanism of formation of fluidization could play a major role in controlling the emplacement mechanism of magma into host rocks.

6.3.1 Thermal fluidization

Thermal fluidization occurs as a result of the heating effect of the magma, changing the heated pore-fluids into a vapour phase, causing rapid expansion in pore-fluid volume, disaggregating the rock and triggering fluidization.

With burial, any confinement of the pore-fluids taking place will lead to an increase in pore-fluid pressure (hydrostatic pressure) within the host rock as the pore-fluid is heated. In such a circumstance pore-fluids will not follow Pathway A (Fig. 6.1) as proposed by Kokelaar (1982). Instead, upon heating, the confinement of pore-fluids will prevent the fluids from instantly flashing to a vapour phase, instead leading to an increase in pore-fluid pressure (Fig. 6.2). For the host rock to then fluidize, the pore-fluid pressure must overcome the yield strength of the grain boundaries. If this occurs, the sudden unconfinement of the pore-fluids will lead to a sudden change to the vapour phase and associated rapid expansion. If in a general sense the mechanical strength of host rock i.e. that caused by grain re-arrangement, compaction, and cementation, is assumed to be linked to permeability, then with increasing mechanical strength of rock, permeability of the sediments will fall, leading to increased confinement of pore-fluids (Fig. 6.2 A2).

The heating/pressure pathways of five arbitrary points are shown in Figure 6.2. As the Coulomb failure envelope becomes larger, pore-fluid pressure must reach increasingly higher pressures above normal hydrostatic pressure to overcome the yield strength of the rock. Delaney (1982) calculated that in host rocks of a lithostatic pressure of 10Mpa (roughly equivalent to a burial depth of 430m in sandstones), a 20% pore pressure increase over normal hydrostatic gradient would be needed to instigate failure in host rock. However on burial, compaction and cementation will act to increase mechanical strength of host, in addition to reducing the fluid volume.

As a result, a critical point will be reached in which mechanical strength of the rock becomes too high, and pore-fluid volume becomes too low that even after heating, the pore-fluid

pressure will be insufficient to cause failure of the host rock. In such a circumstance fluidization will not occur (Fig. 6.2b – pathway 5).

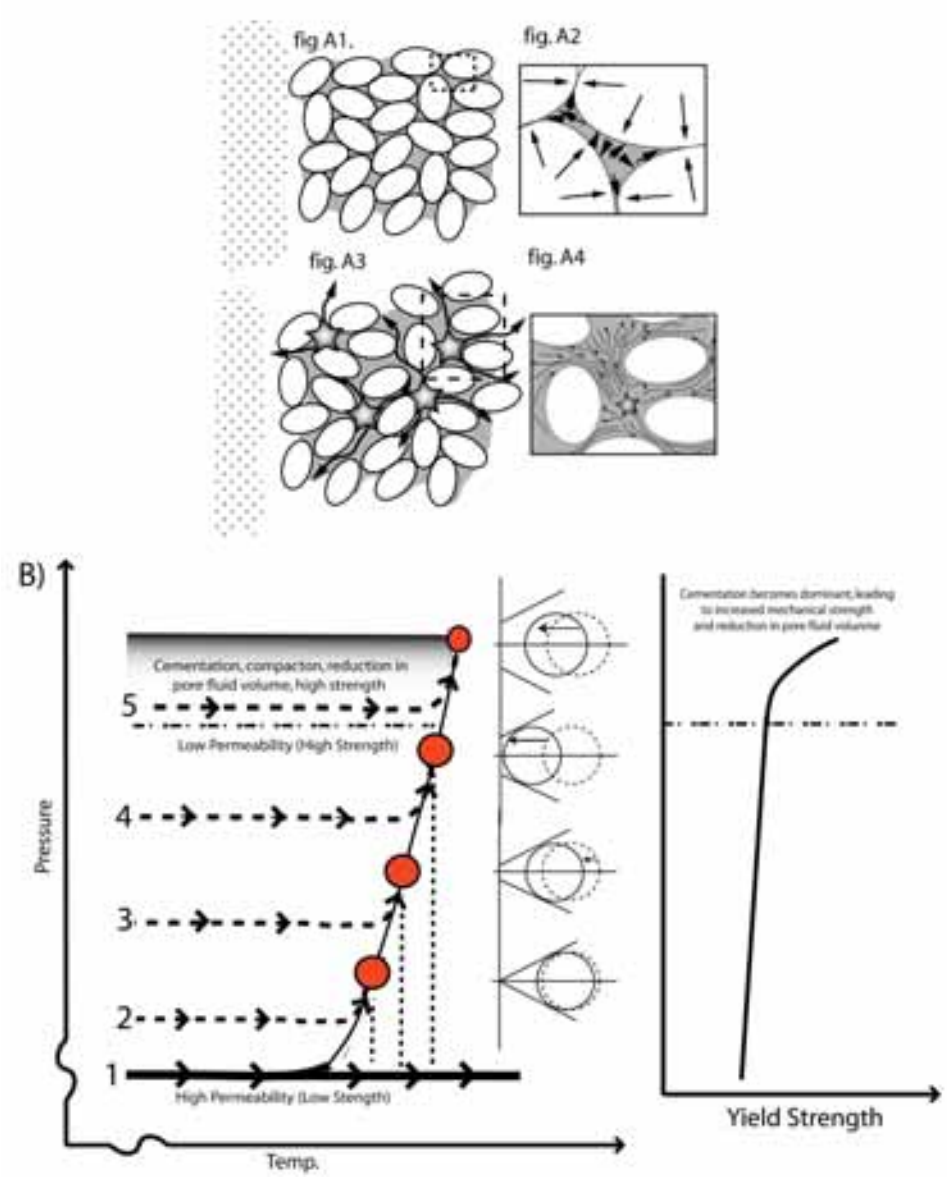

Fig. 6.2 – Illustration of Thermal fluidization. Upon heating of confined pore-fluids (i.e. those confined within pore spaces), for fluidization to occur, the pore-fluid pressure must increase to an extent that it can overcome the strength of the host rock matrix (Fig. A2). Only then can rapid unconfinement of pore-fluid occur (Fig B pathways 2 - 4), to induce fluidization. However with burial, cementation, compaction and reduction in pore-fluid will mean that even upon heating, the increase pore-fluid pressure will be insufficient to cause failure of the host rock matrix, and fluidization (Fig. B – pathway 5).

6.3.2 Triggered fluidization

In the previous section, the type of fluidization of host rock dealt with can effectively be considered to occur in-situ, in such a respect that the fluidization occurs as a result of volatization of pore-fluids by the primary effects of heating by intruding magma. However as Kokelaar (1982) and Curtis and Riley (2003) identified one of the most effective paths in fluidizing host rock was likely to result in rapid unconfinement of fluids (Fig. 6.7). This may happen with the opening of tensile fractures that are sufficient to cause a large temporary drop in pore-fluid pressure (Kokelaar, 1982; Curtis and Riley, 2003). In this respect, the fluidization can be regarded as triggered, as the rapid expansion of heated pore-fluids results from a secondary process.

The major difference from thermal fluidization is that triggered fluidization is initiated by a rapid unconfinement of the pore-fluids, effectively causing the heated pore-fluids to become momentarily under-pressured. This pathway, if large enough, can lead to a rapid crossing of the liquid-vapour phase boundary and flashing to steam (Fig. 6.3) which may be sufficient to disaggregate the host rock matrix and fluidize the rock (Curtis and Riley, 2003).

Understanding the exact process of fluidization is difficult to accomplish, as data is based on examination of rock in which fluidization has already occurred (Kokelaar, 1982; Busby-Spera and White, 1987; Krynauw, 1994). However, Figure 6.4 shows three conceptual models exploring the conditions in which 'triggered' fluidization would and would not occur, and illustrates the role the pore-fluid pressure and host rock strength plays in this. The process, although acting geologically instantaneously, still has a time factor attached, which cannot be easily estimated.

6.3.3 Constraints on depth of fluidization

For host rock fluidization to occur, the vapour must expand quickly enough to create high enough vapour velocities to suspend host particles of the rock/sediment in a buoyant gas matrix, causing fluid-like behaviour (Busby-Spera and White, 1982). The ability for this to occur will be a function of fluid volume, host rock strength, rapidity of vapour expansion and importantly clast size.

Kokelaar (1982) noted that some uncertainty exists under what conditions are required for the host rock to fluidize, but placed a depth constraint of ~ 1.6 km for the fluidization of wet sediments. Kokelaar (1982) concluded that under uniform heating below this depth, the pore-fluid would be above the critical point of pure water (221 bars) and the vapour percentage volume increase would be insufficient to cause fluidization. This figure is

commonly used as a benchmark for the depth at which fluidization will cease (*see* Krynauw et al., 1994; Thomson and Hutton, 2004; Curtis and Riley, 2003; Thomson, 2007).

However, the figure of 1.6 km is incorrect. In the calculation of Kokelaar (1982), the figure of 1.6 km was wrongly derived based on lithostatic pressure, but the pressure-temperature phase relationship of water derived by Kennedy and Holser (1966) and applied by Kokelaar (1982) applies to the pore-fluid pressure (hydrostatic pressure), and is thus unrelated to lithostatic pressure. Therefore, assuming an unconfined interconnected column of water, a hydrostatic pressure of 221 bars equates to a depth of approximately 2.2km. This may be an arbitrary cutoff point, as it is reliant on what form of fluidization is functioning i.e. thermal or triggered (Kokelaar, 1982).

In thermal fluidization, heating of fluids above the critical point is, as Kokelaar (1982) predicted, likely not to induce fluidization. However in the case of triggered fluidization, the pressure drop is a function of the size of fracture opened (*see* Sibson, 1975).

Estimating the exact magnitude of drop in hydrostatic pressure created during the opening of a fracture is difficult. With increasing depth, the pressure drop required to instigate a pressure drop sufficient to trigger fluidization will increase substantially. In pore-fluids heated to ~ 300°C at approximately 1km depth, the pore-fluid must become underpessured by ~ 50 bars to lead to a fluid volume increase by a factor close to 100%. At greater depths, for example ~ 3km, to achieve a 100% volume increase in 300°C pore-fluids, the required drop in fluid pressure is ~ 300 bars. Creating a large enough fracture to allow for such a pressure drop in the region of ~ 300 bars may be unfeasible. In addition, at such depths, even if a fracture of suitable magnitude could cause an expansion in pore-fluid volume suitable enough to cause fluidization, the process could be inhibited by the compaction and cementation within host rocks at this depth resisting pore-fluid pressure and preventing the host rock matrix from undergoing failure.

6.4 Fluidization and sill emplacement

6.4.1 Golden Valley Sill – Host rock characteristics

The Golden Valley Sill (GVS) intruded into flat-lying, unstructured interbedded mudstones and sandstones. The sill at time of emplacement intruded at approximately 1000 – 1500 m below the surface (Polteau et al., 2008), a depth based on approximate extrapolation of the basal basalt of the Drakensberg lavas, which underlie the majority of Lesotho.

Within the inner sill, most host rock is obscured by grazing land, and in the

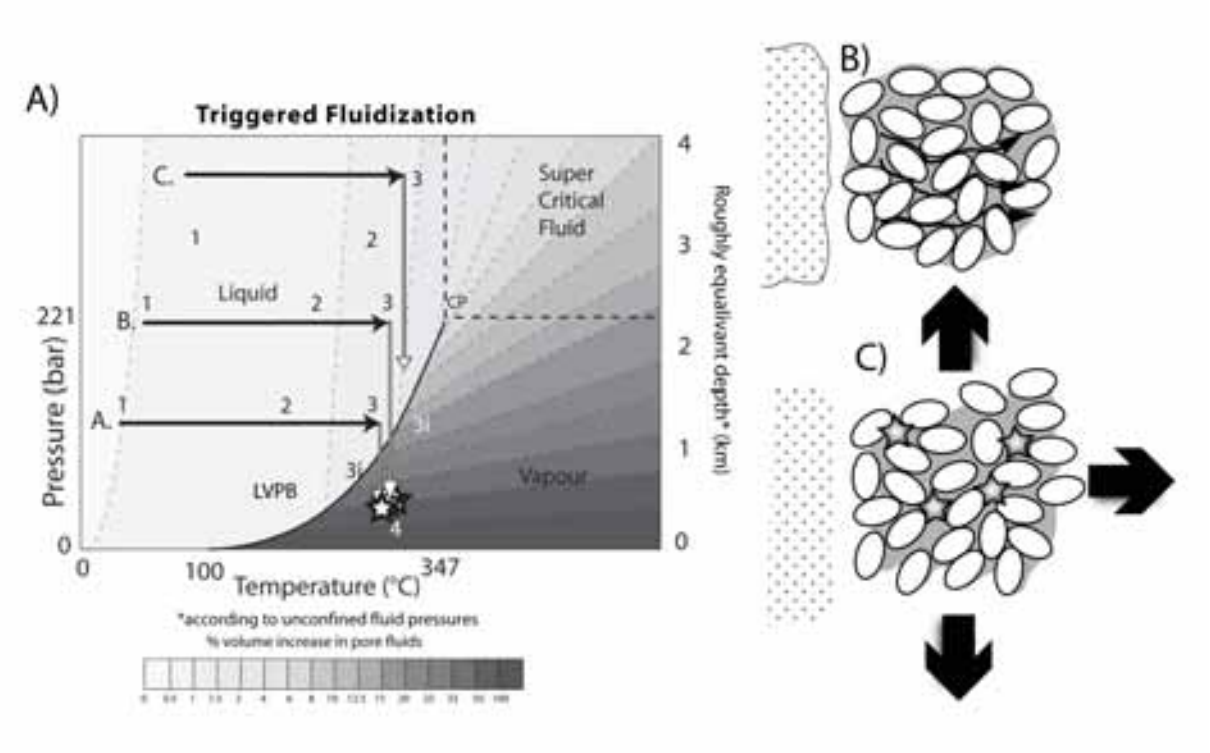

Fig. 6.3 - Triggered fluidization caused by rapid unconfinement of heated pore-fluids by an external force trigger, i.e. opening of a fault of fracture (see text for details). A) Temperature-pressure pathways of heated pore-fluids at increasing depth (A-C). B) Schematic of pore-fluid behaviour before rapid unconfinement, heated pore-fluids will flow in pore-spaces as it is heated C) Schematic of point at which rapid unconfinement of heated pore-fluid occurs, which causes pore-fluids to flash boil and expand.

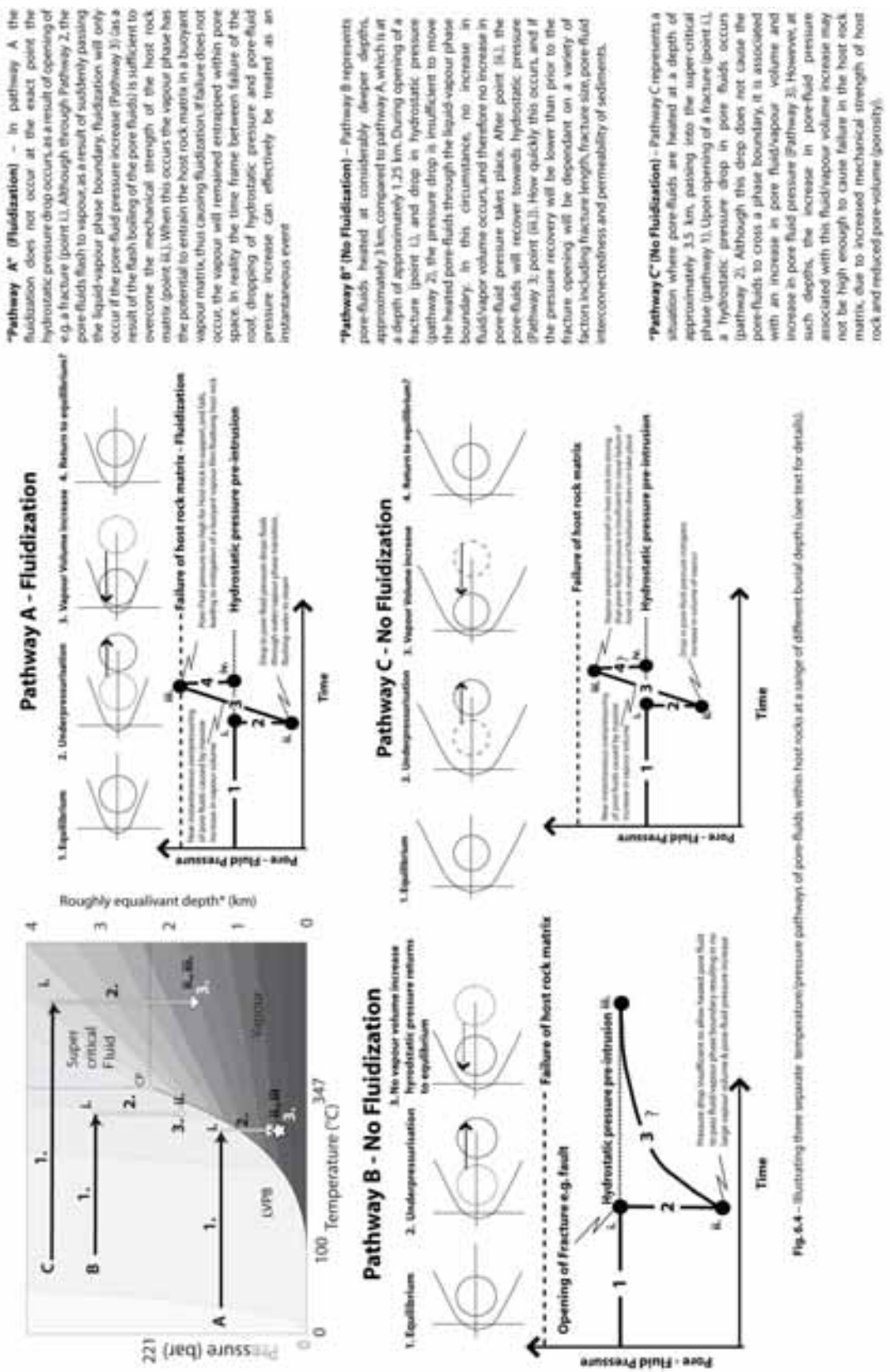

"Pathway A" (Fluidization) – In pathway A the fluidization does not occur at the exact point the hydrostatic pressure drop occurs, as a result of opening of e.g. a fracture (point i.). Although through Pathway 2, the pore-fluids flash to vapour, as a result of suddenly passing the liquid-vapour phase boundary, fluidization will only occur if the pore-fluid pressure increase (Pathway 3) (as a result of the flash boiling of the pore fluids) is sufficient to overcome the mechanical strength of the host rock matrix (point iii.). When this occurs the vapour phase has the potential to entrain the host rock matrix in a buoyant vapour matrix, thus causing fluidization. If failure does not occur, the vapour will remained entrapped within pore space. In reality the time frame between failure of the roof, dropping of hydrostatic pressure and pore-fluid pressure increase can effectively be treated as an instantaneous event

"Pathway B" (No Fluidization) – Pathway B represents pore-fluids heated at considerably deeper depths, approximately 3 km, compared to pathway A, which is at a depth of approximately 1.25 km. During opening of a fracture (point i.), and drop in hydrostatic pressure (pathway 2), the pressure drop is insufficient to move the heated pore-fluids through the liquid-vapour phase boundary. In this circumstance, no increase in fluid/vapor volume occurs, and therefore no increase in pore-fluid pressure takes place. After point iii.), the pore-fluids will recover towards hydrostatic pressure (Pathway 3; point iii.)). How quickly this occurs, and if the pressure recovery will be lower than prior to the fracture opening will be dependant on a variety of factors including fracture length, fracture size, pore-fluid interconnectedness and permeability of sediments.

"Pathway C" (No Fluidization) – Pathway C represents a situation where pore-fluids are heated at a depth of approximately 3.5 km, passing into the super-critical phase (pathway 1). Upon opening of a fracture (point i.), a hydrostatic pressure drop in pore fluids occurs (pathway 2). Although this drop does not cause the pore-fluids to cross a phase boundary, it is associated with an increase in pore fluid/vapour volume and increase in pore fluid pressure (Pathway 3). However, at such depths, the increase in pore-fluid pressure associated with this fluid/vapour volume increase may not be high enough to cause failure in the host rock matrix, due to increased mechanical strength of host rock and reduced pore-volume (porosity).

Fig. 6.4 – Illustrating three separate temperature/pressure pathways of pore-fluids within host rocks at a range of different burial depths (see text for details).

transgressive arcuate inclined sheet, most host rock has been eroded away. However, in certain areas, contacts between host rock and dolerite can still be seen.

Figure 6.5 shows the roof contact between dolerite in the inner sill and host rock. The exact thickness of dolerite in this inner sill is unknown; however, the contact metamorphic zone in the host rock is relatively small, in the region of ~ 20 cm. Within the contact zone, the rock has undergone baking, and some re-crystallization in places, but original bedding is still mostly preserved. Mudstone pods become locally hornfels, taking on a shiny grey appearance. Near cooling joints, veins of partially re-crystallized host rock can be seen to inject into the joints (Fig. 6.6), the centre of the vein shown in Figure 6.6 appears to be formed of clastic material, and does not represent a melt rock. Some re-crystallization occurs mostly at the veins edges and toward the bottom of the vein. In the main body of host rock, connected to the vein is an irregular area approximately 20 cm × 10cm wide, where original bedding becomes incoherent.

This rock is interpreted to represent fluidized host rock, which has been injected into a joint as a result of localized undepressuring of heated pore-fluids in the region of the joint, triggering the host rock to fluidize.

Within the arcuate inclined sheet, the occurrence of exposed host rock – dolerite contacts are rare. However vestiges of country rock are still visible, mainly around the inner sill – arcuate inclined sheet boundary and within the troughs of magma fingers. One such example is shown in figure 6.7. The outcrop is situated in the SE portion of the Golden Valley Sill, approximately ~ 1 – 2m away from the inferred roof contact of the sill.

In the field, the outcrop is characterised by numerous clasts of mudstone ~ 5 – 30 mm in size. The clasts are supported by a sandy matrix, with abundant gas/fluid cavities within the rock (Fig. 6.7a). Under polished section, the fragmental nature of the mudstone clast are visible, which also show lobate contacts in relation to surrounding rock (Fig. 6.7b and 6.7c). Signs of original bedding can be seen in the clasts. The matrix is composed mostly of quartz, but is abundant in gas/fluid cavities containing calcite and chlorite. The lobate nature of the mudstone clasts and loss of bedding towards their margin would suggest some incipient melting/fluidization has occurred. Importantly however, the development of the lobate nature of the clasts would suggest that both the edges of the clasts and host rock matrix were acting in a fluid-like manner simultaneously. The creation of gas/fluid cavities also appears to have occurred in conjunction with this, as they can be seen impinging into lobate edges of the clasts (Fig. 6.7b and 6.7c).

The rock contains no magma-sediment interaction of the type described by Kokelaar (1982), but contains numerous in-filled vugs consisting of hydrothermally deposited calcite. The rock is also abundant in chlorite and contains minor amounts of epidote, all indicative of hot fluids percolating through the system (*see* Krynauw et al., 1994). This kind of texture closely resembles that reported by Krynauw et al. (1994) in a 3.5m zone surrounding the Grunehonga sill, Antarctica, in which extensive fluidization occurred as a result of the emplacement of a 100m thick sill into partially lithified rock/sediment.

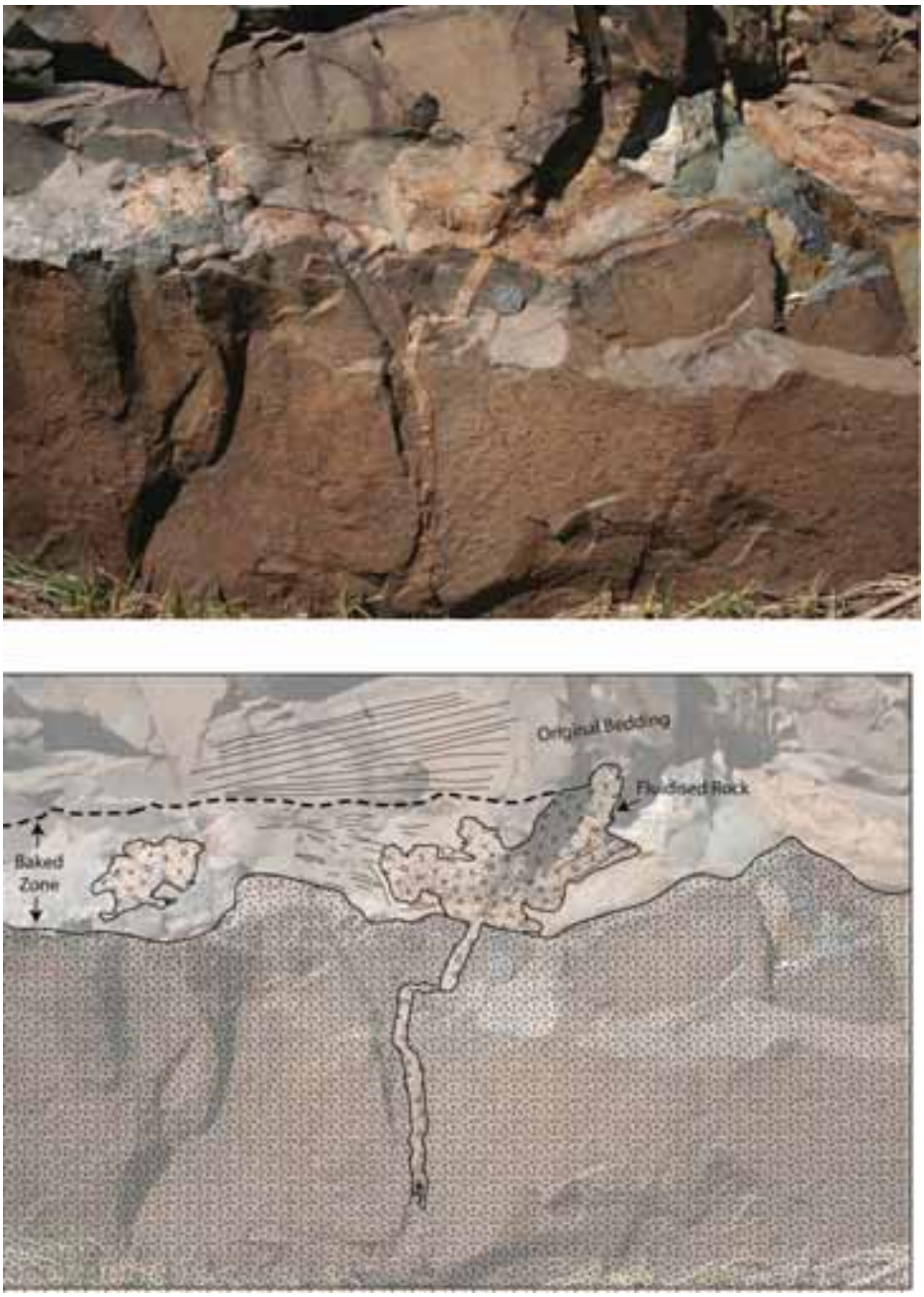

Fig 6.5 – Localised fluidization seen within the roof contact of the inner sill of GVS, interpreted to be the result of opening of a cooling joint within host rock. South African Rand for scale (~ 2cm in diameter)

Fig 6.6 – Plan view of top-dolerite contact within inner sill of golden valley sill, 2m away from last figure, showing injection of fluidized host rock into cooling joints within dolerite

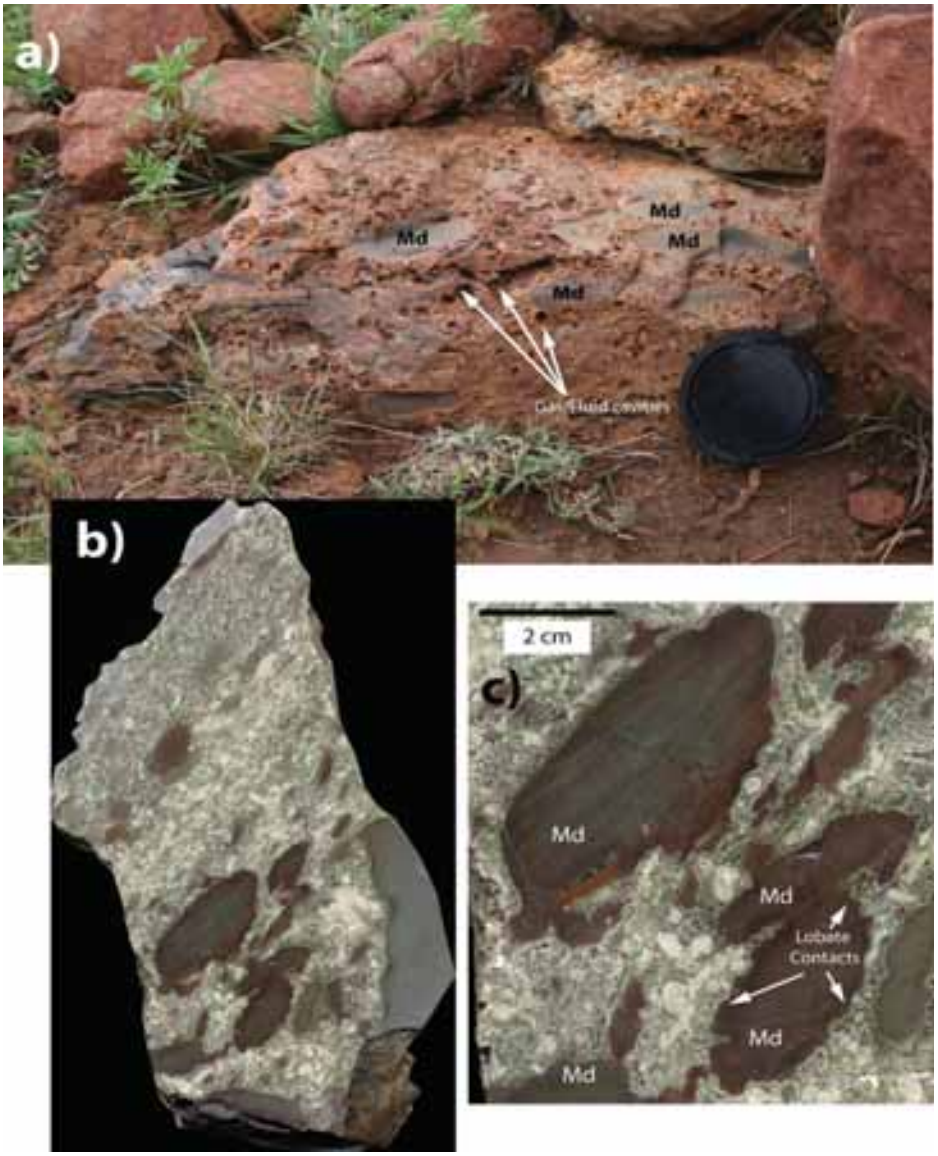

Fig 6.7 – A) Field photograph showing fluidized rock ~ 1m away from top contact of dolerite B) Photograph of cut section showing fragmented mudstone clasts (Md in Fig. C) C) Close-up of polished section. The rock is composed of approximately 40% fragmented mudstone clasts with lobate contacts (Md). The remaining rock consists of ~20% quartz and ~40% in-filled gas/fluid cavities containing calcite and chlorite. Note that the gas cavities (bubbles) impinge the margins of the mudstone clasts indicating that the fragmentation of the mudstone occurred in situ (inset). The lobate nature of the mudstone clasts illustrates that the matrix and fragmented shale were acting in a fluid-like manner simultaneously.

6.4.2 Aspects for emplacement model to satisfy

Several key aspects exist from the GVS which any model of emplacement for the GVS must take into account;

- The transgressive inclined sheet of the sill possesses well developed magma fingers over a circumference of ~ 50 km.
- The magma fingers were only in the inclined sheet, no evidence for their occurrence could be seen in the inner sill.
- Vestiges of country rock, where preserved show chaotically fluidized host rock adjacent to sill contacts. Within the inner sill, this appears to be restricted to localized zones associated with opening of cooling joints within the dolerite. However in the arcuate inclined sheet larger outcrops of highly chaotic fluidized host rock occur between ~ 1-2 m from the contact with dolerite.
- The transition from a flat inner sill to transgressive arcuate inclined sheet is smooth; no evidence for the stair-step morphology as proposed by Malthe-Sørensen et al. (2004) model of sill emplacement exists.

Other factors which need to be considered;

- For magma fingers structures to form *sensu* Pollard et al. (1975) both magma and host rock must be acting as two viscous fluids with one another, with the host rock having a greater viscosity than the intruding magma.
- The occurrence of magma fingers within the transgressive inclined sheet of the sill suggests a causal link between magma finger formation and the point magma begins to transgress bedding.

6.4.3 Fluidization of host rock and role in emplacement of sills: Discussion

Goulty and Schofield (2008) suggested that saucer-shaped sill emplacement is essentially a two-stage process and could be modeled using concepts dealing with simple flexure of the overburden. In the first instance, intrusion of the inner sill occurs along a plane of weakness (e.g. bedding) accompanied by doming of the overburden, which takes place until tensile failure of the doming overburden occurs. Goulty and Schofield (2008) noted that the model was only applicable up to the point of failure, after which no prediction about the subsequent propagation direction of the rupture could be made. Thomson (2007) and Thomson and Schofield (2008) proposed a qualitative sill emplacement model, in which the inflation of the

inner sill results in failure of the roof rock by creation of a series of inwardly dipping reverse faults at the periphery of inner sill. Such results have also been re-produced in analogue experiments of Galland et al (2009) who showed that central inflation of a inner sill caused shear failure in the overlying substrate at the sill peripheries.

Although the exact mechanism in which the inner sill begins to transgress bedding to form a saucer is debatable, it is generally concluded that transition from a propagating concordant inner sill to a climbing sill is the function of opening of some kind of fracture at the periphery of the inner sill (Malthe-Sørensen, 2006; Thomson, 2007; Goulty and Schofield, 2008; Thomson and Schofield, 2008; Galland et al., 2009). As explored in section 6.2.2 the opening of a fracture, e.g. a fault, or joint, can momentarily cause hydrostatic pressure to drop (Kokelaar, 1982; Curtis and Riley, 2003), causing heated pore-fluids (if present) to cross the liquid vapour phase boundary and trigger fluidization in partially lithified wet sediments.

Fluidization of host rock is regarded generally to be a secondary function of igneous emplacement created by heating effects of magma on pore-fluid (*see* Kokelaar, 1982; Busby-Spera and White, 1987; Krynauw, 1994; Jamtveit et al., 2004) and its role in the emplacement of saucer-shaped sills has not been fully considered. This is despite the fact that saucer-shaped sills complexes occur in a greatest abundance at paleo-depth in a 0 - 2km depth range (*see* Thomson and Hutton; 2004; Hansen and Cartwright; 2004; Thomson, 2007; Rocchi et al., 2007), which is within the approximate window for fluidization to be viable in host sediments (Kokelaar, 1982).

In the Golden Valley Sill it is proposed that the sudden drop in hydrostatic pressure resulting from the sudden opening of a fracture at the periphery of the inner sill leads to localized host rock fluidization around the newly opened fracture. At the pressure appropriate for the intrusion of the Golden Valley Sill (~ 1.25 km, i.e. ~ 125 bar hydrostatic pressure) (Fig 6.8), modelling with Heat3D (Wohletz, 2008), assuming a propagation rate in the order of a metre per second (Delaney and Pollard, 1982), shows that as the tip of the sill propagates, the magma will heat pore-fluids to ~300ºC within <1 m of the propagating tip. The drop in pressure associated with failure of the roof will cause flash boiling of these pore-fluids whose rapid expansion would disaggregate and fluidize rock around the fracture.

The major consequence of this is a fluid-fluid interface between intruding magma and the host rock will be created, triggering the formation of magma fingers *sensu* Pollard et al., 1975 and as documented in the GVS (Fig. 6.8). In addition, fluidization would act at the same time to destroy the mechanical anisotropy that forces the intrusion to follow the bedding and so allow the sill to transgress. This process can essentially be viewed as ‘triggered’

fluidization as the onset of fluidization is the result of an external process, i.e. opening of a fracture, causing a rapid drop in fluid pressure (Kokelaar, 1982).

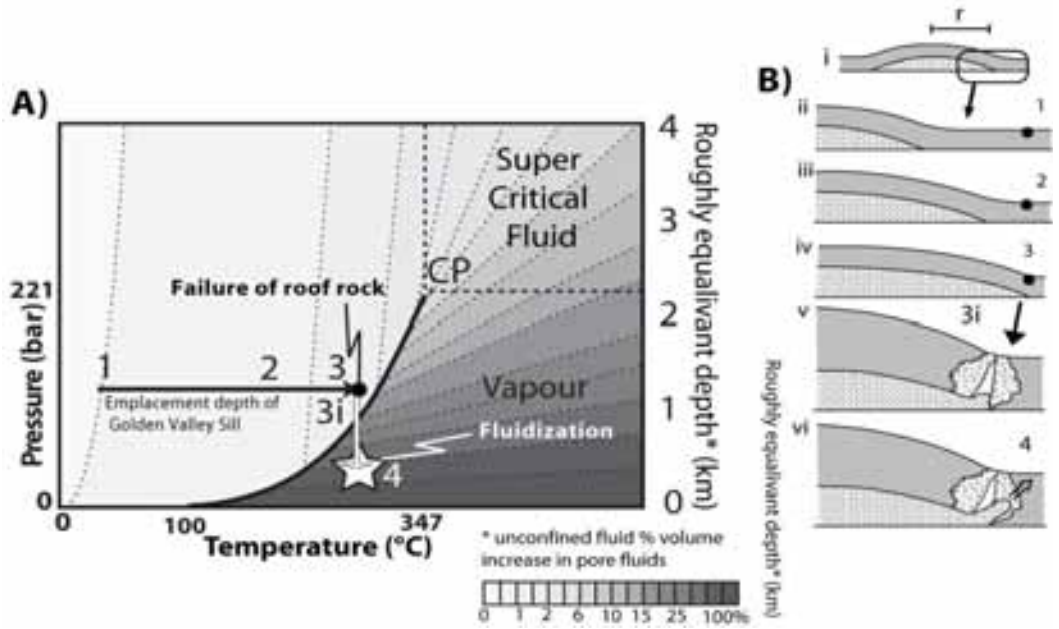

Fig 6.8 – A) Showing the possible fluidization pathway of the rock within the GVS at the point of failure of the overlying host rock B) accompanying geo-schematic interpretation.

6.5 Proposed emplacement model of the GVS and saucer-shaped sills

The intrusion of the Golden Valley Sill can be viewed as a series of sequential events. Several different models of saucer-shaped sill emplacement have been proposed by various workers (see Chapter 2), in particular to explain the transition from flat concordant inner sill to the transgressive outer sill (e.g. Malthe-Sørensen et al., 2004; Thomson and Hutton, 2004; Thomson, 2007; Thomson and Schofield, 2008). Here the model of Goulty and Schofield (2008) is modified to consider what might happen after failure of the roof occurs which is the point the model of Goulty and Schofield (2008) breaks down.

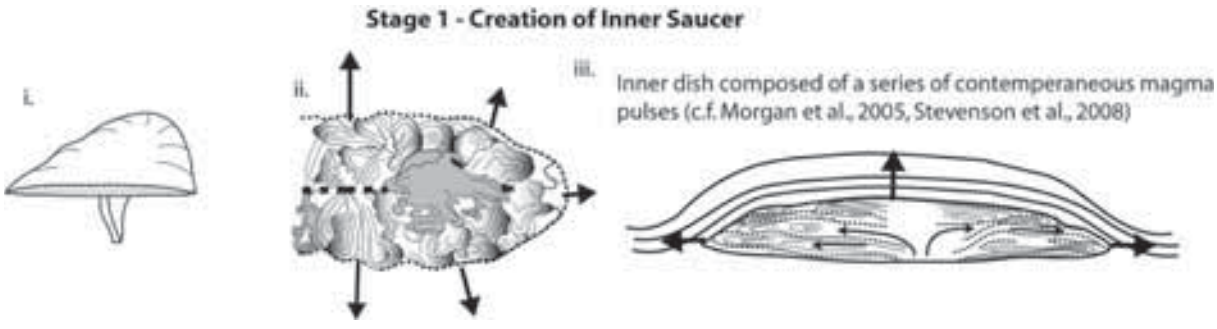

Fig. 6.9 – Schematic illustrating the inferred creation of the inner sill through a series of magma pulses (see text for details)

Stage 1 – Creation of the inner sill: The elliptical nature of the GVS suggests that it is fed from an axial line source, either in the form of a dyke, or lobate protrusion of an inclined sheet of a deeper sill (Thomson and Hutton, 2004; Hansen and Cartwright 2006; Goulty and Schofield, 2008). Upon initiation of the inner sill, possibly the result of exploitation of a preferential sedimentary horizon (*see* Thomson and Schofield, 2008) the magma propagates away from the central feeder zone spreading out in an elliptical fashion (Fig. 6.9ii).

How the inner sill propagates and inflates in the Golden Valley is unknown due to poor exposure. Although Goulty and Schofield (2008) assume a single body of inflating magma, other works have shown magma bodies to be amalgamated from a series of discrete pulses of magma (Habert and Saint-Blanquat, 2004; Morgan et al., 2005; Horsman et al., 2005; Stevenson et al., 2008). Thomson and Hutton (2004) and Thomson, (2007) show that the inner sill of sills can possess a series of interconnecting lobate patterns in the base of a dish. However, lobate elements may not be easily identifiable even if present. Stevenson et al. (2008) identified magma pulses within granites predominantly by the study of microscopic flow fabrics and AMS, despite little evidence of solid-state contacts being preserved in the field. The inner sill could be constructed by a series of magma pulses with breakouts analogous to the inflation and formation of pahoehoe lobes in lava flows (Anderson et al., 1999; Miyamoto and Crown, 2006), (Fig. 6.9i. and 6.9iii.). Such a construction does not necessarily render the approximation of the inner sill as being a continuous body of magma *sensu* of Goulty and Schofield (2008) as an oversimplification, as the stress pattern results from the doming, not from the way the doming develops.

Stage 2 – Failure of overburden: As magma propagates horizontally it will begin to inflate vertically (Hutton, in press) (Fig 6.10i.), if this progresses, the tensile stress, which will be greatest at the periphery of the expanding inner sill, will eventually equal and overcome the level of the tensile stress needed for failure of the overburden (Goulty and Schofield, 2008). In a doming magma lens, Goulty and Schofield (2008) showed that the tensile stress in the roof of the sill along its periphery are at a minimum along the major axis and at a maximum along its minor axis. Subsequently tensile failure in the overburden will first be expected to occur on the minor axis and extend round to the major axis (Fig. 6.10ii., 6.10iii., 6.10iv.). Goulty and Schofield (2008) argue that this type of failure, extending from the minor axis to the long axis will accentuate the elliptical nature of the inner sill (initially created by magma traveling away from the centralized axis), by forming an eye-shaped fracture/fracture pattern (Fig. 6.10iii.).

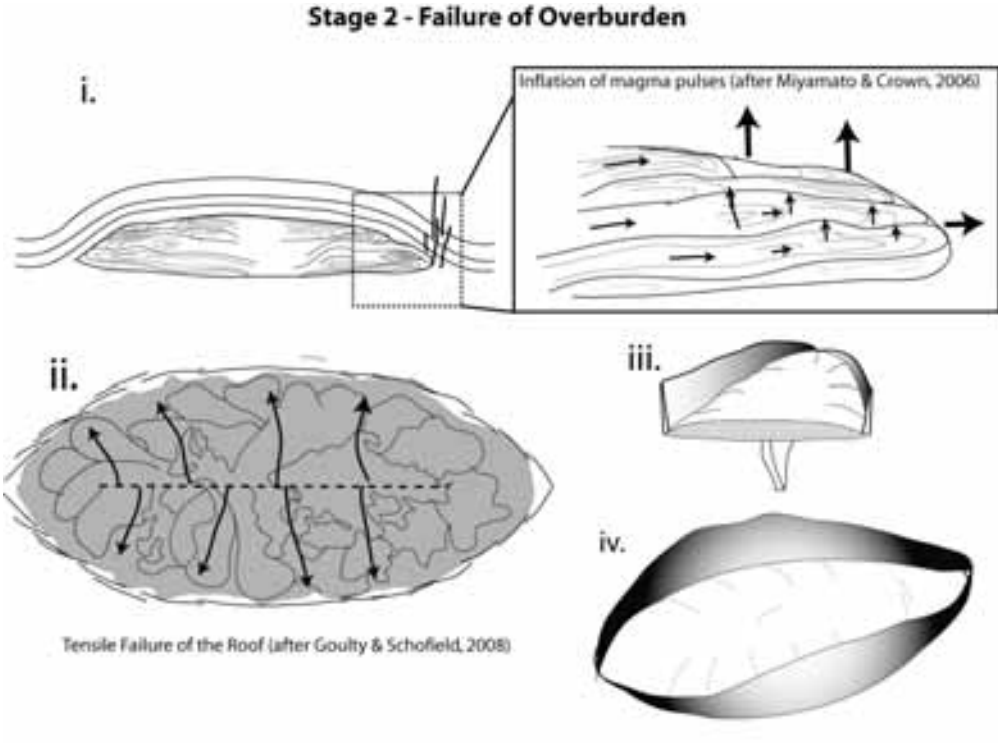

Fig. 6.10 – Schematic showing the inflation of the inner sill (fig i.) and accompanying eye-shaped failure of roof rock which would occur as result of inflation of a elliptical shaped body of magma (*see* Goulty and Schofield, 2008). Failure initially takes place on the short axis of the ellipse, before extending to the long axis (iii and iv.). Therefore one may expect the highest magnitude of displacement to occur on in the regions adjacent to the minor axis of the ellipse, but reduce towards the towards the long axis (Fig. iv) (*see* fault-length displacement; Kim and Anderson, 2005). This may play a role in the lack of development of magma fingers at the south east of the GVS.

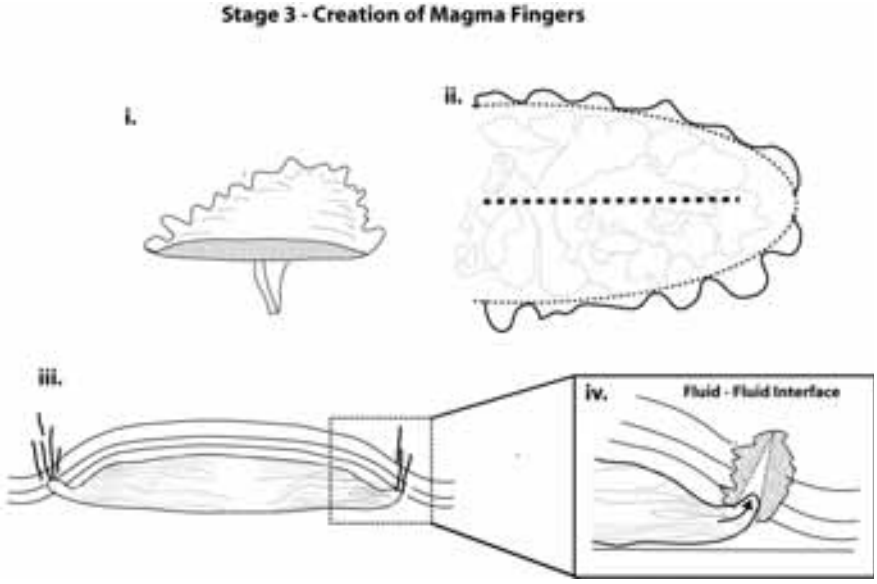

Fig. 6.11 – Schematic illustrating the creation of magma fingers, instigated by the fluid-fluid interface created by magma invading into the cavity of fluidized host rock created by opening of tensile fracture in the overburden (see text for details)

Stage 3 – Creation of magma fingers: With failure of the overburden *sensu* Goulty and Schofield (2008), fluidization of host rock surrounding the fracture would create a fluid-fluid interface between magma and host rock (Fig. 6.11iv.), allowing the initiation of magma fingers *sensu* of Pollard et al. (1975). As the failure of roof rock occurred above the sill tip, magma is deflected out of the horizontal plane, instigating the formation of the transgressive arcuate inclined sheet of the sill.

Stage 4 – Magma finger propagation: After initiation of magma fingers, the front of intruding magma will be constrained to stay in such a configuration (Pollard et al., 1975) (Fig. 6.12i.). The magma fingers will proceed to accelerate ahead of the main sheet (Fig. 6.12ii).

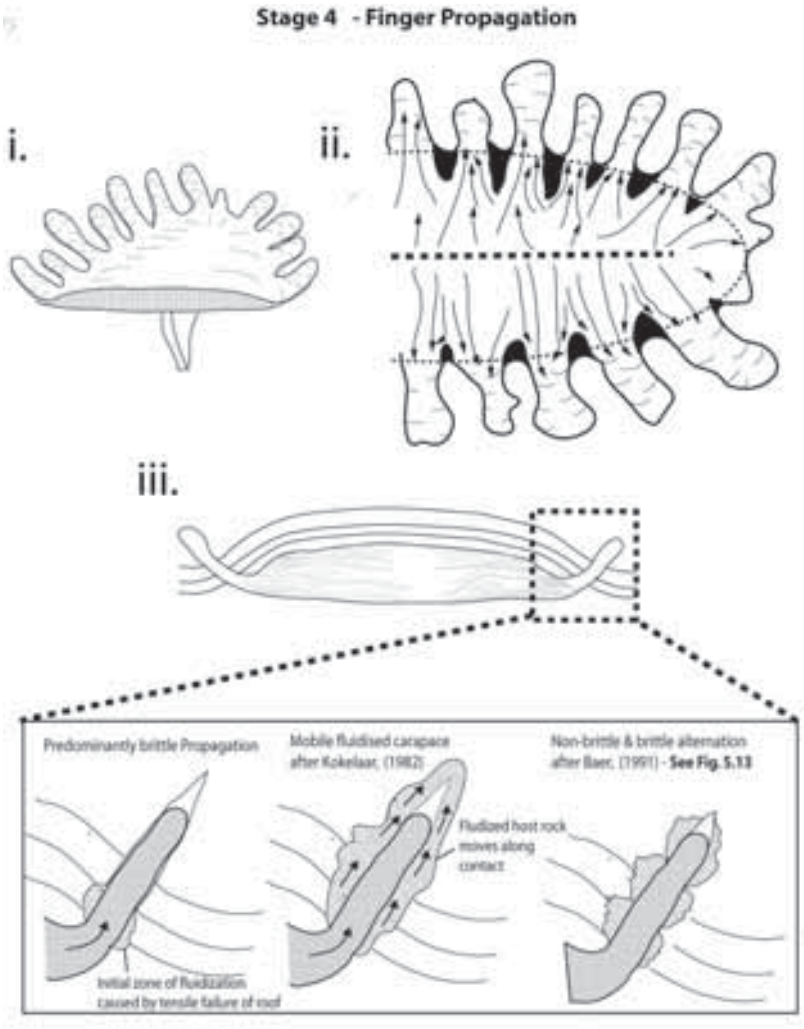

Fig. 6.12 – Schematic showing the propagation of magma fingers (Fig. i. and ii.) and areas between magma finger where stagnation of flow might be expected (solid black, Fig. ii). Fig. iii represents three possible mechanisms in which magma fingers may continue to propagate through host rock.

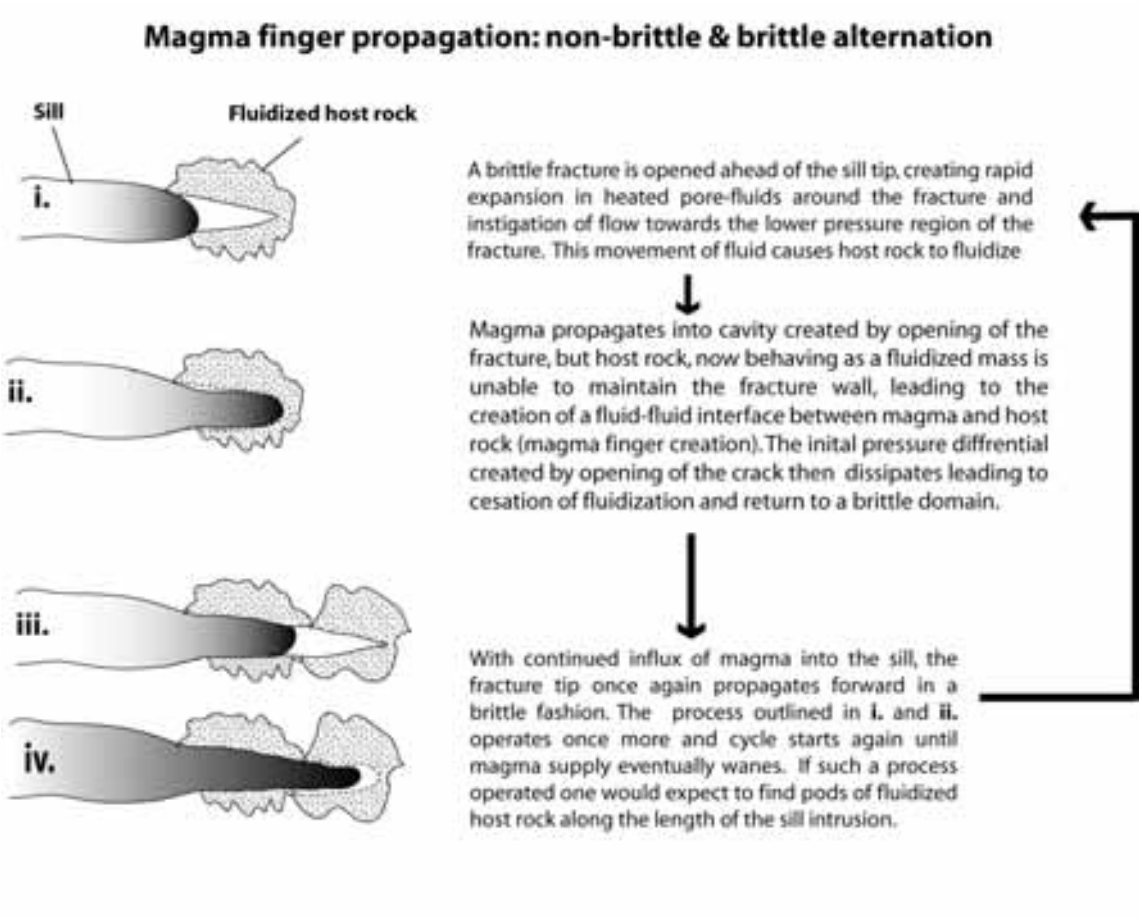

Fig 6.13 – Schematic illustrating possible non-brittle and brittle alternation which may occur because of magma finger propagation.

It is important to assess wheather propagation of magma fingers takes place by continued fluidization of host rock (thermal fluidization), brittle fracture, or a combination of both.

For fluidization to operate, their needs to be sufficient flow of pore-fluid/vapour to separate particles of host rock (Kokelaar, 1982; Jolly and Lonergan, 2002). After the initial opening of the fracture, the fluidization would probably be relatively short lived, as the initial pressure gradient created by the opening of the fracture rapidly dissipates. Under such circumstances, magma finger propagation may resort back to brittle fracture, and propagate through host rock as a mode 1 fracture (Fig. 6.12iii). However, the well formed magma fingers within the GVS extend away from the inner sill and structures related primarily to brittle propagation (e.g. broken bridges, steps) are not evident, suggesting that brittle mode 1 fracture propagation did not occur. Therefore it may be the case that fluidization continues to operate as the magma finger propagates.

With continued input of heat, heated vapour could cause fluidization to continue to operate along the contact zone of magma (Kokelaar, 1982), enveloping the magma fingers of

magma as they propagate through host rock in a carapace of fluidized sediment (6.12iii). The ability for this to occur will be greatest in unconsolidated wet sediments, in which the heated and fluidized mass of sediments can travel along the contact zone by viscous deformation of the surrounding sediment. However, in sediments that contain pore-fluids, but are at least partially lithified, for fluidization of this type to operate, the mechanical strength of host rock matrix must be overcome continuously along the contact to allow continuous transport of sediment along the magma finger contact. Whether this is feasible or not is unclear.

During magma propagation in shallow-level, poorly cemented sandstones, viscous and brittle deformation can operate intermittently with each other. Baer (1991) described dykes in the Ramon Area of Israel showing both structures related to fluid-fluid propagation, e.g. magma finger structures, and structures related to brittle e.g. steps. The magma finger structures of Baer (1991) mainly occurred on the dyke walls and not at the propagating tip. However, Baer (1991) proposed that dyke propagation occurred in a stepwise fashion, in which fluidization of host triggered the formation of magma finger structures on the wall of the dyke. Baer (1991) proposed that emplacement could be intermittently stopped or slowed down if host rock at a given point was resistive to fluidization, in such a case the magma pressure would build until host rock underwent brittle failure. Baer (1991) concluded that the instigation of fluidization and viscous fingering would then resume as crack tip fills up with "dyke fluids". What Baer (1991) meant by "dyke fluids" is difficult to assess, it is also unclear if magma propagation can occur in the stop-start fashion as proposed by Baer (1991) without magma solidifying at the dyke tip (*see* Bruce and Huppert, 1990; Bolchover and Lister, 1999) thus preventing further propagation.

However, in the case of the Golden Valley, in which the rocks would have been at least partially lithified at time of intrusion, the emplacement model proposed by Baer (1991) may apply with modification (Fig. 6.12iii). If, after the opening of the initial tensile fracture, the pressure differential dissipates it will cease the flow of heated fluid/vapour, if this cannot be reinitiated by the process of thermal fluidization, fluidization will cease. In this circumstance, the intrusion may revert to propagating through host rock by mode 1 fracture propagation. However if this occurs, the opening of a brittle fracture ahead of the sill tip will instigate a drop in hydrostatic pressure in host rocks surrounding the fracture, and in turn cause fluidization (Fig. 6.13i). In this fashion, the magma propagation may flip between brittle fracture and fluid-fluid propagation (Fig. 6.13) (Baer, 1991). In such a circumstance instead of a continuous carapace of fluidized sediment surrounding magma fingers *sensu*

Kokelaar (1982), localized pockets of fluidized sediments will occur along the contact with the sill (Fig. 6.13ii. - iv.)

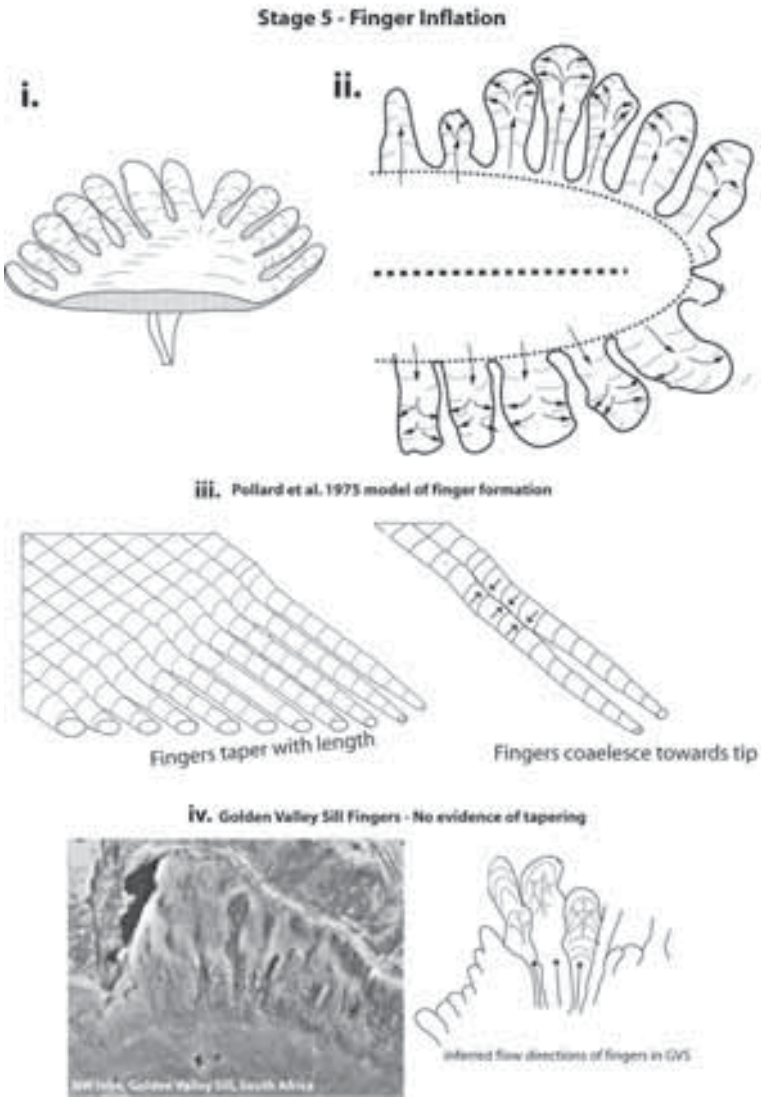

Fig. 6.14 – Schematic illustrating the possible way in which magma fingers inflate (Fig. i. and ii). The method of amalgamation of magma fingers as proposed by Pollard et al. 1975 (Fig. iii) (i.e. magma finger zipping up from the rear), appears incompatible with observations from the GVS (Fig. iv.) were magma fingers show a bulbous nature, appearing to have coalesced in a down-flow direction.

Stage 5 - Magma finger inflation: With continued magma supply, the propagating magma fingers would be expected to begin to expand vertically and laterally (Fig. 6.14i. and Fig 6.14ii.). Pollard et al. (1975) argued that when magma fingers initiated at the front of a propagating sheet, magma fingers would accelerate ahead until cooling and viscous drag forces acting within the magma fingers slowed the propagation of the magma fingers,

effectively enabling the main sheet to 'catch up' with the magma fingers (Fig. 6.14iii.). However observations from the magma finger structures in the GVS clearly show that the magma fingers do not taper, and instead have bulbous terminations, suggesting that they have expanded laterally as magma supply has continued into the magma fingers (Fig. 6.14iv.). This observation would be in agreement with the stop-start propagation of the magma body as proposed by Baer (1991), as with continued input of magma into the magma fingers, if a magma finger cannot propagate forward, the continued in-flow of magma is likely to cause it to expand laterally, forming bulbous tips.

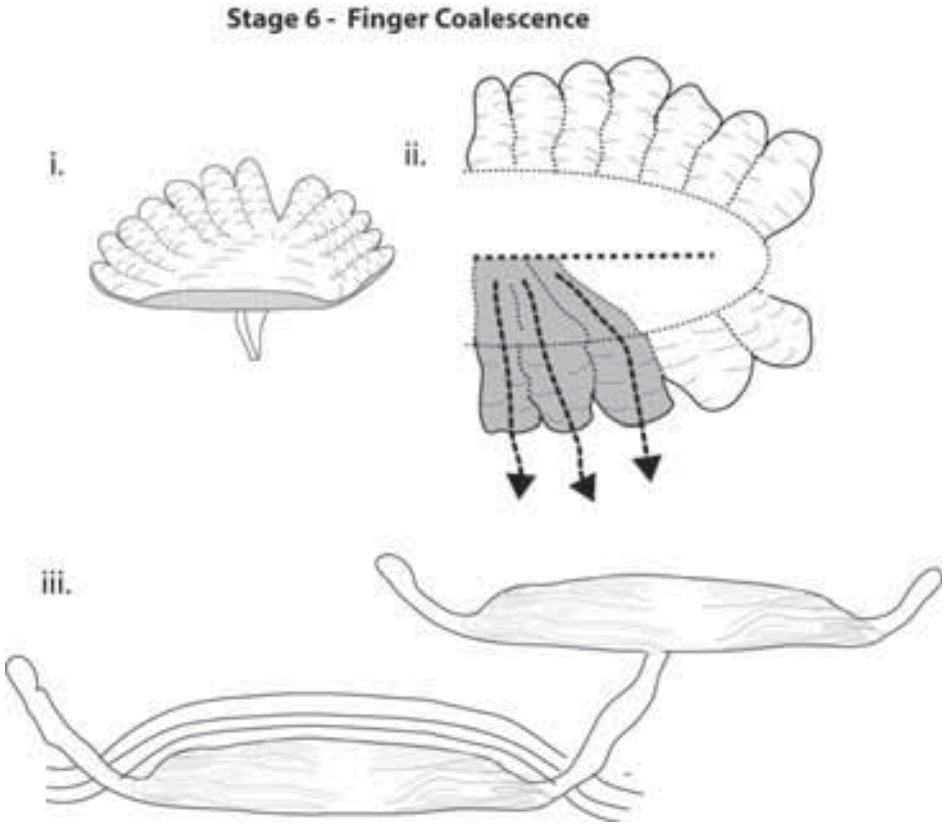

Fig. 6.15 – Schematic illustrating the possible end-member evolution of a fingered saucer-shaped sill in which the magma finger structures have coalesced to form a continuous sheet (Fig. i and ii) but still preserving the undulatory nature. The GVS would fit into this end-member morphology. The magma fingers once coalesced may act as feeders to higher level sills (fig i and iii).

Stage 6 – Magma finger coalescence: If magma supply wanes and heat advected along the magma fingers becomes less than that lost from the magma fingers, then the viscosity of the magma fingers will increase. At a temperature of 1050°C, the magma will have undergone a viscosity increase in the region of 3 orders of magnitude, and although the solidus temperature

of mafic magma is around 950°C, the magma will be relatively immobile (Delaney and Pollard, 1982). In this circumstance, the finger structures will solidify in a configuration prior to that of coalescing, representing either proto-magma fingers or separate magma finger structures. Thus for magma fingers to coalesce into a continuous sheet, magma supply rate into the magma fingers must remain high enough to prevent significant heat loss and choking of the magma fingers as they propagate.

6.6 Discussion - Feeding magma around a sill complex

Cartwright and Hansen (2006) suggested that magma could be moved over 10's km laterally and vertically through the crust via a plexus of interconnected saucer-shaped sills. Cartwright and Hansen (2006) did not explore underlying mechanisms of how this may happen.

Logically for higher levels sills to be fed by lower level sill *sensu* Cartwright and Hansen (2006), (Fig. 6.16), a conduit of magma must exist through the sill complex which allows the transit of magma through sills lower in the succession (e.g. Fig. 6.16, sill 1) to sills higher in the succession (e.g. Fig. 6.16, sill 10). Such a relationship can be seen on 3D seismic data were magma finger-like conduits of one saucer-shaped sill can be seen to feed another saucer-shaped sill (Fig. 6.17). Therefore it seems likely that in the GVS the coalesced magma fingers could have continued to act as long term conduits feeding other saucers higher in the succession after the sill was formed (see Fig. 6.15ii. and 6.15iii.).

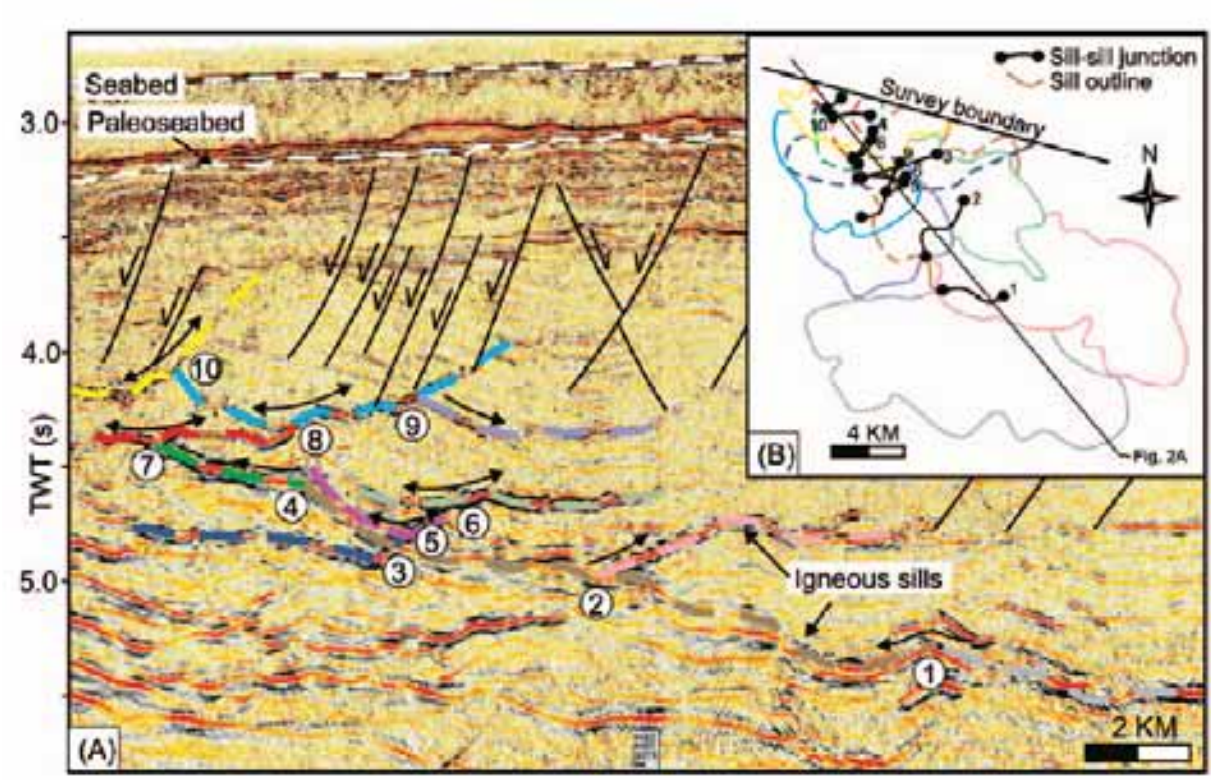

Fig. 6.16 – From Cartwright and Hansen (2006) showing a plexus of interconnected sills. Numbers represent the development of the sills over time, i.e. sill 2 is fed from sill 1. Note that during the formation of sill 10 a conduit of magma must have remained open through sills 1-9.

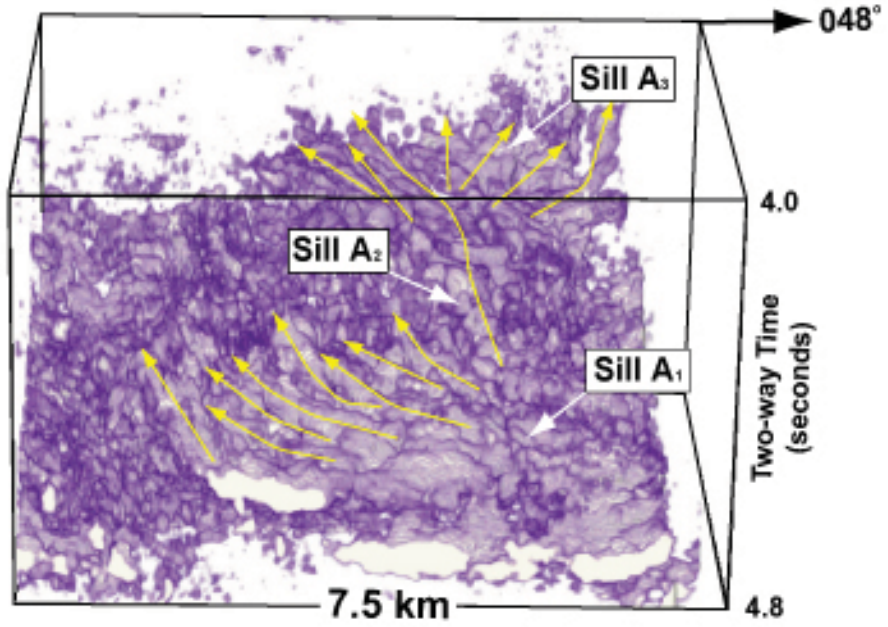

Fig. 6.17 – From Thomson and Schofield (2008) showing an upper sill (A3) being fed from a lower sill (A1) by a magma finger-like conduit (A2).

Chapter 7
Discussion -
Linking sill morphology to emplacement mechanisms

7.1 Introduction

In considering how emplacement mechanisms affect sill morphology it is important to differentiate morphological features seen within sills which are primarily related to brittle fracture propagation in host rock from those related to other processes. This chapter will act to explore some of these constraints; below is a brief recap of points from previous chapters;

- The sills of the Trotternish Peninsula and the Golden Valley saucer-shaped sill possess finger-like features related to flow.
- In the Golden Valley, evidence of host rock fluidisation suggests that finger formation was linked to the ceasing of brittle fracture propagation in host rock as the magma began to transgress stratigraphy at the edge of the inner saucer.
- The formation mechanism of the finger structures within the Trotternish Peninsula, Isle of Skye are not clear, due to lack of exposure, however their morphology appears to closely match that of the fingers exposed within the Golden Valley, suggesting a similar formation mechanism.
- The Skye sills also preserve evidence of brittle structures in the form of steps and broken bridges within the sills.

The chapter will attempt to bring the ideas presented in the preceding chapters with observations from other intrusions, and show how host rock lithology plays a major role in emplacement mechanisms and morphology of sill/sheet intrusions. It starts by describing other examples of less well documented sill/sheet intrusions to assess the general importance of the processes described.

7.2 Raton Basin, Colorado, USA

The Raton Basin, south-east Colorado, USA, is a foreland basin of the Rocky Mountains formed during the Laramide Orogeny (Cooper et al*.,* 2007). Within the basin Oligocene/Miocene sills have extensively intruded into late-Cretaceous medium-rank coal

horizons across the basin (Cornelius et al., 2004; Cooper et al., 2007). At the time of emplacement, the sills post-dated the deposition and burial of coals by at least 30Ma; the ranks of unaltered coal horizons suggest burial occurred in the region of 4.5 – 6km (Cornelius et al., 2004). The sills, as indicated by drilling activity for coal-bed methane stay almost exclusively within the coal horizons across the basin, often being traceable over lateral distances in the region of 10 km (Cornelius, pers. comm.).

Within outcrops across the basin well-formed magma fingers can be seen in cross-section intruding coal horizons (Fig. 7.1 and 7.2). Surrounding the individual magma fingers are zones of chaotic and convoluted coked coal which has deformed in a viscous manner (Fig. 7.3). Contact morphology and thin section evidence for in-situ viscous contacts between intruding magma and coal in the form of liquid–liquid mingling lobate structures and peperitic textures (Fig. 7.4 and 7.5) (Cornelius et al., 2004), suggest that the coal acted in a fluid-like fashion when the magma emplaced.

The ability for coal to act plastically under heating is well known from the coking industry (Gerjarusak et al., 1991; Fukada et al., 2006), upon heating coal softens to form a fluid like mass, referred to as 'metaplast', formed from the physical breakdown of solid constituents in the form of mineral and organic matter within the coal (Lahaye and Prado, 1987; Gerjarusak et al., 1991). Coal plasticity reaches it maximum between approximately 376°C and 476°C (Fig. 7.6) after which the coal resolidifies to form coke (Gerjarusak et al., 1991). In addition the rate at which the coal is heated plays a major role in the plastic behaviour of coal, with rapid heating leading to a lowering of apparent viscosity of the heated coal when compared to coal heated slowly (Fukada et al., 2006).

In the Raton basin, it would appear a similar process is operating within the coals during the intrusion of magma. In this circumstance the prevalence of well-formed magma fingers seen at outcrop in the Raton Basin, and cored from exploration wells (Cornelius, personal communication) can be explained by the magma ceasing to propagate through brittle fracture as a result of the coal acting as a viscous fluid, effectively creating a viscous-viscous interface between host rock coals and magma. Critically for magma fingers to form *sensu* Pollard et al. (1975), the intruding magma must have a lower viscosity compared to country rock that it is intruding, which must also be behaving as a viscous fluid. Such a relationship could be created in the Raton basin if host rock coals in the basin are acting in a plastic fashion during intrusion (*sensu* Fukada et al., 2006). It can be seen that bituminous coal has an apparent viscosity in the region of 10^4 Pa.S at ~ 450°C which is two orders magnitude greater the viscosity of basaltic magma at 1200°C (Fig. 7.6), it therefore seems likely that a suitable fluid-fluid relationship could exist between intruding magma and host rock coals in the Raton basin to form magma fingers *sensu* Pollard et al. (1975).

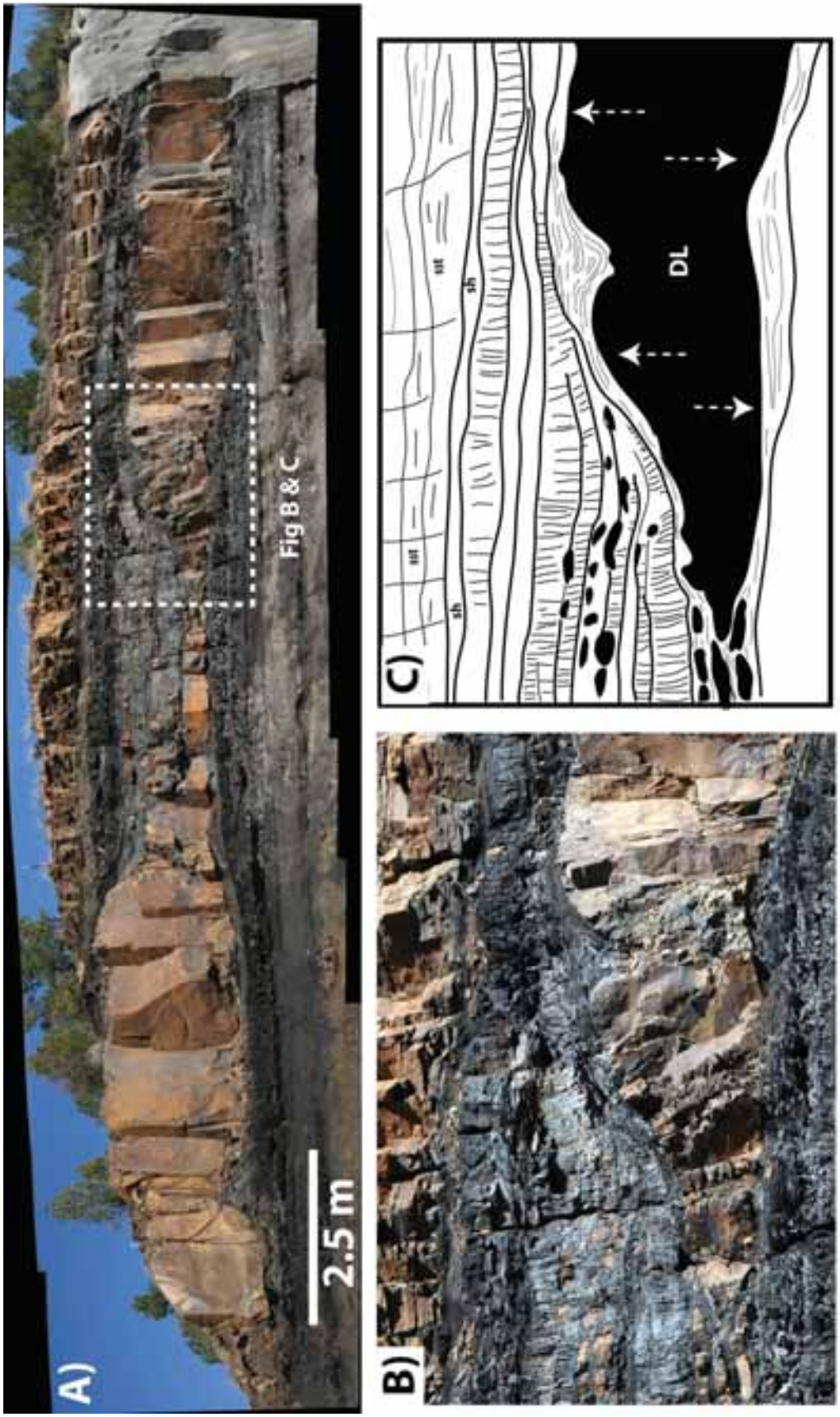

Fig. 7.1 - A) Cross-sectional view of two magma fingers intruding coal horizon, Raton Basin, Colorado, USA. Magma flow axis is interpreted to be perpendicular out of page B) & C) Vertical inflation of the fingers has taken place, deforming the cleated coal horizons above the fingers, however no doming of the overlying sandstone horizons is visible, implying removal of mass has taken place. Note the zone of chaotic convoluted coal surrounding the finger.

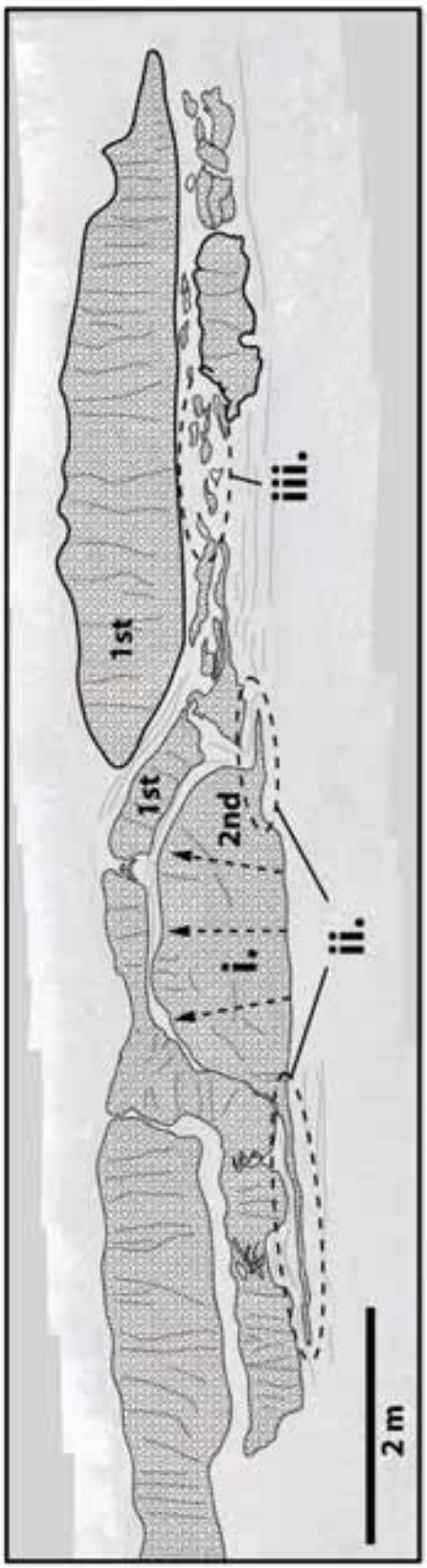

Fig 7.2 - Figure showing several separate generations of magma fingers intruding into coal horizons (flow direction out of page). Vertical inflation of a single finger (i.) has jacked up fingers overlying it. The jacking up of the host rock appears to have opened thin tensile fractures eminating away from the base of the inflating finger, which have become infilled with magma (ii.). Peperitic textures are also visible in the right of the section (iii.).

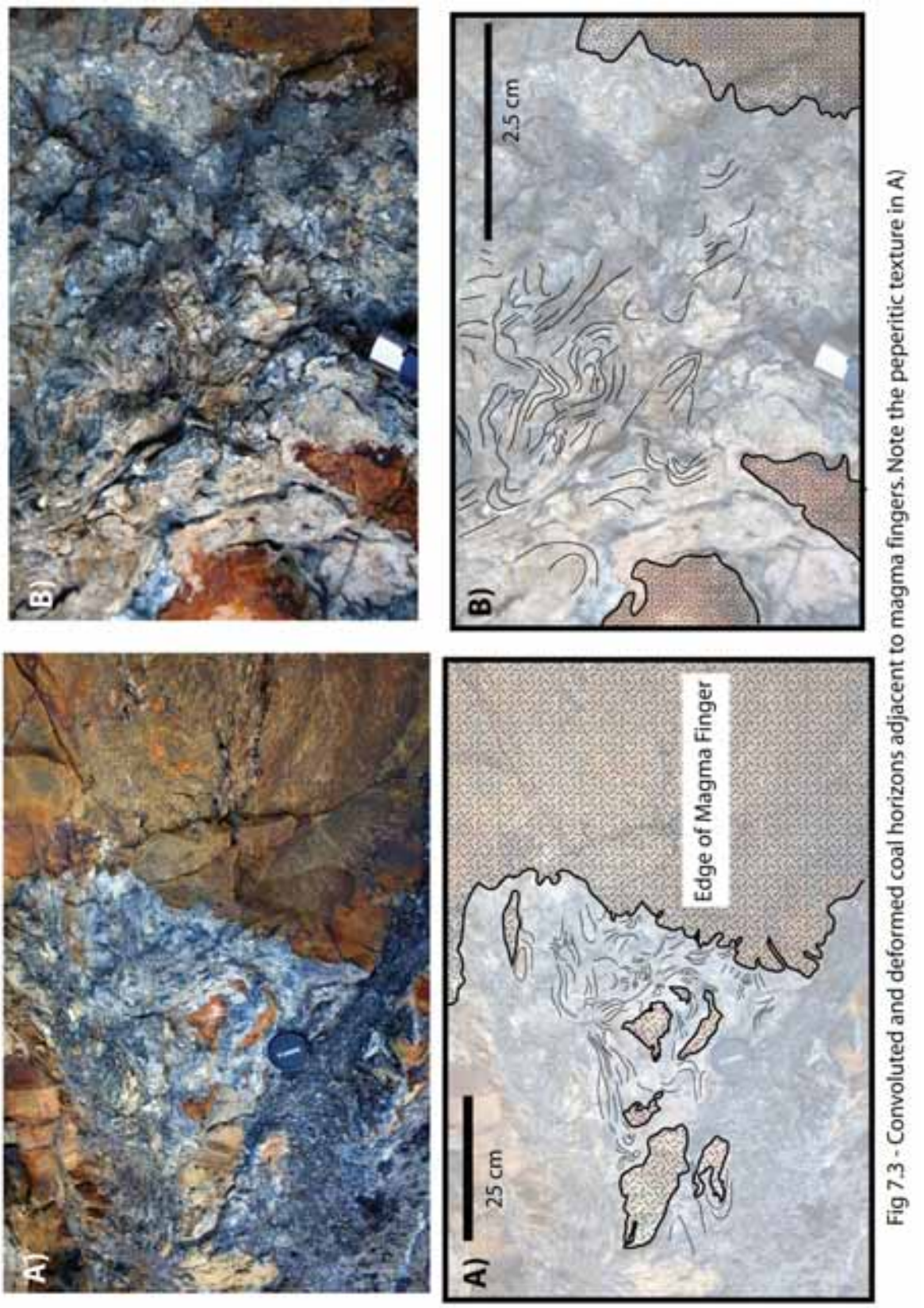

Fig 7.3 - Convoluted and deformed coal horizons adjacent to magma fingers. Note the peperitic texture in A)

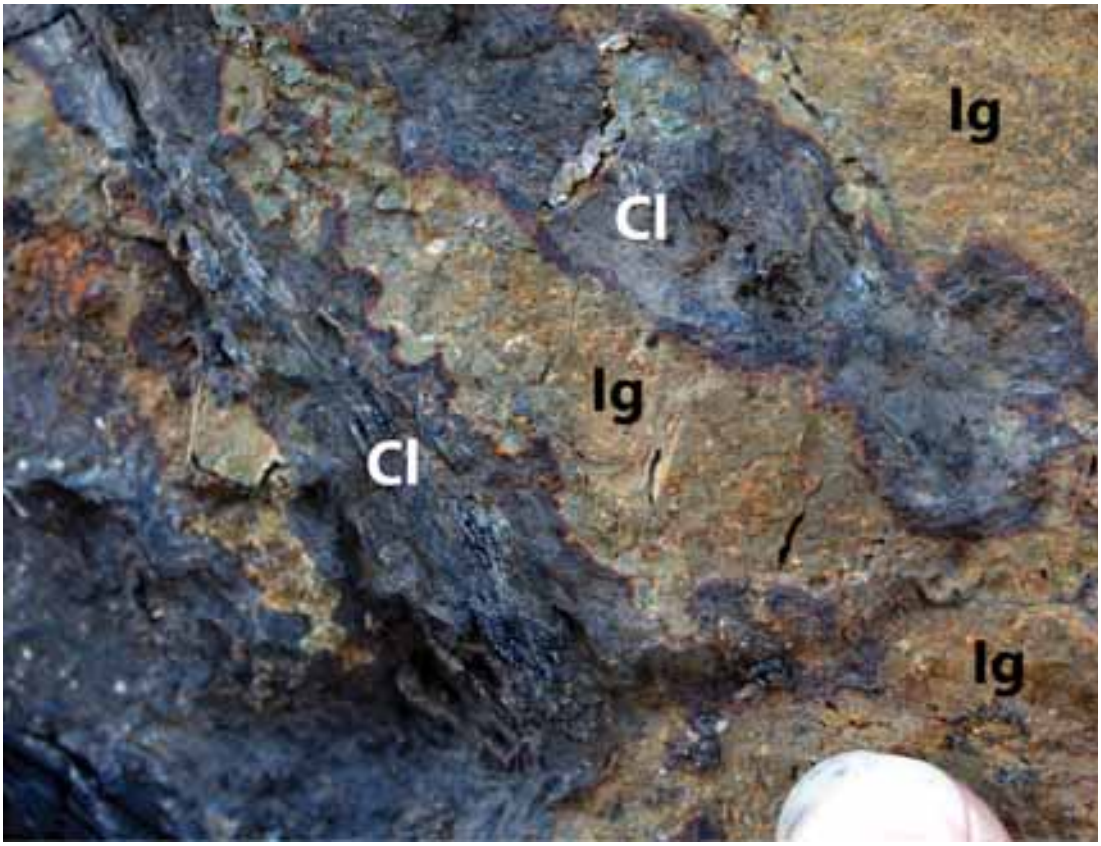

Fig. 7.4 – Viscous-Viscous lobate structures developed at contacts of magma fingers (Ig) and host rock coals (Cl), demonstrating that both the igneous rock and coal were acting in a fluid like state with each other at the same time.

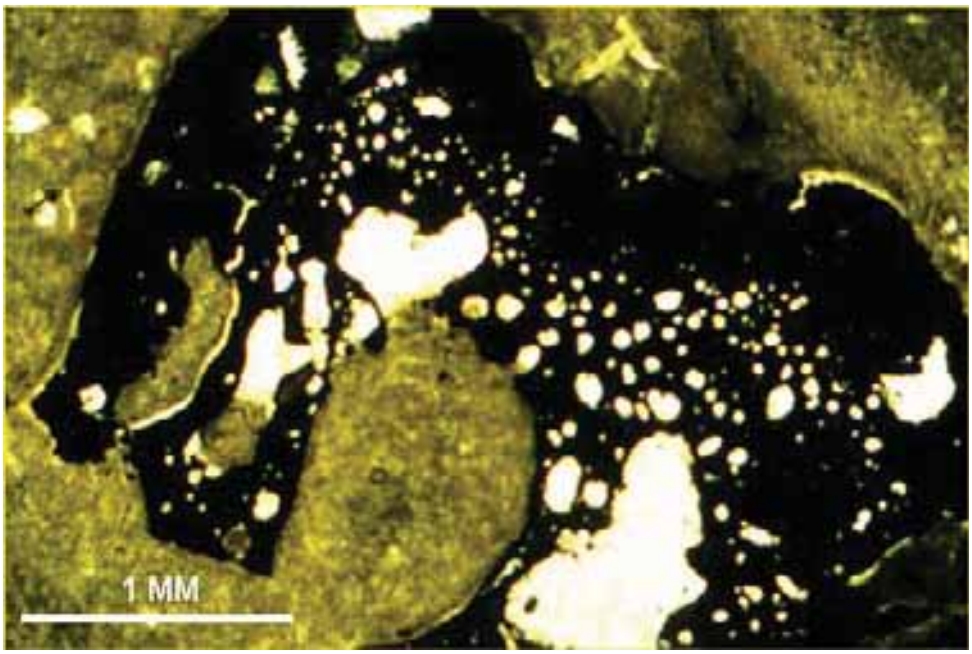

Fig. 7.5 – Thin section photo (courtesy of Chris Cornelius) showing a viscous mingling structure between host rock coals (black) and dolerite which forms the magma fingers.

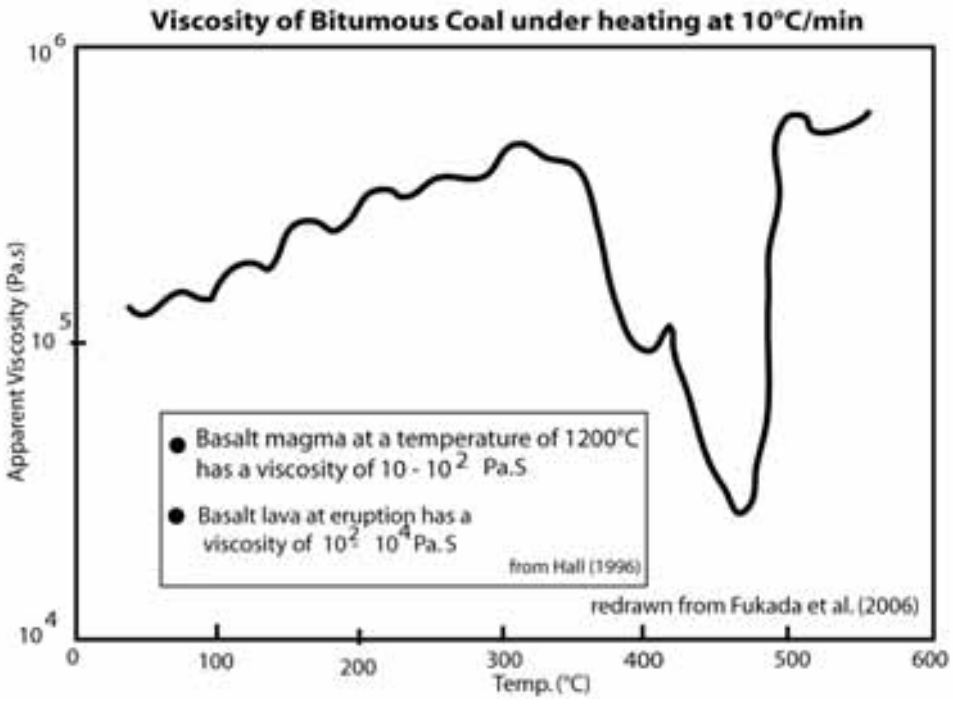

Fig. 7.6 – Graph showing apparent viscosity of Bitumous coal when heated at 10°C/min, and common viscosities of basalt for comparison. For fingers to form *sensu stricto* Pollard et al. (1975), the host rock (acting in a fluid state) must have a higher viscosity compared to intruding magma.

7.3 Whin Sill, Northumberland, United Kingdom

The Whin Sill is a tabular intrusion of dolerite intruded into Carboniferous host rocks in County Durham and Northumberland at a paleo-depth of ~ 1 - 1.5 km (Francis, 1982; Liss, 2004). The occurrence of magma fingers within the Whin Sill occurs on a localized scale, with most outcrops showing no evidence of a fingered morphology (Liss, 2004). The best example of identifiable magma fingers occurs on the coast near to Harkess (OS grid ref., 417600, 636000), north west of Bamburgh. In the foreshore at this location are two well-formed magma fingers, each ~ 0.75 × 3 m in dimension (Fig. 7.7a,b,c). Overlying the fingers is a thin ~ 40 cm – 60 m limestone horizon. Above this is a second tier of dolerite, which shows no fingered morphology. Surrounding the first tier fingers are localized zones of chaotically remobilized sediment, which occurs mainly at the sides and top of the fingers (Fig. 7.7 and Fig. 7.9). The appearance of the material resembles that of a mobilized sandy slurry with abundant gas/fluid cavities in the region of 3 – 6 mm in size. These occurred contemporaneously with the mobilization and deformation of the sediment, as indicated by being entrained in the deformation fabric of the mobilized sediments (Fig. 7.8). The cavities are abundant in hydrothermal quartz, indicating hot, mobile hydrothermal brines where passing through host rock.

Evidence for lateral inflation of fingers is also apparent. In Figures 7.7b and 7.9c, shale, deformed in a ductile manner can be seen sandwiched between two fingers that have inflated laterally towards one-another.

Most outcrops of the Whin Sill show no evidence of fingers and other outcrops show minor evidence of contact metamorphic effects, even on sections in excess of 40m in thickness (Johnson and Dunham, 2001; Liss, 2004). This is in contrast to the Harkess rock outcrop where well developed finger structures occur where the host rock has been affected by the intrusion and heating effect of magma.

Pollard et al. (1975) related finger formation to the intrusion of one viscous fluid into another but gave no indication about the mechanism underpinning this process, or how this may occur in host rocks. Within the fingers at Harkess rock, the fact that the fingers structures occur in conjunction with fluidised and mobilised rock would suggest a causal link between the two.

The extent to which a rock is affected by contact metamorphism may be controlled by the presence and amount of fluid present during metamorphism, coupled with its ability to move around the rock when it is heated (Jamtveit et al., 1997; Hanson, 1995). Without

movement of heated fluids through the host rock during intrusion, contact metamorphism is restricted to conductive heat transfer only, which is an ineffective mode of heat transfer, as rocks in general are poor conductors of heat (Liss, 2004).

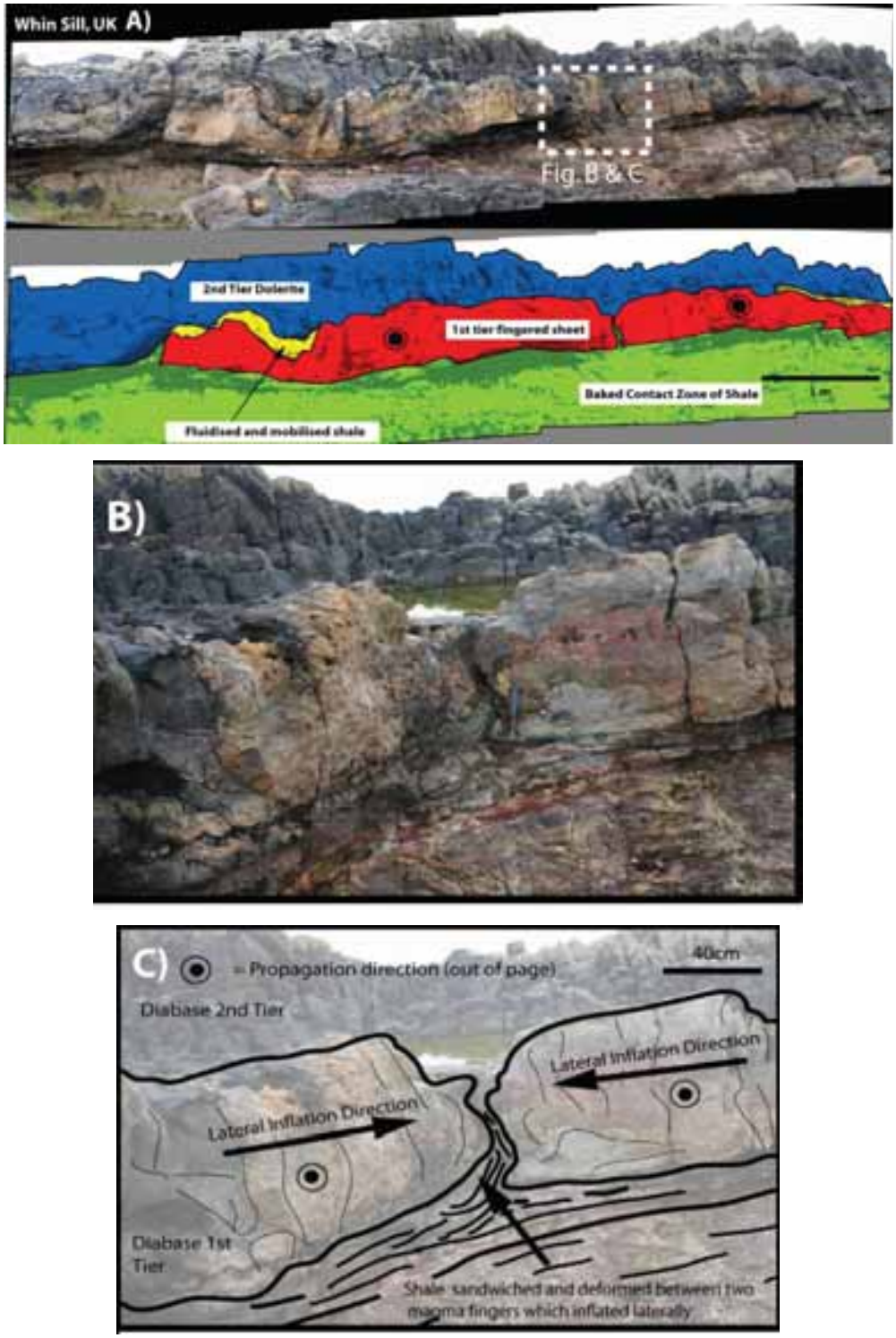

Fig 7.7 – A) Two fingers within the Whin Sill, UK, exposed on the foreshore at Harkess **B)** Field photograph of sandwiched shale between two inflating fingers (hammer for scale). **C)** Sketch of Fig. 7.7b illustrating the sandwiching of a shale horizon between two fingers which have inflated laterally towards one another.

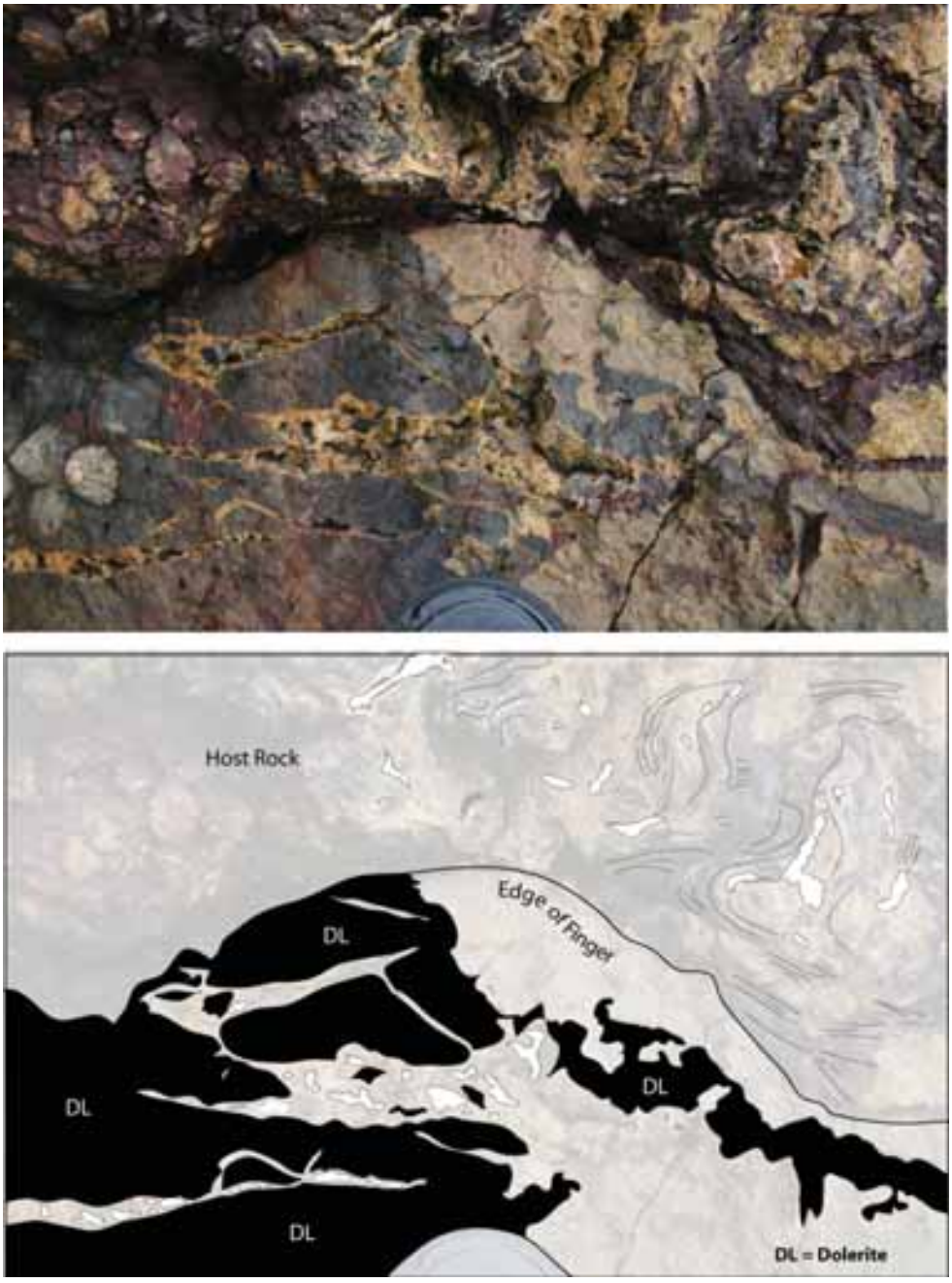

Fig. 7.8 – Field photograph and sketch illustrating a complicated texture developed between host rock and the edge of one of the intruding fingers. The dolerite has become brecciated by the apparent forceful intrusion of hot fluids and sediment into the dolerite. The veins contain hydrothermally deposited quartz, and have numerous vesicles and mineral filled cavities. Also present in the veins is a sand matrix, in places re-crystallized, but appearing to have formed from the sandy slurry injected into the veins.

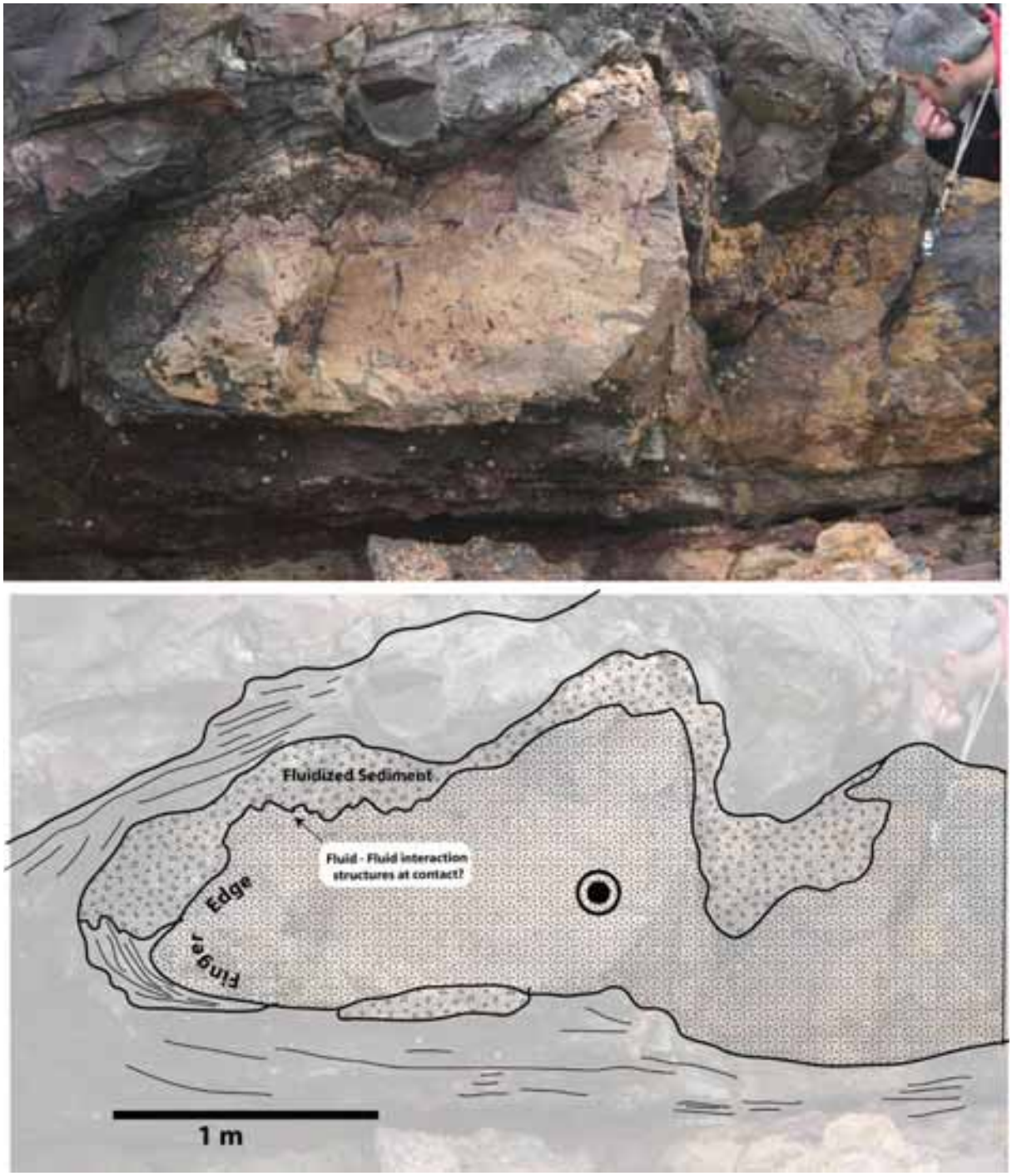

Fig. 7.9 – Field photograph and sketch illustrating contact between magma finger of dolerite and chaotic sediment. Note the contact is not planar, and takes on an undulatory, slightly lobate appearance. This would suggest a viscous-viscous fluid like interaction, indicating the magma and host sediment were acting in a fluid like manner simultaneously.

Within the Whin Sill the general lack of noticeable metamorphic effects in anything but the thickest parts of the sill (Liss, 2004) suggest that during intrusion large amounts of fluids were not available to percolate around host rocks.

Liss (2004) noted that chaotic mobilisation of host rocks seen at outcrops at Harkess occurred in areas were the mobilized beds were overlain by limestone horizons. On this basis Liss (2004) proposed that the limestone had prevented the expulsion of fluid with burial, leading to partially lithified horizons. Therefore upon intrusion of magma into the host rock at Harkess, it contained pore-fluid, which upon heating caused failure of host rock matrix by fluidization (Fig. 7.10). Such an effect would be augmented as such overpressured horizons tend to be poorly consolidated and possess little mechanical strength (Maltman and Bolton, 2001), so that the pore fluid pressure required to overcome the mechanical strength of the host rock and trigger fluidization will be substantially reduced.

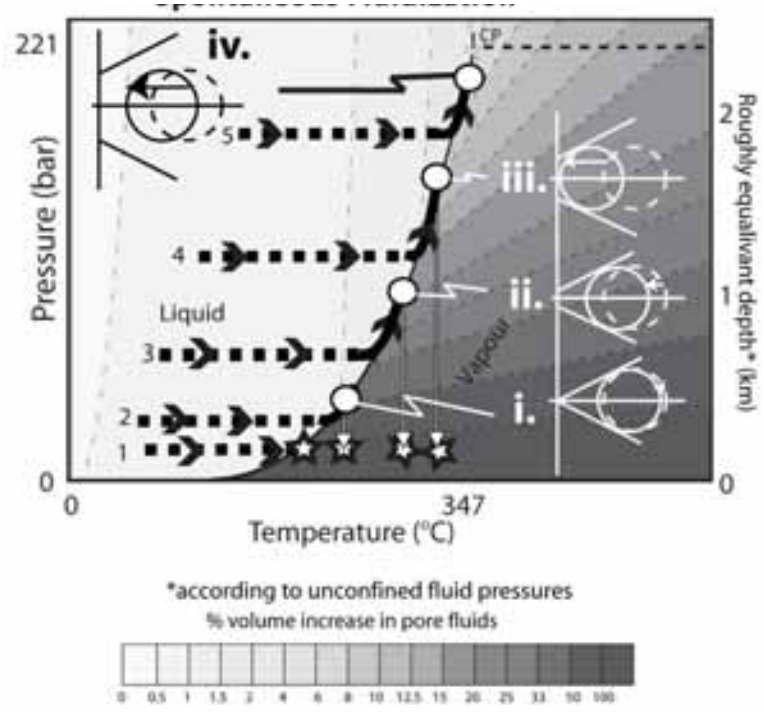

Fig. 7.10 – Figure showing concept of thermal fluidization, the majority of the Whin Sill would fall on line 5, in which even on heating of pore-fluid within host rock, burial and dewatering processes mean that the pore-fluid volume and subsequent pressure increase is insufficient to overcome the strength of host rock matrix and cause fluidization. The fingers at Harkess rock result due to a likely pathway defined by lines 1 and 2, and occur as a result of the host rock being being poorly lithified due to an overlying limestone seal (see text). Upon intrusion and heating the pore-fluid content is sufficient to fluidize host rock instantly (line 1) or after a subsequent pore-fluid pressure increase to overcome mechanical strength of the host rock (line 2).

Therefore, the formation of magma fingers within the Whin Sill appears inherently linked to host rock behavior during intrusion. Specifically it is the burial, dewatering, compaction and cementation history of the host rock which controlled the emplacement mechanism of the sheet and development, or not, of non-brittle structures.

7.4 Ardnamurchan, Scotland

Ardnamurchan forms part of the Hebridian Igneous Province, and forms one of the central complexes, which also consist of Skye, Rum and Mull. Ardnamurchan effectively represents the roots of an eroded volcano (Emeleus and Bell, 2005), and is situated on the mainland adjacent to the northern part of the Isle of Mull. The complex is made of three distinctive volcanic centres (Richey and Thomas, 1930), with numerous sets of cone-sheets associated with each centre. However the most prominent set is related to the intrusion of centre 2 (Emeleus and Gyopari, 1992). The cone-sheets cut up through all of the pre-existing rocks, including Moine psammites, Jurassic and Triassic rocks through to the Paleocene lavas, volcaniclastic breccias and conglomerates of Ben Hiant (Emeleus and Bell; Brown, 2005).

South east of the summit of Ben Hiant, dolerites sheets (cone-sheets) cut up through Paleocene volcaniclastic breccias and conglomerates of the Ben Hiant member. The Ben Hiant member consists of a heterogeneous mix of lithic clasts derived mainly from the Paleocene Lava pile and underlying Moine psammites (Brown and Bell, 2005). The breccias and conglomerates vary between being clast and matrix supported, however typically they are sub-rounded to sub-angular cobbles and boulders set in a fine-grained sand to silt grade matrix (Brown and Bell, 2005; Emeleus and Bell, 2005).

The dolerite sheets which cut up at an angle of ~ 20 – 25° through the volcaniclastic breccias in the region of Ben Hiant shows a distinctive undulatory nature in cross section. Distinctive peaks and troughs (Fig. 7.11), similar to the morphology of the sheets in the Golden Valley Sill occur (Fig. 7.11e), but on a reduced scale, with the Ben Hiant structures being typically in the region of 5-10m across.

The 3D exposure of the undulatory features is poor, rendering it difficult to investigate the exact shape of the contact and nature of the top surface of the sheet. However the cooling joints within the undulations splay in such a way that it suggests that the top contact of the sill closely matches to that defined by the edge of the heather defining the current ground surface (Fig. 7.11d). This suggests the undulations may be representative of the original intrusion morphology and therefore represent magma-fingers.

The undulatory nature to cone-sheets in Ardnamurchan appears to be restricted to the Ben-Hiant cone-sheet. In other areas of the peninsula, the cone-sheets display a typically tabular appearance with no signs of undulations (Fig. 7.12), and the processes operating appear to be essentially brittle with the host rocks being essentially well consolidated and mechanically strong. In the region of the ferry terminal on the south foreshore, the sheets heavily exploit host rock anisotropy, mainly in the form of joints jets within the Moine psammites (Fig. 7.12a and Fig. 7.12b). In the Jurassic shales, the cone-sheets again exploit existing host rock joint sets as well as host rock bedding.

In the case of Ben Hiant the formation of undulatory finger-like features may be attributed to the host rocks intruded. Magma finger formation is not reliant on fluidization and mobilisation of host rocks, although this can be seen to commonly occur. Pollard et al., (1975) reported no evidence of fluidization in his host rocks, where the formation of fingers appears to be more related to poorly consolidated shale horizons acting in a semi-ductile fashion. In addition, Tweto (1951) showed finger formation related to sill intrusion occurring by ductile deformation of shale and in particular clay horizons. However in each of these cases the host rock was and could behave in a incompetent.

During the emplacement of centre 1 intrusions between 59.1 and 58.9 Ma (Brown and O'Driscoll, 2008) the associated doming of the overlying lava pile resulted in mass-wasting (Brown and Bell, 2006), and deposition of the Ben Hiant Member (Brown and Bell, 2006). This was soon followed by the intrusion of the undulatory cone-sheet seen at Ben Hiant. The depth of emplacement of the cone-sheet is hard to estimate, but given the short time frame between deposition of Ben Hiant member and intrusion of the cone-sheet (Brown and Bell, 2006), substantial burial could have not taken place and therefore a depth of emplacement in the region of a few hundred metres is likely to be the case (David Brown, pers. comm.).

The intrusion of magma into unconsolidated host rock, such as the volcaniclastic breccia of the Ben Hiant member could have prevented normal brittle fracture of the host rock. At such shallow levels the host rock may be incapable of supporting brittle fracture and instead ductile deformation of host rocks at the propagating front of the intrusion could have occurred. This would have at least created a pseudo viscous fluid – fluid relationship between magma and host rock, as the partially consolidated volcaniclastic material flowed around the fingers in a non-brittle fashion, analogous to the flow of material around magma fingers of Tweto (1951).

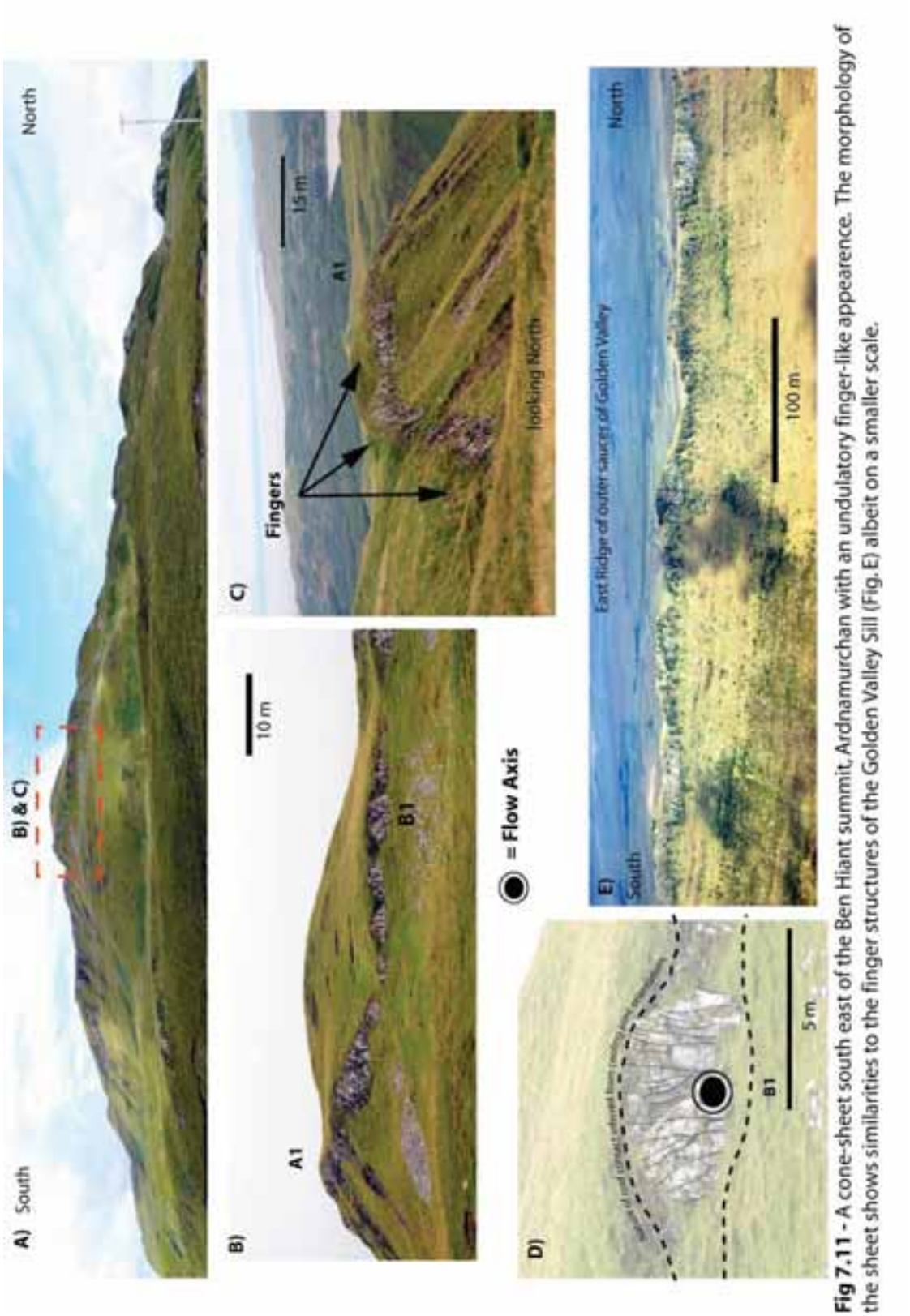

Fig 7.11 - A cone-sheet south east of the Ben Hiant summit, Ardnamurchan with an undulatory finger-like appearence. The morphology of the sheet shows similarities to the finger structures of the Golden Valley Sill (Fig. E) albeit on a smaller scale.

Fig. 7.12 - Cone-sheets of Ardnamurchan (Photos courtesy of Craig Magee) A) & B) Cone-sheets intruding into Moine Psammites C) Cone-Sheet intruding into Limestone. Note the tabular non undulatory appearence to the cone-sheets in contrast to the undulatory nature of the cone-sheet of Ben Hiant (fig. 7.11). The diffrent morphology can be attributed to the fact that the cone-sheet shown within the figure intruded host rock in a brittle fashion. (Craig Magee for scale, note Craig is 1.7 metres tall).

In addition at such a shallow depth high meteoric fluid content in the host rock may be expected (Jamtveit, 1992) which is also likely to aid in the break-down of normal brittle behavior by triggering fluidization in the sequence ahead and around the intruding cone-sheet (Kokelaar, 1982; Chapter 5).

The key factors in the formation of a fingered cone-sheet at Ben-Hiant was the shallow depth of emplacement into a host rock which had only been recently deposited and was essentially unconsolidated and possibly water-saturated at the time of intrusion.

7.5 Linking host rock to sheet morphology

In each of the previously outlined examples within this chapter the morphology of the sheet produced appears to have been controlled by the rheology of the host stratigraphy. Therefore within a given basin, the change in rheological properties of the host rock in response to intrusion of magma will dictate if the morphology of the sill is dominated by essentially brittle or non-brittle structures. As explored in Chapter 5, for fingered sheet intrusion to occur, the host material must behave with effective zero shear strength, i.e. in a fluid-like fashion (Pollard et al., 1975).

In the case of the Raton basin, the host rock coal possessed an inherent mechanical property which allowed them to behave in a viscous manner upon heating by magma. This is also the case in Ardnamurchan where the magma locally intruded unconsolidated host rocks, which could not support a mode 1 fracture and may have acted as a viscous fluid during intrusion.

If the host rock itself does not behave in a primary non-brittle manner, for structures to form (e.g. fingers), which have a non-brittle origin, the rock must be triggered to behave in a non-brittle fashion (see chapter 6). The latter can occur if rapid expansion of pore fluid/gasses occurs at such a velocity that it causes disaggregation effectively suspending particles of the host rock within a buoyant fluid/gas matrix causing the host rock to fluidise and act as a fluid-like mass (Kokelaar, 1982). This process can operate in unconsolidated sediments, enhancing the fluid like behaviour of the rock, but can also act on partially or weakly consolidated rock, if its inherent mechanical strength can be overcome.

The formation of magma fingers (*sensu* Pollard et al., 1975) is linked to the mechanical strength of the host rock and amount of host rock pore fluid (see chapter 6). Fingered sheet intrusions generally occur in higher frequency in shallow intrusions i.e. < 2km (Pollard, 1975; Horsman et al., 2005; this study). This is not necessarily surprising as under

normal burial and lithostatic loading, porosity reduction and cementation begin relatively quickly. Within sand dominated strata compaction arising from grain rearrangement, ductile grain deformation, and brittle failure of grains all act to decrease inter-granular volume at an exponential rate with burial (Lander and Waulderhaug, 1999). Quartz cementation begins at ~ 90 – 100°C and but becomes a major factor after 2km of burial, leading to an increase in overall mechanical rock strength and further drop in pore space volume (Hamilton, 1976; Chuhan et al., 2002). All these factors will act to inhibit host rock behaving in a non-brittle state, and therefore also inhibit the formation of magma fingers. In this circumstance magma will still propagate through host rock but will do so in a brittle fashion which will be represented in the final morphology of the sheet in the form of brittle structures, such as broken bridges. Non-brittle structures, such as magma fingers, will be generally absent. Such a relationship is schematically expressed in Figure 7.13.

The general relationships expressed in Figure 7.13 are simplified. Firstly brittle structures can be present at all levels in the subsurface related to magma intrusion (Gudmundson, 1995). However structures related to non-brittle mechanisms (e.g. magma fingers) will be most common in the shallow sub-surface, where suitable conditions exist for their initiation. The stated 2km transition from sill morphologies being dominated mainly by structures related to brittle or non-brittle processes is only approximate, being based upon the level above which magma finger structures are generally documented (Pollard et al., 1975; Horsman et al., 2005; this study) and the point at which major cementation processes begin and pore space volume is greatly reduced (Lander and Waulderhaug, 1999). The relationship in Figure 7.13 also generally assumes that in a given basin, decrease in porosity, fluid volume and increase in cementation and mechanical strength occur at a linear rate, it does not take into account localised heterogeneities in host rock.

However despite the simplification within Figure 7.13, the relationships highlighted show that no single model of sill emplacement can be applied universally as the emplacement characteristics of sill complexes will be governed by heterogeneities in host rock rheology within the sedimentary basin. This aspect will change both vertically, with depth, and laterally within a given sedimentary basin.

Current models of sill emplacement often assume brittle fracture operating at all points (e.g. numerical models, Malthe-Sørensen, 2004; analogue models, Galland et al., 2009). The example of the Raton basin alone brings into serious question the validity of any model of sill emplacement that does not take into account the changes in rheology of host rocks caused by the heating effects of intruding magma at 1100°C, either triggering cessation of brittle

behaviour directly (e.g. coal horizons of the Raton) or by a secondary process (e.g. fluidization, chapter 6). Although heating dynamics could be built into numerical models, it is hard to see how analogue experimentation exploring shallow level intrusions (e.g. Saucer-shaped sills; Galland et al., 2009) can be used to infer emplacement mechanisms when the temperature-dependent viscous fluids used within the experiments are in the order of temperatures of ~ 50°C (e.g. vegetable oil, Galland et al., 2009), compared to magma at ~ 1100°C, as heating effect by the fluid at ~ 50 °C will have no effect on the rheology of the experimental material being intruded, whereas magma intruded into host rock ~ 1100°C can have massive effect on the host rock rheology.

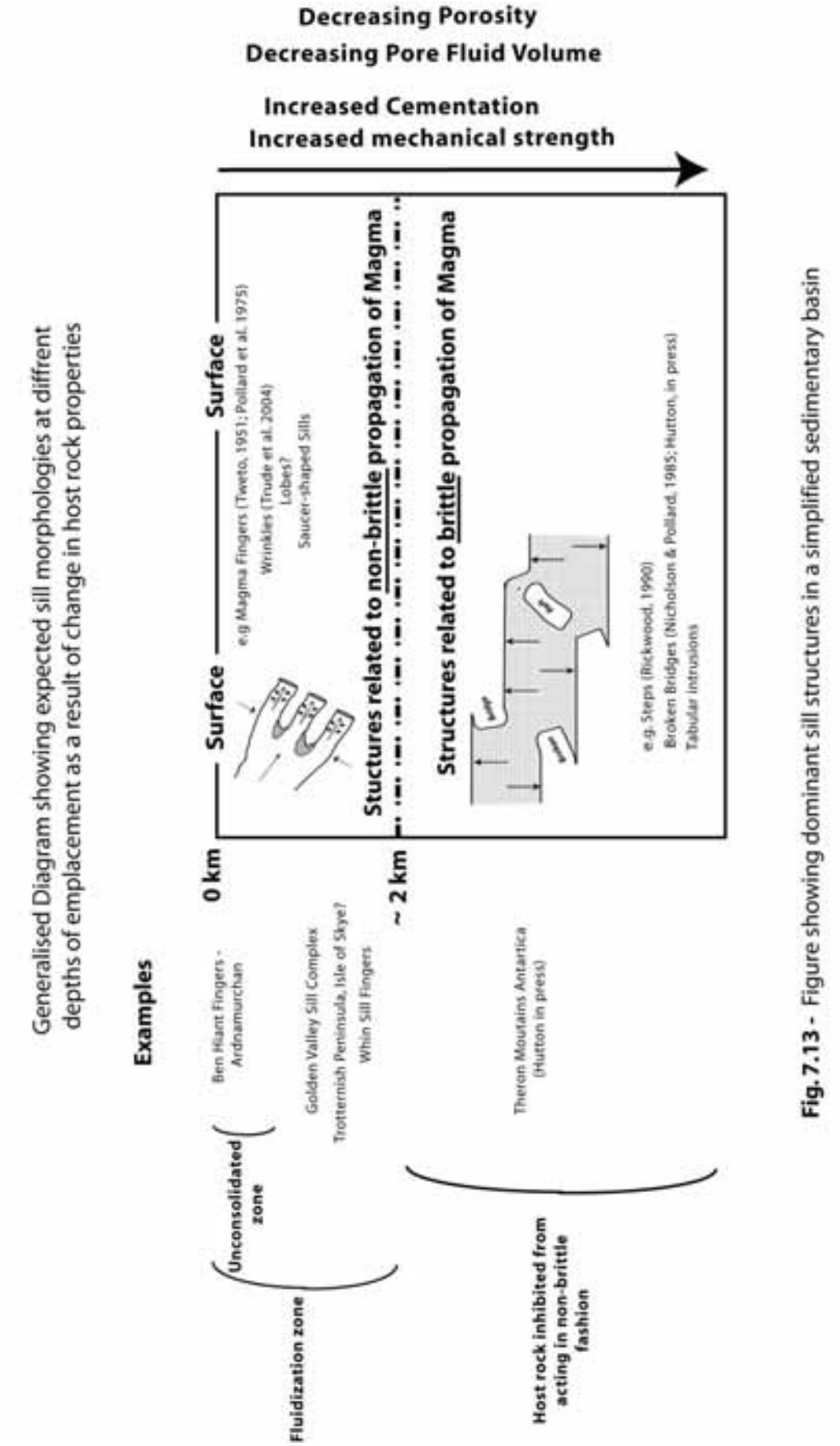

Fig. 7.13 - Figure showing dominant sill structures in a simplified sedimentary basin

Chapter 8
Conclusions

8.1 Overall conclusions regarding thesis

This thesis has acted to understand the underlying mechanisms that govern sill emplacement, specifically addressing the following questions:

- What are the emplacement mechanisms of high-level mafic sill complexes?
- How do saucer-shaped sills form and emplace?
- How does rheology affect sill emplacement mechanisms?
- To what extent does depth act to control sill emplacement mechanisms?

This has been accomplished by a combination of field observations and photo interpretations from sill complexes and sheet intrusions in South Africa, USA, and the UK, combined with observations from 3D seismic data. The detailed findings of this these have been summarized in the previous chapters. However, several overriding conclusions can be drawn across the thesis.

8.1.1 Conclusion 1 – Common occurrence of magma fingers in mafic sheet intrusions

Within the Golden Valley Sill, South Africa, Trotternish sill complex, Skye and Ben Hiant, Ardnamurchan, the dolerite sheets typically possess a corrugated morphology to their top surface. These features can be shown to be the result of magma flow and are interpreted to represent magma fingers *sensu* Pollard et al. (1975). Such features have not been previously identified within published literature related to the sills of the Trotternish peninsula or the cone-sheets of Ardnamurchan. Within the GVS it is suggested that the outer transgressive rim of the sheet did not form by the propagation of single sheet, but by the propagation and coalescence of separate magma fingers. In this respect, fingers are proposed to form a fundamental part of sill intrusion, with magma fingers forming lobes and lobes forming sills.

8.1.2 Conclusion 2 - Host rock controls sill emplacement mechanisms

A key observation presented within this thesis is that it is ultimately the host rock lithology and its coupled rheological response to intrusion of magma that dictates the ongoing morphological evolution of sheet intrusions in high-level magmatic systems.

In the Raton basin, Whin sill and cone-sheets of Ardnamurchan, it is proposed that the burial history and diagenesis of the host rock controlled the morphology of the intruding sill. Within the Whin sill, magma fingers developed as magma intruded into water rich, overpressured horizons, which were susceptible to fluidization. This process only occurred in areas of the Whin sill in which overlying limestone horizons acted as seals to prevent pore-fluid expulsion on burial. Within the Ben-Hiant cone-sheet of Ardnamurchan, the shallow level of emplacement and poor consolidation within host rock appears to have led to the formation of magma fingers, presumably by the viscous deformation of rock around the tip of intruding magma. In the Raton basin, the response of the coal to the heating effects of the magma caused it to behave as a viscous fluid over a sustained period, allowing for the widespread formation of fingers.

In each of the above situations, the development of magma fingers appears to have been a primary function of the response of host rock to magma intrusion, specifically the ability of host rock to act in a viscous manner, either directly or if triggered to do so by a secondary mechanism such as fluidization. The major control in the ability for host rock to do this is reliant on its properties at time of intrusion, i.e. mechanical strength, porosity and volume of pore fluid. These factors in turn will be governed by the burial, diagenesis, dewatering and cementation history of the host rock before the intrusion of magma.

8.1.3 Conclusion 3 – Fluidization of host rock plays a fundamental role in controlling sheet emplacement

Fluidization of host rock has been mostly viewed as a secondary process acting in host rocks due to the result of heating effects of intruding magma. It has not been previously invoked to form a major part in the formation of saucer-shaped sills.

All current models of saucer-shaped sill emplacement invoke brittle failure of host rock at the inner-sill periphery to explain the upwards migration of magma to create the transgressive arcuate inclined sheet of a saucer-shaped sill. The opening of this fracture in the presence of heated pore-fluids is proposed to form a viable trigger to fluidization (and magma finger formation) as a result of a rapid drop in pore-fluid pressure. Saucer-shaped sill complexes are well documented from field and 3D seismic data to generally occur in the 0 –

2 km paleo-depth range. It therefore seems an oversight not to take into account the effect of e.g. fluidization on the emplacement mechanisms of the magma, given that in a 0 – 2 km depth range substantial pore-fluid can be present trapped within host rock at time of intrusion.

The model of saucer-shaped sill emplacement proposed within this thesis invokes fluidization as a key aspect in the ceasing of brittle behaviour and creation of magma fingers at edge of the inner sill periphery.

8.1.4 Conclusion 4 – Analogue modelling is currently incapable of accurately portraying igneous emplacement in high-level magmatic systems

One of the most serious implications of the work in a wider context is questioning the recent upsurge in the trend of using analogue models in the study of sill and igneous emplacement mechanisms. Work in this thesis has shown that behaviour of host rock rheology during intrusion of magma appears to play a major role in the evolution of high-level sheet intrusion. Analogue modelling is currently incapable of replicating the heating effects of magma at ~ 1100°C in an experimental setting. Therefore in such experiments it is currently difficult to assess the importance or not of a heat dependant processes such as fluidization, which raises the question of how valid analogue models are at portraying the 'real world' situation in shallow level sheet emplacement.

8.1.5 Conclusion 5 – Structures within sills need to be classified genetically and not simply by morphology

Sills possess many different structures, which are mainly classified on terms of morphology, but by looking at the structures in terms of understanding the process that formed them, it is possible to use the structures to understand the emplacement mechanism of the sill.

This has been highlighted in observations regarding the occurrence of magma fingers and the behaviour of surrounding host rocks. Specifically when brittle behaviour ceases to operate during the intrusion of a magma sheet, magma fingers are generally formed.

Therefore it is important to classify common structures within sill in terms of if they are formed by predominantly brittle, or non-brittle behaviour and not just on the basis of morphology

8.2 Future work - Toward a new concept in sill emplacement

Many of the relationships presented in this thesis challenge some of the widely accepted

views on how sill complexes intrude into the upper crust. However many of the processes highlighted in this thesis require a great deal of further investigation.

8.2.1 Formation of lobes and fingers

The emplacement of magma fingers, their coalescence into lobes, which in turn form the larger rims of the saucer-shaped sills, is quite different to classical fracture-mechanical models for intrusions, as the development of fingers requires that both the intruding magma and the country rock to behave to some degree as fluids. As a result, the movement of magma through the very shallow crust needs to be completely re-evaluated. Key questions regarding magma finger and lobe formation are as follows;

- How do fingers coalesce to form lobes?
- How do lobes interact to form saucer-shaped sills?
- How do saucer-shaped sills connect with higher saucer-shaped sills to provide the sub-volcanic plumbing system?

How magma fingers coalesce to form lobes and how lobes interact to form saucer-shaped sill can only be easily understood by determining the flow dynamics within magma fingers (at various stages) and in lobes (after magma fingers have coalesced). Although numerical modelling could prove useful in this, little field data is currently available to constrain a numerical model. Therefore, a targeted AMS (anisotropy of magnetic susceptibility) study could prove useful in trying to understand flow fabrics within magma fingers and lobes. Previous AMS studies on saucer-shaped sills (e.g. Polteau et al. 2008) have had insufficient sampling density to elucidate detailed flow fabrics within sill structures, e.g. magma fingers. A targeted AMS study of convex-up undulations structures could confirm how the finger structures formed, either as a result of finger expansion or of flow localisation (Fig. 8.1). In addition, a targeted AMS study across sets of magma fingers may also potentially elucidate information of how one sill feeds another by identifying magma fingers which have acted as long term conduits to higher sills (Fig. 8.1)

8.2.2 Constraints on fluidization

Although good evidence exists for fluidization of host rocks and its effect on emplacement mechanisms of sills, a lot of uncertainty remains. Specifically in the case of the Golden

Valley Sill, the opening of a fracture at the periphery is proposed to have triggered fluidization of host rock and triggered the formation of magma fingers. A key question in regard to this is;

- What magnitude of fracture needs to open to induce fluidization in unconsolidated or partially consolidated host rock and how this is linked to factors such as interconnection of pore-spaces, pore-fluid volume and heating effects of magma?

Realistically the only way to understand how each of these variables affects the process of fluidization and finger formation would be to undertake numerical modelling, taking into account pore-fluids and heating effects of magma.

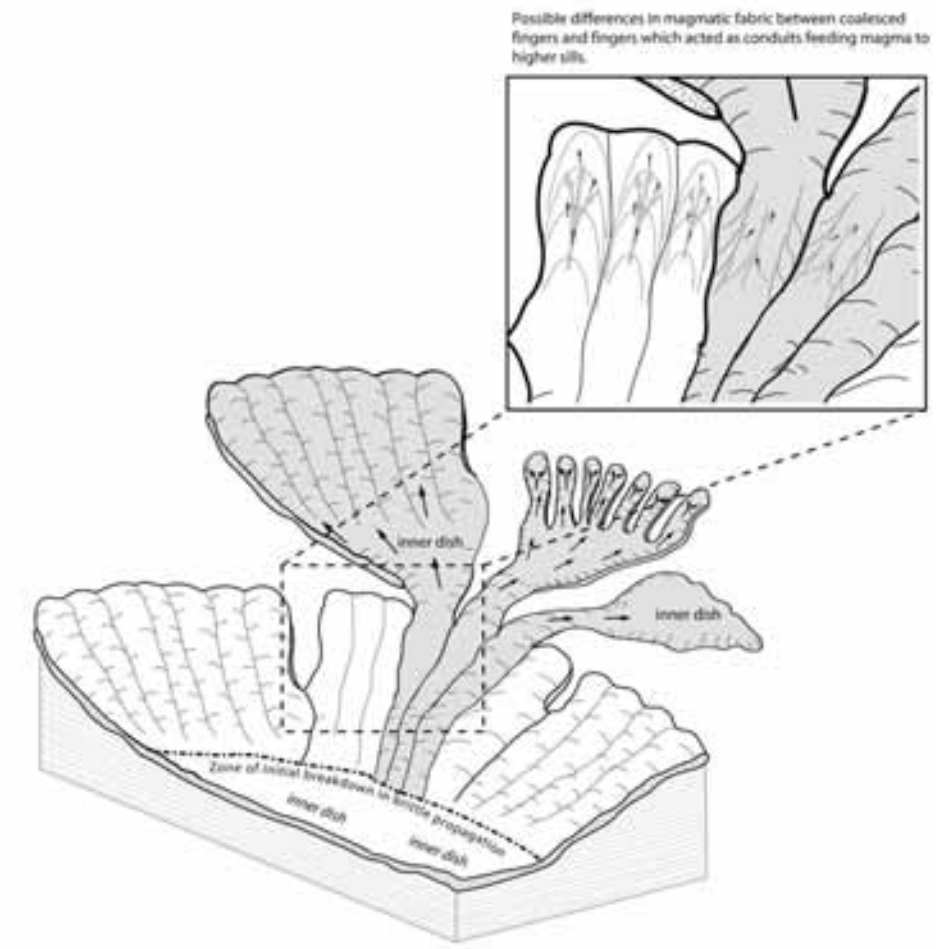

Fig. 8.1 – Schematic showing possible differences in magmatic fabric between coalesced fingers and fingers acting as conduits feeding magma to higher sills.

8.2.3 Role of saucer-shaped sill complexes in acting as shallow-level magma chambers

It is clear from seismic images (e.g. Cartwright and Hansen, 2006) and satellite images that sills can form extensive interconnected networks that have the potential to feed magma around the upper shallow crust (Fig. 8.2). It is feasible to think that such a complex plumbing system must have some capacity to store and release batches or pulses of magma i.e. act as shallow level magma chambers, rather than simply provide an open conduit to a deeper source. Therefore an understanding of the scale of inflation during magma filling and deflation during magma extraction (feeding higher sills or erupting) of individual structures and the entire complex is fundamental. This may then give information regarding distribution of magma in the system, highlighting active parts of the sill complex which were episodically inflating and deflating while feeding overlying eruptions, or higher sills within the complex.

Such an investigation could be carried out primarily using 3D seismic data to investigate structures above sills related to inflation and/or deflation cycles, in particular forced folding and brittle failure. By combining the seismic data with field based observations, it may be possible to understand inflation and deflation cycles within a sill and sill complex.

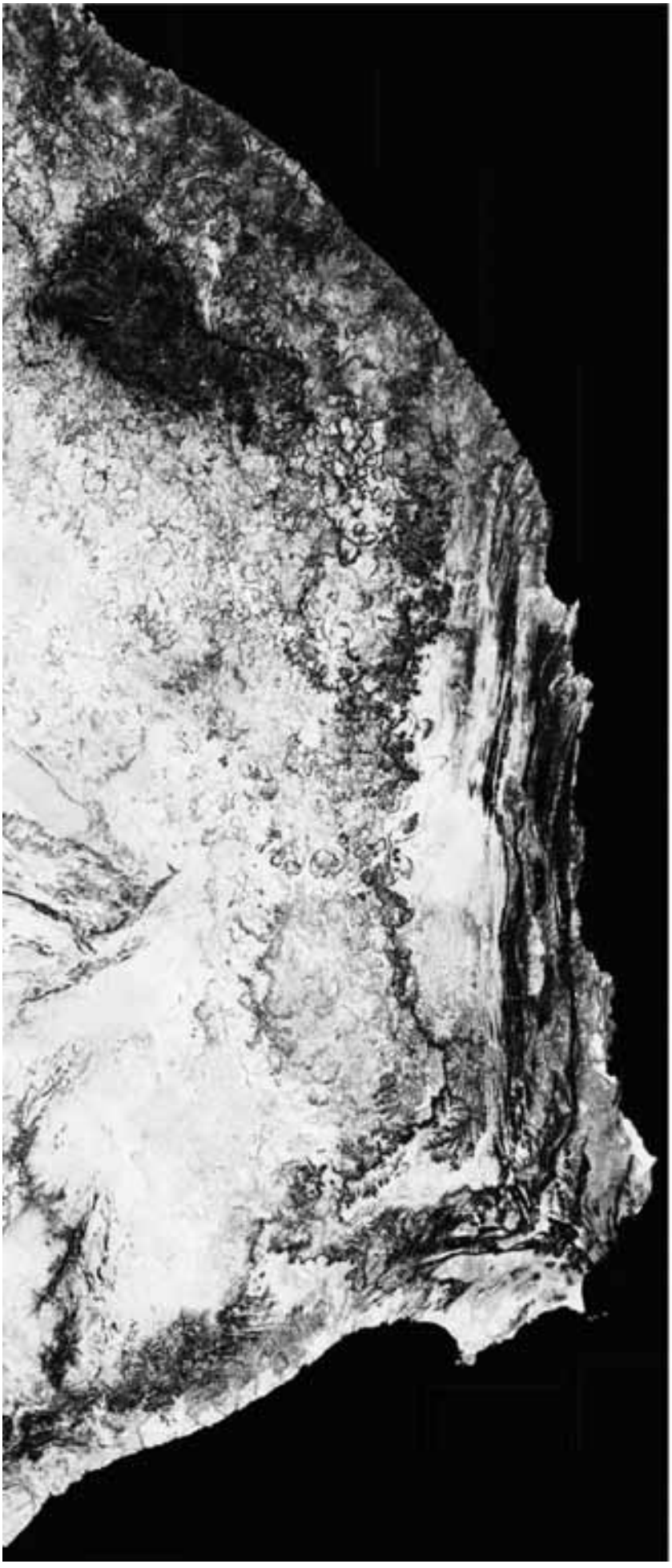

Fig. 8.2 – SRTM-90 satellite image of South Africa rendered as a dip map. The saucer-shaped sills extending across the Karoo Basin are clearly visible (black rings). Could these represent shallow level magma chambers?

References

Anderson, E.M., 1951, The dynamics of faulting and dyke formation with applications to Britain. Edinburgh, Oliver and Boyd, 206 pp.

Anderson, F.W. and Dunham, K.C., 1966, *The Geology of Northern Skye*. Memoir of the Geological Survey of Great Britain, HMSO, Edinburgh.

Anderson, S.W., McColley, S.M., Fink, J.H., and Hudson, R., 2005, The Development of Fluid Instabilities and Preferred Pathways in Lava Flow interiors: Insights from Analog Experiments and Fractal Analysis: Geol.Soc.Am.Special Paper, v. 396, p. 147-161.

Baer, G., 1991, Mechanisms of dyke propagation in massive porous sedimentary rocks. Journal of Geophysical Research, v. 96, p. 11911-11ee4r929.

Baer, G., 1995, Fracture propagation and magma flow in segmented dykes: field evidence and fabric analysis, Makhtesh Ramon, Israel, in Baer, G. and Heinmann, A.A. (eds.), Physics and Chemistry of dykes. Rotterdam, Balkema, p. 125-140.

Ballantyne, C.K., McCarroll, D., Nesje, A., Dahl, S.O., Stone, J.O., and Fifield, L.K., 1998, High-resolution reconstruction of the last ice sheet in NW Scotland: Terra Nova, v. 10, p. 63-67.

Bell, B.R. and Butcher, H., 2002, On the emplacement of sill complexes: evidence from the Faroe-Shetland Basin, *in* Jolly, D.W. and Bell, B., eds., The North Atlantic Igneous Province: stratigraphy, tectonic, volcanic and magmatic processes.: Geol Soc Lond. Spec Pub 197, p. 307-329.

Bell, B.R. and Harris, J.W., 1986, An Excursion Guide to the Geology of the Isle of Skye. Geological Society of Glasgow, 317 pp.

Bell, B.R. and Williamson, I.T., 2002., Tertiary Igneous Activity, in Trewin, N.H. (ed.), The Geology of Scotland (4th edition), The Geological Society (London), 371-407.

Bemudez, A. and Delpino, D., 2008, Concentric and radial joint systems within basic sills and their associated porosity enhancement, Neuquen Basin, Argentina, from Thomson, K with Petford, N. (eds) Structure and Emplacement of High-Level Magmatic Systems, Geol. Soc. London, Special Publication, 302, p. 45-61.

Benn, D.I., 1997, Glacier fluctuations in western Scotland: Quaternary International, v. 38-9, p. 137-147.

Bennett, M.R. and Boulton, G.S., 1993, Deglaciation of the Younger Dryas Or Loch-Lomond Stadial Ice-Field in the Northern Highlands, Scotland: Journal of Quaternary Science, v. 8, p. 133-145.

Binns, P. E., McQuillan, R. Fannin, N. G. T., Kenolty, N. and Ardus, D. A., 1975, Structure and stratigraphy of sedimentary basins in the Sea of the Hebrides and the Minches. *In*: Woodland, A. W. (ed.) *Petroleum and the Continental Shelf of North West Europe. 1. Geology,* Applied Science Publishers, Barking, Essex, p.93–102.

Bjørlykke, K., 993,Fluid flow in sedimentary basins. Sedimentary Geology, 86, p.137–158.

Bolchover, P. and Lister, J.R., 1999, The effect of solidification on fluid-driven fracture, with application to bladed dykes: Proceedings of the Royal Society of London Series A-Mathematical Physical and Engineering Sciences, v. 455, p. 2389-2409.

Bradley, J., 1965, Intrusion of major dolerite sills. Transactions of the Royal Society of New Zealand, Geology, v.3, p. 27-55.

Brown, D.J. and Bell, B.R., 2006, Intrusion-induced uplift and mass wasting of the Palaeogene volcanic landscape of Ardnamurchan, NW Scotland. Journal of the Geological Society, London, 163, (1), p. 29-36.

Brown, D.J. and O'Driscoll, B., 2008, Ardnamurchan "A tribute to the life and works of James E.Richey (1886-1968): 40 years on. Volcanic and Magamatic Studies Group Field Guide, University of Glasgow.

Burchardt, S., 2008, New insights into the mechanics of sill emplacement provided by field observations of the Njardvik Sill, Northeast Iceland, Journal of Volcanology and Geothermal Research, Volume 173, Issues 3-4, p. 280-288.

Burger, C.A.J., Hodgson, F.D.I. and Van der Linde, P.J., 1981, Hidroliese eienskappe van akwifere in die Suid Vrystaat. Die ontwikkeling en evaluering van tegnieke vir die bepaling van die ontginninspotensiaal van grondwaterbronne in die Suid-Vrystraat en in Noord-Kaapland. Institute of Groundwater Studies, University of the Orange Free State, Bloemfontein, South Africa. **2**, 115 pp.

Busby-Spera, C. and White, J.D.L., 1987, Variation in peperites textures associated with different host-sediment properties. Bulletin of Volcanology, v. 49, p. 765-777.

Butler, R.W.H. and Hutton, D.H.W. 1994, Basin structure and Tertiary magmatism on Skye, NW Scotland. Journal of the Geological Society, London, 151, p. 931-944.

Byerlee, J., 1978, Friction of Rocks: Pure and Applied Geophysics, v. 116, p. 615-626.

Callot, J.P. and Helfrich, K.R., 2004, Magma Flow in the East Greenland dyke swarm inferred from study of anistropy of magnetic susceptibility: magmatic growth of a volcanic margin: Geophys.J.Int., v. 159, p. 816-830.

Cartwright, J. and Hansen, D.M., 2006, Magma transport through the crust via interconnected sill complexes: Geology, v. 34, p. 929-932.

Catuneanu, O., Wopfner, H., Eriksson, P.G., Cairncross, B., Rubidge, B.S., Smith R.M.H. and Hancox, P.J, 2005, The Karoo basins of south-central Africa, Journal of African Earth Sciences **43**, p. 211–253.

Chang, H., 2004. Hydraulic fracturing in particulate material. PhD thesis, Georgia Institute of Technology, Athens.

Chevalier, L. and Woodford, A., 1999, Morpho-tectonics and mechanism of emplacement of the dolerite rings and sills of the western Karoo, South Africa, South African Journal of Geology, v.102, p. 43-54.

Chuhan, F.A., Kjeldstad, A., Bjorlykke, K. and Hoeg, K., 2002, Porosity loss in sand by grain crushing-experimental evidence and relevance to reservoir quality. *Mar. Pet. Geol.* **19** (2002), p. 39–53.

Cooper, J.R., Crelling, J.C., Rimmer, S.M., and Whittington, A.G., 2007, Coal metamorphism by igneous intrusion in the Raton Basin, CO and NM: implication for generation of volatiles, *International Journal of Coal Geology* **71** (2007), p. 15–27.

Cornelius, C., Clarke, P., Turner., 2004, Basin scale peperites in cretaceous coals; host rock fluidization ca. 30 million years after lithification, Geological Society of America Abstracts with Programs, Vol. 36, No. 4, p. 85.

Corry, C.E., 1988, Laccoliths: Mechanics of Emplacement and Growth. Geological Society of America Special Paper 220.

Cox, K.G., 1989, The role of mantle plumes in the development of continental drainage patterns. Nature, 342, 873-877.

Cox, K. G., 1992, Karoo igneous activity, and the early stages of the breakup of Gondwana, in Storey, B. C., et al., eds., Magmatism and the causes of continental breakup: Geological Society of London Special Publication 68, p. 137–148.

Curtis, M.L. and Riley, T.R., 2003, Mobilization of fluidized sediment during sill emplacement, western Dronning Maud Land, East Antarctica: Antarctic Science, v. 15, p. 393-398.

Davies, R., Bell, B.R., Cartwright, J.A., Shoulders, S., 2002, Three-dimensional seismic imaging of Palaeogene dike-fed submarine volcanoes from the northeast Atlantic margin: Geology, v. 30, p. 223-226.

DeGraff, J.M. and Aydin, A., 1993, Effect of thermal regime on growth increment and spacing of contraction joints in basaltic lava, Journal of geophysical research, vol. 98, noB4, p. 6411-6430.

Delaney, P.T. and Pollard, D.D., 1981, Deformation of host rocks and flow of magma during growth of minette dikes and breccia-bearing intrusions near ship rock. New Mexico: US Geological Survey Professional Paper, Report, vol. 1202, p. 61.

Delaney, P.T., 1982, Rapid intrusion of magma into wet rock: groundwater flow due to pore pressure increase. Journal of Geophysical Research, v.87, p. 7739-7756.

Delaney, P.T., 1987, Heat transfer during emplacement and cooling of mafic dykes, in Halls, H.C. and Fahrig, W.F (eds.), Mafic Dyke Swarms. Geological Association of Canada Special Paper, 34, p. 31-46.

Delaney, P.T. and Pollard, D. D., 1982, Solidification of basaltic magma during flow in a dyke. American Journal of Sciences. V. 282, p.856-885.

Delaney, P.T., Pollard, D.D., Ziony, J.I., and Mckee, E.H., 1986, Field Relations Between Dikes and Joints - Emplacement Processes and Paleostress Analysis: Journal of Geophysical Research-Solid Earth and Planets, v. 91, p. 4920-4938.

Dowman, I., Balan, P., Renner, K., and Fischer, P., 2003, An Evaluation of Nextmap Terrain Data in the Context of UK National Datasets, unpublished report.

Du Toit, A.L., 1920, The Karoo dolerites of South Africa: a study of hypabassal injection. Trans Geological Soc South Africa 23, p. 1-42.

Duffield, W. A., Bacon, C. R., and Delaney, P. T., 1986, Deformation of poorly consolidated sediment during shallow emplacement of a basalt sill, Coso Range, California: *Bulletin of Volcanology*, v. 48, p. 97-107

Eales, H.V., Marsh, J.S. and Cox, K.G., 1984, The Karoo Igneous Province: An Introduction: Spec. Publ. Geol. Soc.S. Afr, v. 13, p. 1-26.

Elliot, D.H. and Fleming, T.H., 2000, Weddell triple junction: The principal focus of Ferrar and Karoo magmatism during initial breakup of Gondwana: Geology, v. 28, p. 539-542

Emeleus, C.H, and Bell, B.R., 2005, British Regional Geology: the Palaeogene volcanic districts of Scotland (Fourth edition). (British Geological Survey, Nottingham)

England, R.W., 1988, The early tertiary stress regime in NW Britain: Evidence from patterns of volcanic activity, form Morton, A.C., with Parson, L. M., (eds), 1988, Early Tertiary Volcanism and the opening of the NE Atlantic, Geological Society Special Publication No.39, p. 381-389.

Ernst, R.E., Grosfils, E.B., and Mege, D., 2001, Giant dike swarms: Earth, Venus, and Mars: Annual Review of Earth and Planetary Sciences, v. 29, p. 489-534.

Francis, E.H., 1982, Magma and sediment-I. Emplacement mechanism of the late carboniferous tholeiite sills in northern Britain. Journal of the Geological Society, London, v. 139, p. 1-20.

Francis, T.J.G., 1982b, Thermal-Expansion Effects in Deep-Sea Sediments: Nature, v. 299, p. 334-336.

Frid, V., Bahat, D., and Rabinovich, A., 2005, Analysis of en echelon/hackle fringes and longitudinal splits in twist failed glass samples by means of fractography and electromagnetic radiation: Journal of Structural Geology, v. 27, p. 145-159.

Fukada, K., Itagaki, S., and Shimoyama, I., 2006, Effect of rapid preheating on the coking properties of coals: ISIJ International, v. 46, p. 1603-1609.

Gaffney, E.S., Damjanac B. and Valentine, G.A., 2007, Localization of volcanic activity: 2. Effects of pre-existing structure, *Earth and Planetary Science Letters* **263** (2007), pp. 323–338

Galerne, C.Y., Neumann, E.R., and Planke, S., 2008, Emplacement mechanisms of sill complexes: Information from the geochemical architecture of the Golden Valley Sill Complex, South Africa: Journal of Volcanology and Geothermal Research, v. 177, p. 425-440.

Gallagher, J.W. and Dromgoole, P.W., 2007, Exploring below the basalt, offshore Faroes: a case history of sub-basalt imaging: Petroleum Geoscience, v. 13, p. 213-225.

Galland, O., Planke, S., Neumann, E.R., and Malthe-Sorenssen, A., 2009, Experimental modelling of shallow magma emplacement: Application to saucer-shaped intrusions: Earth and Planetary Science Letters, v. 277, p. 373-383.

Gerjarusak, S., Peters, A., and Howard, J.B., 1991, Coal plasticity at high heating rates and temperatures, fifth Technical progress report, Energy laboratory and department of chemical engineering, MIT.

Gibson, S.A. and Jones, A.P., 1991, Igneous Stratigraphy and Internal Structure of the Little Minch Sill Complex, Trotternish Peninsula, Northern Skye, Scotland: Geological Magazine, v. 128, p. 51-66.

Gilbert, G.K., 1877. Report on the geology of the Henry Mountains, U.S. Geographical and Geological Survey of the Rocky Mountains Region, 170 p.

Gretener, P.E., 1969, On the mechanics of the intrusion of sills. Canadian Journal of Earth Sciences, v.6, p. 1415-1420.

Grossenbacher, K.A. and McDuffie, S.M, 1995, Conductive cooling of lava: columnar joint diameter and stria width as functions of cooling rate and thermal gradient, Journal of Volcanology and Geothermal Research, Volume 69, Issues 1-2, P. 95-103.

Goto, Y. and Tsuchiya, N., 2004, Morphology and growth style of a Miocene submarine dacite lava dome at Atsumi, northeast Japan: Journal of Volcanology and Geothermal Research, v. 134, p. 255-275.

Goulty, N.R., 2005, Emplacement mechanism of the Great Whin and Midland Valley dolerite sills. Journal of the Geological Society London, 162, p. 1047-1056.

Goulty, N. and Schofield, N., 2008, Implications of simple flexure theory for the formation of saucer-shaped sills. Journal of Structural Geology, 30, p. 812-817.

Gudmundsson, A., 2003, Surface stresses associated with arrested dykes in rift zones: Bulletin of Volcanology, v. 65, p. 606-619.

Gudmundsson, A., 2005, The effects of layering and local stresses in composite volcanoes on dyke emplacement and volcanic hazards: Comptes Rendus Geoscience, v. 337, p. 1216-1222.

Hälbich, I.W., 1992, The Cape Fold Belt orogeny: state of the art 1970s – 1980s. In: M.J. de Wit and I.G.D. Ransome, Editors, *Inversion Tectonics of the Cape Fold Belt, Karoo and Cretaceous Basins of Southern Africa*, Balkema, Rotterdam, pp. 141–158

Hamilton, E.L., 1976, Variations of Density and Porosity with Depth in Deep-Sea Sediments: Journal of Sedimentary Petrology, v. 46, p. 280-300.

Hamilton, M.A., Pearson, D.G., Thompson, R.N., Kelley, S.P., and Emeleus, C.H., 1998, Rapid eruption of Skye lavas inferred from precise U-Pb and Ar-Ar dating of the Rum and Cuillin plutonic complexes: Nature, v. 394, p. 260-263.

Hansen, D.M., Cartwright, J.A. and Thomas, D., 2004, 3D seismic analysis of the geometry of igneous sills and sill junction relationships. In: Davies, R.J.,Cartwright, J.A., Stewart, S.A., Lappin, M. with Underhill, J.R. (eds) 3D.Seismic Technology: Application to the Exploration of Sedimentary Basins. Geological Society, London, Memoirs, 29, 199–208.

Hansen, D.M. and Cartwright, J., 2006, Saucer-shaped sill with lobate morphology revealed by 3D seismic data: implications for resolving a shallow-level sill emplacement mechanism: Journal of the Geological Society, v. 163, p. 509-523.

Hansen, D.M. and Cartwright, J., 2006b, The three-dimensional geometry and growth of forced folds above saucer-shaped igneous sills: Journal of Structural Geology, v. 28, p. 1520-1535.

Hanson, R.B., 1995, The Hydrodynamics of Contact-Metamorphism: Geological Society of America Bulletin, v. 107, p. 595-611.

Habert, G. and Saint-Blanquat, M., 2004., Rate of construction of the Black Mesa bysmalith, Henry Mountains, Utah., from Breitkreuz, C. with Petford, N. (eds) Physical Geology of High-Level Magmatic Systems, Geol. Soc. London, Special Publication, 264. 163-173.

Hatcher, R.D., 1996, Structural Geology: Principles, Concepts, and Problems (second ed.), Prentice Hall, New Jersey, USA (1995), 525p.

Herrero-Bervera, E., E. Canon-Tapia, G. P. L. Walker, and J. C. Guerrero-Garcia, 2001, The Nuuanu and Wailau giant landslides: Insights from paleomagnetic and anisotropy of magnetic susceptibility (AMS) studies, *Phys.Earth Planet. In.*, 129, 83-98.

Holness, M.B. and Humphreys, M.C.S., 2003, The Traigh Bhan na Sgurra Sill, Isle of Mull: Flow localization in a major magma conduit: Journal of Petrology, v. 44, p. 1961-1976.

Horsman, E., Tikoff, B., Morgan, S., 2005, Emplacement-related fabric and multiple sheets in the Maiden Creek sill, Henry Mountains, Utah, USA: Journal of Structural Geology, v. 27, p. 1426-1444.

Husch, J.M., 1990, Palisades Sill - Origin of the Olivine Zone by Separate Magmatic Injection Rather Than Gravity Settling: Geology, v. 18, p. 699-702.

Hutton, D.H.W. in press, Insights into magmatism in volcanic margins: Bridge structures and a new mechanism of basic sill emplacement-Theron Mountains, Antarctica, in Schofield, N., Turner, J.P.T., Underhill, J. (eds), Petroleum Geoscience.

Hutton, D.H.W and Owens, W.H., unpublished report, The Geometry and flow directions of the Tertiary Trotternish Sills of Skye, Earth Sciences, University of Birmingham.

Jamtveit, B., Dahlgren, S., and Austrheim, H., 1997, High-grade contact metamorphism of calcareous rocks from the Oslo Rift, Southern Norway: American Mineralogist, v. 82, p. 1241-1254.

Jamtveit, B., Svensen, H., Podladchikov, Y.Y. and Planke, S. 2004, Hydrothermal vent complexes associated with sill intrusions in sedimentary basins. *In:* Breitkreuz, C. with Petford, N. (eds) Physical Geology of High-Level Magmatic Systems. Geological Society, London, Special Publications, **234**, 233–241.

Johnson, G.A.L. and Dunham, K.C., 2001, Emplacement of the Great Whin Dolerite Complex and the Little Whin Sill in relation to the structure of northern England. Proceedings of the Yorkshire Geological Society 53, 177–186.

Johnson, A.M. and Pollard, D.D., 1973, Mechanics of growth of some laccolithic intrusions in the Henry Mountains, Utah, I. Tectonophysics, v.18., p. 261-309.

Johnson, M.R., van Vuuren, C.J., Hegenberger, W.F., Key, R., and Shoko, U., 1996, Stratigraphy of the Karoo Supergroup in southern Africa: An overview (vol 23, pg 3, 1996): Journal of African Earth Sciences, v. 23, 607p.

Jolly, R.J.H. and Lonergan, L., 2002, Mechanisms and controls on the formation of sand intrusions: Journal of the Geological Society, v. 159, p. 605-617.

Jourdan, F., Feraud, G., Bertrand, H., Watkeys, M.K., Kampunzu, A.B., and Le Gall, B., 2006, Basement control on dyke distribution in Large Igneous Provinces: Case study of the Karoo triple junction: Earth and Planetary Science Letters, v. 241, p. 307-322.

Kavanagh, J.L., Menand, T and Sparks, R.S.J., 2005, An experimental investigation of sill formation and propagation in layered elastic media. Earth and Planetary Science Letters. 245, 799-813.

Kennedy, G.C. and Holser, W.T., 1966, Pressure-volume-temperature and phase relations of water and carbon dioxide, in Clark, S.P. (ed.), Handbook of physical constants. Memoir of the Geological Society of America, v.97, p. 371-381.

Kerr, A.C., 1993, Current research in the British Tertiary Igneous Province, Journal of the Geological Society*;* 1993; v. 150; issue.6; p. 1193-1194; DOI: 10.1144/gsjgs.150.6.1193.

Kerr, A.D. and Pollard, D.D., 1998, Toward more realistic formulations for the analysis of laccoliths, Journal of Structural Geology **20**, p. 1783–1793.

Kim, Y.S. and Sanderson, D.J., 2005, The relationship between displacement and length of faults: a review: Earth-Science Reviews, v. 68, p. 317-334.

Klausen, M.B., and Larsen, H.C., 2002, East Greenland coast-parallel dike swarm and its role in continental breakup, in Menzies, M.A., et al., eds., Volcanic Rifted Margins: Geological Society of America Special Paper 362, p. 133–158.

Kokelaar, B.P., 1982, Fluidization of wet sediments during the emplacement and cooling of various igneous bodies. Journal of the Geological Society, London, v. 139, p.21-33

Krynauw, J.R., Hunter, D.R. and Wilson, A.H., 1988, Emplacement of sills into wet sediments at Grunehogna, western Dronning Maud Land, Antartica. Journal of the Geolgical Society, London, v.145, p. 1019-1032.

Krynauw, J.R., Behr, H.J., and Vandenkerkhof, A.M., 1994, Sill Emplacement in Wet Sediments - Fluid Inclusion and Cathodoluminescence Studies at Grunehogna, Western Dronning-Maud-Land, Antarctica: Journal of the Geological Society, v. 151, p. 777-794.

Lahaye. J. and Prado, G, 1987, Fundamentals of the physical-chemistry of pulverized coal combustion, orth Atlantic Treaty Organization. Scientific Affairs Division, 502p.

Lander, R.H. and Walderhaug, O., 1999, Predicting porosity through simulating sandstone compaction and quartz cementation. American Association of Petroleum Geologists Bulletin **83**, pp. 433–449.

Leamen, D.E., 1975, Form, Mechanism and control of dolerite intrusion near Hobart, Tasmania. Journal of the Geological Society of Australia, v.22, p. 175-186.

Leat, P.T., 2008, On the long-distance transport of the Ferrar Magmas, from Thomson, K with Petford, N. (eds) Structure and Emplacement of High-Level Magmatic Systems, Geol. Soc. London, Special Publication, 302, p. 45-61.

Liss, D., 2004, Emplacement processes and magma flow geometries of the Whin Sill complex. Unpublished PhD thesis, University of Birmingham. 236p.

Liss, D., Hutton, D.H.W and Owens,W.H, 2002, Ropy Flow Structures-a neglected indicator of magma flow direction in sills and dykes. *Geology,* v. 30, 715-718.

Lister, J.R., and Kerr, R.C., 1990, Fluid-mechanical models of dyke propagation and magma transport, in Parker, A.J., Rickwood, P.C., and Tucker, D.H., (eds), Mafic Dykes and Emplacement Mechanisms. Rotterdam, Balkema, p.69 – 80.

Lister, J.R., and Kerr, R.C., 1991, Fluid-mechanical models of crack propagation and their application to magma transport in dykes. Journal of Geophysical Research, v. 96, p. 10049-52.

Marsh, J.S., Hooper, P.R., Rehacek, J., Duncan, R.A., and Duncan, A.R., 1997, Stratigraphy and age of Karoo Basalts of Lesotho and implications for correlations within the Karoo Igneous Province, *in* Mahoney, J.J., and Coffin, M.F., eds., Large igneous provinces: Continental, oceanic, and planetary flood volcanism: American Geophysical Union Geophysical Monograph 100, p. 247–272.

Malthe-Sørenssen, A., Planke, S., Svensen, H. and Jamtveit, B., 2004, Formation of saucer-shaped sills. In: Breitkreuz, C., Petford, N. (Eds.), Physical Geology of High-Level Magmatic Systems. Special Publication, vol. 234. Geological Society, London, pp. 215–227.

Menand, T., Phillips, J.C., and Sparks, R.S.J., 2008, Circulation of bubbly magma and gas segregation within tunnels of the potential Yucca Mountain repository: Bulletin of Volcanology, v. 70, p. 947-960.

Mcphie, J., 1993, The Tennant Creek porphyry revisted: a synsedimentary sill with peperites margins, Early Proterzoic, Northern Territory. Australain Journal of Earth Sciences, v.41, p. 393-394.

Miyamoto, H. and Crown, D.A., 2006, A simplified two-component model for the lateral growth of pahoehoe lobes: Journal of Volcanology and Geothermal Research, v. 157, p. 331-342.

Morgan, S.S., Horsman, E., Tikoff, B., de Saint Blanquat, M., Nugent, A., and G. Habert, 2005, Sheet-like emplacement of satellite laccoliths, sills, and bysmaliths of the Henry Mountains, southern Utah. In: J. Pederson and C.M. Dehler, Editors, *Interior Western United States Field Guide 6*, Geological Society of America (2005), pp. 283–309.

Mudge, M.R., 1968, Depth control on some concordant intrusions. Geological Society of America, bulletin, v. 79. p. 312-315.

Murata, K.J. and Richter, D.H., 1976, The 1959-1960 eruptions of Kilauea volcano, Hawaii; chemistry of the lavas. U.S. Geological Survey professional Paper 537A, 1-26

Musset, A.E., 1986, 40Ar-39Ar step-heating ages of the Tertiary igneous rocks of Mull, Scotland: Journal of the Geological Society of London, v. 143, p. 887-896

Nicholson, R., 1985, The Intrusion and Deformation of Tertiary Minor Sheet Intrusions, West Suardal, Isle of Skye, Scotland: Geological Journal, v. 20, p. 53-72.

Nicholson, R. and Pollard, D. D., 1985, Dilation and linkage of en-echeleon cracks. Journal of Structural Geology, v.7, p. 583-590.

Parsons, T. and Thompson, G.A., 1991, The Role of Magma Overpressure in Suppressing Earthquakes and Topography - Worldwide Examples: Science, v. 253, p. 1399-1402.

Parsons, T., Howie, J.M., and Thompson, G.A., 1992, Seismic Constraints on the Nature of Lower Crustal Reflectors Beneath the Extending Southern Transition Zone of the Colorado Plateau, Arizona: Journal of Geophysical Research-Solid Earth, v. 97, p. 12391-12407.

Passey, S.R. and Bell, B.R., 2007, Morphologies and emplacement mechanisms of the lava flows of the faroe islands basalt group, faroe islands, NE atlantic ocean: Bulletin of Volcanology, v. 70, p. 139-15

Planke, S., Rasmussen, T., Rey, S.S. and Myklebust, R., 2005, Seismic characteristics and distribution of volcanic intrusions and hydrothermal vent complexes in the Vøring and Møre Basins, *in* Dore, A.G. and Vining, B., eds., Petroleum geology: N.W. Europe and global perspectives: London, Geological Society, p. 833-844.

Pollard, D.D., 1973, Derivation and evaluation of a mechanical model for sheet intrusions. Tectonophysics. v.19, p. 233 – 269.

Pollard, D., 1987, Elementary Fracture Mechanics Applied to the Structural Interpretation of Dykes. *Geologocal Association of Canada*, 34, 5-24

Pollard, D.D., Muller, O.H., and Dockstader, D.R., 1975. The form and growth of fingered sheet intrusions. Geological Society of America Bulletin, v. 86, p. 351-363.

Polteau, S., Galland, O., Haaberg, K. and Podladtchikov, Y., 2006, Post-emplacement processes of saucer-shaped sills constrained by detailed fieldwork, AMS analyses and numerical modeling of the Golden Valley Sill Complex, South Africa, LASI II, Physical Geology of subvolcanic systems; Laccoliths, sills and dykes, 1-3rd April, 2006, Abstract volume.

Polteau, S., E. C. Ferré, S. Planke, E.-R. Neumann, and L. Chevallier, 2008, How are saucer-shaped sills emplaced? Constraints from the Golden Valley Sill, South Africa, *J. Geophys. Res.*, 113, B12104, doi:10.1029/2008JB005620.

Richey, J.E. and Thomas, H.H., 1930, The Geology of Ardnamurchan, Northwest Mull and Coll, *Mem. Geol. Surv., Scotl.* 393p.

Riley, T.R., Curtis, M.L., Leat, P.T., Watkeys, M.K.; Duncan, R.A.; Millar, I.L.; Owens, W.H, 2006, Overlap of Karoo and Ferrar magma types in KwaZulu-Natal, South Africa. Journal of Petrology 47 (3): 541-566.

Roberts, A.M. and Holdsworth, R.E., 1999, Linking onshore and offshore structures: Mesozoic extension in the Scottish Highlands: Journal of the Geological Society, v. 156, p. 1061-1064.

Roberts, A. W., White, R. S., Lunnon, Z. C., Christie, P. A. F. and Spitzer, R., 2005, Imaging magmatic rocks on the Faroes Margin. *In:* Doré, A. G. and Vining, B. A. (eds.) Petroleum Geology: North-West Europe and Global Perspectives - Proceedings of the 6th Petroleum Geology Conference, 755-766.

Rocchi, S., Westerman, D.S., Dini, A., Innocenti, F. and Tonarini, S., 2002, Two-stage growth of laccoliths at Elba Island, Italy. Geology: Vol. 30, No. 11, p. 983–986.

Rocchi, S., Mazzotti, A., Marroni, M., Pandolfi, L., Costantini, P., Giuseppe, B., di Biase, D., Federici, F., and Lo, P.G., 2007, Detection of Miocene saucer-shaped sills (offshore Senegal) via integrated interpretation of seismic, magnetic and gravity data: Terra Nova, v. 19, p. 232-239.

Rohrman, M., 2007, Prospectivity of volcanic basins: Trap delineation and acreage de-risking: Aapg Bulletin, v. 91, p. 915-939.

Roman-Berdiel, T., Gapais, D. and. Brun, J.P, 1995, Analogue models of laccolith formation, Journal of Structural Geology **17**, p. 1337–1346.

Rickwood, P.C., 1990, The anatomy of a dyke and the determination of propagation and nm,magma flow directions, in Parker, A.J, Rickwood, P.C., and Tucker, D.H. (eds.), Mafic Dykes and Emplacement Mechanisms: Rotterdam, Balkema, p.81-100.

Riley, T.R., Knight, K.B., 2001. Age of pre-break-up Gondwana magmatism: a review. Antarctica. Sci. 13, 99 – 110.

Rubin, A.M., 1995, Propagation of magma filled cracks. Annual Reviews of Earth and Planetary Science, v. 23, p. 287-336.

Ryan, R.A., Sammis, C.G., 1978, Cyclic fracture mechanisms in cooling basalt. Geological Society of America Bulletin, 89: 1295-1308.

Saffman, P.G. and Taylor, G., 1958, The penetration of a fluid into a porous medium or Hele-Shaw cell containing a more viscous liquid. Royal Society of London, Proceedings, series A, v. 245, p. 312-329.

Schofield, N., Stevenson, C., Reston, T (in press) – Magma fingers and importance of host rock fluidization in sill emplacement, Geology.

Sibson, R.H., Moore, J.M. and Rankin, A.H., 1975, Seismic pumping — A hydrothermal fluid transport mechansim, *Journal of the Geological Society of London* **131** (1975), pp. 653–659.

Silva, R. and Corcoran, D, 2002, Sub-basalt imaging via pre-stack depth migration an example from the Slyne Basin, offshore Ireland. *First Break* **20,** 295.299.

Smallwood, J.R. and Maresh, J., 2002, The properties, morphology and distribution of igneous sills: modelling, borehole data and 3D seismic data from the Faeroe-Shetland area. In: Jolley DW, Bell BR (eds) The North Atlantic Igneous Province: The North Atlantic Igneous Province: Stratigraphy, Tectonic, Volcanic and Magmatic Processes.Geological Society, London, Special Publications, 197, 271–306.

Smallwood, J.R., *in press,* Backstripped 3D seismic data : A new tool applied to testing sill emplacement models, in Schofield, N., Turner, J.P.T., Underhill, J. (eds), Petroleum Geoscience, Aug issue.

Stevenson, C.T.E., Owens, W.H., and Hutton, D.H.W., 2007, Flow lobes in granite: The determination of magma flow direction in the Trawenagh Bay Granite, northwestern Ireland, using anisotropy of magnetic susceptibility: Geological Society of America Bulletin, v. 119, p. 1368-1386.

Summer, N.S. and Ayalon, A., 1995, Dike Intrusion Into Unconsolidated Sandstone and the Development of Quartzite Contact Zones: Journal of Structural Geology, v. 17, p. 997-1010.

Symonds, P.A., Planke, S., Frey, Ø., and Skogseid, J., 1998, Volcanic development of the Western Australian continental margin and its implications for basin development. In: Purcell, P.G., Purcell, R.R. (Eds.) The Sedimentary Basins of Western Australia 2, Proceedings of the Petroleum Exploration Society of Australia, Symposium, Oxford. Petroleum Exploration Society of Australia, Perth, p. 33-54.

Thomson, K., 2005, Volcanic features of the North Rockall Trough: application of visualisation techniques on 3D seismic reflection data: Bulletin of Volcanology, v. 67, p. 116-128.

Thomson, K., 2007, Determining magma flow in sills, dikes and laccoliths and their implications for sill emplacement mechanisms. Bulletin of Volcanology, 70, p. 183-201

Thomson, K. and Hutton, D., 2004, Geometry and growth of sill complexes: insights using 3D seismic from the North Rockall Trough: Bulletin of Volcanology, v. 66, p. 364-375

Thomson, K. and Schofield, N., 2008, Lithological and structural controls on the emplacement and morphology of sills in sedimentary basins, Structure and Emplacement of High-Level Magmatic Systems, Geol. Soc. London, Special Publication, 302, p. 31-44.

Trendall, A.F., 1994, The Tennant Creek Porphyry Revisited - A Synsedimentary Sill with Peperite Margins, Early Proterozoic, Northern-Territory - Discussion: Australian Journal of Earth Sciences, v. 41, p. 391-392.

Trewin, N. H., (ed.), 2002, The Geology of Scotland, 4th ed. viii + 576 pp. London, Bath: Geological Society of London

Trude, J., Cartwright, J., Davies, R.J., and Smallwood, J., 2003, New technique for dating igneous sills: Geology, v. 31, p. 813-816.

Trude, K.J., 2004, Kinematic indicators for shallow level igneous intrusion from 3D seismic data; evidence of flow direction and feeder location. In: Davies, R.J., Cartwright, J.A., Stewart, S.A., Lappin, M. with Underhill, J.R. (eds) 3D Seismic Technology: Application to the Exploration of Sedimentary Basins. Geological Society, London, Memoirs, 29, 209–217.

Tweto, O., 1951, Form and Structure of Sills Near Pando, Colorado: Geological Society of America Bulletin, v. 62, p. 507-532.

Valentine, G.A. and Krogh, K.E.C., 2006, Emplacement of shallow dikes and sills beneath a small basaltic volcanic centre - The role of pre-existing structure (Paiute Ridge, southern Nevada, USA): Earth and Planetary Science Letters, v. 246, p. 217-230.

van Zijl, J.S.V., 2006, Physical characteristics of the Karoo sediments and mode of emplacement of the dolerites: South African Journal of Geology, v. 109, p. 329-334.

Visser, D.J.L., 1999, The Geotectonic evolution of south Africa and offshore areas, Council for Geoscience, Geological Survey of South Africa, 319.p

Walker, F., 1930, The geology of the Shiant Isles (Hebrides). *Quarterly Journal of the Geological Society of London*, **86**, 355–98.

Walker, G.P.L., 1993, Basaltic-volcano systems *Geological Society, London, Special Publications*; 1993; v. 76; p. 3-38; DOI: 10.1144/GSL.SP.1993.076.01.01

Williamson, I.T. and Bell, B.R., 1994, The Palaeocene Lava-Field of West-Central Skye, Scotland - Stratigraphy, Paleogeography and Structure: Transactions of the Royal Society of Edinburgh-Earth Sciences, v. 85, p. 39-75.

Wohletz, K., 2008, "KWare Geological Software", 10th July 2008. *http://www.ees1.lanl.gov/Wohletz/Heat.htm*, 11th November, 2008.

Wylie, J.J., Helfrich, K.R., Dade, B., Lister, J.R., and Philips, K., 1999, Flow localization in fissure eruptions: Bulletin of Volcanology, v. 60, p. 432-440.